



Rezelj, Veronica Valentina (2017) *Characterization of the non-structural (NSs) protein of tick-borne phleboviruses*. PhD thesis.

<https://theses.gla.ac.uk/8149/>

Copyright and moral rights for this work are retained by the author

A copy can be downloaded for personal non-commercial research or study, without prior permission or charge

This work cannot be reproduced or quoted extensively from without first obtaining permission in writing from the author

The content must not be changed in any way or sold commercially in any format or medium without the formal permission of the author

When referring to this work, full bibliographic details including the author, title, awarding institution and date of the thesis must be given

Enlighten: Theses

<https://theses.gla.ac.uk/>  
[research-enlighten@glasgow.ac.uk](mailto:research-enlighten@glasgow.ac.uk)

# **Characterization of the non-structural (NSs) protein of tick-borne phleboviruses**



**Veronica Valentina Rezelj, BSc.**

Submitted in partial fulfilment of the requirements for the  
Degree of Doctor of Philosophy in Molecular Virology

MRC-University of Glasgow Centre for Virus Research  
Institute of Infection, Immunity and Inflammation  
College of Medical, Veterinary and Life Sciences  
Oilthigh Ghlaschu - University of Glasgow

**February, 2017**

## Abstract

In recent years, a number of newly discovered tick-borne viruses exhibiting a wide spectrum of diseases in humans have been ascribed to the *Phlebovirus* genus of the *Bunyaviridae* family. These viruses have a tripartite RNA genome composed of two negative-sense RNA segments (medium and large) and one ambisense segment (small), which encode four structural proteins and one non-structural protein (NSs). The NSs protein is the major virulence factor of bunyaviruses, and acts as an antagonist of a key component of the first line of defence against viral infections: the interferon (IFN) system (Bridgen *et al.*, 2001; Weber *et al.*, 2002). The work presented herein describes the characterization of tick-borne phlebovirus NSs proteins as IFN antagonists. The development of a reverse genetics system for the apathogenic tick-borne Uukuniemi phlebovirus (UUKV) enabled the recovery of infectious UUKV entirely from cDNA. A recombinant UUKV lacking NSs induced higher amounts of IFN in infected cells compared to wild-type UUKV, suggesting a role of NSs in modulating the IFN response. The weak IFN antagonistic activity of UUKV NSs was evident using transient transfection reporter assays in comparison to the NSs protein of either pathogenic Heartland virus (HRTV) or Severe fever with thrombocytopenia syndrome virus (SFTSV). The sensitivity of UUKV, HRTV and SFTSV to exogenous and virus-induced IFN, as well as their growth kinetics in IFN-competent cells were examined. The molecular mechanisms employed by UUKV, HRTV and SFTSV NSs proteins to evade antiviral immunity were investigated using reporter assays, immunofluorescence, and immunoprecipitation studies. Collectively, these assays showed that UUKV NSs was able to weakly inhibit IFN induction but not IFN signalling, through a novel interaction with MAVS (mitochondrial antiviral signalling protein). On the other hand, HRTV and SFTSV NSs proteins potently inhibited IFN induction through an interaction with TBK1, and type I but not type II IFN signalling via an interaction with STAT2. Finally, the development of a minigenome system for HRTV in conjunction with minigenomes developed for UUKV and SFTSV (Brennan *et al.*, 2015) provided preliminary data to assess possible outcomes of tick-borne phlebovirus reassortment. In summary, the results described in this thesis offer insights into how tick-borne phlebovirus pathogenicity may be linked to the capacity of their NSs proteins to block the innate immune system. The data presented also illustrate the plethora of viral immune evasion strategies utilized by emerging phleboviruses, and provide an insight into the possibility of tick-borne phlebovirus reassortment.

# Table of contents

|  |            |
|--|------------|
| <b>Abstract</b> .....  | <b>I</b>   |
| <b>Table of contents</b> .....   | <b>II</b>  |
| <b>List of tables</b> .....  | <b>VI</b>  |
| <b>List of figures</b> .....   | <b>VII</b> |
| <b>Acknowledgements</b> .....  | <b>X</b>   |
| <b>Author's declaration</b> .....  | <b>XI</b>  |
| <b>List of abbreviations</b> .....   | <b>XII</b> |
| <b>Publications</b> .....  | <b>XV</b>  |
| <b>1 Introduction</b> .....  | <b>2</b>   |
| <i>1.1 Molecular biology of the Bunyaviridae</i> .....                                     | 2          |
| 1.1.1 Classification of the Bunyaviridae.....  | 2          |
| 1.1.2 Virion structure.....  | 6          |
| 1.1.3 Genome organization and coding strategy.....   | 8          |
| 1.1.4 Gene products and their function.....  | 12         |
| 1.1.5 Replication cycle.....   | 20         |
| <i>1.2 Reverse genetics of bunyaviruses and its applications</i> .....                     | 27         |
| 1.2.1 cDNA-based rescue of bunyaviruses.....   | 27         |
| 1.2.2 Minigenome and virus-like particle assays.....                                       | 30         |
| <i>1.3 The Phlebovirus genus</i> .....   | 33         |
| 1.3.1 Classification and transmission.....   | 33         |
| 1.3.2 Geographic distribution.....   | 34         |
| 1.3.3 Disease caused by phleboviruses.....   | 37         |
| 1.3.4 Uukuniemi virus.....   | 38         |
| 1.3.5 Severe fever with thrombocytopenia syndrome virus.....                               | 39         |
| 1.3.6 Heartland virus.....   | 40         |
| <i>1.4 Host innate immune responses to virus infection and viral countermeasures</i> ..... | 42         |
| 1.4.1 The human innate immune system.....  | 42         |
| 1.4.2 Interferon induction.....  | 43         |
| 1.4.3 Interferon signalling.....   | 46         |
| 1.4.4 Phlebovirus NSs proteins as antagonists of the human IFN response.....               | 49         |
| <b>2 Aims</b> .....  | <b>54</b>  |
| <b>3 Materials</b> .....   | <b>56</b>  |
| <i>3.1 Cell culture</i> .....  | 56         |
| 3.1.1 Eukaryotic cell lines.....   | 56         |
| 3.1.2 Competent bacterial strains.....   | 57         |

|  |           |
|--|-----------|
| 3.2 <i>Virus strains and sequence accession numbers</i> .....              | 57        |
| 3.2.1 Virus strains.....   | 57        |
| 3.2.2 Virus sequence accession numbers .....                               | 58        |
| 3.3.2 Enzymes .....  | 59        |
| 3.3.4. Plasmids.....   | 59        |
| 3.3.5 Antibodies .....   | 62        |
| 3.4 <i>Reagents and chemicals</i> .....                                    | 63        |
| 3.4.1 Bacterial culture .....  | 63        |
| 3.4.2 Cell culture .....   | 64        |
| 3.4.3 DNA analysis .....   | 64        |
| 3.4.4 Total cellular RNA extraction .....                                  | 64        |
| 3.4.5 Immunofluorescence .....   | 64        |
| 3.4.6 Protein analysis and western blotting.....                           | 65        |
| 3.4.7 Focus-forming assays .....   | 66        |
| 3.4.8 Immunoprecipitation .....  | 66        |
| 3.5 <i>Software packages</i> .....   | 66        |
| 3.5.1 Bioinformatics .....   | 66        |
| 3.5.2 Graphing and statistical analysis .....                              | 66        |
| 3.5.3 Imaging.....   | 66        |
| <b>4 Methods</b> .....   | <b>68</b> |
| 4.1 <i>Cell culture</i> .....  | 68        |
| 4.1.1 Maintenance of eukaryotic cell lines .....                           | 68        |
| 4.1.2 Transfection of eukaryotic cell lines .....                          | 68        |
| 4.1.3 Minigenome assays .....  | 69        |
| 4.1.4 Virus-like particle assays.....                                      | 69        |
| 4.1.5 Virus rescues .....  | 70        |
| 4.1.6 Virus infections .....   | 70        |
| 4.1.7 Preparation of virus stocks .....                                    | 70        |
| 4.1.8 Determination of virus titre by focus- or plaque-forming assays..... | 71        |
| 4.1.9 Immunofluorescence .....   | 72        |
| 4.1.10 Luciferase assays .....   | 72        |
| 4.1.11 Biological interferon protection assays .....                       | 73        |
| 4.1.12 Biosafety.....  | 74        |
| 4.2 <i>Manipulation of nucleic acids and cloning</i> .....                 | 74        |
| 4.2.1 DNA amplification by PCR .....                                       | 74        |
| 4.2.2 Site-directed mutagenesis.....                                       | 76        |
| 4.2.3 Agarose gel electrophoresis and gel extraction.....                  | 76        |
| 4.2.4 Restriction-free cloning.....  | 76        |
| 4.2.5 Bacterial transformation and plasmid isolation.....                  | 77        |
| 4.2.6 Restriction enzyme digestion .....                                   | 78        |

|  |            |
|--|------------|
| 4.2.7 Total cellular RNA extraction .....  | 78         |
| 4.2.8 cDNA synthesis .....   | 78         |
| 4.2.9 Rapid amplification of complementary DNA ends (RACE).....  | 79         |
| 4.2.10 Real-time qPCR.....   | 79         |
| <i>4.3 Protein analysis</i> .....  | <i>81</i>  |
| 4.1.1 Luciferase assays .....  | 81         |
| 4.1.2 Western blot analysis.....   | 81         |
| 4.1.3 Co-immunoprecipitation .....   | 82         |
| <i>4.4 Statistical analysis</i> .....  | <i>83</i>  |
| <b>5 Establishment of a reverse genetics system for Uukuniemi virus .....</b>                                      | <b>85</b>  |
| <i>5.1 Introduction</i> .....  | <i>85</i>  |
| <i>5.2 Aims</i> .....  | <i>86</i>  |
| <i>5.3 Results</i> .....   | <i>87</i>  |
| 5.3.1 Cloning of cDNA plasmids used for the rescue of UUKV .....   | 87         |
| 5.3.2 Establishment of a UUKV minigenome system.....   | 89         |
| 5.3.3 Generation of UUKV virus-like particles .....  | 93         |
| 5.3.4 Rescue of recombinant UUKV from cDNA .....   | 96         |
| 5.3.5 Rescue of recombinant UUKV lacking the non-structural protein NSs .....                                      | 98         |
| 5.3.6 Replication of rUUKV, rUUKdelNSs and rUUKdelNSsGFP in cell culture ...                                       | 100        |
| 5.3.7 Permissibility of mammalian cell lines to UUKV infection .....   | 104        |
| 5.3.8 Basic characterisation of rUUKV, rUUKdelNSs and rUUKdelNSsGFP in the chicken DF-1 fibroblast cell line. .... | 108        |
| <i>5.4 Discussion</i> .....  | <i>111</i> |
| <i>5.5 Summary</i> .....   | <i>117</i> |
| <b>6 Role of tick-borne phlebovirus NSs proteins in suppressing the human interferon system .....</b>              | <b>118</b> |
| <i>6.1 Introduction</i> .....  | <i>118</i> |
| <i>6.2 Aims</i> .....  | <i>119</i> |
| <i>6.3 Results</i> .....   | <i>120</i> |
| 6.3.1 Evaluation of UUKV NSs as an IFN antagonist .....  | 120        |
| 6.3.2 Inhibition of IFN induction by tick-borne phlebovirus NSs proteins .....                                     | 123        |
| 6.3.3 Effect of tick-borne phlebovirus NSs proteins on NF- $\kappa$ B signalling .....                             | 129        |
| 6.3.4 Effect of tick-borne phlebovirus NSs proteins on type I and type II IFN signalling .....                     | 131        |
| 6.3.5 IFN sensitivity of tick-borne phleboviruses .....  | 135        |
| <i>6.4 Discussion</i> .....  | <i>141</i> |
| <i>6.5 Summary</i> .....   | <i>147</i> |
| <b>7 Molecular mechanism of IFN antagonism by tick-borne phlebovirus NSs proteins .</b>                            | <b>148</b> |
| <i>7.1 Introduction</i> .....  | <i>148</i> |

|  |            |
|--|------------|
| 7.2 <i>Aims</i> .....  | 149        |
| 7.3 <i>Results</i> .....   | 150        |
| 7.3.1 Subcellular localization of UUKV, HRTV and SFTSV NSs.....  | 150        |
| 7.3.2 Dissection of the IFN induction pathway to study the inhibitory effect of UUKV, HRTV and SFTSV NSs proteins.....                                     | 155        |
| 7.3.3 Interaction between UUKV, HRTV and SFTSV NSs proteins and the IFN induction pathway.....   | 159        |
| 7.3.4 UUKV NSs protein interacts with MAVS.....  | 161        |
| 7.3.5 HRTV NSs protein interacts with TBK1.....  | 165        |
| 7.3.6 Interaction between HRTV or SFTSV NSs and the IFN signalling pathway...  | 167        |
| 7.3.7 The effect of HRTV and SFTSV NSs proteins on STAT1 and STAT2 nuclear translocation.....  | 170        |
| 7.4 <i>Discussion</i> .....  | 175        |
| 7.5 <i>Summary</i> .....   | 182        |
| <b>8 Development of a HRTV minigenome system to assess tick-borne phlebovirus genome reassortment.....</b>   | <b>183</b> |
| 8.1 <i>Introduction</i> .....  | 183        |
| 8.2 <i>Aims</i> .....  | 184        |
| 8.3 <i>Results</i> .....   | 185        |
| 8.3.1 Sequencing of the laboratory HRTV stock.....   | 185        |
| 8.3.2 Development of a minigenome system for HRTV.....   | 188        |
| 8.3.3 Investigating the ability of UUKV, HRTV and SFTSV N and L proteins to utilize the M segment minigenome of heterologous tick-borne phleboviruses..... | 194        |
| 8.3.4 Efforts to generate cDNA clones of the HRTV M segment.....   | 202        |
| 8.4 <i>Discussion</i> .....  | 204        |
| 8.5 <i>Summary</i> .....   | 208        |
| <b>9 Conclusions.....</b>  | <b>211</b> |
| 9.1 <i>Fulfilment of the project aims</i> .....  | 211        |
| 9.2 <i>Future directions</i> .....   | 213        |
| <b>10 Appendices.....</b>  | <b>219</b> |
| 10.1 <i>Oligonucleotide primers used in this study</i> .....   | 219        |
| 10.2 <i>Amino acid alignments of UUKV, HRTV and SFTSV N and L proteins</i> .....   | 225        |
| <b>11 References.....</b>  | <b>231</b> |
| <b>12 Publications.....</b>  | <b>264</b> |

## List of tables

|   |            |
|---|------------|
| <b>Table 1-1.</b> Pathogenic viruses within the <i>Bunyaviridae</i> family. ....  | <b>4</b>   |
| <b>Table 3-1.</b> Virus nucleotide sequence accession numbers used in this study .....  | <b>58</b>  |
| <b>Table 3-2.</b> Plasmids used in this study. ....   | <b>60</b>  |
| <b>Table 3-3.</b> Primary antibodies used in this project. ....   | <b>62</b>  |
| <b>Table 3-4.</b> Secondary antibodies used in this project. ....   | <b>63</b>  |
| <b>Table 3-5.</b> Reagents used for native PAGE gels. ....  | <b>65</b>  |
| <b>Table 4-1.</b> Volumes used for transfections in different cell culture vessels. ....  | <b>68</b>  |
| <b>Table 6-1.</b> Percentage amino acid identity of the tick-borne phlebovirus NSs proteins used in this study. ....  | <b>150</b> |
| <b>Table 8-1.</b> Percentage amino acid identity of UUKV, HRTV and SFTSV N proteins. ...  | <b>195</b> |
| <b>Table 8-2.</b> Percentage amino acid identity of UUKV, HRTV and SFTSV L proteins. ....   | <b>195</b> |
| <b>Table 8-3.</b> Summary of UUKV, HRTV and SFTSV M-segment based minigenome activities detected in the presence of N and L proteins from cognate or heterologous viruses. .... | <b>200</b> |
| <b>Table 10-1.</b> Common oligonucleotide primers used throughout this study. ....  | <b>219</b> |
| <b>Table 10-2.</b> Oligonucleotide primers used for the generation of UUKV reverse genetics plasmids. ....  | <b>220</b> |
| <b>Table 10-3.</b> Oligonucleotide primers used for sequencing the UUKV genome and plasmids. ....   | <b>221</b> |
| <b>Table 10-4.</b> Oligonucleotide primers used in Chapter 6. ....  | <b>222</b> |
| <b>Table 10-5.</b> Oligonucleotide primers used for the full-genome sequencing of the HRTV laboratory stock. ....   | <b>223</b> |
| <b>Table 10-6.</b> Oligonucleotide primers utilised for the generation of HRTV minigenome constructs. ....  | <b>224</b> |

## List of figures

|  |            |
|--|------------|
| <b>Figure 1-1.</b> Simplified schematic of arbovirus transmission. ....                                      | <b>5</b>   |
| <b>Figure 1-2.</b> Bunyavirus virion structure. ....   | <b>7</b>   |
| <b>Figure 1-3.</b> Coding capacity of the <i>Bunyaviridae</i> . ....   | <b>10</b>  |
| <b>Figure 1-4.</b> Negative- and ambi-sense coding strategies employed by phleboviruses. ....                | <b>11</b>  |
| <b>Figure 1-5.</b> Crystal structures of RVFV and TOSV N. ....   | <b>13</b>  |
| <b>Figure 1-6.</b> Polyprotein precursor synthesis and processing of phleboviruses. ....                     | <b>17</b>  |
| <b>Figure 1-7.</b> Life cycle of bunyaviruses. ....  | <b>22</b>  |
| <b>Figure 1-8.</b> Transcription initiation of viral mRNA and coupled translation. ....                      | <b>25</b>  |
| <b>Figure 1-9.</b> The bunyavirus rescue system. ....  | <b>29</b>  |
| <b>Figure 1-10.</b> Minigenome and virus-like particle systems. ....   | <b>32</b>  |
| <b>Figure 1-11.</b> Phylogenetic tree of the phlebovirus glycoprotein precursor. ....                        | <b>35</b>  |
| <b>Figure 1-12.</b> Geographical distribution of tick-borne phleboviruses. ....                              | <b>36</b>  |
| <b>Figure 1-13.</b> Simplified representation of RIG-I-mediated IFN induction. ....                          | <b>45</b>  |
| <b>Figure 1-14.</b> Simplified diagram of type I, II and III IFN signalling. ....                            | <b>48</b>  |
| <b>Figure 5-1.</b> Schematic representation of UUKV rescue plasmids. ....                                    | <b>88</b>  |
| <b>Figure 5-2.</b> Schematic representation of the construction of UUKV minigenome plasmids. ....            | <b>91</b>  |
| <b>Figure 5-3.</b> UUKV minigenome assay. ....   | <b>92</b>  |
| <b>Figure 5-4.</b> UUKV VLP production assay. ....   | <b>95</b>  |
| <b>Figure 5-5.</b> Rescue of rUUKV. ....   | <b>97</b>  |
| <b>Figure 5-6.</b> Generation of recombinant UUKV lacking NSs. ....  | <b>99</b>  |
| <b>Figure 5-7.</b> Phenotypic characterization of recombinant viruses in cell culture. ....                  | <b>102</b> |
| <b>Figure 5-8.</b> Growth kinetics of recombinant viruses in BHK-21 cells. ....                              | <b>103</b> |
| <b>Figure 5-9.</b> eGFP expression in rUUKdelNSsGFP-infected cells. ....                                     | <b>106</b> |
| <b>Figure 5-10.</b> wtUUKV yield assay in selected mammalian cell lines. ....                                | <b>107</b> |
| <b>Figure 5-11.</b> Growth properties of recombinant UUKV in DF-1 cells. ....                                | <b>109</b> |
| <b>Figure 5-12.</b> DF-1 cell morphology following rUUKdelNSsGFP infection. ....                             | <b>110</b> |
| <b>Figure 6-1.</b> Recombinant UUKV viruses lacking NSs are better inducers of IFN than wild-type UUKV. .... | <b>122</b> |

|  |            |
|--|------------|
| <b>Figure 6-2.</b> Inhibition of IFN production by tick-borne phlebovirus NSs proteins.....  | <b>125</b> |
| <b>Figure 6-3.</b> Inhibition of IRF-3 phosphorylation and dimerization by tick-borne phlebovirus NSs proteins.....                                  | <b>126</b> |
| <b>Figure 6-4.</b> RIG-I -induced nuclear translocation of IRF-3 in the presence of tick-borne phlebovirus NSs proteins.....                         | <b>128</b> |
| <b>Figure 6-5.</b> The effect of tick-borne phlebovirus NSs proteins on NF- $\kappa$ B activation. ....  | <b>130</b> |
| <b>Figure 6-6.</b> Inhibition of type I IFN signalling by tick-borne phlebovirus NSs proteins.   | <b>133</b> |
| <b>Figure 6-7.</b> Inhibition of type II IFN signalling by tick-borne phlebovirus NSs proteins. ....   | <b>134</b> |
| <b>Figure 6-8.</b> Sensitivity of tick-borne phleboviruses to exogenous IFN.....   | <b>136</b> |
| <b>Figure 6-9.</b> Sensitivity of tick-borne phleboviruses to virus-induced IFN.....   | <b>138</b> |
| <b>Figure 6-10.</b> Replication kinetics and IFN production following tick-borne phlebovirus infection.....  | <b>140</b> |
| <b>Figure 7-1.</b> Amino acid sequence alignment of UUKV, HRTV and SFTSV NSs proteins. ....  | <b>151</b> |
| <b>Figure 7-2.</b> Subcellular localization of UUKV, HRTV and SFTSV NSs proteins.....  | <b>153</b> |
| <b>Figure 7-3.</b> Subcellular localization of V5-tagged UUKV, HRTV and SFTSV NSs proteins. ....   | <b>154</b> |
| <b>Figure 7-4.</b> IFN- $\beta$ promoter activation by effectors of the IFN induction pathway. ....  | <b>156</b> |
| <b>Figure 7-5.</b> UUKV NSs protein inhibits IFN- $\beta$ induction at the level of MAVS, whereas HRTV NSs antagonises at the level of TBK1. ....    | <b>158</b> |
| <b>Figure 7-6.</b> UUKV NSs interacts with RIG-I N and MAVS, whereas HRTV and SFTSV NSs interact with TBK1 in a transient overexpression system..... | <b>160</b> |
| <b>Figure 7-7.</b> Interaction between UUKV NSs and MAVS detected by immunoprecipitation. ....   | <b>163</b> |
| <b>Figure 7-8.</b> Subcellular localization of V5-tagged UUKV NSs and FLAG-tagged MAVS. ....   | <b>164</b> |
| <b>Figure 7-9.</b> Interaction between HRTV NSs and TBK1.....  | <b>166</b> |
| <b>Figure 7-10.</b> Interaction between UUKV, HRTV or SFTSV NSs and STAT proteins....  | <b>169</b> |
| <b>Figure 7-11.</b> Inhibition of IFN- $\beta$ -induced STAT1 nuclear translocation by HRTV and SFTSV NSs proteins.....                              | <b>171</b> |
| <b>Figure 7-12.</b> Inhibition of IFN- $\beta$ -induced STAT2 nuclear translocation by HRTV and SFTSV NSs proteins.....                              | <b>172</b> |

|  |            |
|--|------------|
| <b>Figure 7-13.</b> Inhibition of IFN- $\gamma$ -induced STAT1 nuclear translocation by HRTV and SFTSV NSs proteins. ....  | <b>174</b> |
| <b>Figure 7-14.</b> Schematic summary of the mechanisms utilized by tick-borne phlebovirus NSs proteins to inhibit the canonical IFN induction and signalling pathways. .... | <b>181</b> |
| <b>Figure 8-1.</b> Differences in the sequence of the HRTV laboratory stock compared to the published HRTV sequence. ....  | <b>187</b> |
| <b>Figure 8-2.</b> HRTV S, M and L minigenome assays using constructs based on published HRTV sequences. ....  | <b>191</b> |
| <b>Figure 8-3.</b> HRTV S segment minigenome assay using constructs based on published and newly identified sequences. ....  | <b>193</b> |
| <b>Figure 8-4.</b> Sequence alignment of the M segment 3' UTR of three tick-borne phleboviruses. ....  | <b>197</b> |
| <b>Figure 8-5.</b> Sequence alignment of the M segment 5' UTR of three tick-borne phleboviruses. ....  | <b>198</b> |
| <b>Figure 8-6.</b> Activity of the UUKV, HRTV and SFTSV M segment-based minigenomes using UUKV, HRTV or SFTSV N and L proteins. ....   | <b>201</b> |
| <b>Figure 10-1.</b> Amino acid sequence alignment for UUKV, HRTV and SFTSV N proteins. ....  | <b>225</b> |
| <b>Figure 10-2.</b> Amino acid sequence alignment for UUKV, HRTV and SFTSV L proteins. ....  | <b>229</b> |

## Acknowledgements

First of all I would like to thank you, Richard, for believing in me when I was just an undergraduate student and giving me the opportunity to join your lab. You gave me the chance to do something I really enjoy in life, and for that I will be ever grateful. Although my time as your student was shorter than expected, it has been enough for me to develop a strong bond with a great supervisor, scientist and person. Your contagious determination and passion for science have made my motivation to succeed stronger. You remain alive within everyone you have trained, and I will make sure to make you proud and become the “good virologist” you wanted me to become.

I am hugely indebted to all the people that have formed part of the Elliott lab during my PhD: Agnieszka, Angela, Basma, Ben, Elina, Felix, Gillian, Gustavo, Ing, Junjie, Natasha, Ping, Sophie, Steve, Xiaohong. Thank you all for your making my time in Glasgow so enjoyable, I will miss you all! Special thanks go to Ben and Massimo, for taking care of and dealing with me during my last 1.5 years, and for your support and advice throughout. Also – thank you for reading this thesis! I would also like to thank Dr Alain Kohl, Prof Rick Randall, and my advisors Dr Esther Schnettler and Dr Pablo Murcia for helpful advice and discussions throughout the past 3.5 years.

I am grateful to Prof Jin Dong-Yan at Hong Kong University and his lab, especially Deng, Chaudhary and Sam. Thank you for welcoming me, and making my stay at Hong Kong an unforgettable experience. Thank you all for your hospitality! Our delicious lunches, Yum Cha, as well as the beautiful views from the lab, Victoria peak and the Harbour will remain in my memory forever.

To Nico, Pepi, Ale and especially to my mom, gracias/hvala/thank you for your unconditional perseverance. Thank you mom, for your sedulous efforts in helping me find a career I love. Last but not least, I would like to thank Jacopo for your motivation during the writing of this thesis, for always being there for me, and most importantly, for keeping me sane all these years.

## Author's declaration

I, Veronica Valentina Rezelj, hereby certify that, except where explicit reference is made to the contribution of others, this thesis is the result of my own work and has not been submitted for any other degree at the University of Glasgow or any other institution. Some of the work has been or will be submitted for publication in appropriate journals, as indicated in page XV. I acknowledge that the work undertaken for the completion of this PhD thesis was supported by the Wellcome Trust Senior Investigator Award to Richard M. Elliott (099220/Z/12/Z).

Date \_\_\_\_\_

Signature \_\_\_\_\_

Printed name \_\_\_\_\_

## List of abbreviations

|           |   |
|-----------|---|
| A549/Npro | A549/BVDV-Npro                            |
| A549/V    | A549/PIV5-V                               |
| ADTPV     | American dog tick phlebovirus             |
| agRNA     | Antigenomic RNA                           |
| ANTV      | Antigone virus                            |
| BCCV      | Black Creek Canal virus                   |
| BTPV      | Blacklegged tick phlebovirus              |
| BUNV      | Bunyamwera virus                          |
| BVDV      | Bovine viral diarrhea virus               |
| CARD      | Caspase activation and recruitment domain |
| CBP       | CREB-binding protein                      |
| CCHFV     | Crimean Congo hemorrhagic fever virus     |
| CMV       | Cytomegalovirus                           |
| Cryo-EM   | Cryo-electron microscopy                  |
| DC-SIGN   | Dendritic cell specific ICAM              |
| DMEM      | Dulbecco's modified Eagle's medium        |
| dsRNA     | double-stranded RNA                       |
| DUGV      | Dugbe virus                               |
| eGFP      | Enhanced GFP                              |
| EMCV      | Encephalomyocarditis virus                |
| FCS       | Foetal Calf Serum                         |
| FFU       | Focus-forming unit                        |
| GAF       | Gamma-activated Factor                    |
| GAS       | IFN- $\gamma$ activated site              |
| GFP       | Green Fluorescent Protein                 |
| GMEM      | Glasgow modified Eagle's medium           |
| GOLV      | Gouleako virus                            |
| gRNA      | Genomic RNA                               |
| HIGV      | Hunter Island Group virus                 |
| HRTV      | Heartland virus                           |
| HTNV      | Hantaan virus                             |
| IBs       | Inclusion bodies                          |

|                 |  |
|-----------------|--|
| ICAM            | Intracellular adhesion molecule-3 grabbing non-integrin                |
| ICTV            | International Committee on Taxonomy of Viruses                         |
| IFITM           | Interferon-inducible transmembrane proteins                            |
| IFN             | Interferon   |
| IFNAR           | Type I IFN receptor  |
| IFNGR           | Type II IFN receptor   |
| IFN $\lambda$ R | Type III IFN receptor  |
| IKK             | Inhibitor of nuclear factor kappa-B kinase                             |
| IL              | Interleukin  |
| IP              | Immunoprecipitation  |
| IRF-3           | Interferon regulatory factor   |
| ISG             | Interferon-stimulated gene   |
| ISGF3           | Interferon-stimulated gene factor 3                                    |
| ISRE            | IFN-stimulated response elements                                       |
| I $\kappa$ B    | Inhibitor of NF- $\kappa$ B  |
| I $\kappa$ BSR  | I $\kappa$ B super-repressor   |
| JAK             | Janus activated kinase   |
| L-SIGN          | Liver-specific intercellular adhesion molecule-3-grabbing non-integrin |
| LACV            | La Crosse virus  |
| LSV             | Lone Star virus  |
| MALV            | Malsoor virus  |
| MAVS            | Mitochondrial antiviral signalling protein                             |
| MDA-5           | Melanoma differentiation-associated gene-5                             |
| MOI             | Multiplicity of infection  |
| NCS             | Newborn Calf Serum   |
| NF- $\kappa$ B  | Nuclear factor $\kappa$ -light-chain-enhancer of activated B cells     |
| NLS             | Nuclear localization signal  |
| ORF             | Open reading frame   |
| OROV            | Oropouche virus  |
| PAMP            | Pathogen associated molecular pattern                                  |
| PFU             | Plaque-forming unit  |
| PKR             | Double-stranded RNA-dependent protein kinase                           |
| Pol I           | RNA polymerase 7   |

|       |   |
|-------|---|
| PRR   | Pattern recognition receptor                      |
| PTV   | Punta Toro Virus                                  |
| RdRp  | RNA-dependent RNA polymerase                      |
| RIG-I | Retinoic acid-inducible gene-I                    |
| RIU   | Relative IFN units                                |
| RNAP  | RNA polymerase                                    |
| RNP   | Ribonucleoprotein                                 |
| RVFV  | Rift Valley Fever virus                           |
| SAP30 | Sin3A associated protein 30                       |
| SFNV  | Sandfly fever Naples virus                        |
| SFTSV | Severe fever with thrombocytopenia syndrome virus |
| SNV   | Sin Nombre virus                                  |
| ssRNA | Single-stranded RNA                               |
| STAT  | Signal transducer and activator of transcription  |
| TBK1  | Tank binding kinase 1                             |
| TFIIH | Transcription factor IIH                          |
| TIR   | Toll-IL1-resistance domain                        |
| TLR   | Toll-like Receptors                               |
| TOSV  | Toscana virus                                     |
| TPB   | Tryptose phosphate broth                          |
| TRIF  | TIR-containing adaptor inducing IFN- $\beta$      |
| TRIM  | Tripartite motif-containing protein               |
| TSWV  | Tomato spotted wilt virus                         |
| TULV  | Tula virus  |
| TYK2  | Tyrosine kinase 2                                 |
| UTR   | Untranslated regions                              |
| UUKV  | Uukuniemi virus                                   |
| VLP   | Virus-like particle                               |
| WB    | Western blotting                                  |
| WCL   | Whole cell lysate                                 |

## Publications

**Rezelj, Veronica V.**, Anna K. Överby, and Richard M. Elliott. "Generation of mutant Uukuniemi viruses lacking the nonstructural protein NSs by reverse genetics indicates that NSs is a weak interferon antagonist." *Journal of virology* 89, no. 9 (2015): 4849-4856.

### **Contributed to, but not included in this thesis:**

Donald, Claire L., Benjamin Brennan, Stephanie L. Cumberworth, **Veronica V. Rezelj**, Jordan J. Clark, Marli T. Cordeiro, Rafael Freitas de Oliveira França et al. "Full genome sequence and sfRNA interferon antagonist activity of Zika virus from Recife, Brazil." *PLoS Negl Trop Dis* 10, no. 10 (2016): e0005048.

### **In preparation:**

**Rezelj, Veronica V.**, Ping Li, Vidyanath Chaudhary, Richard M. Elliott, Jin Dong-Yan, and Benjamin Brennan. "A comparative study of emerging tick-borne *Phlebovirus* non-structural proteins reveals differential antagonism of the human innate immune responses."

**Rezelj, Veronica V.**, and Benjamin Brennan. "M segment-based minigenome assays as an approach to assess the potential of tick-borne phlebovirus genome reassortment."

### **Not included in this thesis (in preparation):**

**Rezelj, Veronica V.**, Agnieszka Szemiel, and Benjamin Brennan. "The Uukuniemi virus non-structural NSs protein acts as a strong antagonist of the avian interferon system."

---

Chapter **1**

INTRODUCTION

---

# 1 Introduction

The following chapter will review the basic characteristics of the molecular biology of the *Bunyaviridae*, with particular attention to the *Phlebovirus* genus, followed by a brief history of the methods employed to manipulate the genome of bunyaviruses. A discussion of emerging tick-borne phleboviruses, as well as a short review of the host innate immune responses and countermeasures employed by phleboviruses to suppress these responses is also described.

## 1.1 Molecular biology of the *Bunyaviridae*

### 1.1.1 Classification of the *Bunyaviridae*

The *Bunyaviridae* is the largest family of RNA viruses, and it comprises over 350 members. All bunyaviruses share similar genetic, morphological and replication strategies: they are enveloped, single strand RNA viruses with tripartite genomes of negative- or ambi-sense polarity, they replicate exclusively in the host cell cytoplasm and virus particles are of 80-120 nm diameter. Additionally, bunyaviruses are characterised by their maturation and budding at the Golgi complex (Kuismanen *et al.*, 1984; 1982; Murphy *et al.*, 1973).

The *Bunyaviridae* was recognised as a family by the International Committee on Taxonomy of Viruses (ICTV) in 1975 (Elliott and Blakqori, 2012), and was further classified into 5 genera: *Orthobunyavirus*, *Nairovirus*, *Hantavirus*, *Phlebovirus* and *Tospovirus* according to their genomic and antigenic similarities. Members of the *Bunyaviridae* family are commonly referred to as bunyaviruses. However, the terms orthobunyaviruses, nairoviruses, hantaviruses, phleboviruses and tospoviruses refer to the particular genera, respectively. Some members of these genera are important plant, animal, or human pathogens with a worldwide distribution (Table 1-1).

In general, bunyaviruses are known as arthropod-borne viruses (arboviruses), with the exception of hantaviruses, which are transmitted by rodents via aerosolized excreta. Additionally, all bunyaviruses are known to infect vertebrate hosts, except for tospoviruses, which are the sole group of plant-infecting viruses within the family and are transmitted by thrips. It must be mentioned that some viruses, such as Gouléako virus (GOLV) or Herbert virus (HEBV), are putatively recognized as insect-specific viruses

---

(Marklewitz *et al.*, 2015). However, GOLV and HEBV RNA was detected in pigs in South Korea, suggesting that these viruses may also infect vertebrates (Chung *et al.*, 2014).

Like other arboviruses, arthropod-transmitted bunyaviruses are maintained in nature by enzootic cycles involving haematophagous invertebrate vectors of transmission (such as mosquitoes, sandflies, thrips or ticks) and susceptible vertebrate hosts (Figure 1-1). The diversity of hosts, vectors and disease manifestation of the members of this family, and their remarkable ability to replicate in cells of disparate phylogeny is of interest. These characteristics give an insight into the heterogeneity of virus-host interactions that this family has evolved at the molecular level.

**Table 1-1. Pathogenic viruses within the *Bunyaviridae* family.**

| <b>Virus</b>                  | <b>Vector</b>    | <b>Host</b>                       | <b>Geographic distribution</b>    | <b>Disease manifestation</b>                               |
|-------------------------------|------------------|-----------------------------------|-----------------------------------|--|
| <b><i>Orthobunyavirus</i></b> |                  |                                   |                                   |  |
| Bunyamwera                    | Midge, mosquito  | Human                             | Africa                            | Acute febrile illness, encephalitis                        |
| Oropouche                     | Midge            | Human                             | North America                     | Fever, myalgia, arthralgia, encephalitis                   |
| La Crosse                     | Mosquito         | Human                             | North America                     | Fever, encephalitis  |
| Cache Valley                  | Midges, mosquito | Cattle, sheep                     | North America                     | Febrile illness, encephalitis                              |
| Schmallenberg                 | Midges           | Cattle, sheep, goats              | Europe                            | Stillbirths and birth defects                              |
| <b><i>Hantavirus</i></b>      |                  |                                   |                                   |  |
| Hantaan                       | Field mouse      | Human                             | Eurasia                           | Haemorrhagic fever with renal syndrome                     |
| Puumala                       | Bank vole        | Human                             | Eurasia                           | Nephromathia epidemica                                     |
| Sin Nombre                    | Deer Mouse       | Human                             | North America                     | Hantavirus pulmonary syndrome                              |
| <b><i>Nairovirus</i></b>      |                  |                                   |                                   |  |
| CCHF*                         | Tick             | Human                             | Africa, Eurasia                   | Haemorrhagic fever   |
| Dugbe                         | Tick, mosquito   | Human, cattle                     | Worldwide                         | Abortion in cattle, fever and thrombocytopenia in humans   |
| <b><i>Tospovirus</i></b>      |                  |                                   |                                   |  |
| Tomato spotted wilt           | Thrip            | Plants (weeds, field crops)       | Worldwide                         | Spotting and wilting of plants                             |
| <b><i>Phlebovirus</i></b>     |                  |                                   |                                   |  |
| Rift Valley fever             | Mosquito         | Human, cattle                     | Africa                            | Retinitis, encephalitis, haemorrhagic fever                |
| Toscana                       | Sandfly          | Human                             | Europe                            | Fever, myalgia   |
| SFTS° /Heartland              | Tick             | Human, sheep, cattle, dogs, birds | South East Asia/<br>North America | Fever, thrombocytopenia, leukocytopenia, hemorrhagic fever |

\* Crimean-Congo Haemorrhagic Fever, °Severe Fever with Thrombocytopenia Syndrome

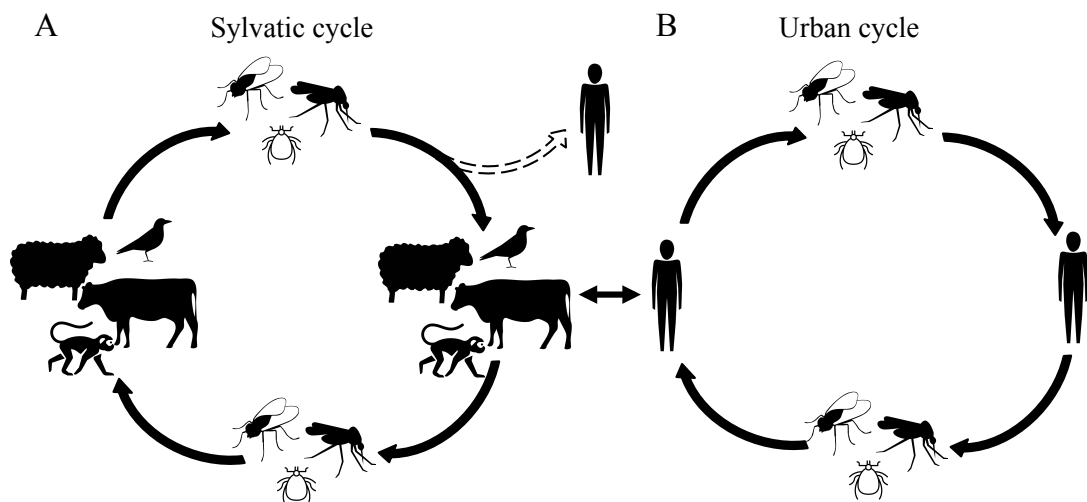


**Figure 1-1. Simplified schematic of arbovirus transmission.**

Arboviruses can be maintained in nature in two cycles. (A) The enzootic sylvatic transmission cycles involves blood-feeding arthropods and wild vertebrates. In rare cases, a spill-over event can occur from the enzootic cycle to humans, which are considered the dead-end hosts. (B) Some viruses are capable of being maintained in an urban cycle. These viruses are able to infect humans and cause high viraemia, which allows humans to act as the main reservoir of arboviruses, allowing infection of new vectors. Close contact between the sylvatic and urban cycles can result in virus spill-over from one cycle to another. Figure modified from (Petersen and Busch, 2010).

### 1.1.2 *Virion structure*

Bunyavirus virions are composed of only four structural proteins: the two surface glycoproteins embedded in a lipid envelope, the nucleocapsid protein (N) and the RNA-dependent RNA polymerase (RdRp, L). The latter two are tightly associated with the three RNA segments to form ribonucleoprotein (RNP) complexes (Figure 1-2 A). These RNPs have been found in virions in a circular panhandle form, with a pseudo-helical structure (Figure 1-2 B) (Obijeski *et al.*, 1976; Pettersson and Bonsdorff, 1975; Samsø *et al.*, 1975). The general view of a bunyavirus particle containing three genome segments has now been revisited, as a recent study used single molecule fluorescence *in situ* hybridization to show that RVFV genome packaging is a non-selective process (Wichgers Schreur and Kortekaas, 2016). This study confirmed that in reality, the majority of mature virions lack one or more genome segments, despite the intracellular S, M and L genome segments averaging a 1:1:1 ratio. Additionally, although the general view is that only genomic segments are packaged into virions, a fraction of antigenomic replication intermediates have been reported to be packaged in Rift Valley Fever (RVFV) and Uukuniemi (UUKV) viral particles (Brennan *et al.*, 2014; Ikegami *et al.*, 2005b; Simons *et al.*, 1990).

Cryo-electron microscopy (cryo-EM) of a number of bunyaviruses has demonstrated that members of different genera exhibit some differences in their morphology, with virion diameter ranging from 80 to 120 nm (Figure 1-2 C). The virion diameter of a number of bunyaviruses has been determined:  $108 \pm 8$  nm for Bunyamwera virus (BUNV) (Bowden *et al.*, 2013), 75-115 nm for La Crosse virus (LACV) (Talmon *et al.*, 1987), 95-125 nm for UUKV (Overby *et al.*, 2008; Pettersson and Bonsdorff, 1975), 100 nm for RVFV (Freiberg *et al.*, 2008; Sherman *et al.*, 2009) and 120-160 nm for Tula virus (TULV) (Huiskonen *et al.*, 2010). Virions are composed of a 4-7 nm thick lipid bilayer envelope, which originates from the host cell Golgi cisternae and is embedded by the heterodimers of the viral glycoproteins Gn and Gc that can be visualised as 5-10 nm protrusions from the envelope by EM (Huiskonen *et al.*, 2009; Overby *et al.*, 2008). As bunyaviruses lack a matrix protein, it is thought that the arrangement of the Gn-Gc heterodimers is crucial in determining virion morphology (Huiskonen *et al.*, 2009; Overby *et al.*, 2008). BUNV glycoprotein spikes were found to follow a tripodal arrangement (Bowden *et al.*, 2013), while UUKV and RVFV Gn-Gc heterodimers exhibit an ordered icosahedral T=12 symmetry (Freiberg *et al.*, 2008; Overby *et al.*, 2008). Comparatively, hantavirus virions have homotetrameric Gn complexes interconnected with Gc homodimers, creating a square grid-like surface pattern (Hepojoki *et al.*, 2010; Martin *et al.*, 1985) (Figure 1-2 D).

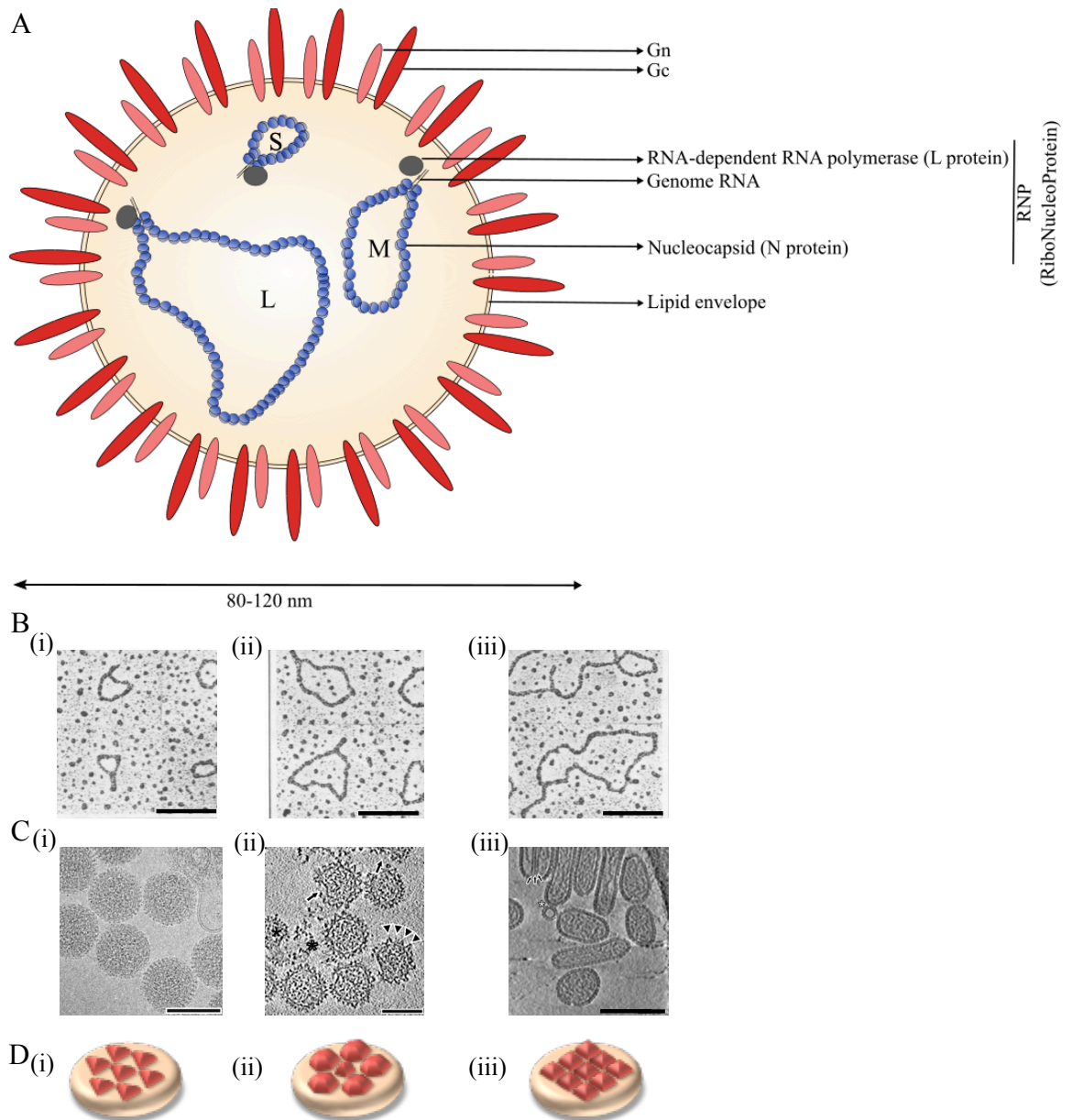


**Figure 1-2. Bunyavirus virion structure.**

(A) Schematic representation of the morphology a bunyavirus virion. Virions are composed of a lipid bilayer embedded by the viral glycoproteins Gn and Gc, which envelopes RNPs composed of the genomic RNA (S, M or L segments) encapsidated by the nucleocapsid protein in association with the RNA-dependent RNA polymerase. (B) Circular panhandle forms of purified UUKV S (i) M (ii) and L (ii) RNPs are shown. Scale bars represent 0.25 nm. Images were modified from (Hewlett *et al.*, 1977). (C) Morphology of RVFV (i), UUKV (ii), and TULV (iii) virions, visualised by cryo-electron microscopy. Scale bars represent 100 nm. Images modified from (Huiskenon *et al.*, 2010; 2009; Overby *et al.*, 2008). (D) Schematic representation of the surface arrangement of Gn and Gc spikes in virions of the *Orthobunyavirus* (i), *Phlebovirus* (ii) and *Hantavirus* (iii) genus. The figures were adapted from (Bowden *et al.*, 2013). RNP: Ribonucleoprotein; UUKV: Uukuniemi virus; RVFV: Rift Valley Fever Virus; TULV: Tula virus.

### 1.1.3 *Genome organization and coding strategy*

Bunyaviruses have a segmented single-strand RNA genome of negative- or ambi- sense polarity. The segments are named according to their nucleotide length, namely the S (small), M (medium) and L (large) segments. Each segment is composed of a coding region flanked by viral 3' and 5' untranslated regions (UTRs). The termini of these UTRs are complementary, and it is this complementarity that enables their self-annealing and results in the formation of the characteristic panhandle-like structure that gives a circular conformation to viral RNPs. These regions have also recently been shown to be important for binding of the RdRp to form the RNPs (Gerlach *et al.*, 2015). RNA secondary structures within the viral UTRs function as *cis*-acting elements to drive transcription and replication of the viral genome (Dunn *et al.*, 1995; Elliott and Blakqori, 2011; Lowen and Elliott, 2005). Importantly, for phleboviruses, the 3' and 5' UTR of all three genome termini contain eight nucleotides that are conserved across most phleboviruses (3'-ACACAAAG...CUUUGUGU-5') (Elliott and Blakqori, 2011).

The genome segments encode four structural proteins: the S segment encodes the nucleocapsid protein (N), the M segment encodes the glycoprotein precursor, which is co-translationally cleaved to generate the glycoproteins (Gn and Gc), and the L segment encodes the viral RdRp (L). In addition, non-structural proteins are encoded by the S segment of most orthobunyaviruses, phleboviruses and tospoviruses (named NSs), and by the M segment of orthobunyaviruses, tospoviruses and some phleboviruses (named NSm) (Bouloy, 2011). The coding capacity of representative viruses from each of the genera is depicted in Figure 1-3.

The M and L segments of phleboviruses are of negative-sense (genomic) polarity, which means that following virus infection, the genomic RNA (gRNA) serves as a template for transcription of positive-sense mRNA for the translation of the glycoprotein precursor or the L protein. In addition, gRNA can be replicated into anti-genomic RNA (agRNA), which can serve as a template for the generation of more gRNA copies (Figure 1-4 A). Their S segment, however, utilizes an ambi-sense coding strategy to encode N in the negative-sense and NSs in the positive-sense from separate sub-genomic mRNAs. Specifically, N is translated from subgenomic mRNA transcribed from the genomic-sense RNA, whereas NSs is translated from subgenomic mRNA transcribed from agRNA (Figure 1-4 B) (Bouloy and Weber, 2010). The ambi-sense nature of phlebovirus S segments has implications in the temporal expression of N and NSs proteins. Because NSs

mRNA is generated from agRNA, the transcription of NSs mRNA occurs only after replication of the viral gRNA into agRNA (Figure 1-4 B). In fact, studies using pulse-chase analysis have shown that the N protein of UUKV is synthesized as early as 4 h p.i., whereas NSs is only synthesized at 8 h p.i. (Simons *et al.*, 1992). Tospovirus M and S segments also employ an ambi-sense coding strategy, where the Gn-Gc and NSm open reading frames (ORFs) or N and NSs ORFs (respectively) have opposite polarities. In contrast, most members of the *Orthobunyavirus* genus do not utilize an ambi-sense coding strategy, but can encode NSs in an overlapping reading frame with the N sequence, thus both proteins can be translated from the same mRNA transcript (Figure 1-3) (Elliott and Schmaljohn, 2013).

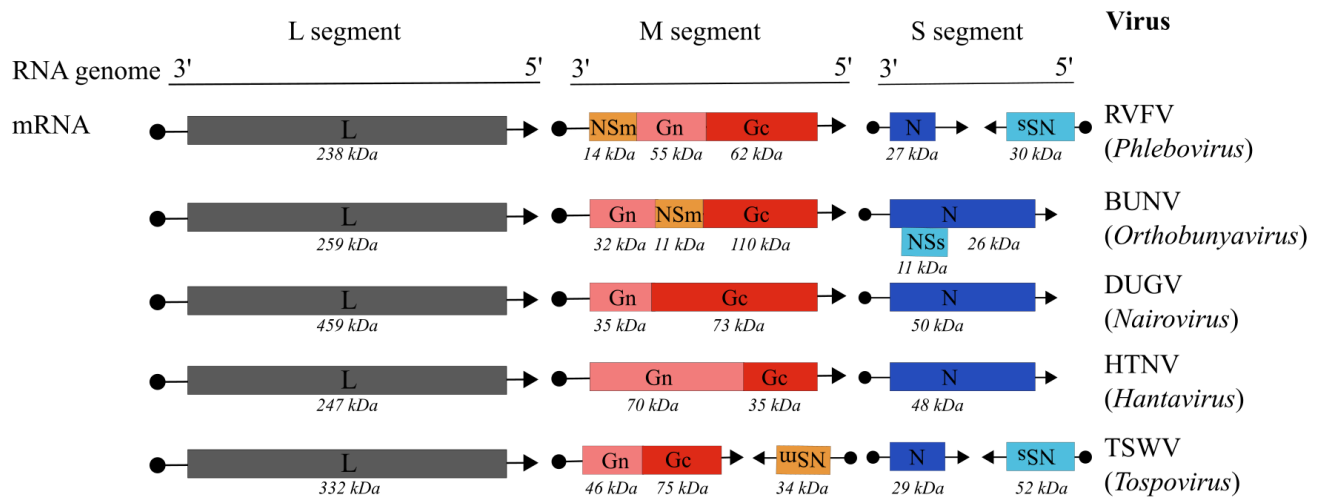


**Figure 1-3. Coding capacity of the *Bunyaviridae*.**

Schematic representation of the coding capacity for all *Bunyaviridae* genera in comparison to the *Phlebovirus* genus, represented by RVFV. BUNV, DUGV, HTNV and TSWV genomes are depicted, representing the *Orthobunyavirus*, *Nairovirus*, *Hantavirus* and *Tospovirus* genera, respectively. The viral RNA segment is shown as a naked line with the 3' and 5' termini shown. The viral mRNA is shown with a host-derived 5' terminal cap (•) and an arrow (→) representing the orientation of transcription elongation (5' to 3'). Note that the length of the genomes are not represented to scale, genome lengths vary between genera. The molecular weight of the encoded proteins is shown below the mRNA. RVFV: Rift Valley Fever Virus; BUNV: Bunyamwera virus; DUGV: Dugbe virus; HTNV: Hantaan virus; TSWV: Tomato spotted wilt virus. Figure adapted from (Elliott and Schmaljohn, 2013).

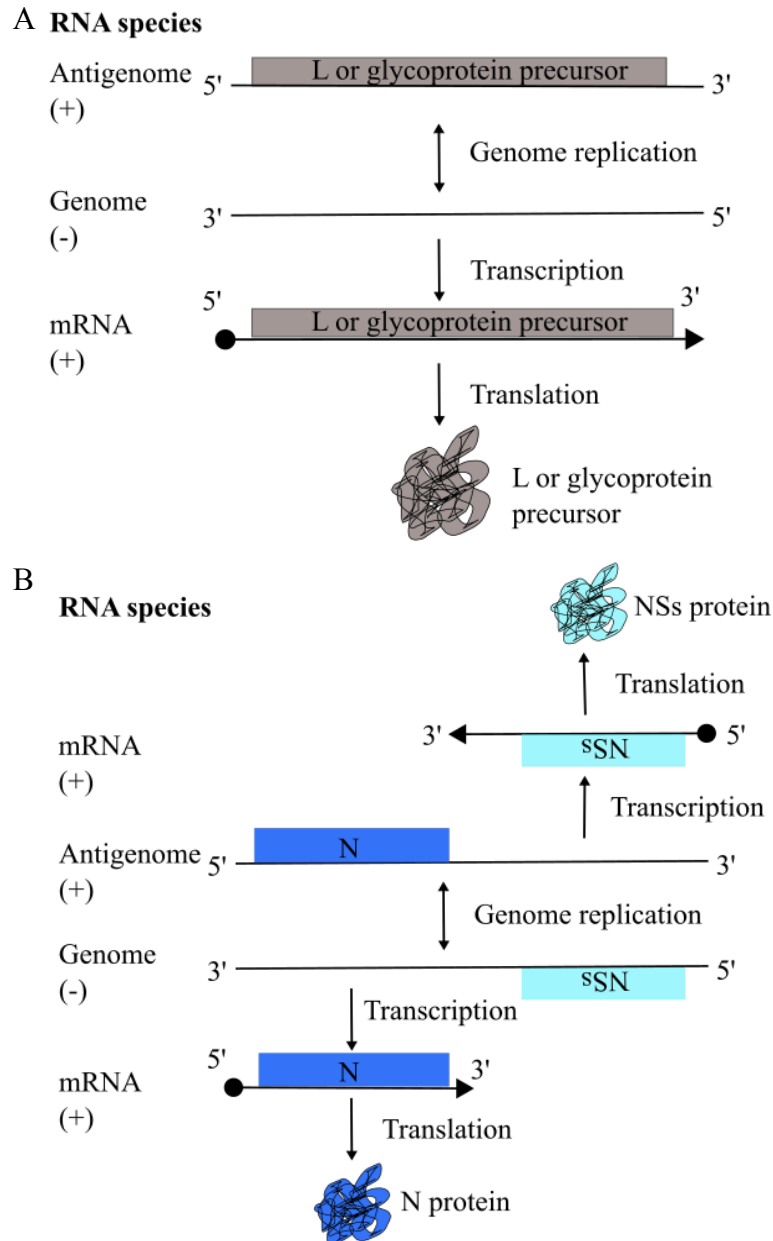


**Figure 1-4. Negative- and ambi-sense coding strategies employed by phleboviruses.**

Transcription and replication strategies employed by phleboviruses for negative- (A) or ambi-sense (B) segments are shown. In negative-sense genomes (such as M or L segments of phleboviruses), subgenomic mRNA is transcribed directly from the viral genome, which also serves as a template for genome replication and the generation of the positive-sense replication intermediate (antigenome). In genomes with an ambisense coding strategy, subgenomic mRNA can also be transcribed after genome replication using the anti-genomic replication intermediate as a template. Only ORFs in the positive sense are shown. The viral genomic or antigenomic-sense RNA segments are shown as a naked line with the 3' and 5' termini. Viral mRNA is shown with a host-derived 5' terminal cap (•) and an arrow (→) representing the orientation of transcription elongation (5' to 3'). Illustration modified from (Elliott and Brennan, 2014).

### 1.1.4 *Gene products and their function*

#### *(i) Nucleocapsid (N) protein*

The N protein is encoded in the genomic-sense S segment RNA of bunyaviruses and plays an indispensable role in the viral life cycle. Following infection of a host cell, N is the most abundant protein expressed by the virus. This is presumably because of its primary function, which entails protecting the viral genome from degradation and tightly binding to viral RNA for the formation of RNPs along with the viral polymerase (L) (Bouloy, 2011). The N protein also plays a major role in the replication and transcription of viral RNA by the viral polymerase, and in packaging of the genome into virions (Elliott and Schmaljohn, 2013). Given that bunyaviruses replicate exclusively in the cytoplasm, it is not surprising that the N protein of bunyaviruses is localized to the cytoplasm, which was demonstrated for UUKV, SFTSV and RVFV (Brennan *et al.*, 2015; 2011a; Katz *et al.*, 2010). Although between genera the homology of the N protein is minimal, the function of this protein to encapsidate the viral genome is conserved.

Initial structural studies showed that UUKV and RVFV N proteins formed dimers and higher oligomers through aromatic residues at the N terminus of the protein (Katz *et al.*, 2010; Le May *et al.*, 2005). The availability of a crystal structure for RVFV and TOSV N proteins provided structural insights into the RNA encapsidation mechanism of phleboviruses. Initially it was shown that an RNA-free form of RVFV N was composed of a dimer in which the amino-terminal “arm” domain of RVFV N was folded into a predicted RNA-binding pocket of the C-terminal globular domain (Raymond *et al.*, 2010). Further studies showed that in the presence of RNA, TOSV and RVFV N proteins form ring-shaped hexameric conformations stabilised by the N-terminal arm, which was bound to a hydrophobic pocket of the globular C-terminal domain of an adjacent subunit through inter-molecular interactions (Figure 1-5) (Ferron *et al.*, 2011; Olal *et al.*, 2014). A number of positively charged residues located in a deep groove formed by the hexameric structures were shown to enable the binding of a single RNA molecule in a sequence-independent manner, with six RNA bases binding to each monomer (and thus a total of 36 RNA bases per hexamer) (Ferron *et al.*, 2011; Olal *et al.*, 2014; Raymond *et al.*, 2012). Additionally, RNA binding to TOSV N was shown to induce an inter-subunit rotation which enabled the transition from a hexameric form to a helical RNP-like assembly through the opening up the RNA-binding tunnel (Figure 1-5 B)(Olal *et al.*, 2014).

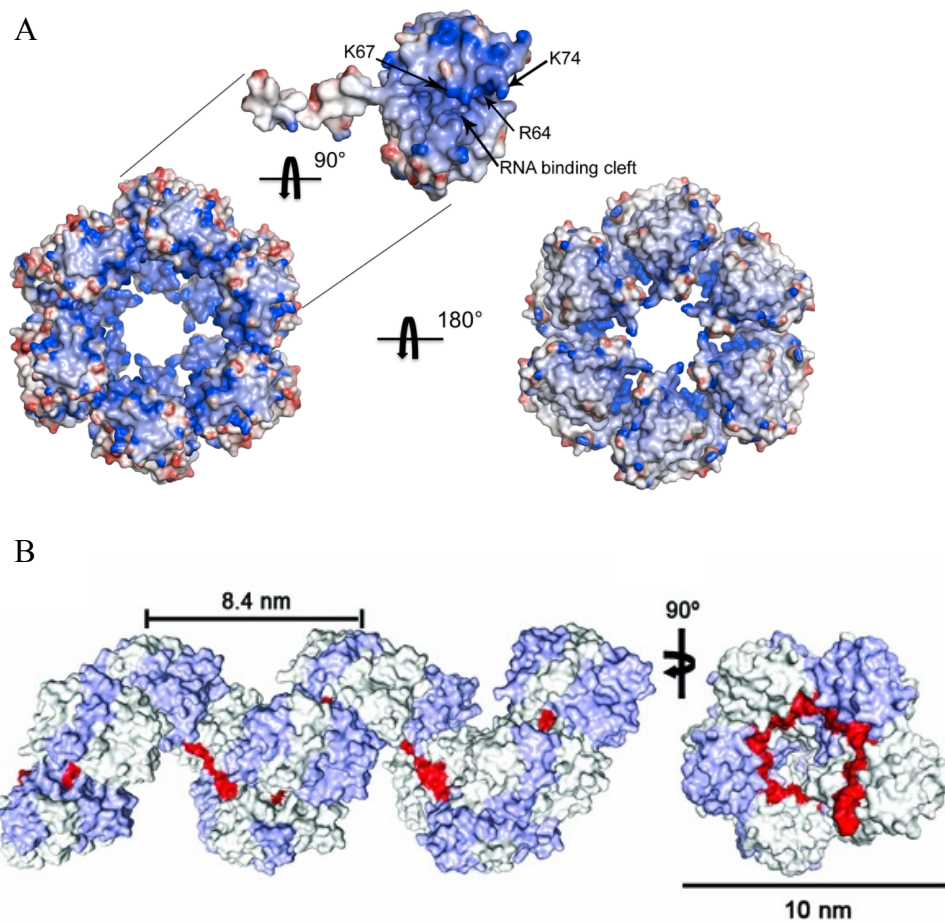


**Figure 1-5. Crystal structures of RVFV and TOSV N.**

The electrostatic surface potential of RVFV and TOSV N hexamers is shown. (A) A patch of positively charged residues (blue) is observed in the inner part of the hexameric ring for RVFV N. (B) The positively charged RNA binding groove for TOSV N is depicted in red in both the model of a left-handed helical RNP (left) and in the hexameric ring viewed from the top (right). RVFV: Rift Valley Fever Virus; TOSV: Toscana Virus; RNP: Ribonucleoprotein. Images taken from (Ferron *et al.*, 2011; Olal *et al.*, 2014).

**(ii) Viral RNA-dependent RNA polymerase (L)**

The L protein of bunyaviruses functions as the viral RdRp, and derives its name because it is the largest encoded protein by the bunyavirus genome (Figure 1-3). The L protein plays an essential role in the virus life cycle, as it is responsible for catalyzing viral RNA synthesis in both, transcription and replication processes (H. Jin and Elliott, 1993a; 1991). While the molecular weight of phlebovirus, hantavirus and orthobunyavirus L proteins is about 250 kDa, tospoviruses encode L proteins of approximately 330 kDa, while nairoviruses encode L proteins of approximately 460 kDa (Figure 1-3). Although little homology is found in the amino acid sequence of L proteins between genera, four main domains that are known as the ‘polymerase module’, were found to be conserved (Aquino *et al.*, 2003; H. Jin and Elliott, 1991; Müller *et al.*, 1994). These domains are also common in RdRps of other positive, negative and double strand RNA viruses (Poch *et al.*, 1989).

Jin and Elliott first identified the ability of the L protein to catalyze viral RNA synthesis in 1991, using a recombinant vaccinia virus expression system for BUNV L (H. Jin and Elliott, 1991). This was followed by the discovery of host-cell derived, capped sequences at the 5’ ends of DUGV viral mRNA transcripts, which suggested that the L protein had, in addition, an endonuclease activity (H. Jin and Elliott, 1993b). A PD-(D/E)XK motif identified in the N-terminus of LACV (and also present in the Influenza virus polymerase) is conserved amongst all *Bunyaviridae*, and was shown to be important for LACV L endonuclease activity *in vitro* (Reguera *et al.*, 2010). It is now known that endonuclease activity of the RdRp is responsible for an important step in the viral life cycle, termed ‘cap-snatching’. Cap-snatching is utilised by the RdRp of many negative sense RNA viruses to cleave 5’ caps of about 10-18 nucleotides in length from host cell pre-mRNAs, in order to prime transcription of the viral genome and the synthesis of 5’ capped, translatable viral mRNAs (Bishop *et al.*, 1983; Bouloy *et al.*, 1990; Kormelink *et al.*, 1992; Simons and Pettersson, 1991).

In terms of subcellular localization, the L protein of a number of bunyaviruses has been shown to be cytoplasmic (Di Bonito *et al.*, 1999; Kukkonen *et al.*, 2004). The generation of recombinant BUNV and RVFV with a V5-tagged L protein showed that in infected cells, N and L proteins co-localise in the cytoplasm forming so-called ‘viral factory’ structures, which are thought to be the site of viral replication (Brennan *et al.*, 2011a; Shi and Elliott, 2009).

### ***(iii) Glycoproteins (Gn and Gc)***

The viral glycoproteins Gn and Gc are encoded by the genomic M segment of bunyaviruses, and are translated as a polyprotein precursor from a single mRNA molecule (Figure 1-3). They serve an essential role in attachment, entry, packaging and budding of the virus. As they are exposed on the surface of the virion, the glycoproteins are recognized by the immune system and elicit the production of neutralising antibodies against glycoprotein epitopes (Bouloy, 2011).

Processing of the polyprotein precursor, which is co-translationally cleaved by host cell proteases, is crucial for viral attachment, as well as virion maturation and budding (Elliott and Schmaljohn, 2013; Shi *et al.*, 2016). The mature Gn and Gc proteins are both type I integral transmembrane proteins, and are trafficked as heterodimers from the endoplasmic reticulum (ER) to the Golgi compartment, which is the site of virus assembly (Bowden *et al.*, 2013; Persson and Pettersson, 1991; Shi *et al.*, 2016; 2005). Viral attachment is thought to occur via an interaction between oligomannose-type glycans present on virion glycoproteins and a tetrameric C-type lectin, called DC-SIGN (DC [Dendritic Cell] specific ICAM [intracellular adhesion molecule]-3 grabbing non-integrin) (Hofmann *et al.*, 2013; Lozach *et al.*, 2011). A glycome analysis of the UUKV virion revealed differential processing of Gn and Gc, with both proteins displaying poly-*N*-acetylactosamines, consistent with the assembly of virions in the medial Golgi complex. However, oligomannose-type glycans required for DC-SIGN cellular attachment were predominant in UUKV Gc (Crispin *et al.*, 2014). N-linked glycans have also been shown to support RVFV infection via DC-SIGN (Phoenix *et al.*, 2016). In addition, N-linked glycosylation of bunyavirus glycoproteins has been shown to play a pivotal role in protein folding and intracellular packaging (Shi *et al.*, 2005; Shi and Elliott, 2004). The importance of glycosylation is illustrated by failure to rescue BUNV lacking a N-terminal Gn N-glycosylation site, which was shown to result in protein misfolding the inability to traffic both Gn and Gc to the Golgi complex (Shi and Elliott, 2004).

The crystal structure of RVFV Gc revealed a class II fusion protein architecture, similar to those found in flaviviruses and alphaviruses and enabled to identify Gc as the membrane anchor that acts as the effector of the fusion between the virus and host cell endosomal membranes (Dessau and Modis, 2013), a hypothesis previously suggested for BUNV, LACV and HTNV (Ogino *et al.*, 2004; Plassmeyer *et al.*, 2005; Shi *et al.*, 2009). Additionally, the crystal structure of the ectodomain of SFTSV Gc identified Histidine

residues that are important in triggering a pH-dependent conformational change required to facilitate fusion of viral and endosomal membranes (Halldorsson *et al.*, 2016).

Virus-like particle studies on UUKV and BUNV suggested that the cytoplasmic tails of UUKV Gn and BUNV Gn and Gc had a critical role in genome packaging into the virus envelope (by a close interaction with viral RNPs), whereas the cytoplasmic tail of UUKV Gc was found to be important for particle generation and budding (Overby *et al.*, 2007; Shi *et al.*, 2007).

#### ***(iv) Non-structural protein NSm***

The M segment of some bunyaviruses encodes an accessory non-structural protein, named 'NSm'. The precise role of this non-essential protein is not well-defined. BUNV NSm is co-translationally cleaved from the polyprotein precursor along with Gn and Gc, localises to the Golgi, and its N terminus is involved in virus assembly and morphogenesis (Nakitare and Elliott, 1993; Shi *et al.*, 2006). The NSm protein of RVFV has been suggested to suppress virus-induced apoptosis by inhibiting the activation of cellular caspase-8, which plays an important role in the initiation of the mitochondrial pathway to apoptosis (Won *et al.*, 2007).

While within the *Phlebovirus* genus the M segment of viruses transmitted by dipterans encode a NSm protein, the M segment of those transmitted by ticks do not (Bouloy, 2011; Elliott and Brennan, 2014). The coding sequence of the NSm protein of dipteran-borne phleboviruses is located in the pre-Gn region of the polyprotein precursor, at the N terminus. Interestingly, while some viruses such as PTV and TOSV encode a unique NSm protein of 30 kDa (Di Bonito *et al.*, 1999; Ihara *et al.*, 1985), the glycoprotein precursor of RVFV can generate two NSm proteins: a 78 kDa NSm protein, also known as p78, and a 14 kDa NSm protein termed NSm (Bouloy, 2011). The two RVFV NSm proteins are generated by alternative usage of in-frame AUG codons present in the precursor: while p78 synthesis is initiated by the use of the first AUG, the second AUG is utilised for synthesis of the smaller NSm (Figure 1-6). The larger, p78 protein can be regarded as an NSm protein that remains fused to Gn, as the N terminus of Gn is not cleaved at its signal peptide (Figure 1-6) (Suzich *et al.*, 1990). NSm has been attributed a number of roles in the replication of RVFV in mosquitoes. For instance, a study has shown that RVFV NSm is important for allowing the virus to cross the mosquito mid-gut barrier, and the replication of recombinant RVFV lacking NSm was attenuated in mosquitoes (Crabtree *et al.*, 2012;

Kading *et al.*, 2014). Additionally, the p78 version of RVFV NSm appears to act as a major determinant of virus dissemination in infected mosquitoes (Kreher *et al.*, 2014).

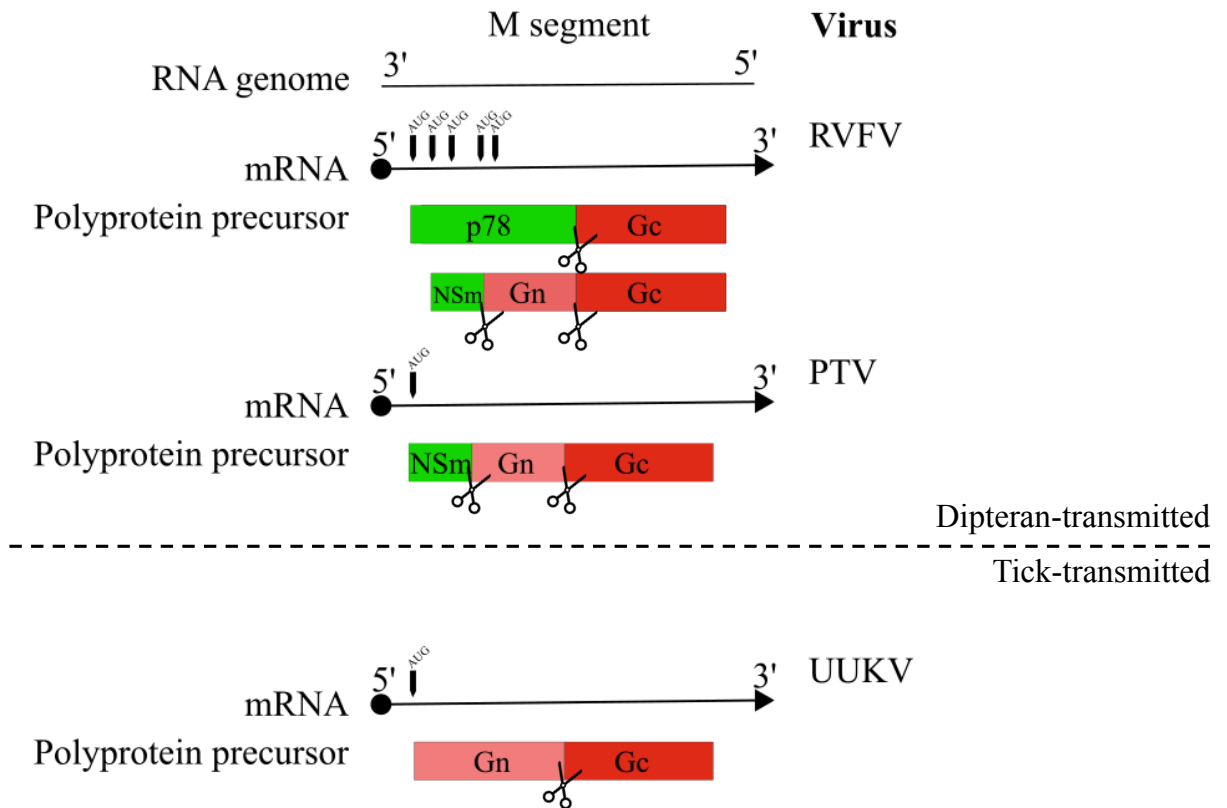


**Figure 1-6. Polyprotein precursor synthesis and processing of phleboviruses.**

Schematic representation of polyprotein precursor synthesis and processing, encoded by the genomic M segment of mosquito-borne Rift Valley fever virus (RVFV) and Punta Toro virus (PTV), and tick-borne Uukuniemi virus (UUKV). The viral mRNA is shown with a host-derived 5' terminal cap (•) and an arrow (→) representing the orientation of transcription (5' to 3'). AUG codons are shown on the mRNAs. The signal peptidase cleavage sites are represented by a scissor. This figure was adapted from (Bouloy, 2011). RVFV: Rift Valley fever virus; PTV: Punta Toro virus; UUKV: Uukuniemi virus.

**(v) Non-structural protein NSs**

The non-structural protein NSs is encoded in the S segment of some bunyaviruses, and although the NSs protein shares little homology within and between genera, the major function of NSs as an antagonist of the interferon (IFN) system appears to be conserved (Elliott and Blakqori, 2012; Wuerth and Weber, 2016). The NSs protein of a number of orthobunyaviruses (BUNV, SBV, LACV, OROV) has been shown to be a non-essential gene product that acts as an IFN antagonist (Blakqori and Weber, 2005; Elliott *et al.*, 2013; Tilston-Lunel *et al.*, 2016; Varela *et al.*, 2013; Weber *et al.*, 2002). While the generation of recombinant BUNV, SBV and OROV viruses lacking NSs demonstrated some attenuation of replication kinetics compared to wild-type viruses in IFN incompetent cells, this was not the case for LACV (Blakqori and Weber, 2005; Elliott *et al.*, 2013; Tilston-Lunel *et al.*, 2016; Weber *et al.*, 2002). These observations suggest that perhaps the NSs proteins of BUNV, SBV and OROV but not LACV play a non-essential role in facilitating virus replication. NSs proteins have also been identified for Tula and Puumala viruses within the *Hantavirus* genus, and were reported to act as antagonists of IFN induction (Jääskeläinen *et al.*, 2007). Recently, a NSs protein was also identified in the S segment of Crimean Congo haemorrhagic fever virus (CCHFV), which disrupts the mitochondrial membrane potential and induces apoptosis (Barnwal *et al.*, 2016). Within the *Tospovirus* genus, the NSs protein of TSWV acts as a suppressor of the RNAi pathway in plant cells and is also implicated in persistent infection and transmission by thrips (Margaria *et al.*, 2014; Oliveira *et al.*, 2011). Phleboviral NSs proteins characterised as IFN antagonists include those belonging to RVFV, TOSV, PTV and SFTSV (Billecocq *et al.*, 2004; Chaudhary *et al.*, 2015; Gori-Savellini *et al.*, 2010; Lihoradova *et al.*, 2013; Ning *et al.*, 2015; Perrone *et al.*, 2007; Santiago *et al.*, 2014).

The NSs protein of BUNV and RVFV were shown to inhibit host cell mRNA transcription, which is facilitated by their nuclear localization (Billecocq *et al.*, 2004; Leonard *et al.*, 2006; van Knippenberg and Elliott, 2015). BUNV NSs was shown to interact with MED8, a component of the Mediator complex that regulates RNA polymerase II-mediated transcription, in order to suppress host cell mRNA transcription as a strategy to inhibit the IFN response (Leonard *et al.*, 2006; Thomas *et al.*, 2004). Specifically, this interaction was shown to result in the ultimate shut off of host cell protein synthesis by the inhibiting the phosphorylation of the C-terminal domain of RNA polymerase II, which is known to regulate its activity (Leonard *et al.*, 2006). Initially, it was believed that the broad inhibition of host cell mRNA transcription of RVFV NSs was also a strategy to inhibit the

IFN response, by blocking the transcription of IFN-related genes (Billecocq *et al.*, 2004). The mechanism by which RVFV NSs blocks host cell mRNA transcription was demonstrated to be by inhibiting the assembly of the basal transcription factor IIIH (TFIIH). Briefly, RVFV NSs was shown to sequester the p44 subunit of TFIIH within characteristic nuclear filaments formed by RVFV NSs, therefore preventing its interaction with the XPD subunit of TFIIH (natural partner of the p44 subunit) and thus inhibiting the helicase activity of XPD (Le May *et al.*, 2004). Additionally, RVFV NSs was shown to halt host cell transcription by promoting the proteasomal degradation of the TFIIH p62 subunit at early stages of infection through a  $\Omega$ XaV motif ( $\Omega$ : aromatic, 266 X: any, a: acidic, V: valine), found at the C-terminal region of RVFV NSs (Cyr *et al.*, 2015; Kalveram *et al.*, 2011). Recently, the RVFV NSs-driven proteasomal degradation of p62 was demonstrated to occur by an interaction of RVFV NSs with the F-box protein FBXO3 (Kainulainen *et al.*, 2014; Le May *et al.*, 2004), a subunit of E3 ubiquitin ligases, which mediate ubiquitination for rapid degradation by the proteasome. It was later shown that RVFV NSs is capable of suppressing IFN- $\beta$  mRNA synthesis specifically, using a separate mechanism to that utilized to suppress general host cellular transcription (Le May *et al.*, 2008). Details about the molecular mechanism of RVFV NSs to inhibit the induction of IFN- $\beta$  mRNA synthesis are described in Section 1.4.4. The general host cell transcription suppression by RVFV NSs likely induces an unfavourable environment for viral replication within host cells. However, RVFV NSs was shown to also alter the unfavourable environment to support virus replication by promoting the post-transcriptional proteasome-dependent down-regulation of the double-stranded RNA-dependent protein kinase (PKR), which prevents the inhibition of translation (Ikegami *et al.*, 2009a; 2009b). Because this function is a strategy utilized as a countermeasure of the IFN response, further details regarding the RVFV NSs-induced proteasomal degradation of PKR (and the IFN antagonist activity of other phlebovirus NSs proteins) are discussed in Section 1.4.4.

In addition to antagonizing the innate immune system, the NSs protein of BUNV, LACV and SFTSV inhibit minigenome activity (described in Section 1.2.2) in a dose-dependent manner and have been suggested to regulate the activity of the RdRp L (Blakqori *et al.*, 2003; Brennan *et al.*, 2015; Weber *et al.*, 2001). A similar effect by RVFV NSs on the RVFV S segment-based minigenome was reported (Brennan *et al.*, 2011a). However, contrasting data showing that RVFV NSs promotes viral replication and transcription in minigenome systems derived from all viral segments were also shown (Ikegami *et al.*, 2005a).

### 1.1.5 Replication cycle

#### (i) Attachment and entry

Bunyaviruses utilise similar mechanisms to other enveloped viruses to enter host cells. As discussed earlier, the glycoproteins Gn and Gc are exposed on the surface of virions and their glycosylation patterns have been shown to play a role in virus entry (Hofmann *et al.*, 2013; Lozach *et al.*, 2011) (Ludwig *et al.*, 1991; Phoenix *et al.*, 2016). Interactions between the viral glycoproteins and cellular receptors mediate host cell attachment (Step 1; Figure 1-7), and will determine the tropism of the virus (Elliott and Schmaljohn, 2013). Recent progress has been made to characterize receptors and cellular factors utilised by bunyaviruses to enter host cells. It is not surprising that the receptors utilised for attachment by hantaviruses (which are transmitted by aerosols) are different to those employed by viruses belonging to the other genera, which are transmitted through arthropod bites (Albornoz *et al.*, 2016). Upon inhalation, hantaviruses encounter the epithelium of the lung, and infection of the capillary network endothelial cells tightly attached to epithelial cells results in capillary permeability and vascular leakage, causing haemorrhagic fever in infected patients. So far, receptors such as integrins  $\beta_1$ ,  $\beta_2$ , and  $\beta_3$  (Gavrilovskaya *et al.*, 1999; 1998; Matthys *et al.*, 2010; Raftery *et al.*, 2014), as well as Decay Accelerating Factor (DAF)/C55 and gC1QR/p32 (Choi *et al.*, 2008; Krautkrämer and Zeier, 2008) have been documented for hantavirus attachment to endothelial and epithelial cells. In contrast, arthropod-borne bunyaviruses enter the skin dermis of mammalian hosts via the bite of an infected arthropod and encounter dermal macrophages and dendritic cells at the site of infection (Léger and Lozach, 2015). DC-SIGN, highly expressed on dermal dendritic cells, has been shown to promote attachment and entry of the orthobunyavirus Germiston virus (Lozach *et al.*, 2011), the nairovirus CCHFV (Suda *et al.*, 2016), and phleboviruses SFTSV, UUKV, TOSV, PTV, and RVFV (Hofmann *et al.*, 2013; Lozach *et al.*, 2011). As well as DC-sign, phleboviruses UUKV, TOSV and RVFV have been shown to exploit another C-type lectin expressed in liver endothelial cells, Liver-Specific Intercellular adhesion molecule-3-Grabbing Non-integrin (L-SIGN), as an attachment receptor (Léger *et al.*, 2016).

Heparan sulfate is ubiquitously expressed in virtually all mammalian tissues and is known to be a polysaccharide that serves as a non-specific first docking site for many viruses through low affinity electrostatic interactions, in comparison to the more specific and multivalent virus-receptor interactions (Albornoz *et al.*, 2016). So far, heparan sulfate has

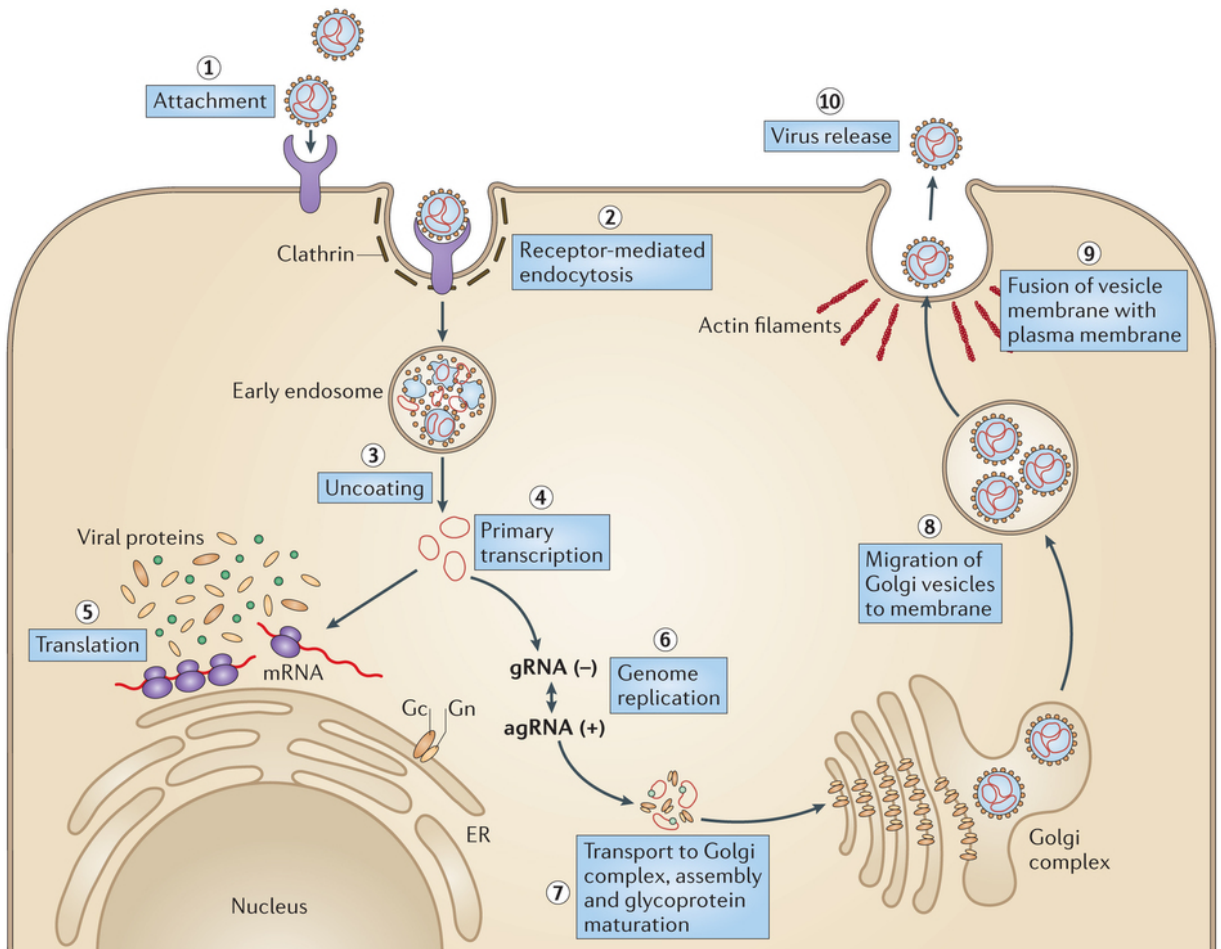
been shown to promote infection of phleboviruses RVFV and TOSV (de Boer *et al.*, 2012a; Pietrantoni *et al.*, 2015), however its role in attachment for other bunyaviruses remains to be determined.

Following attachment, bunyaviruses rely on endocytic processes for their uptake into the host cell (Step 2 in Figure 1-7). While studies with orthobunyaviruses OROV and LACV (Hollidge *et al.*, 2012; Santos *et al.*, 2008), hantavirus HTNV (Jin *et al.*, 2002) andairovirus CCHFV (Simon *et al.*, 2009) have suggested that virion internalization likely occurs through clathrin-mediated endocytosis, UUKV internalization was shown to be mainly clathrin-independent (Lozach *et al.*, 2010). Upon internalization, virions must be released from vesicles in order to allow viruses to access the host cell machinery. Lozach *et al.* utilized UUKV as a model bunyavirus, to show that endocytosed virions are sorted into vesicles, which are trafficked through the host cell endocytic machinery from Rab5a+ early endosomes (pH~6.5) to Rab7a+ late endosomes (pH ~5.5–5.0) (Lozach *et al.*, 2010). Acidification of late endosomes occurred 20-40 min after internalization, and triggered fusion of the viral and endosomal membranes, consequently enabling the release of RNPs into the host cell cytoplasm for transcription and replication (Step 3 in Figure 1-7).

As mentioned in section 1.1.3, fusion of viral and host cell endosomal membranes is mediated by bunyavirus glycoproteins, which also function as fusion proteins. Early studies on UUKV showed a pH-dependent conformation in UUKV glycoproteins (Overby *et al.*, 2008). Acid-activated structural reorganization of the RVFV Gc fusion protein was also observed, and was suggested to be triggered by protonation of conserved histidine residues (de Boer *et al.*, 2012b). Similar histidine residues identified in the structure of SFTSV Gc were also found to be important in the pH-dependent conformational change of Gc (Halldorsson *et al.*, 2016). Thus, it is thought that acidification of endosomes triggers a conformational change in pre-fusion glycoproteins, which facilitates the fusion of the viral and endosomal membranes.

### ***(ii) Primary transcription and translation***

For negative-strand RNA viruses, the classical view is that following virus infection, the genomic RNA is transcribed into mRNA by the incoming viral polymerase or transcriptase (Elliott and Schmaljohn, 2013). However, unlike other negative-strand RNA viruses such as influenza, which replicate in the cell nucleus, the site of RNA synthesis for bunyaviruses is localised to the cytoplasm (Elliott and Schmaljohn, 2013; Rossier *et al.*, 1986).



Nature Reviews | Microbiology

**Figure 1-7. Life cycle of bunyaviruses.**

Schematic representation of the stages of the bunyavirus life cycle. 1. Attachment is mediated via the interaction of cell surface proteins and viral glycoproteins. 2. Internalization of the viruses occurs via endocytosis, which can be clathrin-dependent or independent. 3. Acidification of the endosomes results in fusion of the endosomal and virion membranes, leading to virion uncoating. 4. Primary transcription of viral mRNAs from genomic RNA occurs, which enabled the translation of viral proteins (5). 6. The translated viral proteins replicate the viral genome to generate positive-sense antigenome intermediates, which can serve for the replication and generation of more progeny negative-sense viral genome. Ribonucleoprotein (RNPs) are transported to the Golgi complex (7), the site of viral glycoprotein maturation. Virus particles bud into Golgi membrane-derived vesicles, which migrate to the cell surface (8). Fusion of the Golgi-derived vesicle and the plasma membrane (9) results in the release of infectious virions (10). Illustration modified from (Elliott, 2014).

The first event following release of viral RNPs to the cytoplasm is primary transcription from genomic RNA (Step 4 in Figure 1-7). Primary transcription involves cap-snatching of 10-18 nucleotide long caps from host cell pre-mRNAs by the endonuclease domain of the L protein (Bishop *et al.*, 1983; Bouloy *et al.*, 1990; Kormelink *et al.*, 1992; Simons and Pettersson, 1991) (Patterson *et al.*, 1984). The 5' 7-methylguanosine cap cleaved from the host cell pre-mRNAs is transferred to the 5' end of the viral transcript by the L protein, and this allows the generation of mRNA that can be recognized by host cell ribosomes (Figure 1-8).

Minigenome assays have shown that naked RNA alone cannot act as a template for transcription, but both N and L are necessary for transcription to occur (Dunn *et al.*, 1995; Elliott and Blakqori, 2011; Lopez *et al.*, 1995; Lowen and Elliott, 2005). Additionally, the viral UTRs enable binding of the L protein to the RNPs (Gerlach *et al.*, 2015). Base pairing of complementary viral UTRs and their secondary structures have been shown to determine promoter strength by acting as *cis*-acting elements to drive RNA synthesis (Dunn *et al.*, 1995; Elliott and Blakqori, 2011; R. Flick *et al.*, 2002; Lowen and Elliott, 2005).

While viral mRNA transcripts are not polyadenylated at their 3' ends, the mRNAs have been shown to be shorter than their respective genome template, suggesting that transcription termination signal sequences are present within the genome (Barr *et al.*, 2006; Plassmeyer *et al.*, 2005; Vera-Otarola *et al.*, 2010). Although no consensus sequence has been identified as a transcription termination signal for all bunyaviruses, some sequences have been identified for specific viruses (Barr *et al.*, 2006; Ikegami *et al.*, 2007; Vera-Otarola *et al.*, 2010). A conserved sequence motif acting as a transcription termination signal (3'-C<sub>1-3</sub>GUCG/A-5') for the ambisense S segment of phleboviruses RVFV, SFSV and TOSV was found in the intergenic region (Albariño *et al.*, 2007; Ikegami *et al.*, 2007; Lara *et al.*, 2011).

Following primary transcription, translation is initiated on the growing mRNA strands (Step 5 in Figure 1-7, and Figure 1-8). Coupled transcription and translation has been suggested to be obligatory, as otherwise early transcription termination would result in the generation of truncated transcripts (Barr, 2007). Specifically, ribosomes translating nascent mRNAs prevent the interactions of RNA termination signals in the coding region of the viral genome template RNA and the nascent complementary mRNA, which are required for transcription termination. Termination signals found in the viral UTRs however are

active, as these regions are not translated, therefore allowing RNA interactions to occur and stop transcription (Barr, 2007).

### ***(iii) Genome replication***

Primary transcription occurs prior to the replication of the viral genome, as N and L proteins generated from primary transcription and translation are required to encapsidate the RNA replication product for the formation of RNPs. During replication, the viral genome RNA (gRNA) is used as a template to synthesize the exact copy of the viral genomic RNA, in a positive, antigenomic sense (Figure 1-4 A). The antigenomic RNA (agRNA) can then be utilized as a template to generate more progeny gRNA that can either serve as a secondary transcription template or be assembled into virions (Step 6 in Figure 1-7). In the case of genomes that employ ambi-sense coding strategy (such as that of the *Phlebovirus* S segment), agRNA can not only be utilised for replication and the generation of gRNA, but also serves as a template for transcription of subgenomic mRNA encoded in the positive sense in the viral genome (Figure 1-4 B).

Unlike transcription, replication is cap-independent and full-length copies of the template are generated. The nascent antigenome transcript is encapsidated by N, which prevents translation (Elliott and Schmaljohn, 2013). Because the viral polymerase is responsible for transcription and replication, the ability to regulate the switch between these two processes is still undefined, yet host and viral factors have been implicated in this regulation. For instance, RVFV NSs has been shown to bind to the p44 subunit of the host cell transcription factor TFIIF (as explained in Section 1.1.4) (Le May *et al.*, 2004). Consequently, impairment of host cell mRNA transcription by RVFV NSs favours cap-independent replication over cap-dependent transcription. In this way, the subsequent impairment of host cell mRNA transcription would favour cap-independent replication over cap-dependent transcription. It must be mentioned that encapsidation by the N protein may also play a role in regulating the switch from transcription to replication, as suggested for other negative-strand RNA viruses (Kolakofsky and Lamb, 2001; Rose and Whitt, 2001).

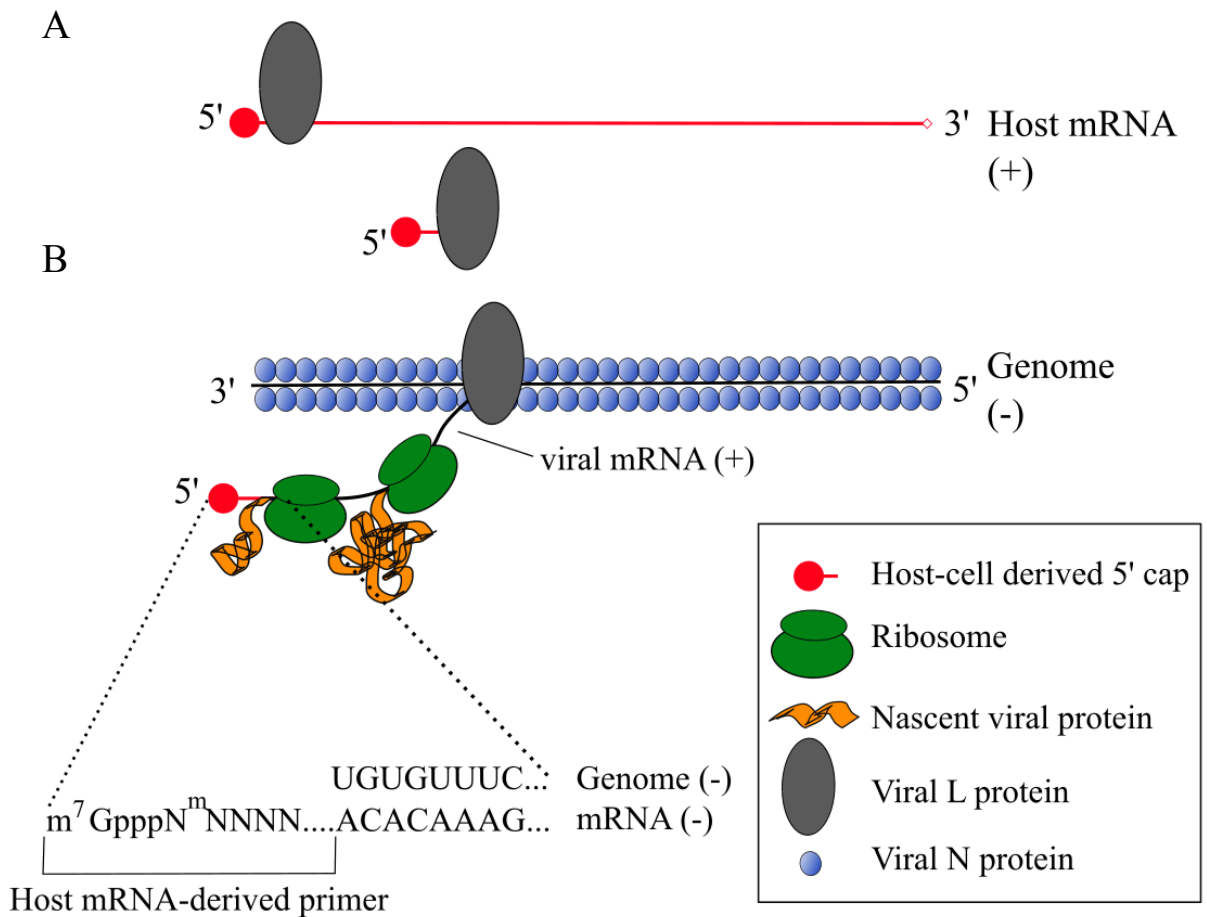


**Figure 1-8. Transcription initiation of viral mRNA and coupled translation.**

(A) The endonuclease activity of the viral L protein enables the cleavage of the host cell pre-mRNA 5' 7-methylguanosine cap. (B) The host-cell derived 5' cap is used to initiate the transcription of viral mRNA transcripts from the viral genome. The 5' cap serves to recruit host cell ribosomes to the nascent mRNA strand, to initiate the translation of viral proteins. Figure adapted from (Mir *et al.*, 2008).

***(iv) Assembly, budding and release***

In order to generate an infectious particle, at least one of each of the genome segments needs to be packaged into a virion. Little is known about genome packaging of bunyaviruses. Minigenome studies of BUNV demonstrated that the UTR regions of BUNV are required for packaging (Kohl *et al.*, 2006). A recent study on RVFV genome packaging has revealed that the majority of mature virions lack one or more genome segments, suggesting that bunyavirus genome packaging is a non-selective process (Wichgers Schreur and Kortekaas, 2016). However, other studies investigating the role of the viral UTRs in co-packaging have indicated that specific intermolecular interactions between the UTRs of the viral segments drive copackaging of the three viral RNA segments to produce infectious RVFV (Terasaki *et al.*, 2011).

EM studies for UUKV and BUNV suggested that bunyaviruses bud from the Golgi apparatus, as viral factories could be visualised at this site within infected cells (Kuismanen *et al.*, 1982; Salanueva *et al.*, 2003). The viral glycoproteins are post-translationally modified by N-linked glycosylation in the ER and are targeted to and accumulate in the Golgi apparatus, where virus assembly takes place (Step 7 in Figure 1-7) (Elliott and Schmaljohn, 2013; Shi *et al.*, 2005; Shi and Elliott, 2004). Studies using UUKV or BUNV virus-like particles suggested RNPs are targeted to glycoprotein-rich regions in the Golgi membrane, where the RNPs closely interact with the cytoplasmic tails of the viral glycoproteins, which promotes budding of Golgi-derived vesicles (Step 8 in Figure 1-7) (Overby *et al.*, 2007; Shi *et al.*, 2007). This is in comparison to other negative-strand RNA viruses that assemble and bud from the plasma membrane, such as influenza viruses. However, RVFV and the hantaviruses Sin Nombre virus (SNV) and Black Creek Canal virus (BCCV) have been shown to bud from both the Golgi and plasma membranes (Anderson and J. F. Smith, 1987; Goldsmith *et al.*, 1995; Ravkov *et al.*, 1997).

Progeny virions derived from the Golgi apparatus are transported to the plasma membrane to be consequently released to the extracellular space via the exocytic pathway (Steps 9 and 10 in Figure 1-7). These steps were visualized by the generation of recombinant BUNV with a Green Fluorescent Protein (GFP) -tagged Gc (Shi *et al.*, 2010).

Finally, the NSs protein of SFTSV has been shown to form unique cytoplasmic structures that are believed to be derived from the endosomal pathway because the structures colocalize with the endosomal marker Rab5 (Santiago *et al.*, 2014). A recent study

suggested that the cytoplasmic structures formed by SFTSV NSs harbour infectious virus, and are secreted to the extracellular space to mediate the receptor-independent endocytosis of SFTSV to neighbouring cells (Silvas *et al.*, 2015).

## **1.2 Reverse genetics of bunyaviruses and its applications**

### ***1.2.1 cDNA-based rescue of bunyaviruses***

Reverse genetics is an approach to investigate the phenotypic effects caused by the modification of a target gene, and thus allows to infer gene functions. Reverse genetics systems for RNA viruses proved to be difficult because they require the conversion of viral RNA into cDNA for the introduction of mutations, due to the instability of the RNA molecule. Until 1996, reverse genetics system of negative strand segmented RNA viruses did not exist, and bunyavirus research was limited to utilising forward genetics as an approach to determine the genetic basis of a virus phenotype. This was mostly carried out by generating and isolating temperature-sensitive virus mutants (Gahmberg, 1984; Pringle, 2011). Although useful, this method to investigate virus phenotype did not allow the targeted alteration and manipulation of the virus genome.

The first non-segmented negative-sense RNA virus recovered entirely from cDNA clones was rabies virus in 1994, where authors showed that recovery of an infectious negative-sense virus required the cDNA copies of the viral genome to be in an antigenomic (positive) sense (Schnell *et al.*, 1994). This was because in order to form RNPs, ‘helper’ expression plasmids encoding protein components of the rabies RNP (nucleocapsid protein, phosphoprotein, and the RdRp) needed to be provided along with cDNA plasmids encoding the cDNA copies of the genomic (negative) sense RNA genome. However, such experimental setup would result in simultaneous transcription of the genomic sense RNA from cDNA copies of the viral genome and antigenomic sense RNA from helper plasmids, leading to RNA-RNA hybridization and interfering with encapsidation of the genomic RNA and thus subsequent transcription and replication.

It was in 1996, that Bridgen and Elliott pioneered the recovery of an infectious bunyavirus (specifically, BUNV) entirely from cDNA clones (Bridgen and Elliott, 1996), which paved the way for the development of reverse genetics systems for other negative strand, segmented RNA viruses such as influenza A virus (Fodor *et al.*, 1999; Neumann *et al.*, 1999). The system was based on that already described for rabies virus (Schnell *et al.*, 1994), and uses transcription plasmids encode cDNA copies of the three viral segments in

the antigenomic sense, under the control of a bacteriophage T7 RNA polymerase (T7 RNAP) promoter. The 3' UTR of the antigenome cDNA is directly followed by a Hepatitis  $\delta$  ribozyme (H $\delta$ r) and a T7 terminator sequence. The function of the H $\delta$ r is to allow self-cleavage of the antigenome transcript to generate the exact 3' end of the viral segment (Figure 1-9 A). Three plasmids (henceforth referred to as 'rescue plasmids') encoding antigenomic cDNA copies of the viral S, M and L RNA segments cDNA clones of the viral segments S, M and L are transfected into cells which were provided T7 RNAP *in trans*, or cells constitutively expressing the T7 RNAP, such as the BSR-T7/5 cell line (Buchholz *et al.*, 1999). Following transfection, the T7 RNAP generates antigenome (positive-sense) RNA transcripts (Bridgen and Elliott, 1996). Helper expression plasmids encoding the viral proteins N and L can be transfected, in order to increase the efficiency of RNP formation following transcription of the T7 RNAP-driven rescue plasmids (Bouloy and R. Flick, 2009; Neumann and Kawaoka, 2004). However, since BUNV was successfully recovered by the transfection of rescue plasmids only, and because transcripts generated by the T7 RNAP are neither capped nor polyadenylated, 'leaky' translation of the antigenome-sense RNA copies of the viral segments must occur that would be enough for the generation of N and L proteins required for RNP formation, replication and transcription (Billecocq *et al.*, 2008). The RNPs can then be assembled and packaged into virions, as it occurs following virus infection of a host cell (Figure 1-9 B). Some T7 RNAP systems utilize rescue plasmids in which the T7 RNAP promoter sequence is immediately followed by a single G residue or two G residues, which was shown to increase the efficiency by which the T7 RNAP utilizes the T7 promoter (Billecocq *et al.*, 2008).

It must be noted that bunyavirus reverse genetic systems driven by the cellular RNA polymerase I (Pol I) have also been demonstrated. This system was initially developed for negative-strand RNA viruses that replicate in the nucleus such as influenza A virus (Fodor *et al.*, 1999; Neumann and Kawaoka, 2004). The use of a Pol I-driven system for the rescue of bunyaviruses can be regarded as disadvantageous, because bunyaviruses replicate exclusively in the cytoplasm. However, a minigenome and virus-like particle system for UUKV (R. Flick and Pettersson, 2001; Överby *et al.*, 2006) and the rescue of RVFV and AKAV (Billecocq *et al.*, 2008; Ogawa *et al.*, 2007) have all been reported to work under the control of Pol I. Importantly, a comparative study of the Pol I- and the T7 RNAP-driven RVFV rescue systems demonstrated that infectious RVFV could only be generated in the absence of helper plasmids expressing N and L using the T7 RNAP system, but not Pol I (Billecocq *et al.*, 2008).

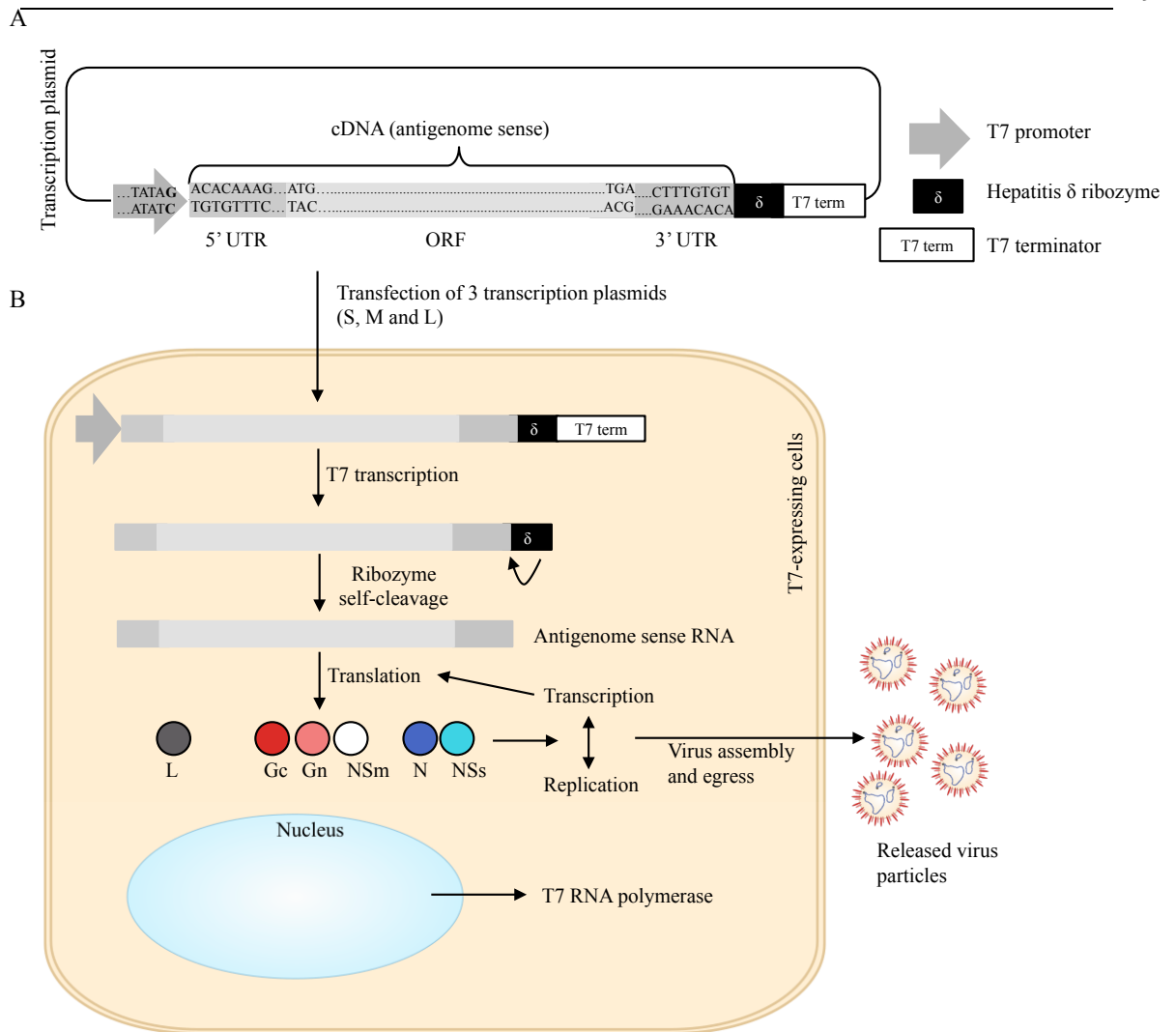


**Figure 1-9. The bunyavirus rescue system.**

(A) Schematic representation of the T7 RNAP-driven transcription plasmids encoding the full-length cDNA of each of the three segments S, M or L, in the antigenomic sense. The plasmid also contains a T7 promoter, Hepatitis  $\delta$  ribozyme and T7 terminator sequences. The G residue in the T7 promoter sequence (shown in bold) increases T7 transcription efficiency. The terminal sequences of genome segments, which are strictly conserved within a genus are shown within the UTR termini (using representative *Phlebovirus* terminal sequences). (B) Three transcription plasmids encoding the full-length S, M and L cDNAs shown in (A) are transfected into T7 RNAP-expressing cells, where transcription and ribozyme self-cleavage occurs. mRNA is produced from antigenome-sense RNA through leaky translation, which allows translation of viral proteins. Production of N and L enables the formation of RNPs, to initiate replication of agRNA to gRNA. gRNA can then be packaged into virions and infectious virus is produced. UTRs: Untranslated regions; T7RNAP: T7 RNA polymerase; RNP: Ribonucleoprotein; agRNA: antigenome RNA; gRNA: genome RNA.

To date, the rescue of a number of bunyaviruses has been reported, such as BUNV (Bridgen and Elliott, 1996), LACV (Blakqori and Weber, 2005), RVFV (Ikegami *et al.*, 2006), AKAV(Ogawa *et al.*, 2007), SBV (Elliott *et al.*, 2013; Varela *et al.*, 2013), SFTSV (Brennan *et al.*, 2015), CCHFV (Bergeron *et al.*, 2015) and OROV (Tilston-Lunel *et al.*, 2016). Intriguingly, no rescue of viruses belonging to the *Hantavirus* or *Tospovirus* genera has been reported. Nevertheless, the rescue of other bunyaviruses entirely from cDNA clones has proven to be an invaluable tool for the field of bunyavirus research. For example, the ability to manipulate the viral genome has allowed the fusion of GFP with BUNV Gc, and enabled the investigation of virus entry, budding and morphological changes in the Golgi complex in real time using live-cell imaging (Shi *et al.*, 2010). Introduction of targeted mutations in the viral genome allowed the investigation of the role of various proteins, such as NSs, in the virus life cycle (Weber *et al.*, 2002). The generation of RVFV encoding a luciferase reporter gene as also been reported (Ikegami *et al.*, 2006). Finally, the remarkable flexibility of bunyavirus genomes has also been demonstrated by the creation of a RVFV with a 2- or 4- segmented genome (Brennan *et al.*, 2011b; Wichgers Schreur *et al.*, 2014), the exchange of BUNV UTR sequences (Lowen *et al.*, 2005), the shortening of BUNV UTR sequences (Mazel-Sanchez and Elliott, 2012), or by the creation of BUNV with an ambisense S segment (van Knippenberg and Elliott, 2015). These examples are only a few that highlight the enormous contribution that the reverse genetics systems of bunyaviruses have provided to fundamental virus research.

### **1.2.2 Minigenome and virus-like particle assays**

While the plasmid-based recovery of infectious virus has allowed the study of virus life cycles in their entirety, minigenomes and virus-like particles provide insights into specific steps of the virus life cycle, without the need to generate infectious virus. These systems also prove to be useful in the study of highly pathogenic viruses, such as CCHFV, outside of high biosafety laboratory conditions. They are based on the expression of the viral N and L proteins, along with a transcription plasmid encoding a reporter gene, flanked by the viral UTRs in the genomic sense. The expressed N and L proteins can encapsidate, replicate and transcribe the negative-sense reporter genes to generate artificial RNPs, utilising the viral UTRs as promoters of replication and transcription. Thus, activity of the reporter gene serves as a measure to assess the functionality of the viral UTRs, as well as the viral protein N and L (Figure 1-10 A). The system has served as a key tool to understand bunyavirus encapsidation (Dong *et al.*, 2013; Eifan and Elliott, 2009), promoter strength (K. Flick *et al.*, 2004; Gaudiard *et al.*, 2006), recognition of viral UTRs by the

polymerase (Mazel-Sanchez and Elliott, 2015), and many other transcriptional and replicative processes.

Including a plasmid expressing the viral glycoprotein precursor in the minigenome assay enables the generation of transcription-competent virus-like particles (VLPs) (Figure 1-10 B), which enables the study of virus maturation, assembly and egress. Following the formation of artificial RNPs, these can be packaged into VLPs using similar processes that occur during virus assembly, through interactions with the cytoplasmic tails of the viral glycoproteins (Overby *et al.*, 2007; Shi *et al.*, 2007). The VLPs can be used to infect naïve cells to deliver the packaged RNPs, which can undergo transcription and replication. A study comparing authentic UUKV virions and UUKV VLPs showed that their morphology is identical (Overby *et al.*, 2008). Since VLPs package the reporter minigenome RNP, and not genome segments encoding essential viral proteins required for virus replication, they can only undergo a single-cycle infection. However, VLPs can be amplified by infection of cells that were pre-transfected with plasmids encoding viral L, N, and the glycoprotein precursor, as shown for CCHFV, which can be used as a tool for the development of vaccines and antivirals (Devignot *et al.*, 2015).

Minigenome and VLP assays are also of crucial significance before attempting virus rescue, to ensure all viral components required for the rescue are functional. This is best exemplified by the inability to rescue OROV. Through the development of the aforementioned assays, the inability to rescue infectious OROV entirely from cDNA clones was found to be attributed to a mistake in the published sequence of the OROV S segment (Acrani *et al.*, 2015). The revised OROV S segment sequence had a longer 3' UTR that resulted in an active minireplicon system (unlike the published sequence), and later enabled the successful rescue of OROV entirely from cDNA clones (Tilston-Lunel *et al.*, 2016).

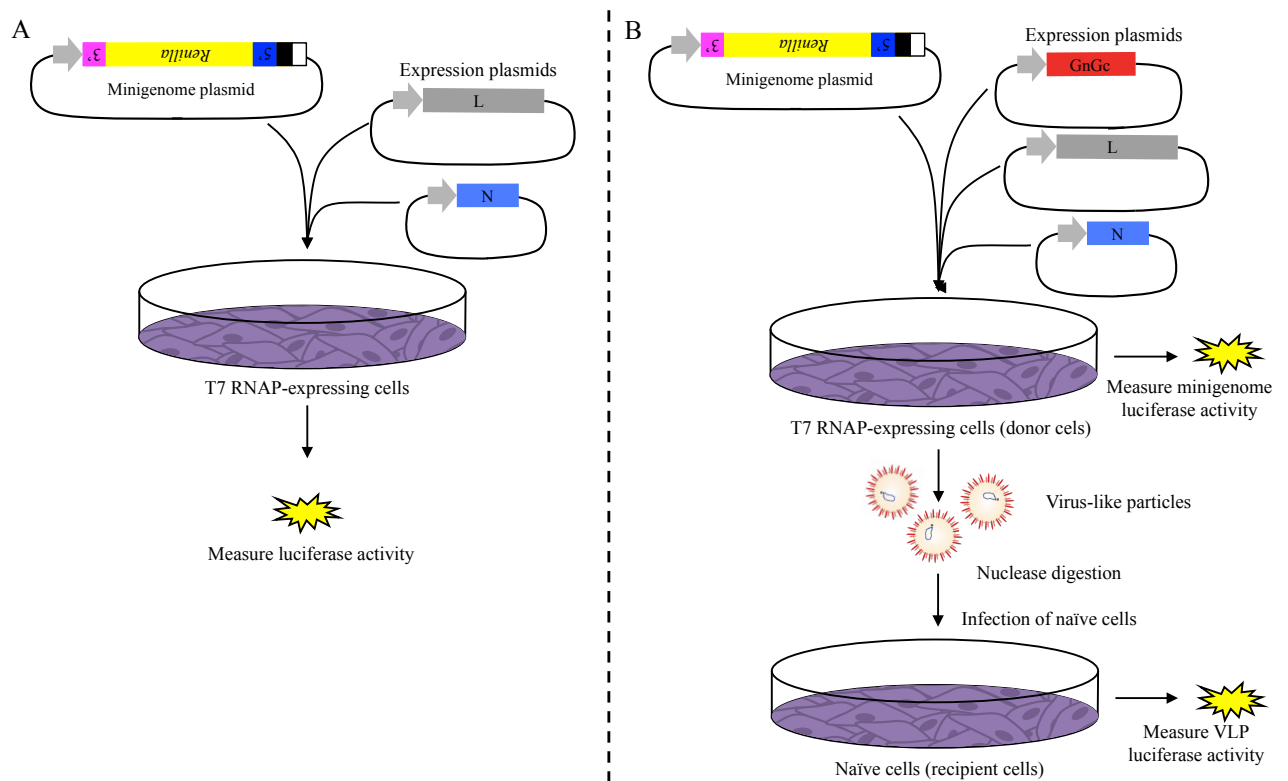


**Figure 1-10. Minigenome and virus-like particle systems.**

(A) Schematic diagram of the bunyavirus minireplicon system. The minigenome plasmid for a specific segment contains a reporter gene (*Renilla*) flanked by the viral UTRs in the genomic (negative) sense orientation, relative to the T7RNAP promoter. Co-transfection with expression plasmids encoding N and L in T7 RNAP-expressing cells will result in the formation of an active minigenome RNP if the viral UTRs, and the N and L proteins are functional. (B) Schematic diagram on a virus-like particle assay. If the minigenome assay is supplemented with an expression plasmid encoding the viral glycoprotein precursor, virus-like particles containing the minigenome reporter produced in donor cells can be used to infect naïve recipient cells upon nuclease treatment of the supernatant from donor cells. Infection can be confirmed by measuring reporter activity in recipient cells. UTRs: Untranslated regions; T7RNAP: T7 RNA polymerase; RNP: Ribonucleoprotein

### 1.3 The *Phlebovirus* genus

This section will give a brief overview of the *Phlebovirus* genus, and describe the emergence of a number of tick-borne phleboviruses concerning this PhD study: Uukuniemi virus, Heartland virus, Severe fever with thrombocytopenia syndrome virus.

#### 1.3.1 *Classification and transmission*

The *Phlebovirus* genus comprises over 70 viruses, with 10 species and 33 tentative species (Plyusnin *et al.*, 2001) that can be broadly divided into two groups based on their antigenic, vector and genomic similarities: the Sandfly fever (or Phlebotomus) group and the Uukuniemi-like virus group (Bouloy, 2011). Initially, UUKV and related viruses were classified as a separate genus within the *Bunyaviridae* (*UUKuvirus*), but due to their genetic and antigenic similarities, these viruses were reclassified as members of the *Phlebovirus* genus (Plyusnin *et al.*, 2001). While all recognized Uukuniemi-like viruses are transmitted by ticks, phlebotomines or mosquitoes transmit those belonging to the sandfly fever group. In addition to vector differences, an important difference noted at the molecular level between these two groups is the lack of the non-structural protein NSm in Uukuniemi-like viruses, which is encoded at the N terminus of the glycoprotein precursor in the M segment of sandfly fever viruses.

Important pathogens within the Sandfly fever group include RVFV (recognised as the type species) (Plyusnin *et al.*, 2001), Punta Toro virus (PTV) Sandfly fever Sicilian virus (SFSV), sandfly fever Naples virus (SFNV) and Toscana virus (TOSV). Notable Uukuniemi-like group viruses include the prototype UUKV, Bhanja virus (BHAV) and the recently emerged Heartland virus (HRTV) and severe fever with thrombocytopenia syndrome virus (SFTSV). In recent years many novel and emerging viruses have been assigned to the *Phlebovirus* Uukuniemi-like group, including Lone Star virus (LSV) (Nasci *et al.*, 2014), Hunter Island Group virus (HIGV) (Gauci *et al.*, 2015), Malsoor virus (MALV) (Mourya *et al.*, 2014), Antigone virus (ANTV) (Papa *et al.*, 2016), blacklegged tick phlebovirus (BTPV) and American dog tick phlebovirus (ADTPV) (Tokarz *et al.*, 2014). Recently, a virus that appears to be restricted to arthropod hosts only (specifically to mosquitoes) named Gouléako virus (GOLV) was discovered and found to be closely related to the genus *Phlebovirus* (Marklewitz *et al.*, 2011). Interestingly, the GOLV genome does not encode an NSm protein, unlike the genome of other mosquito-borne phleboviruses. GOLV was also suggested to constitute a tentative novel genus within the *Bunyaviridae* (Marklewitz *et al.*, 2011).

In light of the growing number of novel tick-borne phleboviruses identified, a recent study characterized the Uukuniemi-like group using full-length genome sequences, including newly discovered viruses (Palacios *et al.*, 2013). Phylogenetically, Uukuniemi-like group viruses clustered together, separate from those phleboviruses transmitted by phlebotomines. A representative phlebovirus phylogenetic tree (of the M segment ORF) is shown in Figure 1-11. Based on phylogenetic and serologic relationships, the authors proposed that Uukuniemi-like group viruses should be assigned to seven different species, namely the Uukuniemi, Murre, SFTSV/HRTV, Precarious Point, Grand Arbaud, Manawa and Bhanja species. The continuing identification of novel tick-borne phleboviruses, as well as their increasing host range and movement into naïve geographical locations highlights the risk posed to human and animal health by these emerging viruses.

### **1.3.2 Geographic distribution**

Phleboviruses are emerging pathogens that are geographically distributed according to the distribution of their vectors in North and South America, Europe, Asia and Africa (Bouloy, 2011). This is illustrated by the distribution of SFSV and SFNV, which concomitantly agrees with the geographical distribution of sandflies, extending from the Mediterranean basin to the Arabian Peninsula and as far east as Pakistan and India (Elliott and Schmaljohn, 2013). TOSV, a virus transmitted by phlebotomines which can cause aseptic meningitis and meningoencephalitis, has been isolated in central Italy, Spain, France, Portugal, Cyprus and other countries in the Mediterranean basin (Cusi, 2010). RVFV is transmitted mainly by *Aedes* and *Culex* mosquito species and is widespread in Africa, causing recurrent epizootics and epidemics particularly in East and West Africa. However, in the year 2000 it extended its geographic range to reach Yemen and Saudi Arabia, leading to human deaths and major livestock losses (Chevalier *et al.*, 2010).

Until recently, only a few phleboviruses transmitted by ticks had been identified. UUKV was known to be distributed in central and eastern Europe (Hubálek and Rudolf, 2012). BHAV cases were reported in southern and central Asia, Africa, and southern Europe (Hubálek, 2009). With the discovery of HRTV, SFTSV, LSV, HIGV, MALV, ANTV, BTPV and ADTPV, it became apparent that tick-borne phleboviruses have a global distribution (Figure 1-12). A sensitive RT-PCR system was recently developed, which can target a broad range of tick-borne phleboviruses (Matsuno *et al.*, 2015). This tool will aid surveillance efforts to detect known and unidentified tick-borne phleboviruses in diverse geographic locations.

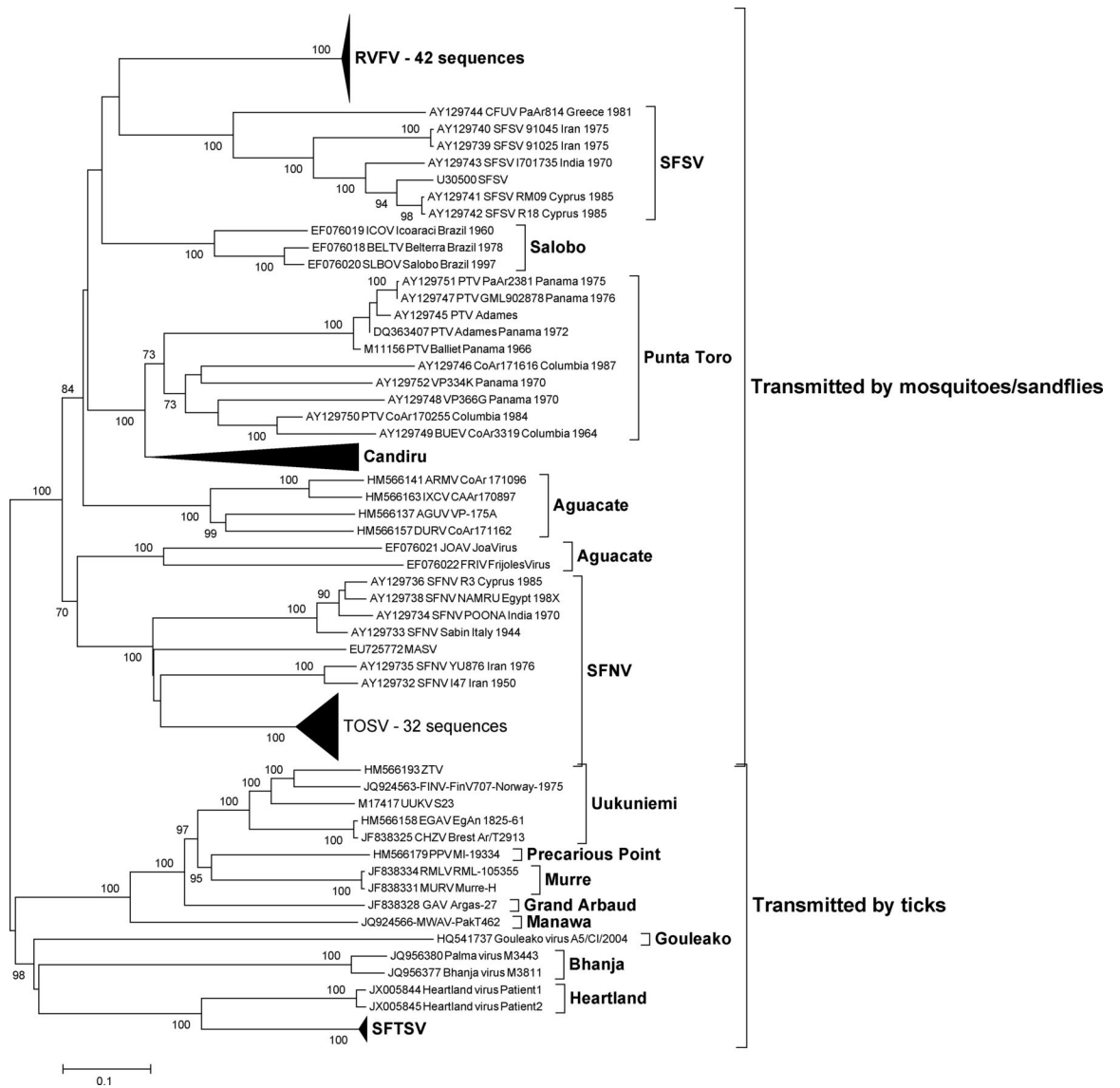


**Figure 1-11. Phylogenetic tree of the phlebovirus glycoprotein precursor.**

The phylogenetic tree shows 133 phleboviral sequences of the M segment open reading frame, analysed by a Neighbour-Joining analysis. Tentative species of the Uukuniemi-like group (transmitted by ticks) are shown. SFSV: sandfly fever Sicilian virus; SFNV: sandfly fever Naples virus. Modified from (Palacios *et al.*, 2013).

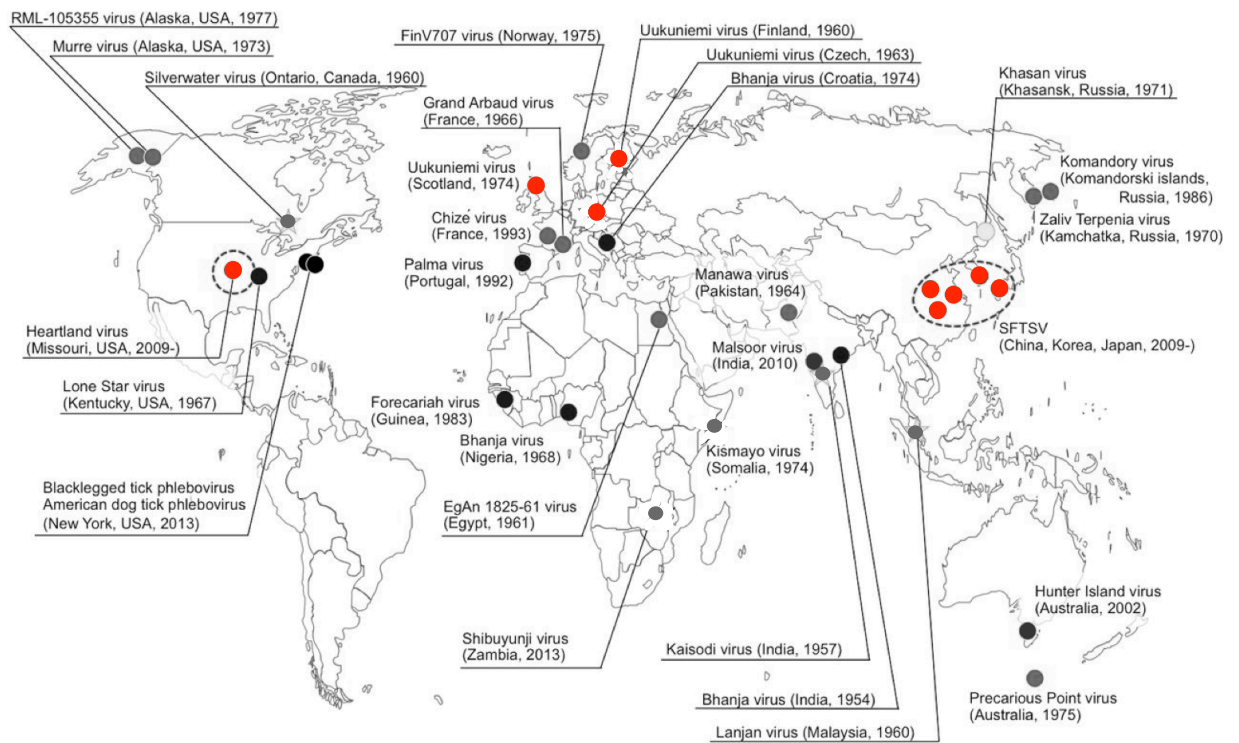


**Figure 1-12. Geographical distribution of tick-borne phleboviruses.**

Circles indicate the location where the tick-borne phleboviruses have been found. Dashed circles represent areas where the noted viruses are endemic. Red circles depict the distribution of viruses that are relevant to this study (UUKV, HRTV and SFTSV). UUKV: Uukuniemi virus; HRTV: Heartland virus; SFTSV: Severe fever with thrombocytopenia syndrome virus. Modified from (Matsuno *et al.*, 2015).

### 1.3.3 *Disease caused by phleboviruses.*

It is important to note the broad spectrum of clinical outcomes elicited by phlebovirus infections in humans. Among the Sandfly fever group, a number of viruses can cause disease. While SFSV and SFNV are aetiologic agents of an acute, self-limiting illness that involves fever, myalgia and malaise, TOSV can cause aseptic meningitis and meningoencephalitis (Cusi, 2010; Hemmersbach-Miller *et al.*, 2004; Sanbonmatsu-Gómez *et al.*, 2009). TOSV infection has also been reported to result in asymptomatic infections, and influenza-like symptoms during the summer season (Hemmersbach-Miller *et al.*, 2004; Portolani *et al.*, 2002). RVFV is perhaps the phlebovirus that poses most concern for human and animal health (Mandell and R. Flick, 2010). Disease in ruminants (the principal amplifying host of RVFV) (Gerdes, 2004) manifests itself with febrile illness, diarrhea, and abortion (Ikegami and Makino, 2011). In newborn lambs, the mortality rate of RVFV may reach 90-100%, resulting in a significant socio-economic burden to society (Bouloy, 2011). Infection in humans primarily leads to a benign self-limited febrile illness, however a small proportion of infected patients develop haemorrhagic fever, neurological disorders and blindness (Rolin *et al.*, 2013).

Until the emergence of highly pathogenic HRTV and SFTSV, Uukuniemi-like group viruses were not recognised as a public health threat, as no human illness caused by these viruses had been reported even though antibodies to some of the members of this group have been detected in humans in serologic surveys (Bouloy, 2011; Hubálek and Rudolf, 2012; Saikku and Brummer-Korvenkontio, 1973; Traavik and Mehl, 1977). This is with the exception of BHAV, which can induce neurotropic disease in young ruminants (Mádr *et al.*, 1984) and in some cases a febrile-like illness in humans (Calisher and Goodpasture, 1975). Serological surveys have suggested that BHAV is endemic in Eastern Europe, however causing asymptomatic human infections (Punda *et al.*, 1987).

Understanding the differences in the molecular mechanisms of virulence of different tick-borne phleboviruses is of interest to elucidate the determinants that contribute to the wide spectrum of disease outcomes. The following sections present an overview of the current knowledge of the molecular biology of UUKV (apathogenic in humans), HRTV and SFTSV (both of which can cause serious disease in humans).

### 1.3.4 *Uukuniemi virus*

UUKV is the prototype of the Uukuniemi-like virus group. It was originally isolated from a tick (*Ixodes ricinus* species) in southern Finland (Oker-Blom *et al.*, 1964). Subsequent isolations of UUKV were also reported in central and eastern Europe, as well as in Norway, southern Russia and central Asia (CDC Arbovirus catalog [wwwn.cdc.gov/arbocat]). While antibodies to UUKV (or UUKV-like viruses) have been isolated in humans and other vertebrates such as birds, rodents and cows (Hubálek and Rudolf, 2012; Saikku and Brummer-Korvenkontio, 1973), no clinical signs of disease have been reported in these species.

Various strains of UUKV have been isolated from ticks collected in nesting areas of seabirds and passerine birds, or from tick nymphs collected on migrant birds (S. R. Moss, 1986; Nuttall *et al.*, 1981; 1984; Traavik and Mehl, 1977; Watret and Elliott, 1985), which could suggest that birds may act as hosts of UUKV and could play a role in the widespread distribution of tick-borne viruses in Europe (Hubálek and Rudolf, 2012).

UUKV has served as a prototype virus to understand basic characteristics of viruses within the *Bunyaviridae* family. In fact, UUKV was the first bunyavirus shown to consist of a tripartite negative-sense RNA genome, a distinctive feature of the *Bunyaviridae* (Pettersson *et al.*, 1977). An icosahedral T=12 symmetry of Gn-Gc heterodimers was first observed in UUKV virions, a unique arrangement not previously observed for viruses and later found in RVFV (Freiberg *et al.*, 2008; Overby *et al.*, 2008). UUKV has also served as a model phlebovirus to investigate phlebovirus entry in mammalian and tick cell lines (Lozach *et al.*, 2010) (Mazelier *et al.*, 2016). Lozach *et al.* showed that unlike other bunyaviruses, UUKV internalization in mammalian cells was mainly clathrin-independent (Lozach *et al.*, 2010). UUKV minigenome systems have aided the understanding of role of the non-coding regions of bunyaviruses. Flick *et al.* showed that complementarity at the 5' and 3' ends of the viral UTRs are crucial for promoter activity and that the IGR in the ambisense S segment serves as a regulator of transcription termination (K. Flick *et al.*, 2004). Finally, UUKV-like particles have been used to understand bunyavirus genome packaging and budding, and it was shown that UUKV Gn had a critical role in genome packaging by a close interaction with viral RNPs, while its Gc was important for budding (Overby *et al.*, 2007). Although a minigenome and a virus-like particle system for UUKV exist, there is a need to develop a reverse genetics system that allows the rescue of UUKV entirely from cDNA. Such a tool could serve to allow UUKV to be utilized as a

comparative model for other more pathogenic tick-borne phleboviruses, to understand the molecular basis for their virulence and pathogenicity.

### 1.3.5 *Severe fever with thrombocytopenia syndrome virus*

Severe fever with thrombocytopenia syndrome virus (SFTSV) (also known as Huaiyangshan virus, DaBie Mountain virus and Henan fever virus) was the first tick-borne phlebovirus discovered that caused severe disease in humans. Between 2007 and 2010, patients in the Henan and Hubei provinces of China were presenting gastrointestinal symptoms, joint pain, thrombocytopenia, leukocytopenia, haemorrhagic manifestations and multi-organ dysfunction as a result of an unknown infectious disease, which was causing a fatality rate of 12-30% (Yu *et al.*, 2011). The causative agent was identified as the novel tick-borne phlebovirus SFTSV (Stone, 2010; Xu *et al.*, 2011; Yu *et al.*, 2011; Zhang *et al.*, 2012a; 2011). SFTSV was later identified in patients presenting with similar symptoms in Japan and South Korea (Kim *et al.*, 2013; Takahashi *et al.*, 2014).

Sequencing of the SFTSV genome revealed low similarity to other phleboviruses, with 33%, 30-41% 11-13% and 30-36% similarity to RVFV or UUKV L, N, NSs and glycoprotein precursor proteins, respectively ( Yu *et al.*, 2011). However, as with other tick-borne phleboviruses, the SFTSV genome does not encode an NSm protein. Phylogenetic studies ( Yu *et al.*, 2011; Zhang *et al.*, 2011) subsequently supported by serological studies (Palacios *et al.*, 2013) have thus suggested that the novel virus represents a distinct lineage within the *Phlebovirus* genus.

The primary vector of SFTSV in China is the *Haemaphysalis longicornis* species of ticks, as both infectious virus and viral RNA has been isolated from this species (Yu *et al.*, 2011; Zhang *et al.*, 2012b). The wide geographical distribution of these ticks throughout China and other parts of Asia and Oceania such as Korea, Japan, Australia and Fiji (Hoogstraal *et al.*, 1968) poses a concern for the potential spread of the virus to these locations (Y. Wu and Gao, 2013; Xiong *et al.*, 2012). It is not entirely clear which is the vertebrate host of SFTSV. In a survey of domesticated animals in China, SFTSV-specific antibodies and viral RNA were detected in sheep (69.5%), cattle (60.5%), dogs (3.1%), pigs (3.1%) and chickens (47.4%) (Niu *et al.*, 2013). Others have also found SFTSV-specific antibodies in goats (66.8%), rodents (4.4%) and hedgehogs (2.7%) (Li *et al.*, 2014; Ni *et al.*, 2015). Furthermore, antibodies against SFTSV were detected in two migratory bird species in China (Li *et al.*, 2016). Yun *et al.* recently analysed phylogenetic relationships of SFTSV and migratory bird routes in Asia and proposed that migratory birds, well-known carriers

of ticks, could be a potential source of the spread of SFTSV across China, South Korea and Japan (Yun *et al.*, 2015). Finally, some evidence exists for human-to human transmission of SFTSV, as documented in a family cluster in China (Bao *et al.*, 2011; Jiang *et al.*, 2015).

The emergence of SFTSV focused research interests on understanding its underlying molecular mechanisms of pathogenicity. The virus was able to infect and replicate in the human monocytic cell line THP-1 without causing a cytopathic effect (CPE) (B. Qu *et al.*, 2012), in comparison to severe CPE caused by RVFV (Won *et al.*, 2007). The authors reported that the virus was able to suppress IFN and NF- $\kappa$ B responses. In addition to the NSs protein, SFTSV N was also able to inhibit the activation of the IFN- $\beta$  promoter and NF- $\kappa$ B responses (B. Qu *et al.*, 2012). The mechanisms employed by SFTSV to inhibit the human IFN system have been extensively studied, and are described in Section 1.4.4.

Expression of the SFTSV glycoproteins in lentiviral and rhabdoviral pseudotypes showed that entry into a broad range of human and animal cell lines, including human macrophages and dendritic cells, is mediated by these proteins in a pH-dependent-manner (Hofmann *et al.*, 2013). Additionally, the authors showed that DC-SIGN served as a receptor for the viral pseudotypes (Hofmann *et al.*, 2013), which was subsequently confirmed with wild-type SFTSV (Tani *et al.*, 2016). Unlike RVFV (Ikegami *et al.*, 2009b), SFTSV was shown to be unable to shut off host cell protein synthesis (Brennan *et al.*, 2015). An infectious model for SFTS which resulted in the hallmark symptoms of thrombocytopenia and leukopenia was established in B57/BL6 mice (Jin *et al.*, 2012). Interestingly, while viral RNA was detected in blood, spleen, liver and kidneys, virus replication was only observed in the spleen of the mice. Additionally, the authors reported that SFTSV was found to adhere to mouse platelets, which results in phagocytosis by primary macrophages. Thus, thrombocytopenia induced by SFTSV is presumed to be caused by clearance of virus-bound platelets by macrophages (Jin *et al.*, 2012). Finally, the development of a reverse genetics system for SFTSV (Brennan *et al.*, 2015) now serves an invaluable tool to manipulate the viral genome in order to further characterize the molecular biology of SFTSV.

### 1.3.6 *Heartland virus*

Following the identification of SFTSV, Heartland virus (HRTV) was isolated from two patients living in Northwestern Missouri, who reported tick bites prior to disease and presented with fever, fatigue, anorexia, diarrhea, thrombocytopenia and leukocytopenia

(McMullan *et al.*, 2012). Seven additional cases were later reported in Missouri, Tennessee and Oklahoma, two of which were fatal (Muehlenbachs *et al.*, 2014; Williams, 2014). Despite being most closely related to SFTSV, comparison of the viral L and N (the two most conserved proteins within the *Bunyaviridae*) showed 27% and 38% difference with SFTSV (McMullan *et al.*, 2012).

A study on field-collected arthropods detected HRTV RNA in 10 pools of *Amblyomma americanum* ticks (lone star tick), 8 of which yielded infectious virus. This finding implicated lone star ticks as the primary vector of HRTV (Savage *et al.*, 2013). The authors in this study also suggested that presumably the ticks become infected by feeding on a viremic host during their larval stage, and transmission to humans occurs when nymphs are host seeking during spring and summer seasons. Though initially associated with disease in Missouri, Tennessee and Oklahoma, a serological survey suggested a more widespread distribution of HRTV in the United States, with seropositive wildlife detected in 13 different states in Central and Eastern United States (Riemersma and Komar, 2015). Seropositive wildlife in this study included deer, raccoons, coyotes and moose. A recent serological survey examined 8 mammalian species and 26 bird species to identify candidate vertebrate amplification hosts of HRTV (Bosco-Lauth *et al.*, 2015). HRTV-specific antibodies were identified in raccoons and deer as in the previous study, as well as horses, dogs and opossums, but not in any bird species. The authors suggested that the high antibody prevalence in deer and raccoons, as well as their high abundance in northwest Missouri indicates that these species may act as the vertebrate amplification hosts of HRTV (Bosco-Lauth *et al.*, 2015).

To date, there is a lack of understanding of the molecular determinants of virulence of HRTV. However, a recent study assessed the viremic potential of a number of vertebrates (raccoons, goats, chickens, rabbits, hamsters, mice and IFN- $\alpha/\beta/\gamma$  receptor-deficient mice) following HRTV infection (Bosco-Lauth *et al.*, 2016). Although all animals showed immune responses against HRTV following primary or secondary exposure, only IFN- $\alpha/\beta/\gamma$  receptor-deficient mice showed viremia and associated illness, indicating that the innate immune response mounted following virus infection plays an important role in the development disease. The understanding of the molecular biology of HRTV could be aided by the availability of a reverse genetics system.

## **1.4 Host innate immune responses to virus infection and viral countermeasures**

### ***1.4.1 The human innate immune system***

Following infection of a susceptible vertebrate host, viruses confront two major types of host defense mechanisms: the adaptive and the innate immune systems. Adaptive immune responses are composed of humoral immunity (mediated by the production of antibodies by B lymphocytes), and T-cell mediated immunity (which involves the induction of apoptosis in virus-infected cells displaying epitopes of the foreign antigen). Although the adaptive immune response is crucial to develop immunological memory and enables enhanced long-lasting anti-viral responses in subsequent exposures to the pathogen, it is a slow response because it requires the activation of specific B and T cells, which can take a week to become effective (Alberts *et al.*, 2014).

Instead, vertebrate hosts depend on innate immunity as the first line of defence against viral infections. Unlike adaptive immune responses, which are highly specific, innate immune responses are non-specific, and begin immediately or within a few hours following exposure to a pathogen. The IFN system plays an important role in innate immunity, and is capable of controlling most virus infections in the absence of adaptive immunity (Goodbourn *et al.*, 2000; Randall and Goodbourn, 2008). IFNs were discovered in 1957 by Isaacs and Linderman, and were described by the authors as a factor that was inducing interference with the growth of live influenza A virus in chick chorio-allantoic membranes which were pre-treated with heat-inactivated influenza virus (Isaacs and Lindenmann, 1957). IFNs are now known as a group of cytokines that are responsible for myriad of roles in innate as well as adaptive immunity. IFNs are produced and secreted by cells following the recognition of foreign molecular patterns associated with infection, known as pathogen associated molecular patterns (PAMPs). There are three types of IFN: type I, II and III, grouped according to their sequence homology. In humans, type I IFNs are encoded on chromosome 9 and include IFN- $\alpha$  (includes 13 different subtypes), IFN- $\beta$ , IFN- $\epsilon$ , IFN- $\kappa$ , and IFN- $\omega$  (Pestka, 1987; Pestka *et al.*, 2004). IFN- $\alpha$  and IFN- $\beta$  are well-known to be induced en masse as a response to virus infection in many different cell types, whereas the role of other type I IFNs is less well-defined (Randall and Goodbourn, 2008; Taniguchi and Takaoka, 2002). A single member of type II IFN exists, IFN- $\gamma$ , which is encoded on the human chromosome 10 and is structurally different from type I IFNs (Chen *et al.*, 2004; Pestka *et al.*, 1997; Plataniias and Fish, 1999). Type III IFNs are composed of

three subtypes of IFN- $\lambda$ . Following the induction of IFNs by mechanisms described in Section 1.4.2, secreted IFNs activate intracellular signalling cascades in neighbouring cells by binding to receptors on the cell surface, which subsequently leads to the induction of an antiviral state through the up-regulation of a number of genes that can have anti-viral activity (Goodbourn *et al.*, 2000; Hoffmann *et al.*, 2015; Randall and Goodbourn, 2008; Schneider *et al.*, 2014). These genes are known as IFN-stimulated genes (ISGs). Type I, type II and type III IFNs have evolved to bind to distinct receptors on the cell surface, and while type I and type III IFNs can activate the same signalling pathway, the pathway activated by type II IFNs differs slightly (described in section 1.4.2) (Uzé and Monneron, 2007).

### 1.4.2 Interferon induction

In order to recognize pathogens, host cells must discriminate between self- and viral RNAs. RNA viruses produce products such as double-stranded (ds) RNA and 5'-triphosphorylated single-stranded (ss) uncapped RNAs during replication of their viral genome. These products, or PAMPs, are detected as 'non-self RNA' by pattern recognition receptors (PRRs), including transmembrane Toll-like Receptors (TLRs) and cytosolic host cell DExD/H box RNA helicases such as melanoma differentiation-associated gene-5 (MDA-5) or retinoic acid-inducible gene-I (RIG-I) (Goodbourn *et al.*, 2000; Randall and Goodbourn, 2008). TLRs are mainly expressed in antigen-presenting cells, such as dendritic cells and localise to the plasma membrane, with the exception of TLR3, TLR7 and TLR9, which are embedded in endosomal compartments and can detect dsRNA upon virus endocytosis (Nishiya and DeFranco, 2004; Schaefer *et al.*, 2004). On the other hand, cytosolic RIG-I and MDA-5 are widely expressed in many cell types. While RIG-I recognizes 5'-triphosphorylated, uncapped RNA (Rehwinkel *et al.*, 2010), both RIG-I and MDA-5 can detect short and long dsRNA molecules, respectively, allowing them to detect distinct classes of RNA viruses (Kato *et al.*, 2008; 2006). Negative-strand RNA viruses, such as bunyaviruses, produce little or undetectable amounts of dsRNA during replication (Weber *et al.*, 2006). Thus, it is hypothesised that these viruses are sensed mainly by RIG-I, by generation of ssRNA with uncapped 5' triphosphate ends (Hornung *et al.*, 2006; Pichlmair *et al.*, 2006).

Binding of viral RNA to RIG-I results in its activation and the initiation of downstream signalling pathways. Upon binding viral RNA, polyubiquitination of the N-terminus of RIG-I by the tripartite motif-containing protein 25 (TRIM25) E3 ubiquitin ligase is crucial

for its activation (Gack *et al.*, 2007; Zeng *et al.*, 2009). RNA-bound RIG-I is believed to undergo a conformational change that exposes the N terminus of RIG-I consisting of tandem caspase activation and recruitment domains (CARD), which are repressed when inactive (Saito *et al.*, 2007). The exposed CARDS promote multimerization, but also interactions with the CARD domains of the adaptor mitochondrial antiviral signalling protein (MAVS, also known as IPS-1, Cardif or VISA) (Saito *et al.*, 2007). Activation of MAVS through CARD-CARD interactions induces the formation of prion-like aggregates (Hou *et al.*, 2011). These functional MAVS polymers acts as a scaffold to recruit and activate cytosolic kinases Inhibitor of nuclear factor kappa-B kinase (IKK) and tank binding kinase 1 (TBK1). The activation of TBK1/IKK $\epsilon$  and IKK $\alpha$ /IKK $\beta$  subsequently leads to the activation of interferon regulatory factor 3 (IRF-3) and nuclear factor  $\kappa$ -light-chain-enhancer of activated B cells (NF- $\kappa$ B), respectively and their translocation to the nucleus. Although IRF-3 and NF- $\kappa$ B play a role in the induction of IFN, other members of the IRF family, such as IRF-7, have been shown to be involved in IFN induction (Honda and Taniguchi, 2006). Activation of IRF-3 occurs through the phosphorylation at its C terminus, which results in its dimerization and exposure of a nuclear localization signal (NLS) (Dragan *et al.*, 2007; Lin *et al.*, 1998). On the other hand, the NLS of NF- $\kappa$ B, which is located within its p65 subunit, is unveiled once its inhibitor molecule I $\kappa$ B (inhibitor of NF- $\kappa$ B) becomes phosphorylated and degraded by proteasomes (J. Hu *et al.*, 2005). Once in the nucleus, IRF-3 and NF- $\kappa$ B can assemble on the promoter of the IFN- $\alpha/\beta$  gene, in a cooperative manner along with other factors, to form the multi-protein enhanceosome complex, which promotes the assembly of the host cell transcriptional machinery for the initiation of IFN- $\alpha/\beta$  mRNA synthesis (Figure 1-13) (Randall and Goodbourn, 2008). TLR-3 signalling follows a slightly different route to that of RIG-I and MDA-5. Briefly, following TLR-3 activation, the Toll-interleukin (IL)-1-resistance (TIR) domain-containing adaptor inducing IFN- $\beta$  (TRIF) induces the activation of TBK1/IKK $\epsilon$ , subsequently leading to the phosphorylation and nuclear translocation of IRF-3 (García-Sastre and Biron, 2006; Hoffmann *et al.*, 2015).

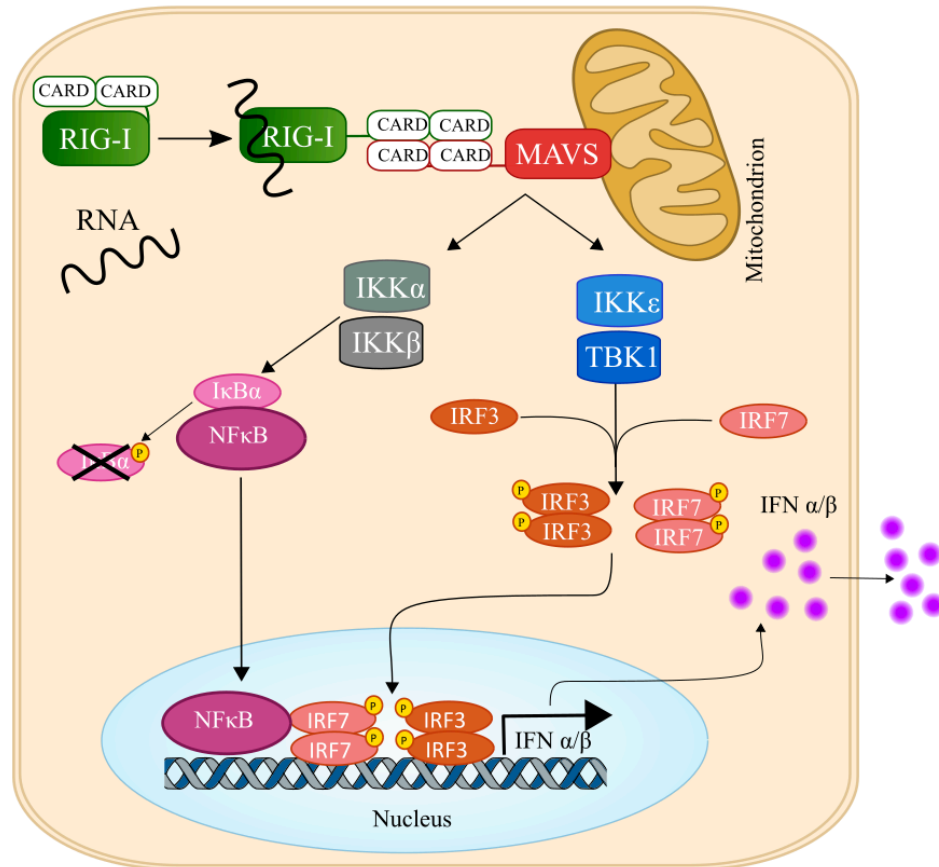


**Figure 1-13. Simplified representation of RIG-I–mediated IFN induction.**

Viral RNA products generated during virus replication (such as dsRNA or 5'-triphosphorylated, uncapped single-stranded ssRNA) are detected by RNA helicases RIG-I or MDA-5. Binding of RNA triggers a conformational change in RIG-I that results in the exposure of N-terminal CARD domains. CARD-CARD interactions enable the recruitment of the adaptor protein MAVS. MAVS acts as a scaffold to recruit and activate cytosolic kinases IKK and TBK1. The activation of kinases subsequently leads to the activation and nuclear translocation of IRF-3 or IRF-7 and NF- $\kappa$ B, respectively. While IRF-3 translocation is driven by the phosphorylation-induced dimerization, NF- $\kappa$ B is free to translocate to the nucleus upon phosphorylation and degradation of its inhibitor molecule I $\kappa$ B. Once in the nucleus, IRF-3, IRF-7 and NF- $\kappa$ B can act as transcription factors to enhance the transcription of the IFN- $\beta$  promoter gene. Adapted from (Randall and Goodbourn, 2008). dsRNA: double-stranded RNA; ssRNA: single-stranded RNA; RIG-I, retinoic acid-inducible gene I; MDA-5: melanoma differentiation-associated gene-5; CARD: caspase recruitment domain; MAVS: mitochondrial antiviral signalling protein; IKK: inhibitor of nuclear factor kappa-B kinase; TBK1: TANK-binding kinase 1, IRF: IFN-regulatory factor; NF- $\kappa$ B: nuclear factor  $\kappa$ -light-chain-enhancer of activated B cells.

### 1.4.3 Interferon signalling

Following IFN induction, secreted IFN activates the IFN signalling pathway in neighbouring cells by binding to IFN receptors. Type I IFN engages with the type I IFN receptor (IFNAR), which has a broad cell type distribution and is composed of two subunits: IFNAR1 and IFNAR2. Type II IFN (or IFN- $\gamma$ ) binds to the type II IFN receptor (IFNGR), which is also has broad cell type distribution but is a tetrameric complex, composed of two subunits of IFNGR1 and two subunits of IFNGR2. Type III IFN signals through binding to the type III IFN receptor (IFN $\lambda$ R), a heterodimeric receptor formed by IFNLR1 and IL10R2 subunits (Kotenko *et al.*, 2003). Importantly, while IL10R2 is expressed in a wide range of cell types and forms part of a separate receptor (namely the IL-10 cytokine receptor complex), IFNLR1 is primarily restricted to epithelial cells, limiting cell-specific responsiveness and explaining why many other cell types respond poorly to type III IFN stimulation (Sommerreyns:2008ez; de Weerd and Nguyen, 2012).

Once IFN binds to their cognate receptors, the receptor chains come into close proximity and propagate the signal through the JAK/STAT signalling pathway, for the ultimate induction of ISGs. A simplified illustration of the JAK/STAT signalling pathway is shown in Figure 1-14. Type I and Type III IFN signalling cascades have some redundancy, as they signal using the canonical JAK/STAT pathway, utilising identical JAKs (Janus activated kinase) and STATs (signal transducer and activator of transcription) (de Weerd and Nguyen, 2012). While the cytoplasmic tails of IFNAR1 and IL10R2 are constitutively associated with the JAK family tyrosine kinase 2 (TYK2) (Uzé *et al.*, 1990), IFNAR 2 and IFNLR1 are associated with JAK1 (Chen *et al.*, 2004; Darnell *et al.*, 1994). Studies have shown that STAT-2 may also be associated with the receptors, and weakly bound to STAT1 prior to IFN stimulation (Stancato *et al.*, 1996). The IFNGR1 and IFNGR2 subunits of the type II IFN receptor are, comparatively, associated with JAK1 and JAK2, respectively.

Ligand-induced rearrangement and dimerization of the IFN receptors causes the receptor-associated kinases to transphosphorylate the cytoplasmic receptor chains, which enables the activation of STATs (Figure 1-14). For instance, following type I IFN binding to the IFNAR receptor, TYK2 phosphorylates Tyr466 on the cytosolic tail of IFNAR1, which generates a docking phosphorylation site for STAT2. STAT2 is consequently phosphorylated at Tyr 690 by TYK2 and STAT1 at Tyr701 by JAK1 (Müller *et al.*, 1993). The phosphorylation of the STATs induces their dimerization via SH2-phosphotyrosine

interactions, and results in the generation of a novel NLS (Banninger and Reich, 2004; Fagerlund *et al.*, 2002). In addition, monomeric IRF-9 is acetylated by IFNAR2, and assembles with STAT1-STAT2 heterodimers to form a heterotrimer complex, named Interferon-stimulated gene factor 3 (ISGF3) (Tang *et al.*, 2007). The ISGF3 complex then translocates to the nucleus, where it can bind IFN-stimulated response elements (ISRE) present in the promoter of many ISGs, to initiate their transcription. Importantly, acetylation plays an important role in IFN signalling, as acetylation of IRF-9 is required for DNA binding, and STAT acetylation is thought to aid in the assembly of ISGF3 (Tang *et al.*, 2007). The up-regulated ISGs can have direct antiviral activity, such as the interferon-inducible transmembrane (IFITM) proteins, which inhibit virus entry by modulating membrane fluidity (S. Smith *et al.*, 2014). Other ISGs can instead act indirectly, as positive or negative regulators of the IFN signalling pathways. For instance, the production of IRF3 and IRF7 as a result of IFN signalling results in induction of more IFN, thus creating a positive feedback loop (Marié *et al.*, 1998; Sato *et al.*, 1998). In contrast, Tripartite motif-containing protein (TRIM)-28 has been shown to act as a negative regulator of IFN induction, by binding directly to IRF-7 and preventing its translocation to the nucleus (Liang *et al.*, 2011). Such immunomodulatory strategies are important because excessive IFN responses could harm the host, as demonstrated in patients with autoimmune disorders (Niewold, 2014).

Whereas the formation of the ISGF3 heterotrimer is the canonical form of ISG induction, other transcription factor complexes with the ability to regulate the expression of ISGs have been described (Randall and Goodbourn, 2008). For instance, type I, II and III IFN can lead to the formation of STAT1-STAT1 homodimers (Gamma-activated Factor [GAF]), which can translocate to the nucleus to bind to and promote the transcription of the IFN- $\gamma$  activated site (GAS) in the promoter of IFN- $\gamma$  regulated genes (Ramana *et al.*, 2002). As opposed to type I and type III IFN signalling, in which ISGs are mainly induced by STAT hetero-dimers, type II IFN signalling is majorly mediated only by STAT1 homodimers (Figure 1-14) (Borden *et al.*, 2007; Plataniias, 2005).

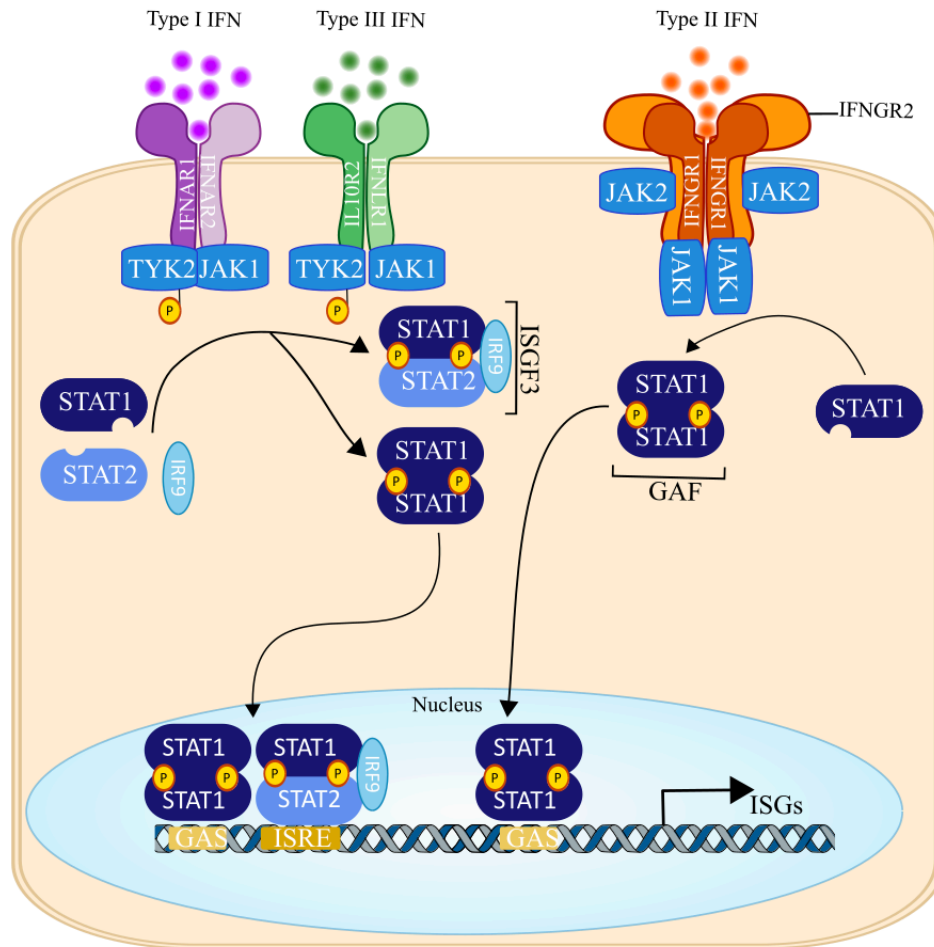


**Figure 1-14. Simplified diagram of type I, II and III IFN signalling.**

Receptor chains undergo dimerization upon binding to their cognate interferon (IFN). Consequently, proteins of the Janus Kinase (JAK) family associated with the cytosolic domains of receptor chains become activated and phosphorylate (P) signal transducer and activator of transcription (STAT) proteins. Phosphorylated STATs can form homodimers such as the gamma-activated factor (GAF), or heterodimers, which in association with the interferon regulatory factor 9 (IRF-9) forms a heterotrimer complex referred to as IFN-stimulated gene factor 3 (ISGF3). GAF and ISGF3 can translocate to the nucleus to bind to promoters of IFN-stimulated genes (ISGs), namely the IFN- $\gamma$  activated site (GAS) and the IFN-stimulated response elements (ISRE), respectively. Adapted from (Hoffmann *et al.*, 2015). IFN: interferon; JAK: janus kinase; STAT: signal transducer and activator of transcription; GAF: gamma-activated factor; ISGF3: IFN-stimulated gene factor 3; ISG: IFN-stimulated gene.

#### 1.4.4 *Phlebovirus NSs proteins as antagonists of the human IFN response*

IFN production can have protective effects against bunyavirus infection, which can be illustrated by the high susceptibility to RVFV infection in IFNAR knock out mice, compared to wild-type mice (Bouloy *et al.*, 2001; Cyr *et al.*, 2015; Yadani *et al.*, 1999). During bunyavirus replication, products of each of the three viral RNA segments have the potential to activate IFN induction by the stimulation of RIG-I. As a consequence, bunyaviruses require efficient mechanisms to antagonise the IFN response. It is well-known that the NSs protein of bunyaviruses acts as a major virulence factor, contributing to pathogenesis by assisting the virus to evade the host innate immune system, first demonstrated for BUNV NSs (Bridgen *et al.*, 2001; Weber *et al.*, 2002). The NSs proteins of phleboviruses have also evolved a plethora of countermeasures to block the IFN response.

Within the Sandfly fever group of the *Phlebovirus* genus, the NSs protein of RVFV has been extensively studied. Unlike most phleboviruses, the NSs protein of RVFV localizes to the nuclei of infected cells, forming distinct filamentous structures (Brennan *et al.*, 2014; Cyr *et al.*, 2015; Struthers and Swanepoel, 1982; Yadani *et al.*, 1999). Part of its IFN antagonistic activity is attributed to its nuclear localization, which enables RVFV to inhibit IFN- $\beta$  mRNA synthesis. Initially, RVFV NSs was shown to inhibit general host cell mRNA transcription by inhibiting the assembly of the basal transcription factor IIIH (TFIIH), as described in section 1.1.4 (Billecocq *et al.*, 2004; Cyr *et al.*, 2015; Kalveram *et al.*, 2011; Le May *et al.*, 2004). However, RVFV NSs was shown to employ a different mechanism for the suppression of IFN- $\beta$  mRNA synthesis specifically. This mechanism involved an interaction between RVFV NSs and SAP30 (Sin3A associated protein 30), a protein which forms part of a repressor complex that regulates IFN- $\beta$  gene expression (Le May *et al.*, 2008). The interaction of SAP30 with RVFV NSs and its recruitment to the IFN- $\beta$  promoter results in chromatin structure reorganization, which physically inhibits the recruitment of the CREB-binding protein (CBP) to the IFN- $\beta$  promoter, therefore suppressing histone acetylation and consequently transcriptional activation. RVFV NSs was also shown to support virus replication in infected cells by promoting the post-transcriptional proteasome-dependent down-regulation of the double-stranded RNA-dependent protein kinase (PKR) (Ikegami *et al.*, 2009b; 2009a). Following IFN induction, PKR levels are up-regulated. A dsRNA-binding domain in PKR binds dsRNA generated during virus replication, which triggers its activation (F. Zhang, 2001). Once active, PKR can phosphorylate the eukaryotic initiation factor eIF2 $\alpha$  (Srivastava *et al.*, 1998). eIF2 $\alpha$  is

a subunit of the IF2 initiation complex that is responsible for recruiting initiator<sup>Met</sup>tRNA to the 40S ribosomal subunit in a guanosine triphosphate (GTP)-dependent manner. Phosphorylation of eIF2 $\alpha$  by PKR inhibits the exchange of GDP for GTP, thereby resulting the inhibition of translation initiation due to the inability to recruit the initiator<sup>Met</sup>tRNA to the 43S pre-initiation complex (de Haro *et al.*, 1996). Thus, the proteasomal degradation of PKR by RVFV NSs suppresses the phosphorylation of eIF2 $\alpha$  and in this way prevents the inhibition of translation initiation induced by the IFN response (Habjan *et al.*, 2009b; Ikegami *et al.*, 2009b). Recently, it was shown that the degradation of PKR is mediated by the interaction of RVFV NSs with the F-box proteins FBXW11 and/or FBCW1, through a ‘degron’ sequence in RVFV NSs, which, curiously overlaps with the  $\Omega$ XaV motif at its C terminus (Kainulainen *et al.*, 2016; Mudhasani *et al.*, 2016). It was suggested that perhaps the down-regulation of PKR turns the unfavourable environment induced by suppression of host cell mRNA transcription (by RVFV NSs) in infected host cells to one that supports viral replication, by preventing the inhibition of viral translation (Ikegami *et al.*, 2009a). In this way, the dual functions of RVFV NSs could function concomitantly to inhibit host innate immune responses and to enable efficient RVFV replication (Ikegami *et al.*, 2009b).

Early studies showed that TOSV induced IFN despite the ability of its NSs protein to antagonise the IFN response, which the authors indicate may be a result of a weak IFN antagonistic activity of TOSV NSs (Gori-Savellini *et al.*, 2010). The ability to induce the proteasomal-mediated degradation of PKR by RVFV NSs is a property that is conserved in TOSV NSs (Kalveram and Ikegami, 2013). However, in comparison to RVFV, cellular transcription levels are unaffected following TOSV infection (Kalveram and Ikegami, 2013). Additionally, the type I IFN response was shown to be blocked by TOSV NSs by a direct interaction with RIG-I, and its targeting for proteasomal degradation, thereby preventing RIG-I-mediated IFN induction (Gori-Savellini *et al.*, 2013). In a study where recombinant RVFV encoding PTV or SFSV NSs proteins instead of RVFV NSs were generated, the viruses encoding PTV and SFSV NSs proteins did not affect PKR levels (Kalveram and Ikegami, 2013; Lihoradova *et al.*, 2013). However, the virus encoding PTV NSs was able to suppress host cell mRNA transcription similarly to RVFV, whereas that encoding SFSV NSs had no inhibitory effect of host cell mRNA synthesis (Kalveram and Ikegami, 2013; Lihoradova *et al.*, 2013).

Whilst within the *Phlebovirus* genus most studies have focused on understanding the mechanism employed by mosquito-borne virus NSs proteins to antagonize the IFN response, the role of tick-borne phlebovirus NSs proteins in innate immunity was neglected until the emergence of the novel highly pathogenic SFTSV. Upon the discovery of SFTSV, research efforts focused on understanding its underlying molecular mechanisms of virulence and pathogenicity. Consequently, SFTSV NSs was quickly characterized and was found to form cytoplasmic viroplasm-like structures, also known as inclusion bodies (IBs). The structures were described in infected cells, but also when NSs is expressed in the absence of other viral proteins (Ning *et al.*, 2014; Santiago *et al.*, 2014). The IBs were found to colocalise with lipid droplets and viral dsRNA (X. Wu *et al.*, 2014). Inhibitors of fatty acid synthesis hindered the formation of IBs and virus replication, thus suggesting that NSs-formed IBs play a role in virus replication (X. Wu *et al.*, 2014). However, the confirmation of such conclusion would require the generation of a recombinant SFTSV lacking NSs. Another study found that IBs colocalised with the early endosomal marker Rab5, but not with Golgi apparatus or endoplasmic reticulum markers, suggesting the endosomal system is utilised for the formation of IBs (Santiago *et al.*, 2014). Finally, it was suggested that SFTSV NSs-formed IBs are secreted into the extracellular space, and that the extracellular vesicles containing infectious virions could mediate the receptor-independent transmission of SFTSV, through endocytosis into uninfected neighbouring cells, where they could sustain virus replication (Silvas *et al.*, 2015). As well as the roles suggested by NSs-induced IBs in virus replication and receptor-independent endocytosis, the IBs were described as a novel, elegant strategy that SFTSV employs to antagonise the IFN response. In fact, SFTSV NSs was characterized as a potent antagonist of IFN induction through the spatial isolation and sequestration of TRIM25 and RIG-I (Santiago *et al.*, 2014), TBK1 (Ning *et al.*, 2014; X. Wu *et al.*, 2014), and IRF-3 (Ning *et al.*, 2014; X. Wu *et al.*, 2014) into the IBs. The interaction between IKK $\epsilon$  or IRF-3 and SFTSV NSs was reported to be indirect, facilitated by the interaction with TBK1 (X. Wu *et al.*, 2014). However, one study also showed a direct interaction with IKK $\epsilon$  (Ning *et al.*, 2014). Similarly, while the direct interaction between SFTSV NSs and RIG-I was reported in one study (Santiago *et al.*, 2014), such an interaction was not observed by others (Ning *et al.*, 2014). As well as inhibiting IFN induction, a potent inhibitory activity of SFTSV NSs on IFN signalling was described, and was attributed to the interaction between SFTSV NSs and STAT1 or STAT2. This interaction results in the spatial isolation of STAT1 and STAT2, therefore inhibiting the JAK/STAT signalling pathway (Chaudhary *et al.*, 2015; Ning *et al.*, 2015). Interestingly, a study using liver epithelial cells showed that while

SFTSV NSs strongly inhibited IFN- $\beta$  promoter activation, NF $\kappa$ B activation was enhanced by SFTSV NSs (Q. Sun *et al.*, 2015). The differential effect of SFTSV NSs on IFN- $\beta$  and NF $\kappa$ B promoter activities may explain elevated levels of proinflammatory cytokines and chemokines regulated by NF $\kappa$ B signalling in liver tissues of mice infected with SFTSV (Q. Sun *et al.*, 2015).

Despite our understanding of the role of SFTSV NSs in impairing the IFN response, little is known about the mechanisms utilised by other tick-borne phleboviruses. Recent reviews have highlighted the need of comparative studies to elucidate the countermeasures that phleboviruses have evolved to hinder the IFN response (Ly and Ikegami, 2016; Wuerth and Weber, 2016), as viruses belonging to this genus are continuously emerging and appear to have evolved divergent mechanisms to suppress host cell responses to virus infection.

---

Chapter **2**

AIMS

---

## 2 Aims

It well-known that the main virulence factor evolved by bunyaviruses to counteract the host innate immune system is their non-structural protein NSs. However, it is also evident that we have limited information about the role of tick-borne phlebovirus NSs proteins in modulating the innate immune system.

The overall aim of this project was to carry out a molecular characterization of the NSs protein of the tick-borne phleboviruses UUKV and HRTV, utilizing reverse genetics as a tool to assist with these investigations.

Specifically, I aimed to:

- (i) Develop minigenome and virus-like particle assays for UUKV, as a first step towards developing a reverse genetics system for this virus.
- (ii) Rescue UUKV and exploit the ability to manipulate the UUKV genome to generate recombinant viruses lacking its NSs protein.
- (iii) Compare the ability of UUKV and recombinant UUKV lacking NSs to hinder interferon production.
- (iv) Compare the ability of UUKV and HRTV NSs proteins to block interferon production and interferon signalling, using the well-characterized SFTSV NSs as a comparison.
- (v) Investigate the molecular mechanisms of antagonism employed by UUKV and HRTV NSs proteins at the level of interferon induction and interferon signalling.
- (vi) Sequence the genome of the HRTV stock available in our laboratory and compare it to the published sequence.
- (vii) Develop a reverse genetics system for HRTV.
- (viii) Use the available reverse genetics systems of tick-borne phleboviruses as a molecular tool to assess the possibility of reassortment between tick-borne phleboviruses.

---

Chapter **3**

**MATERIALS**

---

## 3 Materials

### 3.1 Cell culture

#### 3.1.1 Eukaryotic cell lines

The following cell lines were used in this project:

- A549: cell line derived from human lung adenocarcinomic basal epithelial cells. Maintained in Dulbecco's modified Eagle's medium (DMEM) (Thermo Fisher Scientific), supplemented with 10% (v/v) FCS. Their derivative cell line A549/BVDV-Npro (A549/Npro) expresses the bovine viral diarrhea virus (BVDV) Npro protein, which acts as an IFN antagonist by targeting IRF-3 for proteasomal degradation (Hale *et al.*, 2009; Hilton *et al.*, 2006). The A549/PIV5-V (A549/V) cell line is also an A549 derivative, however constitutively expressing the V protein of parainfluenza virus type 5, which blocks type I IFN signalling by targeting STAT1 for degradation (Killip *et al.*, 2013). Selection of the derivative A549 cell lines was maintained by supplementing the medium with 2 µg/ml (Melford Laboratories Ltd.).
- BHK-21 (clone 13): cell line derived from baby hamster kidneys (MACPHERSON and STOKER, 1962). Maintained in Glasgow modified Eagle's medium (GMEM) (Gibco) with 10% (v/v) newborn calf serum (NCS) and 10% (v/v) tryptose phosphate broth (TPB) (Gibco).
- BSR: a BHK-21-derived clone. BSR-T7/5: BSR cells stably expressing the bacteriophage T7 RNA polymerase (Buchholz *et al.*, 1999). Provided by Dr Karl-Klaus Conzelmann (Ludwig-Maximilians-Universität München). Cells were maintained in GMEM with 10% (v/v) foetal calf serum (FCS) and 10% (v/v) TPB, supplemented with 1 mg/ml G418 (Promega) for the selection of cells expressing the T7 RNA polymerase.
- DF-1: chicken fibroblast immortalised cell line derived from 10-day old East Lansing Line (ELL-0) eggs (Foster, 1998), and was maintained in DMEM, supplemented with 10% (v/v) FCS.
- HeLa: cell line derived from human epithelial carcinoma cells (Gey and Coffman, 1952). Maintained in DMEM supplemented with 10% (v/v) FCS.

- HEK-293T: cell line derived from human embryonic kidney cells. Maintained in DMEM with 10% (v/v) FCS, supplemented with 0.1 mM non-essential amino acids (Gibco).
- Huh-Lunet-T7: cell line constitutively expressing the bacteriophage T7 RNA polymerase (Kaul *et al.*, 2007), derived from Huh-7 cells, which are derived from liver carcinoma cells (Nakabayashi *et al.*, 1982). Provided by Dr Ralf Bartenschlager (Universitätsklinikum Heidelberg). The cells were maintained in DMEM supplemented with 10% (v/v) FCS and 0.1 mM non-essential amino acids. Selection was maintained by supplementing the medium with Zeocin (100 µg/ml) (Thermo Fisher Scientific).
- Vero E6: cell line derived from African green monkey kidney cells. Maintained in DMEM, supplemented with 10% (v/v) FCS.

Trypsin-EDTA (0.05%), phenol red was purchased from Gibco.

### **3.1.2 Competent bacterial strains**

Plasmid stocks were generated using the bacterial strain of *E. coli* JM109, genotype *endA1, recA1, gyrA96, thi, hsdR17* ( $r_k^-$ ,  $m_k^+$ ), *relA1, supE44, Δ(lac-proAB)*, [*F' traD36, proAB, laqI<sup>q</sup>ZΔM15*] or CopyCutter<sup>TM</sup> Epi400 chemically competent *E. coli* (Epicentre) genotype *F<sup>-</sup>mcrA Δ(mrr-hsdRMS-mcrBC)Φ80dlacZΔM15 ΔlacX74 recA1 endA1 araD139Δ(ara, leu)7697 galKλ<sup>-</sup> rpsL nupG tonA ΔpcnB dhfr*. Competent bacteria were made chemically competent using the Mix & Go *E. coli* Transformation Kit and Buffer set (Zymo research).

Bacteria were grown at 37°C or room temperature, either on Luria-Bertani (LB) broth or LB agar plates, in the presence of ampicillin (100 µg/ml) for selection of successfully transformed cells.

## **3.2 Virus strains and sequence accession numbers**

### **3.2.1 Virus strains**

The UUKV strain used in this project was derived from the prototype tick isolate S-23 (Oker-Blom *et al.*, 1964), and plaque-purified in chicken embryo fibroblasts (Pettersson and Kääriäinen, 1973). Working stocks of UUKV were generated by passaging the virus at a low multiplicity of infection (MOI) (0.001 FFU/cell) in BHK-21 cells and harvesting the medium 7 days post infection (p.i.).

The HRTV strain used was isolated from a 67-year-old man who received 20 daily tick bites approximately for a period of two weeks (patient 2 in (McMullan *et al.*, 2012)). The patient was hospitalised for twelve days and presented with fatigue, myalgia, severe thrombocytopenia and leukopenia. The patient isolate was a kind gift by Dr Robert Tesh (World Reference Center for Emerging Viruses and Arboviruses, Galveston, TX).

The SFTSV strain used was a plaque-purified cell culture-adapted stock called Hubei 29pp (HB29pp), provided by Amy Lambert (CDC Arbovirus Diseases Branch, Division of Vector-Borne Infectious Diseases, Fort Collins, CO) (Brennan *et al.*, 2015).

Working stocks of HRTV and SFTSV were generated by passaging the viruses once in Vero E6 cells at a low MOI (0.001 PFU/cell), and harvesting the medium 7 days p.i..

Other viruses included in this study are Encephalomyocarditis virus (EMCV), Bunyamwera virus (BUNV), and rBUNVdelNSs2. rBUNVdelNSs2 is a recombinant BUNV that does not express the NSs protein (Hart *et al.*, 2009).

### 3.2.2 Virus sequence accession numbers

Nucleotide sequences for the generation of plasmids were based on the following accession numbers:

**Table 3-1. Virus nucleotide sequence accession numbers used in this study**

| Virus name | Segment | GenBank accession number |
|------------|---------|--------------------------|
| UUKV       | S       | M33551.1                 |
|            | M       | M17417.1                 |
|            | L       | D10759.1                 |
| HRTV       | S       | JX005843.1               |
|            | M       | JX005845.1               |
|            | L       | JX005847.1               |
| SFTSV      | S       | KP202165.1               |
|            | M       | KP202164.1               |
|            | L       | KP202163.1               |

### **3.3 Molecular biology**

#### **2.3.1 Oligonucleotides**

Standard desalted synthetic oligonucleotides at 25nM scale were purchased from Integrated DNA Technologies. All primers used in this project and the purposes for their use are listed in the Appendices (Tables 10-1 to 10-6).

#### **3.3.2 Enzymes**

##### **(i) Restriction enzymes**

Restriction enzymes were purchased from New England BioLabs (BamHI, PstI-HF, Sall-HF) or Promega (BamHI, DpnI, NcoI, NotI, PstI, XhoI) and used throughout the project to confirm successful cloning by restriction enzyme digestion, prior to sequencing cloned plasmids.

##### **(ii) Modifying enzymes**

For PCR, either GoTaq<sup>®</sup> G2 Flexi DNA polymerase (Promega), KOD Hot Start DNA polymerase (Novagen, Merck Millipore) or Q5<sup>®</sup> high fidelity DNA polymerase (New England Biolabs) were used. RQ1 RNase-Free DNase was purchased from Promega. Reverse-transcription (RT) reactions were performed using either GoScript reverse transcriptase (Promega) or PrimeScript RT Reagent Kit with gDNA Eraser (Takara). Quantitative PCR was carried out using SYBR<sup>®</sup> Premix Ex Taq<sup>™</sup> II Mix (Takara). For 3' Rapid Amplification of cDNA Ends (RACE) analysis, RNA was polyadenylated using a Poly(A) Tailing Kit (Thermo Fisher Scientific). Benzonase<sup>®</sup> Nuclease was purchased from Sigma.

#### **3.3.3 Cloning**

In-Fusion<sup>®</sup> HD Cloning Plus kit (Clontech) was used for restriction-free cloning.

#### **3.3.4. Plasmids**

The plasmids used in this project are described in Table 3-2. All listed plasmids contain an ampicillin resistance gene (amp<sup>R</sup>).

**Table 3-2. Plasmids used in this study.**

| Plasmid   | Description   | Source                              |
|---|---|-------------------------------------|
| pT7UUKS(+)<br>pT7UUKM(+)<br>pT7UUKL(+)          | Full-length, antigenomic sense UUKV S, M and L segments, respectively, subcloned into the plasmid pTVT7 (0,0)(Johnson <i>et al.</i> , 2000). The segments are flanked by a bacteriophage T7 promoter at the 5' end, and a hepatitis $\Delta$ ribozyme at the 3' end, followed by a T7 terminator. A silent mutation was introduced in position 963 of pT7UUKS(+), which introduces an XhoI restriction site in UUKV S segment cDNA. | Made during this project            |
| pT7UUKdelNSs(+)                                 | Modified pT7UUKS(+), in which the UUKV NSs open reading frame (ORF) is excised (nucleotides 874-1695), such that the intergenic region is followed directly by the genomic 5' untranslated region (UTR)   | Made during this project            |
| pT7UUKdelNSseGFP(+)                             | Modified pT7UUKS(+), in which the UUKV NSs ORF is replaced by that of enhanced GFP (eGFP), in the same negative-sense orientation.  | Made during this project            |
| pTMUUKN<br>pTMUUKL<br>pTMUUKGnGc                | UUK N and L or GnGc glycoprotein precursor ORFs, respectively, cloned into the expression plasmid pTM1, originally provided by B. Moss (Moss <i>et al.</i> , 1990). The plasmid backbone contains a bacteriophage T7 promoter to drive transcription, followed by an Internal Ribosome Entry Site (IRES) to drive translation.  | Made during this project            |
| pTMFFluc  | pTM1 plasmid encoding <i>Photinus</i> (firefly) luciferase ORF, as previously described (Weber <i>et al.</i> , 2001).   | Provided by Prof Richard M. Elliott |
| pT7UUKSRen(+)<br>pT7UUKMRen(-)<br>pT7UUKLRen(-) | pTVT7 plasmids encoding <i>Renilla</i> luciferase in a negative sense, flanked by the genomic UUKV M or L UTRs, respectively. In the case of pT7UUKSRen(+), the NSs ORF in pT7UUKS(+), was replaced by the <i>Renilla</i> luciferase ORF in the same (negative-sense) orientation.  | Made during this project            |
| pT7HRTS(+)<br>pT7HRTM(+)<br>pT7HRTL(+)          | Full-length, antigenomic sense HRTV S, M and L segments, respectively, subcloned into the plasmid pTVT7 (0,0), as for UUKV.   | Made during this project            |
| pTMHRTN<br>pTMHRTL                              | HRTV N and L ORF, respectively, cloned into the expression plasmid pTM1.  | Made by Dr Benjamin Brennan         |
| pTM1HRTLA3309U                                  | Modified pTMHRTL with a A $\rightarrow$ T mutation at position  | Made during this                    |

|   |   |  |
|---|---|--|
|   | 3309 (genomic sense)  | project  |
| pT7HRTSren(+)<br>pT7HRTMren(-)<br>pT7HRTLren(-) | pTVT7 plasmids encoding <i>Renilla</i> luciferase in a negative sense, flanked by genomic HRTV M or L UTRs, respectively. In the case of pT7HRTSren(+), the NSs ORF in pT7HRTS(+) was replaced by the <i>Renilla</i> luciferase ORF in the same (negative-sense) orientation. | Made during this project   |
| pT7HRTSren(+) <sub>A1751G</sub>                 | Modified pT7HRTSren(+) with a A→G mutation in the HRTV S segment genomic 5' UTR (position 1751).  | Made during this project   |
| pTM1SFTSN<br>pTM1SFTSL                          | SFTSV N and L ORFs, respectively, cloned into the expression plasmid pTM1.  | Dr Benjamin Brennan<br>From (Brennan <i>et al.</i> , 2015).                          |
| pCMVUUKNSs<br>pCMVHRTNSs<br>pCMVSFTNSs          | Mammalian expression vector pCMV (Addgene) encoding wild-type UUKV, HRTV or SFTSV NSs ORFs, respectively, under the control of a cytomegalovirus (CMV) promoter.  | Made during this project   |
| pCMVUUKNSs-V5<br>pCMVHRTNSs-V5<br>pCMVSFTNSs-V5 | Mammalian expression vector pCMV (Addgene) encoding UUKV, HRTV or SFTSV NSs ORF, respectively, which were tagged at the C-terminus with the simian virus 5 (SV5) V5 epitope tag.  | Made during project  |
| p(125)luc                                       | Firefly luciferase reporter construct driven by the murine interferon-β promoter.   | Provided by Ben Hale. From (Yoneyama <i>et al.</i> , 1998).                          |
| pISREluc  | Firefly luciferase reporter construct driven by tandem repeats of the interferon stimulated response element (ISRE).  | Provided by Ben Hale. From (King and Goodbourn, 1998).                               |
| pNFκBluc  | Firefly luciferase reporter construct driven by five tandem copies of the canonical κB element (Chaudhary <i>et al.</i> , 2015).  | Provided by Prof Dong-Yan Jin  |
| pCMV-IκBαSR                                     | CMV-driven plasmid encoding IκBα mutant super-repressor containing mutations S32A and S36A. This mutant acts as an antagonist of NFκB signalling by sequestering NFκB in the cytoplasm.   | Provided by Prof Dong-Yan Jin. Generated as described in (Karl <i>et al.</i> , 2009) |
| phRL  | CMV-driven <i>Renilla</i> luciferase, used as a transfection  | Provided by Ben  |

|                          |  |   |
|--------------------------|--|---|
|                          | control for data normalisation.  | Hale. Initially purchased from Promega.   |
| pCMVRIG-I-N              | Plasmid encoding the RIG-I N-terminus ORF under the control of a CMV promoter.   | Provided by Ben Hale. As described in (Varga <i>et al.</i> , 2011).                                   |
| pCMVRIG-I-N-FLAG         | Plasmids encoding the RIG-I N-terminus, MAVS, TBK-1, IKK $\epsilon$ and TRIF ORFs, respectively, under the control of a CMV promoter in the pcDNA3.1 N-FLAG vector. All ORFs are FLAG-tagged at their N-terminus.  | Provided by Mirco Schmolke. As described in (Varga <i>et al.</i> , 2011, Prins <i>et al.</i> , 2009). |
| pCMVMAVS-FLAG            |  |   |
| pCMVTBK-1-FLAG           |  |   |
| pCMVIKK $\epsilon$ -FLAG |  |   |
| pCMVTRIF-FLAG            |  |   |
| pCMVIRF-3(5D)            | Plasmid encoding the human IRF-3 ORF in its constitutively active form (IRF-3[5D]), under the control of a CMV promoter. In the active, IRF-3(5D), form of IRF-3 the serine-threonine cluster from amino acid 396 to 405 has been mutated to phosphomimetic aspartic acid. | Provided by Mirco Schmolke. As described in (Lin <i>et al.</i> , 1998).                               |

### 3.3.5 Antibodies

#### (i) Primary antibodies

**Table 3-3. Primary antibodies used in this project.**

| Antibody  | Target    | Dilution |       |       |
|---|-----------|----------|-------|-------|
|   |           | WB       | IF    | IP    |
| Mouse anti-UUKV N (generated from hybridoma 8B11A3, kindly provided by Anna Overby) | UUKV N    | 1:100    | -     | -     |
| Rabbit anti-UUKV NSs (IgG purified, kindly provided by Anna Övererby)               | UUKV NSs  | 1:1000   | 1:200 | -     |
| Rabbit anti-HRTV N (Eurogentec)   | HRTV N    | 1:1000   | -     | -     |
| Rabbit anti-HRTV NSs (Eurogentec)   | HRTV NSs  | 1:1000   | 1:200 | 1:100 |
| Rabbit anti-SFTSV N (Eurogentec)  | SFTSV N   | 1:1000   | -     | -     |
| Rabbit anti-SFTSV NSs (Eurogentec)  | SFTSV NSs | 1:1000   | 1:200 | -     |
| Mouse anti- $\alpha$ tubulin (Sigma)  | Tubulin   | 1:5000   | -     | -     |

|  |                                 |        |       |       |
|--|---------------------------------|--------|-------|-------|
| Mouse anti- $\beta$ -Actin (Sigma)                         | Actin                           | 1:5000 | -     | -     |
| Mouse anti-SV5 V5 epitope (Provided by Richard E. Randall) | V5 epitope                      | 1:3000 | 1:250 | 1:250 |
| Mouse anti-FLAG M2 (Sigma)                                 | FLAG M2                         | 1:2000 | -     | 1:500 |
| Rabbit anti-IRF-3 (Santa Cruz Biotech)                     | IRF-3                           | 1:2000 | 1:250 | 1:250 |
| Rabbit anti-IRF-3 Ser386P (Abcam)                          | IRF-3 phosphorylated at Ser386  | 1:1000 | -     | -     |
| Rabbit anti-TBK-1/NAK (Cell signalling)                    | TBK-1/NAK                       | 1:1000 | -     | -     |
| Rabbit anti-STAT 1 (Santa Cruz Biotech)                    | STAT 1                          | 1:1000 | 1:200 | -     |
| Rabbit anti-STAT 2 (Santa Cruz Biotech)                    | STAT 2                          | 1:1000 | 1:200 | -     |
| Rabbit anti-STAT 3 (Santa Cruz Biotech)                    | STAT 3                          | 1:1000 | -     | -     |
| Rabbit anti-STAT 1 Tyr701P (Cell Signalling)               | STAT 1 phosphorylated at Tyr701 | 1:1000 | -     | -     |
| Rabbit anti-STAT 1 Ser727P (Cell Signalling)               | STAT 1 phosphorylated at Ser727 | 1:1000 | -     | -     |
| Rabbit anti-STAT 2 Tyr690P (Cell Signalling)               | STAT 2 phosphorylated at Tyr701 | 1:1000 | -     | -     |

### (ii) Secondary antibodies

**Table 3-4. Secondary antibodies used in this project.**

| Antibody   | Target     | Dilution |       |
|--|------------|----------|-------|
|  |            | WB       | IF    |
| Anti-mouse IgG HRP-linked (Sigma)                      | Mouse IgG  | 1:5000   | -     |
| Anti-rabbit IgG HRP-linked (Cell signalling)           | Rabbit IgG | 1:5000   | -     |
| Anti-mouse Alexa fluor 568 (Thermo Fisher Scientific)  | Mouse IgG  | -        | 1:500 |
| Anti-rabbit Alexa fluor 488 (Thermo Fisher Scientific) | Rabbit IgG | -        | 1:500 |
| Anti-mouse Alexa fluor 488 (Thermo Fisher Scientific)  | Mouse IgG  | -        | 1:200 |
| Anti-rabbit Alexa fluor 532 (Thermo Fisher Scientific) | Rabbit IgG | -        | 1:200 |

## 3.4 Reagents and chemicals

### 3.4.1 Bacterial culture

- Ampicillin sodium was purchased from Formedium and used at 100  $\mu$ g/mL.
- LB agar: 4% (w/v) LB-Agar-Miller (Formedium) diluted in de-ionised H<sub>2</sub>O.
- LB broth: 2.5% (w/v) LB-Broth-Agar-Miller (Formedium) diluted in de-ionised H<sub>2</sub>O.

### **3.4.2 Cell culture**

- PBS: 137 mM NaCl, 15 mM KCl, 10 mM Na<sub>2</sub>HPO<sub>4</sub> ; pH 7.4
- GMEM, DMEM and TPB were purchased from Gibco.
- 2X MEM: 20% (v/v) 10X Modified Eagle's Medium (MEM) (Gibco), 2% (v/v) L-glutamine, 0.435% (v/v) NaHCO<sub>3</sub>, diluted in H<sub>2</sub>O.
- 0.6% Avicel overlay: 1.2% Avicel (purchased from FMC) (w/v in H<sub>2</sub>O) was diluted in a 1:1 ratio with 2X MEM prior to use.
- 10X Neutral Red: PBS, 0.6% neutral red (w/v).
- Crystal violet staining solution: 20% (v/v) ethanol, 1% (v/v) methanol, 0.1% (w/v) crystal violet, diluted in H<sub>2</sub>O.
- Formaldehyde fixing buffer: 8% or 4% (v/v) formaldehyde in PBS.
- TransIT-LT1 transfection reagent was purchased from MirusBio.
- GeneJuice transfection reagent was purchased from EMD Millipore.
- Lipofectamine 2000 was purchased from Invitrogen.
- Opti-Minimum Essential Medium (Opti-MEM) was purchased from Gibco
- Dual Luciferase Assay Reporter Kit was purchased from Promega.
- Ruxolitinib JAK1/2 inhibitor was purchased from Selleck Chemicals.

### **3.4.3 DNA analysis**

- For plasmid isolation from bacterial cultures, the QIAprep Spin Miniprep kit (Qiagen), or the NucleoBond Xtra midiprep kit (Macherey-Nagel) were used.
- Agarose gel: 1-2% (w/v) molecular grade agarose (Bioline) in TAE buffer.
- 10X TAE buffer: 0.4M Tris, 1.142% (v/v) acetic acid, 0.01 M EDTA diluted in H<sub>2</sub>O.
- 1 kb DNA ladder, DNA loading buffer and Ethidium Bromide solution were purchased from Promega.
- Purification and extraction of DNA from agarose gels were performed using the NucleoSpin<sup>®</sup> Gel and PCR Clean-up kit (Macherey-Nagel), or the Wizard<sup>®</sup> SV Gel and PCR Clean-up System (Promega).

### **3.4.4 Total cellular RNA extraction**

Total cellular RNA was extracted using TRIzol<sup>®</sup> (Thermo Fisher Scientific).

### **3.4.5 Immunofluorescence**

- Poly-L-lysine was purchased from Sigma and used at a concentration of 0.1 mg/mL in H<sub>2</sub>O.
- Fixation agent: 4% (v/v) formaldehyde in PBS.
- Permeabilisation solution: 0.5% (v/v) Triton X-100, 20mM sucrose in PBS.
- Mounting medium: Fluoromont-G with DAPI (eBioscience)
- Confocal microscopy was carried out in a Carl Zeiss LSM 710 microscope.

### 3.4.6 Protein analysis and western blotting

- Protein Disruption buffer (PDB): 50 mM Tris-HCl (pH 6.8), 10% (v/v) glycerol, 4% (w/v) SDS, 0.02% (w/v) bromophenol blue. 200 mM dithiothreitol (DTT) was added prior to use.
- NuPAGE Novex (4-12%) Bis-Tris protein gels were purchased from Thermo Fisher Scientific.
- NuPAGE MES SDS running buffer was purchased from Thermo Fisher Scientific.
- 10% Native-PAGE gels were made in house with the following reagents:

**Table 3-5. Reagents used for native PAGE gels.**

| Reagent                                  | Resolving gel | Stacking gel |
|--|---------------|--------------|
| Acrylamide/Bis-acrylamide 30%/0.8% (w/v) | 3.4 mL        | 4.275 mL     |
| 0.375 M Tris-HCl (pH 8.8)                | 6.49 mL       | 0.67 mL      |
| 10% (w/v) ammonium persulfate            | 100 µL        | 50 µL        |
| TEMED                                    | 10 µL         | 5 µL         |

- Native gel running buffer: 25 mM Tris and 192 mM glycine.
- NuPAGE transfer buffer was purchased from Thermo Fisher Scientific.
- Amersham Hybond ECL nitrocellulose membrane was purchased from GE Healthcare Life Sciences.
- Standard blocking buffer: 4% (w/v) skimmed milk powder in PBS/ 0.1% (v/v) Tween-20.
- Standard washing buffer: PBS 0.1% (v/v) Tween-20.
- Tris-buffered saline (TBS): 50 mM Tris-HCl pH 7.5, 150 mM NaCl.
- Blocking buffer for phosphorylated proteins: 3% Bovine Serum Albumin (BSA) (Sigma) in TBS/ 0.1% (v/v) Tween-20.
- Washing buffer for phosphorylated proteins: TBS 0.1% (v/v) Tween-20.

- Western blotting substrate: Clarity™ ECL western blotting substrate (BioRad).

### ***3.4.7 Focus-forming assays***

- Permeabilisation buffer: 0.5% Triton X-100, 20 mM sucrose in PBS.
- Immunodetection substrate: TrueBlue Peroxidase Substrate was purchased from KPL.

### ***3.4.8 Immunoprecipitation***

- RIPA lysis buffer: 50 mM Tris pH 7.5, 150 mM NaCl, 1 mM EDTA, 10% glycerol, 1% nonidet P-40, supplemented with a cocktail of cOmplete protease inhibitors (Roche).
- UUKV NSs immunoprecipitation lysis buffer: 25 mM HEPES pH 7.5, 150 mM NaCl, 50 mM MgCl<sub>2</sub>, 1% Triton X-100, supplemented with a cocktail of cOmplete protease inhibitors (Roche).
- Washing buffer: 50 mM Tris pH 7.5, 150 mM NaCl, 1 mM EDTA, 10% glycerol.
- Magnetic protein A and protein G Dynabeads® were purchased from Thermo Fisher Scientific.
- Protein G agarose beads were purchased from Sigma.
- Anti-FLAG® M2 magnetic beads were purchased from Sigma.

## **3.5 Software packages**

### ***3.5.1 Bioinformatics***

Primer design and sequence analysis were performed with CLC Genomics Benchwork version 7.

### ***3.5.2 Graphing and statistical analysis***

Graphing and statistical analysis were performed using GraphPad Prism version 5.

### ***3.5.3 Imaging***

ZEN (Zeiss) software and ImageJ (Rasband, 1997) were used for imaging and processing of confocal microscopy images.

---

Chapter **4**

METHODS

---

## 4 Methods

### 4.1 Cell culture

#### 4.1.1 Maintenance of eukaryotic cell lines

Cells grown in either 10 cm dishes, 75 cm<sup>2</sup> or 175 cm<sup>2</sup> vented flasks were split 1:10 when 80-90 % cell confluence was reached. Briefly, after the removal of medium, the cells were washed two times with PBS before adding trypsin. Trypsin-treated cells were incubated for 5 min at 37° C. Upon detachment, the cells were resuspended in appropriate fresh cell culture medium. Cultured cells were incubated in a humidified atmosphere at 37° C with 5% CO<sub>2</sub>, except DF-1 cells, which were maintained in a humidified atmosphere at 39° C with 5% CO<sub>2</sub>.

#### 4.1.2 Transfection of eukaryotic cell lines

Transfections were performed using Lipofectamine 2000 (Invitrogen), TransIT-LT1 (MirusBio), or GeneJuice (EMD Millipore) at least 18h after seeding (or when cells reached 70-80% confluence). The total volumes of OptiMEM (Gibco) and transfection reagent used for cell culture vessels of different surface areas (independent of DNA amounts) are shown in Table 4-1.

**Table 4-1. Volumes used for transfections in different cell culture vessels.**

| Cell culture vessel | Volume per well (mL) | Transfection reagent volume (μL) | Total OptiMEM volume (μL) |
|---------------------|----------------------|----------------------------------|---------------------------|
| 24-well plate       | 0.5                  | 1.25                             | 100                       |
| 12-well plate       | 1                    | 2.5                              | 150                       |
| 6-well plate        | 2                    | 5                                | 500                       |

Half of the total volume of recommended OptiMEM (Table 4-1) was mixed with the required amount of plasmid DNA in microcentrifuge tubes (Eppendorf). For experiments performed under Advisory Committee on Dangerous Pathogens (ACDP) category 3 conditions, 2 mL screw-cap micro tubes (Starstedt) were used. The appropriate amount of transfection reagent was resuspended in the remaining OptiMEM, and mixed with the OptiMEM/DNA mix. After incubation at room temperature for 20 min, the mixture was added to the cell culture medium.

### 4.1.3 Minigenome assays

UUKV, HRTV and SFTSV minigenome assays were based on a previously published protocol, developed for the minigenome system of BUNV (Weber *et al.*, 2001). Briefly, sub-confluent monolayers of BSR-T7/5 cells in a 24-well plate were seeded at approximately  $2.5 \times 10^4$  cells per well. The cells were co-transfected the next day with 25 ng pTMFFluc (to measure firefly luciferase activity as an internal control of transfection efficiency and data normalisation), 125 ng of a *Renilla* luciferase-based minigenome plasmid pT7XSren(+), pT7XMren(-) or pT7XLren(-), 250 ng of the expression plasmid pTMXN, and increasing amounts (0-375 ng) (or the indicated amount) of pTMXL (where X refers to UUKV, HRTV or SFTSV). The total amount of plasmid DNA in all reactions was kept constant by addition of empty control plasmid pTM1 to the DNA mix. 24 h post transfection, the cells were washed twice with PBS, lysed and firefly and *Renilla* luciferase activities measured using the Dual Luciferase Reporter Assay system (Promega), as per the manufacturer's instructions.

The *Renilla* luciferase activity was normalised to firefly luciferase activity in the negative control, where no pTMXL was transfected, unless stated otherwise.

### 4.1.4 Virus-like particle assays

UUKV virus-like particle assays were carried out in a similar manner to minigenome assays. Briefly, sub-confluent monolayers of BSR-T7/5 cells in a 24-well plate (seeded at approximately  $5 \times 10^4$  cells per well) were co-transfected with the plasmids described for the UUKV M segment-based minigenome assays: 25 ng pTMFFluc, 125 ng of pT7UUKMren(-), 250 ng of pTMUUKN, and 250 ng pTMUUKL per well. The minigenome transfection mix was supplemented with 125 ng or 250 ng of pTMUUKGnGc, encoding the UUKV glycoproteins. 48 h post transfection, the cell culture supernatant was harvested and clarified by centrifugation at 10,000 rpm for 5 min, digested with 0.5 u/ $\mu$ L benzonase nuclease (Sigma) for 4 h at room temperature, and used for infection of naïve subconfluent BSR-T7/5 cells seeded in 12 well plates, or cells pre-transfected with 250 ng pTM1UUKN and 250 ng pTM1UUKL. Infections were carried out as described in section 4.1.6. *Renilla* and firefly activities were measured 18 h post infection (p.i.) using the Dual Luciferase Reporter Assay system (Promega), as per the manufacturer's instructions.

#### **4.1.5 Virus rescues**

Virus rescues from cDNA clones were carried out using a three- or five-plasmid, T7 RNA polymerase-driven rescue system, as described elsewhere (Lowen *et al.*, 2004). Briefly, BSR-T7/5 cells were seeded in 6-well plates at approximately  $2 \times 10^5$  cells per well, to reach 60-70% confluence the next day. Before transfection, the cell culture medium was replaced by fresh medium containing 2% FCS. In a three-plasmid rescue system, the sub-confluent cells were transfected with 1  $\mu$ g of each rescue plasmid; pT7UUKL(+), pT7UUKM(+), and either pT7UUKS(+), pT7UUKdelINSs(+), or pT7UUKdelINSs(+) for the generation of recombinant UUKV (rUUKV), rUUKdelINSs, or rUUKdelINSsGFP, respectively. In a five-plasmid rescue system, 250 ng pTM1UUKN and 250 ng pTM1UUKL were added to the DNA mix. Transfected cells were incubated at 37 °C for 7 days, the supernatant clarified by centrifugation at 10,000 rpm for 5 min, and stored at -80 °C for future use. Viral titres of rescued viruses were determined by focus-forming assays on BSR cells.

HRTV rescues were carried out as described for UUKV, with the appropriate plasmids.

#### **4.1.6 Virus infections**

Cells were seeded at  $1-3 \times 10^5$  or  $2-6 \times 10^5$  cells per well in 12- or 6-well plates, respectively, to reach approximately 70% confluence the next day. Appropriate virus dilutions were made in PBS with 2% (v/v) FCS. The cell culture medium was removed, replaced with virus inoculum (150 or 300  $\mu$ L per well in 12-well or 6-well plates) and incubated at 37 °C for one hour. Following virus adsorption, the inoculum was removed, the infected cells were washed three times with PBS, and replaced with the appropriate cell culture medium. Replacement with cell culture medium was considered time point 0 h p.i.

#### **4.1.7 Preparation of virus stocks**

Stocks of wild-type and recombinant UUKV were generated by passaging the viruses at a low multiplicity of infection (MOI) (0.01 focus forming units [FFU]/cell) in BSR cells. The cell culture medium from sub-confluent BSR cells in a 75 cm<sup>2</sup> flask was removed and replaced with the virus inoculum in PBS 2% (v/v) FCS. After 1 h incubation at 37 °C, the inoculum was removed, infected cells washed three times with PBS, and fresh cell culture medium containing 2% (v/v) NCS added. Flasks were incubated at 33 °C and harvested 6 or 7 days p.i. The supernatant was then clarified by centrifugation at 5,000 rpm for 10 min, aliquotted and stored at -80 °C for future use.

HRTV and SFTSV stocks were prepared by Dr Benjamin Brennan in a similar manner as described above, except the viruses were grown in Vero E6 cells (Brennan *et al.*, 2015).

#### ***4.1.8 Determination of virus titre by focus- or plaque-forming assays***

Focus-forming assays for UUKV were performed in monolayers of confluent BSR or BHK-21 cells. After removal of the medium, 10-fold serial dilutions of the virus inoculum (in PBS/2% (v/v) FCS) were added to the cell monolayers. Following 1 h incubation at 37 °C, the cells were overlaid with an MEM overlay supplemented with 2% FCS or NCS and 0.6% Avicel. The assays were incubated for 5 to 6 days, and fixed with formaldehyde fixing buffer for 1 h. After fixation, the monolayer was treated for 30 min with permeabilisation solution, and incubated for 2 h with mouse anti-UUKV N antibody 8B11A3 (1:100 (v/v) in standard blocking buffer). Next, the plates were washed three times in standard washing buffer, and incubated for 1 h with anti-mouse HRP-linked antibody (1:5000 (v/v) in standard blocking buffer). After repeated washing with PBS, foci were detected by adding TrueBlue peroxidase substrate (enough to cover the wells) at room temperature for approximately 20 min. The plates were finally rinsed with distilled water and let to dry upside down protected from light.

For HRTV and SFTSV, virus titres were determined through plaque assays in Vero E6 cells, as described for UUKV, except following fixation, the cell monolayers were stained using crystal violet staining solution to visualise virus plaques.

Virus titres were calculating using the following equation:

$$\text{Virus titre} \left( \frac{\text{PFU or FFU}}{\text{mL}} \right) = \frac{\text{Number of plaques or foci (p.f.u. or f.f.u.)}}{d \times v \text{ (mL)}}$$

, where d= dilution for the well where the number of plaques was counted, v = volume of inoculum, PFU=plaque-forming unit and FFU= focus-forming unit.

When investigating the effect of the JAK1/2 inhibitor Ruxolitinib (Selleck Chemicals) on focus size, focus assays were performed as described above for UUKV, and the avicel overlay was supplemented with 0.4 µM ruxolitinib, or the equivalent volume of the vehicle control DMSO. For HRTV and SFTSV, the primary antibodies used in focus assays were rabbit anti-HRTV N antibody (1:1000 (v/v) in blocking buffer), or rabbit anti-SFTSV N antibody (1:1000 (v/v) in blocking buffer), and the secondary antibody used was anti-rabbit HRP-linked antibody (1:5000 (v/v) in blocking buffer).

### 4.1.9 Immunofluorescence

For immunofluorescence of infected cells, Vero E6, BHK-21, or A549 cells were seeded in 12-well plates with 30 mm coverslips at a cell density of  $1 \times 10^5$  cells per well. For immunofluorescence of transfected cells, HEK293T cells were seeded in coverslips pre-treated with poly-L-lysine (Sigma). Briefly, before seeding the cells, enough poly-L-lysine (0.1 mg/mL in H<sub>2</sub>O) was added to the coverslips to cover the surface, and incubated at room temperature for 30 min. Next, the poly-l-lysine was removed, the coverslips washed three times in distilled H<sub>2</sub>O, and the cells seeded at a cell density of  $1.5 \times 10^5$  cells per well in a 12-well plate.

Transfections or infections were carried out as explained in sections 4.1.2 or 4.1.6, respectively. At the indicated time points, the cells were fixed in fixation agent for 1 h and permeabilised in permeabilisation solution for 30 min. The coverslips were then probed with the primary antibody diluted at the appropriate concentration (see Table 3-3) in PBS 2% (v/v) FCS and incubated overnight at 4 °C in a humid chamber. Following washing five times with PBS 0.1% (v/v) Tween-20, the coverslips were incubated for 1 h at room temperature with the secondary antibodies diluted in PBS 2% (v/v) FCS (see Table 3-4). A second washing step was performed, followed by washing twice with distilled H<sub>2</sub>O, prior to mounting the coverslips in microscope slides using 5µL mounting medium with DAPI. The slides were stored at 4 °C until use.

### 4.1.10 Luciferase assays

#### (i) IFN- $\beta$ reporter assays

To assess the effect of tick-borne phlebovirus NSs proteins had on antagonising the IFN induction pathway,  $5 \times 10^4$  HEK293T cells were seeded per well in a 24-well plate. The next day, subconfluent cell monolayers were co-transfected with 250 ng pCMVXNSs or pCMVXNSs-V5 (where X refers to UUKV, HRTV or SFTSV), along with 50 ng of plasmids encoding various stimuli of the IFN- $\beta$  promoter (pCMVRIG-I-N-FLAG, pCMVMAVS-FLAG, pCMVTBK-1-FLAG, pCMVIKK $\epsilon$ -FLAG, or pCMVIRF-3[5D]) per well. Additionally, 375 ng p(125)luc and 2.5 ng of the *Renilla* control phRL per well were included in the plasmid mastermix. The total amount of plasmid added to each reaction was kept constant by topping up the DNA mix with empty pCMV plasmid. 18 h post transfection, cell monolayers were washed once in PBS and lysed for *Renilla* and firefly

quantification using the Dual-Luciferase Reporter system (Promega) following the manufacturer's instructions.

**(ii) ISRE reporter assay**

The protocol for investigating the effect of NSs proteins on antagonising IFN signalling was carried out similarly to the IFN- $\beta$  reporter assays, except 375 ng of pISREluc (and not p[125]luc) was used per well. 24 h post transfection, the cell culture medium was replaced by fresh medium with or without 250 U of IFN- $\beta$  per well. 18 h post treatment, the cell monolayers were washed with PBS and lysed for *Renilla* and firefly quantification using the Dual-Luciferase Reporter system (Promega) following the manufacturer's instructions.

**(iii) NF $\kappa$ B reporter assay**

To assess the effect of NSs proteins on NF- $\kappa$ B signalling, HEK293T cells were seeded at a cell density of  $5 \times 10^4$  cells per well in a 24-well plate. The next day, subconfluent cell monolayers were co-transfected with 150 ng pCMVXNSs, pCMVXNSs-V5, (where X refers to UUKV, HRTV or SFTSV) or the control pCMV-I $\kappa$ B $\alpha$ SR, along with 200 ng pNF- $\kappa$ Bluc and 5 ng of the *Renilla* control phRL, per well. The total amount of plasmid added to each reaction was kept constant by topping up the DNA mix with empty pCMV plasmid. 18 h post transfection, the cell culture supernatant was replaced by fresh medium containing TNF- $\alpha$  (5 ng per well), or mock-treated. 24 h post treatment with TNF- $\alpha$ , transfected cells were lysed using the Dual-Luciferase Reporter system (Promega), and *Renilla* and firefly values quantified following the manufacturer's instructions.

**4.1.11 Biological interferon protection assays**

Biological IFN protection assays were performed upon transfection or infection of HEK293T cells or A549 cells, respectively. When measuring the biological IFN response following virus infection, IFN-competent A549 cells seeded at  $3 \times 10^5$  cells per well in a 6 well plate were infected with the relevant virus at the indicated MOI, as described in section 4.1.6, and incubated at 37 °C. 24 h p.i. the cell culture supernatant was collected and transferred to a fresh 6-well plate for ultraviolet (UV) light inactivation. Virus was inactivated by UV irradiation using a UV lamp (8W, 254 nm at a distance of approximately 2 cm for 4 min with occasional shaking).

In the case of transfections, HEK293T cells seeded at  $4 \times 10^5$  cells per well in 6-well plates were co-transfected with 0-250 ng pCMXNSs, or pCMVXNSs-V5 (where X refers to

UUKV, HRTV or SFTSV), along with and 12.5 ng pCMVRIG-I N-FLAG. 24 h post transfection, the cell culture supernatant was collected and handled as described below.

Two-fold serial dilutions of the inactivated supernatant or supernatant from transfected cells were made in fresh cell culture medium containing 2 % (v/v) serum. The serial dilutions were used to replace the cell culture medium of IFN-incompetent A549/Npro cells, which were seeded the day before at  $1 \times 10^4$  cells per well in a 96-well plate. 24 h following pre-treatment of A549/Npro cells, 100  $\mu$ L of encephalomyocarditis virus (EMCV) (which was diluted in cell culture medium) was added to each well, at an MOI 0.03 PFU per cell. Four days post infection with EMCV, the cells were fixed with formaldehyde fixing buffer for 30 min and stained with crystal violet staining solution to visualize EMCV-induced destruction of monolayers. The relative amount of biological IFN produced was calculated as  $2^N$ , where N is the number of two-fold dilutions resulting in protection of A549/Npro cells.

#### ***4.1.12 Biosafety***

All work involving infectious Hazard Group 3 pathogens (HRTV and SFTSV) was performed under containment level 3 conditions to ensure appropriate and effective biocontainment, as approved by the UK Health and Safety Executive. UUKV work was performed under containment level 2 conditions

## **4.2 Manipulation of nucleic acids and cloning**

### ***4.2.1 DNA amplification by PCR***

Polymerase Chain Reactions (PCR) were performed to amplify DNA, using KOD HotStart DNA polymerase (Merck) or Q5<sup>®</sup> high fidelity DNA polymerase (New England Biolabs) for high-fidelity reactions, and GoTaq<sup>®</sup> G2 Flexi DNA polymerase (Promega) for low-fidelity PCR reactions. The following conditions for 50  $\mu$ L reactions were used for each of the polymerases, according to the manufacturer's instructions:

*KOD HotStart DNA polymerase*Reaction components

|        |                           |
|--------|---------------------------|
| 5 µL   | 10X KOD polymerase buffer |
| 5 µL   | dNTP mix (2 mM each)      |
| 3 µL   | MgSO <sub>4</sub> (25 mM) |
| 1.5 µL | Forward 5' primer (10 µM) |
| 1.5 µL | Reverse 3' primer (10 µM) |
| 1 µL   | template DNA (1-10 ng)    |
| 1 µL   | KOD polymerase (1 U)      |
| 32 µL  | ddH <sub>2</sub> O        |

PCR conditions

|                      |          |           |           |
|----------------------|----------|-----------|-----------|
| Initial denaturation | 95 °C    | 5 min     | 30 cycles |
| Denaturation         | 95 °C    | 30 sec    |           |
| Annealing            | 52-56 °C | 30 sec    |           |
| Extension            | 70 °C    | 25 sec/kb |           |
| Final extension      | 70 °C    | 10 min    |           |
| Hold                 | 95 °C    | ∞         |           |

*Q5<sup>®</sup> high fidelity DNA polymerase*Reaction components

|         |                            |
|---------|----------------------------|
| 10 µL   | 5X Q5 reaction buffer      |
| 1 µL    | dNTP mix (10 mM)           |
| 2.5 µL  | Forward 5' primer (10 µM)  |
| 2.5 µL  | Reverse 3' primer (10 µM)  |
| 1 µL    | template DNA (1-10 ng)     |
| 0.5 µL  | Q5 HF DNA polymerase (1 U) |
| 32.5 µL | ddH <sub>2</sub> O         |

PCR conditions

|                      |          |           |           |
|----------------------|----------|-----------|-----------|
| Initial denaturation | 98 °C    | 5 min     | 30 cycles |
| Denaturation         | 98 °C    | 10 sec    |           |
| Annealing            | 52-56 °C | 30 sec    |           |
| Extension            | 72 °C    | 25 sec/kb |           |
| Final extension      | 72 °C    | 2 min     |           |
| Hold                 | 4 °C     | ∞         |           |

*GoTaq<sup>®</sup> G2 Flexi DNA polymerase*Reaction components

|          |                                     |
|----------|-------------------------------------|
| 5 µL     | 5X GoTaq Flexi buffer               |
| 1 µL     | dNTP mix (10 mM)                    |
| 3 µL     | MgSO <sub>4</sub> (25 mM)           |
| 1.5 µL   | Forward 5' primer (10 µM)           |
| 1.5 µL   | Reverse 3' primer (10 µM)           |
| 1 µL     | template DNA (1-10 ng)              |
| 0.25 µL  | GoTaq G2 Flexi DNA polymerase (1 U) |
| 36.75 µL | ddH <sub>2</sub> O                  |

PCR conditions

|                      |          |         |           |
|----------------------|----------|---------|-----------|
| Initial denaturation | 95 °C    | 5 min   | 30 cycles |
| Denaturation         | 95 °C    | 30 sec  |           |
| Annealing            | 52 -56°C | 30 sec  |           |
| Extension            | 72 °C    | 1min/kb |           |
| Final extension      | 72 °C    | 10 min  |           |
| Hold                 | 4 °C     | ∞       |           |

PCR products were analysed by agarose gel electrophoresis, as described in section 4.2.1. Primer annealing temperatures varied between 52-56 °C, depending on the primer melting temperature. Extension times varied according to the length of the DNA to be amplified and the rate of DNA polymerase extension rate.

### ***4.2.2 Site-directed mutagenesis***

Site-directed mutagenesis was performed by quick-change PCR, allowing the introduction of specific point mutations into plasmids. Complementary primers were designed such that they were between 30 and 40 nt long and the desired point mutation introduced in the center of the primer, flanked by nucleotides complementary to the target region of the plasmid. The PCR was performed using KOD HotStart DNA polymerase or Q5<sup>®</sup> high fidelity DNA polymerase, as described in section 3.2.1, except 18 cycles were performed and 1 ng of template plasmid used. Following the PCR, the reaction was digested with 2 units of DpnI enzyme at 37 °C for 2-4 h. 4 µL of the Dpn-I treated PCR products were then used to transform JM109 bacteria, as described in section 4.1.5.

### ***4.2.3 Agarose gel electrophoresis and gel extraction***

PCR, or restriction digest DNA fragments were separated in agarose gels consisting of 1-2% (w/v) agarose and 0.04 µg/mL ethidium bromide in 1X TAE buffer. The gel was submerged in 1X TAE buffer and samples with 1X loading dye (Promega) loaded, along with a 1kb DNA ladder (Promega). Electrophoresis was performed at 100V for at least 20 min, until the desired separation of DNA fragments was achieved. DNA was visualized under a UV transilluminator. If the fragments were required for purification, gel extraction from the gel matrix was carried out using the NucleoSpin<sup>®</sup> Gel and PCR Clean-up kit (Macherey-Nagel), or the Wizard<sup>®</sup> SV Gel and PCR Clean-up System (Promega), according to the manufacturer's instructions.

### ***4.2.4 Restriction-free cloning***

Insertion of desired gene targets into vectors was carried out using restriction-free cloning. Vectors were linearized using restriction enzymes, or by excision PCR, using excision primers designed such that their 5' end would anneal to the 3' boundary of the region to be excised, in order to generate blunt-ended products of the vector. Primers for the desired insert were designed such that their 5' end contained 15 bases homologous to each end of the linearised vector. Their 3' end was designed to be of 15-25 nucleotides in length and homologous to the target sequence that was going to be cloned into the vector. In this way, the target insert contains 15 nt overhangs at each end, which are complementary to the blunt-ended vector. Digests or amplified products were gel-purified as described above, and used for an In-Fusion cloning reaction using the In-Fusion<sup>®</sup> HD Cloning Plus kit (Clontech). Briefly, a reaction was set up containing 100 ng of insert with 15 nt overhangs,

100 ng of linearised vector, 2  $\mu\text{L}$  5X In-Fusion HD enzyme premix, and the volume adjusted to 10  $\mu\text{L}$  with ddH<sub>2</sub>O. The reaction was incubated for 15 min at 50 °C and placed on ice. 5  $\mu\text{L}$  of the reaction were used to transform 100  $\mu\text{L}$  competent JM109 as described below.

#### ***4.2.5 Bacterial transformation and plasmid isolation***

##### ***(i) Bacterial transformation***

The *E. coli* strain JM109 were made chemically competent using the Z-competent *E. coli* Transformation kit and Buffer set (Zymo Research). 100  $\mu\text{L}$  competent JM109 were thawed on ice and transformed with 2-10  $\mu\text{L}$  plasmid DNA (1-50 ng) by incubating the cells with DNA for 5 min on ice. Cells were then spread on LB agar plates with ampicillin (100  $\mu\text{g}/\text{ml}$ ), and incubated at room temperature for 48 h, or at 37 °C overnight.

##### ***(ii) Small scale, single colony bacterial culture plasmid preparation***

Single colonies of transformed *E. coli* were picked using a P200 pipette tip and incubated by shaking at 180 revolutions per minute (rpm) in 5 mL LB broth containing ampicillin (100  $\mu\text{g}/\text{ml}$ ). The culture was incubated at room temperature for 48 h, or at 37 °C overnight. Plasmid DNA was isolated using the Qiagen QIAprep Spin Miniprep Kit (Qiagen), according to the manufacturer's instructions. To confirm whether cloning was successful, isolated plasmids were screened using restriction enzyme digestion (section 3.2.6) and the DNA fragments analysed by agarose gel electrophoresis (section 3.2.3). If the digested plasmid DNA products were correct, the small-scale plasmid preparation was sent for Sanger sequencing (Source BioScience) before preparation of large-scale bacterial cultures.

##### ***(iii) Large scale bacterial culture plasmid preparation***

Large-scale bacterial cultures were generated by inoculating 100 mL LB containing ampicillin (100  $\mu\text{g}/\text{ml}$ ) with 100  $\mu\text{L}$  of a small-scale bacterial culture, and grown at room temperature for 48 h or at 37 °C overnight in a shaking incubator (180 rpm). Plasmid DNA isolation was carried out using the NucleoBond Xtra midiprep kit (Macherey-Nagel), following the manufacturer's instructions.

#### ***(iv) Quantification of DNA***

Quality and quantity of isolated DNA was analysed using the NanoDrop-2000 spectrophotometer (Thermo Fisher Scientific).

#### ***4.2.6 Restriction enzyme digestion***

Endonuclease restriction digests were performed in order to linearise vectors for cloning, or to corroborate cloning results. The reaction was made up to a final volume of 50  $\mu$ L with nuclease-free water, 1X appropriate restriction enzyme buffer, 2 units of restriction enzyme, and 0.5-2  $\mu$ g DNA. The reaction was incubated at 37 °C for 1-4 h, and subjected to agarose gel electrophoresis and gel extraction before use (if needed).

#### ***4.2.7 Total cellular RNA extraction***

Total cellular RNA was extraction from infected or transfected cells was carried out by washing the cell monolayer in 6-well plates with PBS. This was followed by the addition of 1000  $\mu$ L TriZol reagent (Thermo Fisher Scientific) and incubation for 5 min at room temperature. Next, the TriZol reagent was placed in 2 mL screw-cap micro tubes and 240  $\mu$ L chloroform added to the samples. The tube was inverted 10 times before centrifugation at 12,000 rpm for 20 min at 4 °C. The aqueous phase was removed, transferred to a fresh tube containing 500  $\mu$ L isopropanol, mixed and incubated at room temperature for 5 min. The samples were centrifuged at 12,000 rpm for 10 min at 4 °C, the supernatant removed, and the pellet washed with 500  $\mu$ L ice-cold 75% (v/v) ethanol. The ethanol-soaked pellets were then centrifuged at 12,000 rpm for 10 min at 4 °C, the supernatant removed, and the pellet left to air-dry prior to resuspension in 30-50  $\mu$ L nuclease-free water. The quality and quantity of isolated RNA was analysed using the NanoDrop-2000 spectrophotometer (Thermo Fisher Scientific).

#### ***4.2.8 cDNA synthesis***

Reverse-transcription (RT) was used for the generation of cDNA, which was used for real-time qPCR analysis, or for sequencing of the HRTV genome and confirming sequences of recombinant UUKV.

PrimeScript RT reagent kit with gDNA eraser (Takara) was used for generation of cDNA to perform gene expression analysis through real-time qPCR. Briefly, 1  $\mu$ g of extracted RNA was mixed with 2  $\mu$ L 5X gDNA eraser buffer and 1  $\mu$ L gDNA eraser, and the volume adjusted to 10  $\mu$ L with nuclease-free H<sub>2</sub>O before incubation at 42 °C for 2 min.

The reaction was mixed with 10  $\mu\text{L}$  of a prepared mastermix, which contained 4  $\mu\text{L}$  5X PrimeScript Buffer 2, 1  $\mu\text{L}$  PrimeScript RT Enzyme mix I, 4  $\mu\text{L}$  RT primer mix (containing Oligod(T) primer and random 6-mers), and 1  $\mu\text{L}$  nuclease-free  $\text{H}_2\text{O}$ . The 20  $\mu\text{L}$  reaction was incubated at 37  $^\circ\text{C}$  for 15 min, followed by 85  $^\circ\text{C}$  for 5 sec, and stored at -20  $^\circ\text{C}$  for future use in RT-qPCR.

For the preparation of UUKV and HRTV cDNA for full-genome sequencing, the GoScript reverse transcription kit (Promega) was used. Briefly, 1 or 2  $\mu\text{g}$  extracted RNA and 1  $\mu\text{L}$  of the appropriate gene-specific primer (1  $\mu\text{M}$ ) were diluted to a total volume of 5  $\mu\text{L}$  in nuclease-free water, and heated at 70  $^\circ\text{C}$  for 5 min. The reaction was immediately chilled on ice for at least 5 min, before adding 15  $\mu\text{L}$  of a RT reaction mix (4  $\mu\text{L}$  GoScript 5X reaction buffer, 3  $\mu\text{L}$   $\text{MgCl}_2$  [25 mM], 1  $\mu\text{L}$  PCR nucleotide mix [10 mM each dNTP], 20 units RNasin, 1  $\mu\text{L}$  GoScript reverse transcriptase, made up to 15  $\mu\text{L}$  with nuclease-free  $\text{H}_2\text{O}$ ). The 20  $\mu\text{L}$  reaction was annealed at 25  $^\circ\text{C}$  for 5 min, extended at 42  $^\circ\text{C}$  for 60 min, and inactivated at 70  $^\circ\text{C}$  for 15 min. The cDNA was stored at -20 $^\circ\text{C}$  for amplification by PCR as described in section 3.2.1. All incubations were performed in a thermocycler.

#### ***4.2.9 Rapid amplification of complementary DNA ends (RACE)***

3' Rapid Amplification of cDNA Ends (RACE) analysis on total cellular RNA of virus-infected cells allowed the determination of 5' and 3' terminal viral S, M, and L sequences using sequence-specific primers, as described elsewhere (Tilston-Lunel *et al.*, 2015). Briefly, DNase-treated extracted RNA was polyadenylated a Poly(A) Tailing Kit (Ambion) at 37  $^\circ\text{C}$  for 1 h, following the manufacturer's instructions. The reaction was purified using an RNeasy kit (QIAGEN), and 12  $\mu\text{L}$  of the polyadenylated RNA used for RT using an oligo-d(T) primer (Primer sequence found in Table 10-1, Appendices) and GoScript reverse transcriptase, as described in section 3.2.8. 2  $\mu\text{L}$  of the cDNA reaction were then used for PCR using a 5' gene-specific primer to amplify genomic or antigenomic S, M or L segment terminal sequences, and a 3' PCR anchor primer (Roche) (Primer sequences found in Table 10-1, Appendices). The resulting PCR fragments were analysed through agarose gel electrophoresis, gel extracted, and subjected to Sanger sequencing.

#### ***4.2.10 Real-time qPCR***

Real-time quantitative PCR (RT-qPCR) was used for gene expression analysis, to measure the mRNA levels of various genes in HEK293T cells in response to different stimuli. Following RT, the cDNA was diluted 1: 10 (v/v) in nuclease-free water, and 2  $\mu\text{L}$  of the

diluted cDNA were used to set up a 20  $\mu\text{L}$  RT-qPCR reaction. The remaining 18  $\mu\text{L}$  were made as a mastermix which contained 0.4  $\mu\text{L}$  forward primer (10  $\mu\text{M}$ ), 0.4  $\mu\text{L}$  reverse primer (10  $\mu\text{M}$ ), 0.4  $\mu\text{L}$  50X ROX reference dye, 10  $\mu\text{L}$  SYBR Premix Ex Taq II, and 6  $\mu\text{L}$  nuclease-free  $\text{H}_2\text{O}$ . These reagents were provided in the SYBR® Premix Ex Taq™ II Mix (Takara). The RT-qPCR reactions were carried out in triplicate in a ABI StepOnePlus (Applied Biosystems) RT-PCR machine, using the following cycling conditions:

|                         |       |        |                           |
|-------------------------|-------|--------|---------------------------|
| Initial denaturation    | 95 °C | 30 sec |                           |
| Denaturation            | 95 °C | 5 sec  | 40 cycles                 |
| Annealing and extension | 60 °C | 30 sec |                           |
| Melt curve              | 95 °C | 15 sec |                           |
|                         | 60 °C | 1 min  | 0.1°C increase per second |
|                         | 95 °C | 15 sec |                           |

The relative expression of mRNA was calculated using a double delta Ct analysis, whereby the cycle threshold (Ct) of a target gene ( $Ct_x$ ) is compared to a reference, housekeeping gene that has constitutive expression. In this project, GAPDH was used as the reference gene. The following steps were followed to calculate relative mRNA expression:

The double  $\Delta\Delta\text{Ct}$  was calculated as:

$$\Delta\Delta\text{Ct} = (Ct_{x,\text{Control}} - Ct_{\text{GAPDH},\text{Control}}) - (Ct_{x,\text{Sample}} - Ct_{\text{GAPDH},\text{Sample}})$$

, where

$Ct_{x,\text{Control}}$  = Ct value of gene of interest in untreated, control sample

$Ct_{\text{GAPDH},\text{Control}}$  = Ct value of GAPDH in untreated, control sample

$Ct_{x,\text{Sample}}$  = Ct value of gene of interest in experimental sample

$Ct_{\text{GAPDH},\text{Sample}}$  = Ct value of reference gene GAPDH in experimental sample

Assuming that the amount of PCR product for each sample and each primer is inversely proportional to  $2^{\text{Ct}}$ , then the ratio of the target gene to GAPDH is calculated as:

$$\text{Ratio} = \frac{2^{(Ct_{x,\text{Control}} - Ct_{\text{GAPDH},\text{Control}})}}{2^{(Ct_{x,\text{Sample}} - Ct_{\text{GAPDH},\text{Sample}})}}$$

Or

$$\text{Ratio} = 2^{\Delta\Delta\text{Ct}}$$

## **4.3 Protein analysis**

### **4.1.1 Luciferase assays**

Luciferase assays were carried out using the Dual-Luciferase Reporter system (Promega) following the manufacturer's instructions. *Renilla* and firefly luciferase were measured using a GloMax 20/20 single tube luminometer (Promega), with a 10 second integration time for each reading.

### **4.1.2 Western blot analysis**

#### **(i) Preparation of cell lysates**

Cell monolayers in 12-well or 6-well plates were lysed in 150 or 300  $\mu$ L protein disruption buffer (PDB), respectively, and collected in 2 mL screw-cap tubes. The samples were boiled at 100 °C for 10 min and stored at -20 °C until use.

#### **(ii) Polyacrylamide gel electrophoresis (PAGE)**

20 to 30  $\mu$ L of the cell lysates were loaded on to precast NuPAGE Novex 4-12% Bis-Tris gels for PAGE under denaturing conditions, or on 10% native PAGE gels for PAGE under native conditions. Gel electrophoresis for the separation of protein was achieved by using using 1X MES SDS running buffer for denaturing conditions, or native gel running buffer for native conditions, at 180 V for 50-60 min.

#### **(iii) Protein transfer**

Proteins were transferred using a semi-dry method on to a nitrocellulose membrane (0.45  $\mu$ m pore size, Amersham) with a Trans-Blot Turbo Blotting system (BioRad). All components of the transfer were soaked in 1X NuPage transfer buffer, and the transfer performed at a constant voltage of 10V for 50 min.

#### **(iv) Detection**

Following transfer, the membrane was blocked for 1h at room temperature in western blotting standard blocking buffer, or blocking buffer for phosphorylated proteins. Primary antibodies were diluted in blocking buffer and incubated with the membrane at either room temperature for 1 h or at 4 °C overnight in constant rotation in 50 mL falcon tubes. The overnight incubation step was especially important for the following antibodies: UUKV N, UUKV NSs, anti-IRF-3, anti-IRF-3 Ser386, anti-STAT 1, anti-STAT 2, anti-STAT 3, anti-

STAT 1 Tyr701P, anti-STAT 1 Ser727P, anti-STAT 2 Tyr690P (Table 3-3). After washing, the membrane was washed at least three times with western blotting washing buffer, and incubated with the relevant secondary antibody diluted in blocking buffer for 1 h at room temperature.

Following incubation with the secondary antibody, the membrane was washed three times in washing buffer and placed on a plastic film. Proteins were detected using Clarity™ ECL western blotting substrate (BioRad) and visualised in a ChemiDoc MP Imaging system (BioRad).

### ***4.1.3 Co-immunoprecipitation***

Co-immunoprecipitation (Co-IP) was carried out either on transfected or infected cell monolayers. For transfections,  $4 \times 10^5$  HEK293T cells were seeded in 6-well plates and transfected with 1  $\mu$ g pCMVXNSs-V5 (where X refers to UUKV, HRTV or SFTSV), or mock-transfected. In some cases, the plasmids were transfected along with with 1  $\mu$ g pCMVRIG-I-N-FLAG, pCMVMAVS-FLAG, pCMVTBK-1-FLAG, pCMVIKK $\epsilon$ -FLAG, or pCMVIRF-3(5D). For Co-IP of NSs proteins in virus-infected cells, HEK293T or A549 cells were infected with UUKV or HRTV at an MOI of 20 or 10 FFU/cell, respectively. At the indicated time point, cells were lysed in RIPA lysis buffer or UUKV NSs IP lysis buffer (specifically for UUKV NSs IP), and incubated by rotation at 4°C for 30 min. For the IP of HRTV NSs, cells were lysed on ice for 30 min, the cell lysates transferred to a tube and removed from containment level 3 conditions, before incubation by rotation for another 30 min at 4°C. The cell lysates were clarified by centrifugation at 12,000 rpm for 20 min at 4°C, and transferred to a fresh tube. Note at this stage the whole cell lysate (WCL) fraction was also taken.

For co-IP of FLAG-tagged proteins, anti-FLAG M2 magnetic beads (Sigma) were used. For co-IP of UUKV or HRTV NSs proteins, clarified cell lysates were incubated overnight at 4°C with rabbit polyclonal anti- UUKV or HRTV NSs antibodies, followed by the addition of Protein A magnetic Dynabeads® (Thermofisher). For co-IP of V5-tagged proteins, clarified cell lysates were incubated overnight at 4°C with mouse anti-V5 antibody, followed by the addition of Protein G magnetic Dynabeads® (Thermofisher). All beads were used according to the manufacturer's instructions. Following incubation of the cell lysates with the beads for 1.5 h at 4°C, the beads were washed five times with RIPA lysis buffer (or UUKV NSs IP lysis bufer) without detergent, and two times with PBS before elution of antibody complexes. Elution of proteins was carried out by the addition of

reducing protein disruption buffer and boiling at 95°C for 10 min. Eluates were analysed by western blotting analysis as described in section 4.1.2.

#### **4.4 Statistical analysis**

All data were analysed using Prism 5 software (GraphPad) and presented as mean  $\pm$  standard deviation (SD) or standard error of the mean (SEM). Statistical significance for the comparison of means between groups was determined by one-way analysis of variance (ANOVA), followed by post-hoc tests.  $p$ -values  $\leq 0.05$  were considered significant (\*\*\*\*,  $p \leq 0.0001$ ; \*\*\*,  $p \leq 0.001$ ; \*\*,  $p \leq 0.01$ ; \*,  $p \leq 0.05$ ).

---

Chapters **5-8**

**RESULTS**

---

# 5 Establishment of a reverse genetics system for Uukuniemi virus

## 5.1 Introduction

Reverse genetics is an approach used for studying the effect of targeted gene modifications on phenotype. Reverse genetics tools in virus research range from minigenome systems to virus-like particles (VLPs) and virus rescue systems. While minigenome systems and VLPs allow studying specific aspects of a virus' life cycle, virus rescue systems enable the investigation of the life cycle in its entirety. Minigenome systems consist of an analogue of the virus genome, in which the open reading frame (ORF) of a virus segment is replaced by a reporter gene. Supplementing the genome analogue with *trans*-acting viral nucleocapsid (N) and RNA-dependent RNA polymerase (L) proteins results in reporter gene activity, which can be measured to investigate the promoter strength of untranslated regions (UTRs), functionality of viral UTRs and N and L proteins, or the effect that other viral or cellular factors may have on minigenome activity. Therefore, minigenome systems allow modelling and simulating virus transcription and replication processes. So far, minigenome systems have been established for a number of bunyaviruses, such as BUNV (Kuismanen *et al.*, 1984; 1982; Murphy *et al.*, 1973), SBV (Elliott and Blakqori, 2012), OROV (Acrani *et al.*, 2015), LACV (Blakqori *et al.*, 2003), RVFV (Ikegami *et al.*, 2005a), SFTSV (Brennan *et al.*, 2015), and CCHFV (Devignot *et al.*, 2015).

Supplementing a minigenome system with viral glycoproteins allows the generation of transcription and replication-competent virus-like particles (VLPs), which have a lipid envelope embedded with the viral glycoproteins. VLPs can package the reporter minigenome and infect target cells to deliver ribonucleoprotein complexes (RNPs), which are able to undergo replication and transcription. In addition to enabling the study of transcription and replication, utilizing VLPs allows to investigate packaging and budding processes, as well as virus morphogenesis.

Uukuniemi virus (UUKV) is a tick-borne phlebovirus originally isolated in 1964 in Finland (Oker-Blom *et al.*, 1964). While antibodies to UUKV (or UUKV-like viruses) have been isolated in humans and other vertebrates such as birds, rodents and cows, there is no evidence of disease in these species (Hubálek and Rudolf, 2012; Saikku and Brummer-Korvenkontio, 1973). Therefore, it serves as a safe laboratory model to study

tick-borne phleboviruses. Indeed, UUKV has served as a prototype virus of the *Bunyaviridae* family for many years, contributing to advances in bunyavirus structure and architectural studies (Freiberg *et al.*, 2008; Overby *et al.*, 2008), glycoprotein studies (Overby *et al.*, 2007) and bunyavirus entry into mammalian cells (Lozach *et al.*, 2010) (Mazelier *et al.*, 2016).

For UUKV, an M segment-based minigenome system utilising chloramphenicol acetyltransferase (CAT) or GFP as reporter genes has already been reported (R. Flick and Pettersson, 2001). Moreover, the authors reported the generation of VLPs containing the reporter minigenomes following superinfection with UUKV. UUKV VLPs generated using a glycoprotein precursor expression plasmid instead of superinfection has also been reported (Överby *et al.*, 2006). However, these systems rely on constructs driven by RNA polymerase I (Pol I), which is disadvantageous because while Pol I localises to the nucleus, bunyaviruses replicate exclusively in the cytoplasm (Plyusnin and Elliott, 2011). In fact, most bunyavirus reverse genetics systems have been developed using a bacteriophage T7 RNA polymerase (RNAP) (Brennan *et al.*, 2015; Tilston-Lunel *et al.*, 2016) (Bergeron *et al.*, 2015; Elliott *et al.*, 2013; Lowen *et al.*, 2004; Varela *et al.*, 2013), which localises to the cytoplasm (Elroy-Stein and B. Moss, 1990).

Finally, even though UUKV Pol I-driven minigenome and VLP systems have been developed, no virus rescue entirely from cDNA has been described. The availability of a rescue system allows the generation of recombinant infectious virus from cDNA clones, enabling the genetic engineering of the viral genome. In this way, the effect of genetic changes on the viral life cycle in its entirety can be explored. There is a need to develop a reverse genetics system for UUKV for the ultimate manipulation of the UUKV genome. Such a system would facilitate the use of UUKV as a safe comparative model to understand the molecular basis for virulence and pathogenicity of highly pathogenic tick-borne phleboviruses, such as Heartland virus (HRTV) and Severe Fever with Thrombocytopenia Syndrome virus (SFTSV).

## **5.2 Aims**

The primary aim of the studies described in this chapter was to establish a T7 RNAP-driven reverse genetics system for UUKV. This included the development of a UUKV minigenome system for all segments using luciferase reporter genes, the generation of virus-like particles, and finally the recovery of UUKV entirely from cDNA clones.

Secondly, I aimed to manipulate the UUKV genome to generate recombinant viruses lacking the NSs protein, which could be used in the future to gain an understanding of the function that UUKV NSs may play in the virus life cycle. Finally, I aimed to generate a recombinant UUKV encoding eGFP in the NSs locus, such that it could be used as a quick tool to investigate permissibility of various mammalian cell lines to UUKV infection.

## **5.3 Results**

### ***5.3.1 Cloning of cDNA plasmids used for the rescue of UUKV***

cDNA plasmids used for virus rescue (henceforth referred to as ‘rescue plasmids’) were designed as it has been previously described for other bunyaviruses (Brennan *et al.*, 2015; Bridgen and Elliott, 1996; Lowen *et al.*, 2004). cDNA copies of the UUKV genome segments were amplified from Pol I-driven plasmids (provided by Dr Anna Överby, Umeå University, Sweden), which encode the full-length antigenome cDNA copies of the S, M and L UUKV RNA segments (pRF202, pRF7 and pRF280, respectively, unpublished). Using restriction-free cloning, the amplified cDNAs were inserted into a pTVT7 plasmid (0,0) (Johnson *et al.*, 2000) which contains an extra G residue at the 5’ end of the antigenome cDNA copy (Billecocq *et al.*, 2008). Inclusion of one or two non-viral G nucleotide residues at the 5’ end of the transcripts have been reported to enhance T7 RNAP transcription efficiency (Pattnaik *et al.*, 1992).

Thus, in the pTVT7 vector the RNA transcript produced by the T7 RNAP is in the antigenome sense, as illustrated in Figure 5-1. In addition, the antigenomic 3’ UTR is directly followed by a Hepatitis  $\delta$  ribozyme (H $\delta$ r) and a T7 terminator sequence. While the T7 terminator sequence allows termination of transcription by the T7 RNAP, the H $\delta$ r enables self-cleavage of the antigenomic transcript to generate the exact end of the 3’ UTR. The rescue plasmids were sequenced and named pT7UUKS(+), pT7UUKM(+), and pT7UUKL(+) (encoding cDNA copies of the UUKV antigenomic S, M and L segments, respectively). The nucleotide sequences of the rescue plasmids are based on the sequences available on GenBank with the accession numbers: M33551.1 for UUKV S, M17417.1 for UUKV M and D10759.1 for UUKV L. Importantly, the UUKV strain used in this study (wtUUKV) was sequenced by the late Prof Richard Elliott (personal communication) and corresponds to the database sequences noted above. Finally, a silent point mutation was introduced as a genetic marker in pT7UUKS(+) at the nucleotide position 963 (A $\rightarrow$ G), which generates a XhoI restriction site in the S segment antigenomic cDNA (Figure 5-1).

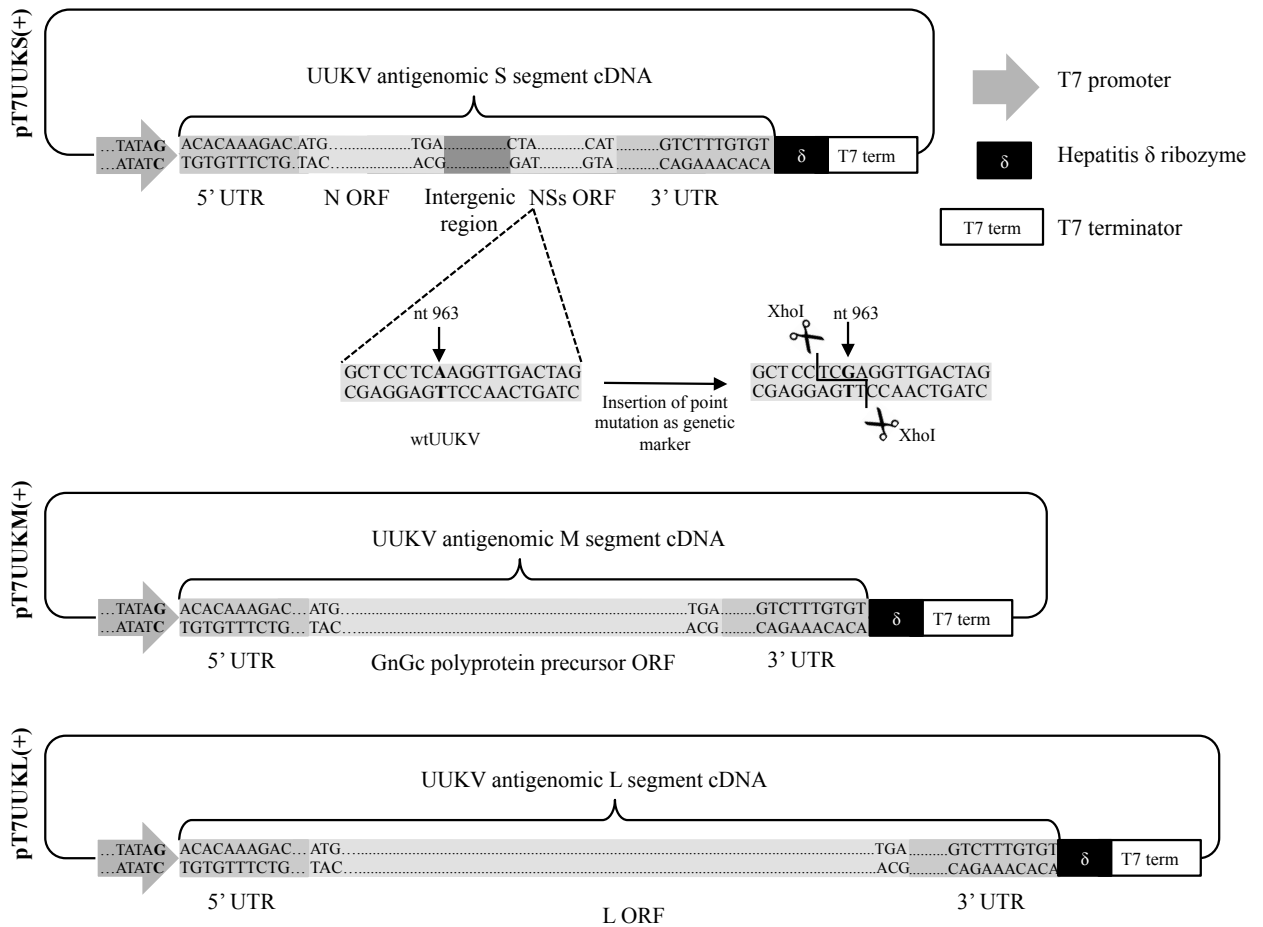


**Figure 5-1. Schematic representation of UUKV rescue plasmids.**

Full-length cDNA copies of the antigenomic UUKV S, M and L RNA segments were cloned into the pT7UUK plasmid (0,0) with an extra G residue at the 5' end of the cDNA (in bold). Rescue plasmids were named pT7UUKS(+), pT7UUKM(+), and pT7UUKL(+). The A→G point mutation introduced at nucleotide position 963 in pT7UUKS(+) for the generation of an XhoI restriction site as a genetic marker is shown. UUKV: Uukuniemi virus; UTR: Untranslated region; ORF: Open reading frame.

### 5.3.2 Establishment of a UUKV minigenome system

Minigenome systems and the generation of VLPs should be considered as the first step before attempting virus rescue, to ensure the accuracy and functionality of UTR sequences, viral N and L proteins in minigenome assays, and viral glycoproteins in VLP assays. Firstly, the transcription plasmids for the establishment of UUKV M and L segment-based minigenome systems were designed. The *Renilla* luciferase open reading frame (ORF) was used as a reporter gene in the negative sense orientation and was designed to be flanked by the genomic sense viral 3' and 5' UTRs in the pTVT7 plasmid (0,0) (Johnson *et al.*, 2000). The cloning strategy carried out for the generation of minigenome plasmids is illustrated in Figure 5-2. Briefly, the viral ORFs in the rescue plasmids pT7UUKM(+) and pT7UUKL(+) was replaced with the humanised *Renilla* luciferase ORF (henceforth referred to as *Renilla* luciferase), such that *Renilla* luciferase was flanked by the antigenomic sense viral UTRs (Figure 5-2 A, first step). Next, the cassette containing luciferase flanked by the antigenomic viral UTRs was amplified and inverted in pTVT7 (0,0) to enable the generation of genomic sense transcripts by the T7 RNAP (Weber *et al.*, 2001) (Figure 5-2 A, second step). In the case of the S segment minigenome system, the NSs ORF in pT7UUKS(+) was replaced by the *Renilla* luciferase ORF in the same (negative-sense) orientation (Figure 5-2 B). The correct sequence of the plasmids was confirmed by Sanger sequencing, and the UUKV S, M and L segment-based minigenome plasmids were named pT7UUKS<sub>Ren</sub>(+), pT7UUKM<sub>Ren</sub>(-) and pT7UUKL<sub>Ren</sub>(-), respectively.

Helper plasmids expressing UUKV N and L were generated by amplifying the UUKV N and L ORFs from pT7UUKS(+) and pT7UUKL(+), respectively, and sub-cloning the ORFs into the expression vector pTM1 (Moss *et al.*, 1990). The plasmids were sequenced and named pTM1UUKN and pTM1UUKL. pTM1 contains a T7 promoter and the encephalomyocarditis virus (EMCV) internal ribosome entry site (IRES), allowing efficient translation of proteins encoded in the transcripts generated by the T7 RNAP.

Minigenome assays were performed in BSR-T7/5 cells, which are a clone derived from the BHK-21 cell line and constitutively express a T7 RNAP (Buchholz *et al.*, 1999). Briefly, sub-confluent BSR-T7/5 cells were co-transfected with constant amounts of pT7UUKS<sub>Ren</sub>(+), pT7UUKM<sub>Ren</sub>(-) or pT7UUKL<sub>Ren</sub>(-), pTM1UUKN, a plasmid expressing firefly luciferase (pTM1FFluc) as an internal control for transfection efficiency, and increasing amounts (0-375 ng) of pTM1UUKL. The total amount of plasmid DNA in

all reactions was kept constant by the addition of empty control plasmid pTM1 to the DNA mix. Cells were lysed 18 h post transfection, and *Renilla* and firefly luciferase activity measured. Experiments were performed in triplicate wells in three independent experiments. *Renilla* values were normalised to firefly values and minigenome activity expressed as fold increase of normalised luciferase units relative to the background control (absence of L protein).

An increase in minigenome activity when the helper plasmid encoding the UUKV L protein was supplemented (compared to the background control) confirmed the functionality of the S, M and L segment-based minigenome assays (Figure 5-3). Interestingly, the highest increase in luciferase activity of the S and L segment-based minigenomes was observed when 125 ng of pTM1UUKL was supplemented, and increasing amounts of UUKV L-expressing plasmid resulted in a drop in minigenome activity (Figure 5-3 A and C). Relative to the background control, a peak 27-fold increase in activity was observed for the S segment-based minigenome, compared to a peak 22.5-fold increase for the M segment-based minigenome (Figure 5-3 B), and a peak 14.6-fold increase for the L segment-based minigenome. Although this data would suggest that the S segment-based minigenome is the most active, it is important to note that this minigenome was constructed in the antigenomic sense, whereas the M and L segment-based minigenome constructs are in the genomic sense. Thus, the relative promoter strengths are not comparable.

Taken together, these results show that the viral UTRs used in this study act as functional promoters and that the cDNA copies of the UUKV N and L proteins used in this study are also functional, leading to the activity of the reporter *Renilla* from the genome analogues.

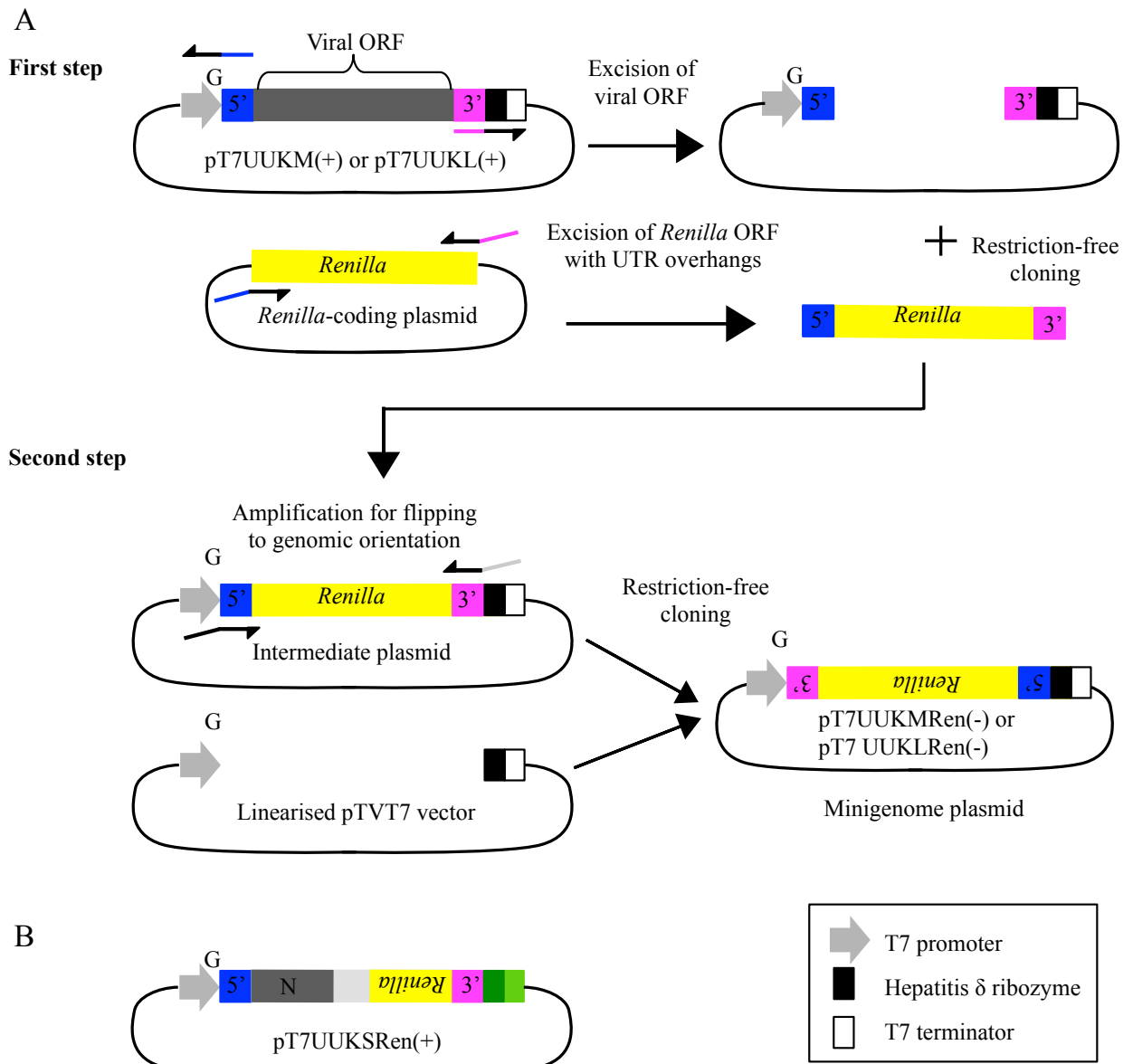


**Figure 5-2. Schematic representation of the construction of UUKV minigenome plasmids.**

(A) **First step:** Generation of an antigenomic intermediate plasmid. Primers were designed to bind the 3' and 5' UTR of pT7UUKM(+) and pT7UUKL(+), such that the viral ORF was excised, leaving the UTRs intact. The *Renilla* ORF was amplified from a *Renilla* encoding plasmid, using primers containing 15 nt overhangs complementary to the corresponding viral UTR. **Second step:** the *Renilla* ORF was cloned into the linearised UTR-containing pTVT7 vector using restriction-free cloning. The minigenome cassette was flipped to the viral genomic sense by amplification using primers containing 15 nt overhangs homologous to the T7 promoter (3' end) and T7 terminator (5' end). The amplified product was inserted into pTVT7 (0,0) with an extra G residue at the 5' end of the cDNA (in bold) by restriction-free cloning. (B) Schematic representation of pT7UUKSren(+). The NSs ORF of the S segment in pT7UUKS(+) was replaced by the *Renilla* ORF. UTR: Untranslated region; ORF: Open reading frame.

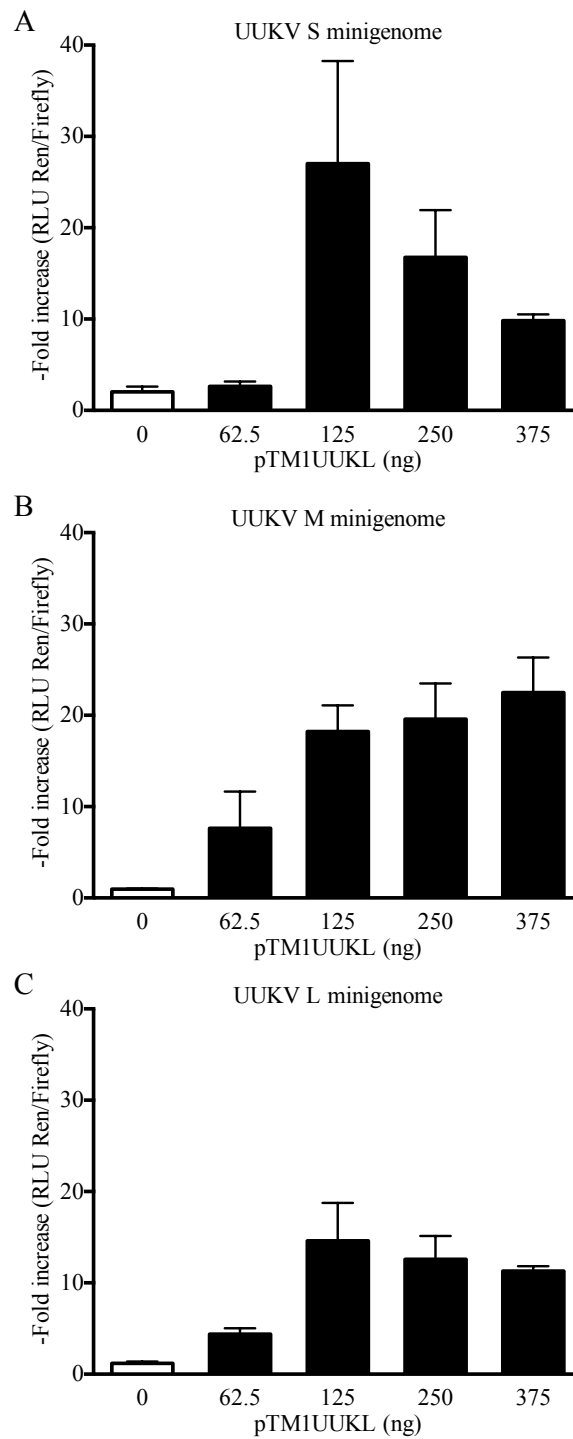


**Figure 5-3. UUKV minigenome assay.**

BSR-T7/5 cells were transfected with constant amounts of (A) pT7UUKS $Ren(+)$ , (B) pT7UUKM $Ren(-)$  or (C) pT7UUKL $Ren(-)$ , pTM1UUKN, pTMFFluc, and the indicated amounts of pTMUUKL. The total amount of plasmid DNA in all reactions was kept constant by addition of empty control plasmid pTM1 to the DNA mix. Cells were lysed 18 h post transfection and the *Renilla* and firefly luciferase units measured. Minigenome activity is expressed as the fold increase of normalised luciferase units relative to the background control (no L). Error bars represent the standard deviation (SD) from the mean of one representative experiment of three, performed in triplicate (n=3). UUKV: Uukuniemi virus; RLU: Relative light units.

### 5.3.3 Generation of UUKV virus-like particles

In order to determine whether the UUKV glycoprotein precursor gene was functional, a VLP assay was developed. Because many other bunyavirus VLP assays utilize an M segment-based minigenome (Acraani *et al.*, 2015; Habjan *et al.*, 2009a; Shi *et al.*, 2006; Soldan *et al.*, 2010), pT7UUKM<sup>Ren(-)</sup> was chosen as the reporter construct to be packaged by the VLPs. A plasmid expressing the UUKV glycoprotein precursor, named pTM1UUKGnGc, was generated by the amplification of UUKV M segment ORF from pT7UUKM(+), and sub-cloning the amplified ORF into the expression vector pTM1 (Moss *et al.*, 1990). For the generation of VLPs, BSR-T7/5 cells were transfected with pTM1UUKGnGc in combination with the plasmids transfected in the UUKV M segment-based minigenome assay (Section 5.3.2). The transfected cells (donor cells) were lysed 48h post transfection and luciferase activities measured. *Renilla* values were normalised to firefly values and activity expressed as the fold increase in normalised luciferase units relative to the background control (absence of L protein).

A mean 317-fold increase in minigenome activity was observed in control donor cells that were not supplemented with glycoprotein expressing plasmid. Minigenome activity was enhanced in cells which were supplemented with 125 ng pTM1UUKGnGc (mean 757-fold increase), presumably due to the generation and spread of VLPs within the donor cells, but not when supplemented with 250 ng pTM1UUKGnGc (Figure 5-4 A). This suggests that the UUKV glycoprotein precursor could have an inhibitory effect on minigenome activity, or that a fine balance of protein amounts is required for efficient VLP production.

The supernatant was endonuclease-treated to remove contaminant DNA and used to infect naïve BSR-T7/5 cells, or BSR-T7/5 cells which were pre-transfected with pTM1UUKN and pTM1UUKL, in order to boost and supplement transcription of the incoming RNPs. These cells, which are infected with VLPs, are referred to as ‘recipient’ cells. Infected recipient cells were lysed at 24 h post infection (p.i.) and the *Renilla* and firefly luciferase activities measured. *Renilla* values normalised to firefly values and minigenome activity expressed as the fold increase in normalised luciferase units relative to the background control (recipient cells infected with VLPs generated in donor cells that were not supplemented with pTM1UUKL).

As expected, no minigenome activity was detected in recipient cells infected with VLPs generated in donor cells that were not supplemented with the viral glycoprotein-expressing plasmid.

However, a mean 300-fold increase in minigenome activity was detected in recipient cells infected with supernatants from donor cells that were co-transfected with 125 ng pTM1GnGc, and a mean 135-fold increase detected in recipient cells infected with supernatants from donor cells that were co-transfected with 250 ng pTM1GnGc (Figure 5-4 B). The lower minigenome activity observed in recipient cells that were infected with VLPs generated in donor cells transfected with higher amounts of pTM1GnGc is in agreement with the effect of pTM1GnGc on minigenome activity noted in donor cells (Figure 5-4 A). In addition, an overall increase in minigenome activity was observed when recipient cells were pre-transfected with pTM1UUKN and pTM1UUKL, with a mean 19700 and 337- fold increase in minigenome activity detected in recipient cells infected with VLPs generated by co-transfection of 125 ng or 250 ng pTM1GnGc, respectively (Figure 5-4 B).

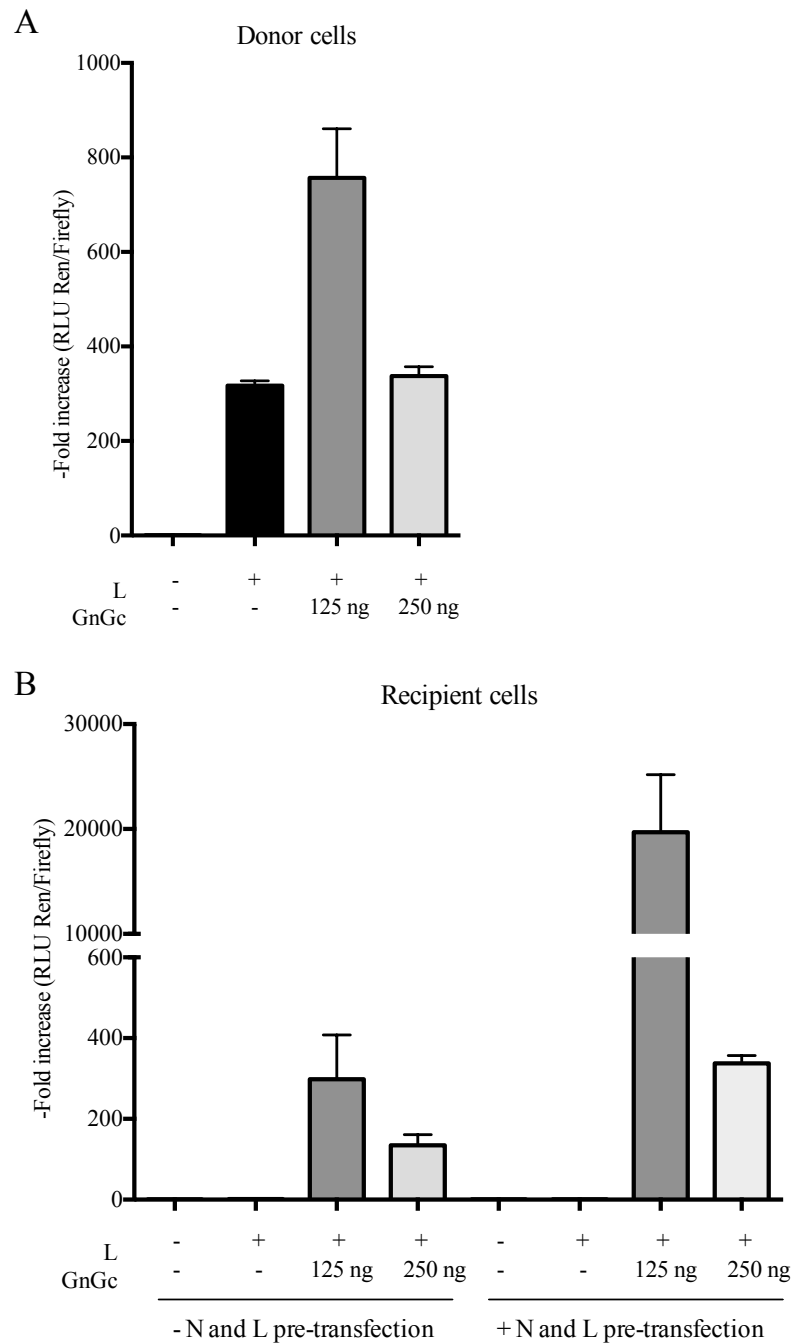


**Figure 5-4. UUKV VLP production assay.**

BSR-T7/5 cells were transfected with constant amounts of pTMFFluc as a transfection efficiency control, pT7UUKM<sup>Ren(-)</sup>, pTMUUK<sup>N</sup>, and pTMUUK<sup>L</sup>. The minigenome transfection mix was supplemented with the indicated amounts of pTMUUK<sup>GnGc</sup>. 48 h post transfection, the clarified cell culture supernatant was used for infection of naïve BSR-T7/5 cells, and luciferase activity measured 18 h p.i. (A) Minigenome activity in donor cells transfected with VLP production assay plasmids and harvested 48 h post transfection. (B) Minigenome activity following infection with VLP supernatant in recipient BSR-T7/5 cells, which were left untransfected, or pre-transfected with pTM1UUK<sup>N</sup> and pTM1UUK<sup>L</sup>. Error bars represent the SD from the mean of one representative experiment of two performed in triplicate (n = 3). VLP: Virus-like particle; RLU: Relative light units.

### 5.3.4 *Rescue of recombinant UUKV from cDNA*

The ability of the UUKV UTR sequences to be recognized for the transcription and replication of a genome analogue by viral N and L proteins (demonstrated by minigenome assays), and the ability of the viral glycoproteins to package the UUKV M segment genome analogue (demonstrated by the successful generation of VLPs) were important pre-requisites for the successful generation of recombinant UUKV from cDNA clones. Thus, since the minigenome and VLP assays were functional, pT7UUKS(+), pT7UUKM(+) and pT7UUKL(+) (described in section 5.3.1) were used to attempt the rescue of recombinant UUKV entirely from cDNA. Briefly, subconfluent BSR-T7/5 cells were transfected with pT7UUKS(+), pT7UUKM(+) and pT7UUKL(+) in a 3-plasmid rescue system, or supplemented with pTM1UUKN and pTM1UUKL in a 5-plasmid rescue system. The supernatant from transfected cells was harvested 7 days post transfection and the viral titre determined by focus-forming assays on BSR cells. In 4 independent experiments, the 3-plasmid rescue system yielded a mean virus titre of  $4.9 \times 10^4$  ( $\pm 1.9 \times 10^4$ ) FFU/mL, and the 5-plasmid rescue system yielded  $2.9 \times 10^4$  ( $\pm 2.7 \times 10^4$ ) FFU/mL. These results suggested that supplementing the 3-plasmid rescue system with UUKV N and L had no effect on the efficiency of virus rescue. Working stocks of the recombinant viruses were prepared in BSR cells with low MOI infections (0.01 FFU/mL), and titres of about  $10^8$  FFU/mL were obtained.

In terms of focus phenotype, recombinant UUKV (rUUKV) exhibited similar foci size and shape to wtUUKV in BSR and BHK-21 cells (Figure 5-5 A). Interestingly, foci were larger in BHK-21 cells (5-6 mm in diameter) than in BSR cells (3-4 mm in diameter).

In order to confirm whether rUUKV was indeed generated from cDNA clones, BSR cells were infected with either wtUUKV or rUUKV at a multiplicity of infection (MOI) of 3 focus forming unit/cell (FFU/cell). 48h p.i. the total cellular RNA from infected cells was extracted and the full S segment RNA subjected to RT-PCR using sequence-specific primers. The generated S segment cDNA products were subjected to XhoI digestion. As expected, no digestion was observed in cDNA derived from wtUUKV S segment, whereas two products of the expected size (963 bp and 757 bp) were visualised upon XhoI digestion of rUUKV S segment cDNA (Figure 5-5 B). RT-PCR products of the S segment were also sequenced to confirm the silent mutation introduced at nt position 963 in rUUKV (described in Section 5.3.1) (Figure 5-5 C).

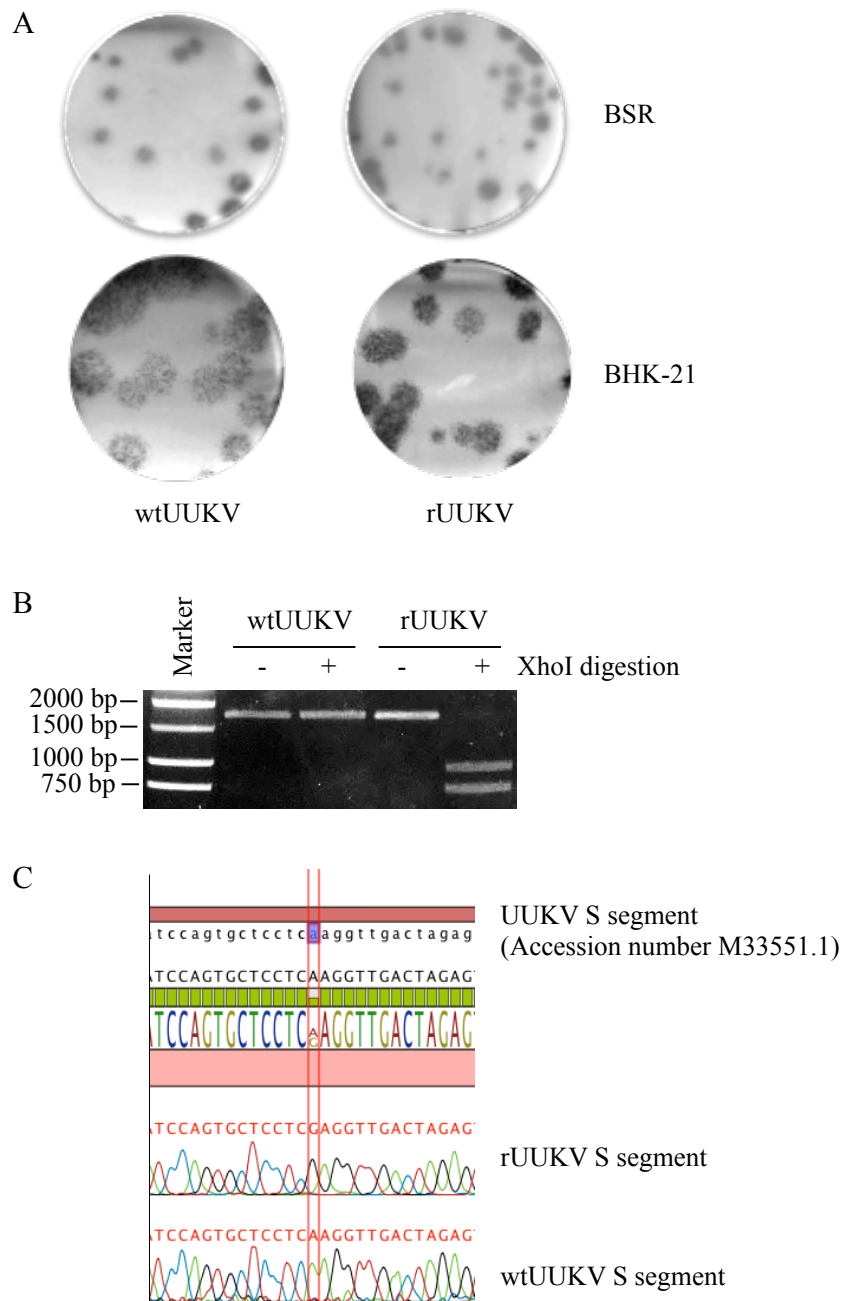


**Figure 5-5. Rescue of rUUKV.**

(A) Focus phenotypes of wtUUKV and rUUKV on BSR or BHK-21 cells. Infected cells were fixed 6 days p.i. and probed with an anti-UUKV N antibody. (B) Confirmation of the insertion of a silent genetic marker into the rUUKV genome. RT-PCR products of the full-length S segment of wtUUKV and rUUKV were subjected to XhoI digestion and the digested products visualised on an agarose gel. (C) Sequencing results for RT-PCR products of full-length S segments of wtUUKV and rUUKV, showing the silent mutation introduced at nt position 963 in rUUKV. UUKV: Uukuniemi virus.

### 5.3.5 *Rescue of recombinant UUKV lacking the non-structural protein NSs*

The established reverse genetics system was also used to generate recombinant UUK viruses lacking the non-structural protein NSs, with the aim of investigating the role of UUKV NSs in the virus life cycle. Two strategies were employed to generate NSs-lacking UUK viruses, illustrated in Figure 5-6 A. Firstly, pT7UUKSdelNSs(+) was cloned by excision of the NSs ORF from pT7UUKS(+) in such way that the intergenic region is immediately followed by the genomic 5'UTR, resulting in the generation of a smaller S segment (898 nt compared to the 1720 nt long wild-type S segment). Secondly, the NSs ORF in pT7UUKS(+) was replaced by that of the enhanced GFP (eGFP) ORF in the same orientation, using restriction-free cloning. This resulted in an eGFP-expressing S segment 1618 nt in length, named pT7UUKSdelNSsGFP(+).

3-plasmid rescues were performed as described in Section 5.3.4, and the mean titre obtained from 4 independent experiments was  $3.75 \times 10^4$  ( $\pm 1.2 \times 10^4$ ) FFU/mL for rUUKdelNSs and  $1 \times 10^4$  ( $\pm 5.2 \times 10^3$ ) FFU/mL for rUUKdelNSsGFP. These titres are similar to those obtained for the rescue of wild-type UUKV (noted in Section 5.3.4). Working stocks of the recombinant viruses were prepared in BSR cells with low MOI infections (0.01 FFU/mL), and titres of about  $10^7$  FFU/mL obtained.

In order to sequence the S segment of the recombinant viruses, BSR cells were infected at a high MOI (3 FFU/cell), the total cellular RNA extracted 24 h p.i. and subjected to RT-PCR for amplification of the full length UUKV S segment. The cellular RNA of infected cells was also subjected to 3' Rapid amplification of cDNA ends (RACE) to determine 3' and 5' UTR S segment termini. Sanger sequencing confirmed that the RACE and RT-PCR products were correct and matched the cDNA sequences used for the rescue of the recombinant viruses. The sizes of the S segment RT-PCR products are shown in Figure 5-6 B. Finally, to validate that NSs was not being expressed at the protein level, BSR cells were mock-infected or infected with wtUUKV or the recombinant viruses at a high MOI (5 FFU/cell) and lysed at 18h post p.i. for western blotting. As expected, while N and NSs were detected in BSR cells infected with wtUUKV or rUUKV, only N was detected in BSR cells infected with rUUKdelNSs or rUUKdelNSsGFP (Figure 5-6 C).

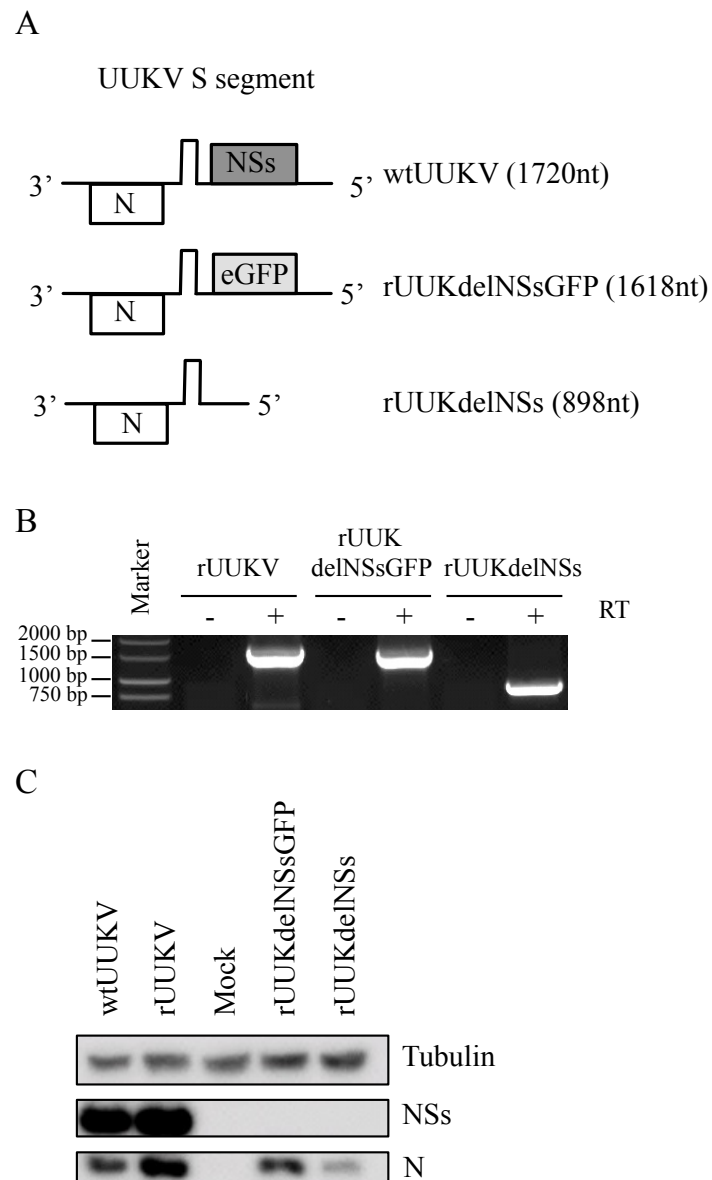


**Figure 5-6. Generation of recombinant UUKV lacking NSs.**

(A) Schematic diagram of the S segment (genomic sense) of wtUUKV and recombinant UUKV lacking the NSs ORF. (B) RT-PCR products of full-length S segments belonging to rUUKV, rUUKdelNSsGFP and rUUKdelNSs, showing size differences corresponding to the S segments designed in panel A. (C) Western blot analysis of BSR cells infected at an MOI of 5 with wtUUKV, rUUKV, rUUKdelNSsGFP, rUUKdelNSs, or mock-infected. Cell lysates were prepared 18 h p.i. and western blots probed with anti-tubulin, anti- UUKV NSs, and anti-UUKV N antibodies. UUKV: Uukuniemi virus.

### 5.3.6 Replication of rUUKV, rUUKdelNSs and rUUKdelNSsGFP in cell culture

The focus phenotype and replication properties of the recombinant viruses rUUKV, rUUKdelNSs and rUUKdelNSsGFP were compared to wtUUKV. In terms of focus phenotype, focus-forming assays showed that viruses lacking NSs exhibited smaller foci (1-2 mm or 0.5-1.5 mm in diameter) compared to wtUUKV and rUUKV (5-6 mm or 3-4 mm in diameter) in BHK-21 or BSR cells (respectively) (Figure 5-7 A).

A time course of BHK-21 cells infected with rUUKdelNSsGFP at a low MOI (0.01 FFU/cell) shows that at 24 h p.i., eGFP expression can be detected in only a few cells. The number of cells exhibiting eGFP expression increases over time as the virus spreads through the cell monolayer, with most cells infected within 4 days (Figure 5-7 B).

The growth properties of the recombinant viruses and wtUUKV were compared in BHK-21 cells, which were infected at a low MOI (0.1 FFU/cell) and maintained at 37°C. The supernatant was harvested at the indicated time points, and the virus titre determined by focus-forming assays in BSR cells. At the same time points, infected cell lysates were prepared for western blot analysis. As shown in Figure 5-8 A, rUUKV exhibited similar growth properties as wtUUKV, reaching titres of  $10^9$  FFU/mL by 96 h p.i. As a general trend, recombinant viruses lacking NSs exhibited slower growth kinetics compared to wtUUKV and rUUKV. Interestingly, rUUKdelNSsGFP reached higher titres (peak titre  $10^8$  FFU/mL) than rUUKdelNSs (peak titre  $10^7$  FFU/mL), which had no sequences added in the NSs locus. These results demonstrate that while NSs is not essential for virus replication, the slower growth kinetics of UUKV lacking NSs suggests that NSs may play a contributory role that enables efficient virus replication.

Analysis of viral protein expression in the time course by western blotting showed that the NSs protein was detected as early as 24 h p.i., and accumulated thereafter in wtUUKV and rUUKV-infected cells, whereas N protein was only detected at 48 h p.i (Figure 5-8 B). As expected, no NSs was detected in rUUKdelNSs- and rUUKdelNSsGFP- infected cells. However, N was detected earlier in rUUKdelNSsGFP-infected cells compared to rUUKdelNSs-infected cells, reflecting the difference observed in virus growth kinetics between these viruses (shown in Figure 5-8 A). Because of the ambisense nature of the *Phlebovirus* S segment, NSs protein expression is delayed relative to N protein expression. This is because NSs mRNA is generated only after replication of the genome to antigenome, whereas N mRNA is generated from the viral genome. In fact, using pulse-chase analysis, Simons *et al* have estimated that UUKV N is synthesized within 4 h p.i.

and is stable for several hours, whereas the NSs protein is synthesized only at 8 h p.i. and has a half-life of approximately 1.5 h (Simons *et al.*, 1992). It is important to note that while in the time course carried out in this study UUKV NSs was detected earlier than N by western blotting (Figure 5-8 B), this may simply relate to differences in antibody affinity to the respective antigen epitopes.

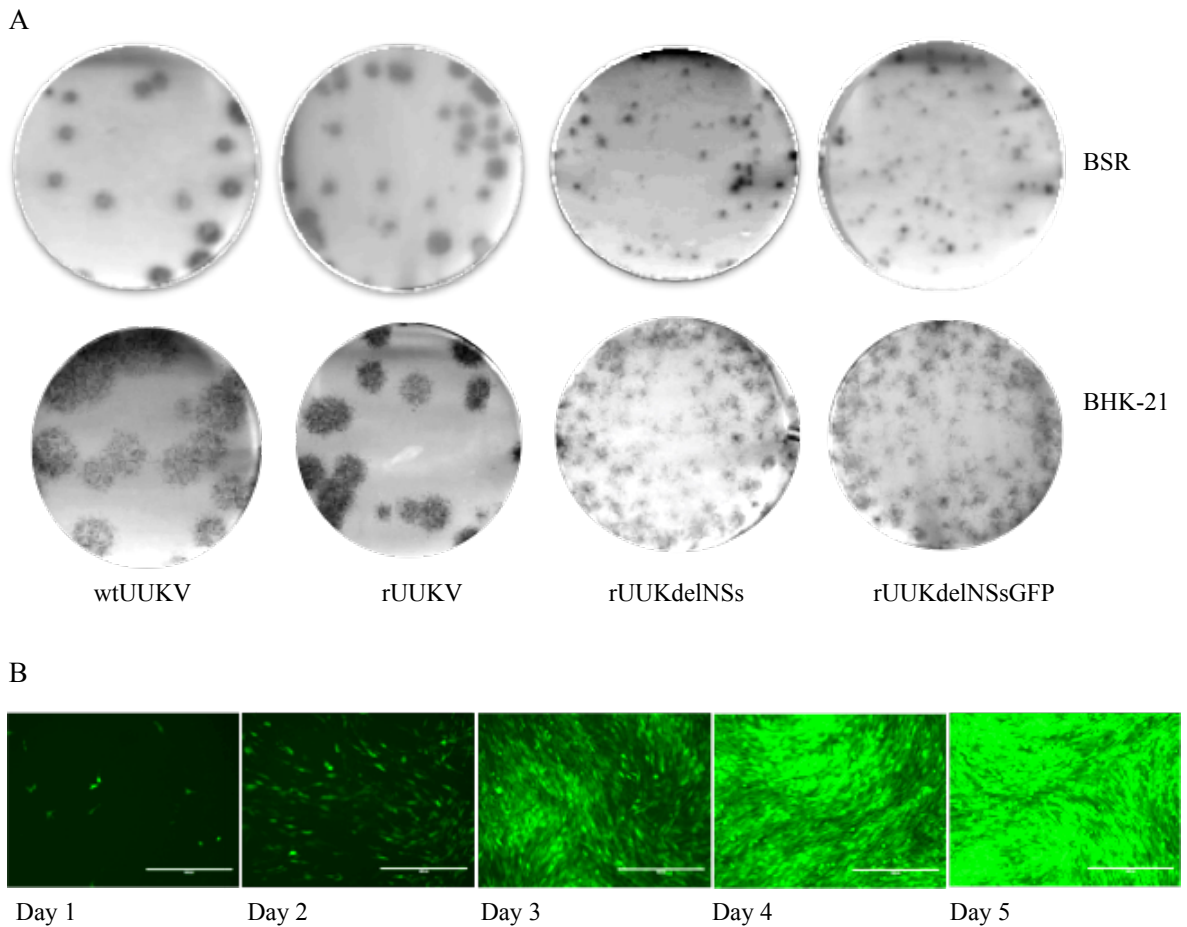


**Figure 5-7. Phenotypic characterization of recombinant viruses in cell culture.**

(A) Focus assay for wtUUKV, rUUKV, rUUKdelINSs, or rUUKdelINSsGFP on BSR or BHK-21 cells 6 days p.i. Foci were detected using an anti-UUKV N antibody. (B) Time course of infection in BHK-21 cells with rUUKdelINSsGFP at 37°C over 5 days to monitor eGFP fluorescence. Cells were infected at an MOI of 0.01 FFU/cell. UUKV: Uukuniemi virus.

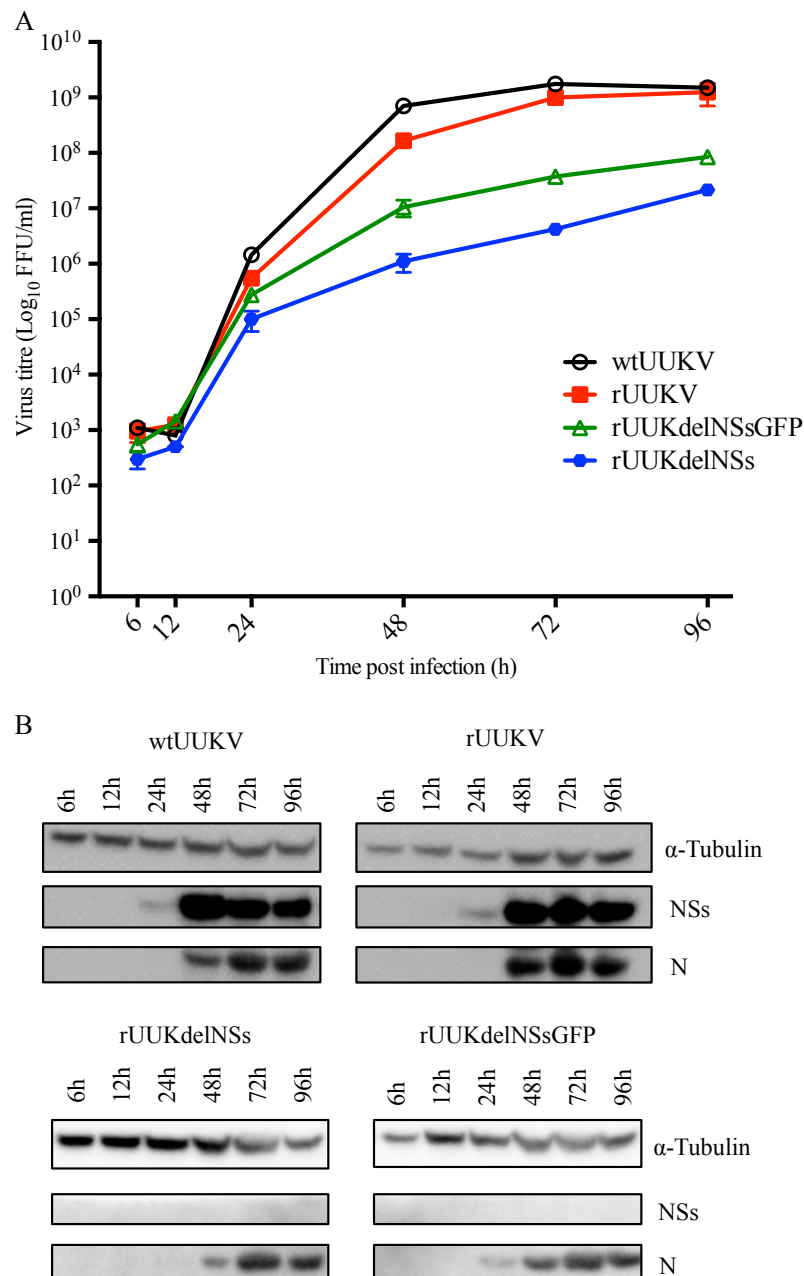


**Figure 5-8. Growth kinetics of recombinant viruses in BHK-21 cells.**

Cells were infected at an MOI 0.1 FFU/cell. The cell culture supernatant or cell lysates were harvested at the indicated time points. (A) Growth curves. Infections were carried out in duplicate and error bars represent the standard error of the means (SEM), for a representative experiment ( $n=2$ ) of three. (B) Analysis of viral protein synthesis. Cell lysates from the growth curve samples were harvested and western blots probed with anti-tubulin, anti-UUKV NSs and anti UUKV-N antibodies, as indicated. UUKV: Uukuniemi virus.

### 5.3.7 Permissibility of mammalian cell lines to UUKV infection

With the aim of investigating whether rUUKdelNSsGFP could be used as a quick tool to monitor virus infection, mammalian cell lines available in our laboratory (A549, A549/V, HeLa, HEK-293T, Huh-7, Vero E6, BHK-21, BSR-T7/5) were infected with rUUKdelNSsGFP at an MOI of 0.005 FFU/cell and eGFP expression monitored at 24 h, 48 h and 72 h p.i. using an EVOS FL imaging microscope.

To examine whether visualizing eGFP expression upon rUUKdelNSsGFP could be used as a method to assess permissibility of various cell lines to UUKV infection, the results of this experiment were compared to a yield assay of wtUUKV in the same cell lines. Briefly, cells were infected with wtUUKV at a low and high MOI (0.005 or 3 FFU/mL, respectively). At 72 h p.i. cell culture supernatants were harvested and virus titres determined by focus-forming assays in BSR cells.

From all the human-derived cell lines tested, Huh-7 cells were the most susceptible to rUUKdelNSsGFP infection, as eGFP signal increased over time and yielded the highest wtUUKV titres (mean titre  $4.3 \times 10^3$  FFU/mL for low MOI infections and  $1.3 \times 10^6$  FFU/mL for high MOI infections) (Figure 5-9 and Figure 5-10). HEK-293T cells yielded slightly lower wtUUKV titres compared to Huh-7 cells (mean titre  $4 \times 10^4$  FFU/mL for low MOI infections and  $3 \times 10^5$  FFU/mL for high MOI infections), and visibly less eGFP expression was observed following rUUKdelNSsGFP infection compared to Huh-7 cells. No eGFP expression was observed in HeLa cells, and this is in agreement with the wtUUKV yield assay results, as only a mean titre of  $1.3 \times 10^2$  FFU/mL for low MOI infections and  $2.3 \times 10^3$  FFU/mL for high MOI infections was observed. It must be noted that these titres could be residual from the virus inoculum. A549/V cells are human lung epithelial cells expressing the V protein of parainfluenza virus 5 (PIV5) which targets STAT1 for degradation, rendering cells unable to respond to interferon (Andrejeva *et al.*, 2002; Killip *et al.*, 2013). In comparison to the IFN-competent parental cell line A549, a 15- and 5-fold increase in wtUUKV titre was observed in A549/V cells at a low and high MOI infection, respectively (Figure 5-10 A and B). These results are in agreement with lower eGFP expression levels in A549 cells compared to A549/V cells in Figure 5-9.

Vero E6 cells are African green monkey kidney epithelial cells commonly used in cell culture for the propagation of viruses, as they are type I IFN-incompetent and can result in the production of high virus yields. However, despite lacking an active type I IFN system, wtUUKV was unable to reach high titres at either a low MOI infection (mean titre  $4.3 \times$

$10^3$  FFU/mL) or a high MOI infection (mean titre  $4.7 \times 10^4$  FFU/mL) in Vero E6 cells. eGFP expression was noted in Vero E6 cells infected with rUUKdelINSsGFP, suggesting the virus is able to infect and enter the cells. However the eGFP expression signal was not amplified later than 48 h p.i., indicating poor virus growth in this cell line.

The rodent cell lines BHK-21 and BSR-T7/5 cells were the most susceptible to virus infection. eGFP expression in these rodent-derived cell lines quickly increased over time following rUUKdelINSsGFP infection (Figure 5-9). Consistent with the results observed using rUUKdelINSsGFP, the highest wtUUKV yields of all cell lines screened were observed in BHK-21 and BSR-T7/5 cells (Figure 5-10). In BHK-21 cells, a mean titre of  $5.6 \times 10^6$  FFU/mL for low MOI infections and  $1 \times 10^7$  FFU/mL for high MOI infections was observed, whereas in BSR-T7/5 cells the mean titre for a low MOI infection was  $4.3 \times 10^6$  FFU/mL and a mean titre of  $1.3 \times 10^7$  FFU/mL for a high MOI infection. It is necessary to note that both cell lines are IFN incompetent, and BSR-T7/5 cells are derived from BSR cells, which are a clone of BHK-21. Therefore, it is not surprising that both cell lines have similar susceptibilities to UUKV infection. Increased susceptibility to UUKV infection in BHK-21 and BSR-T7/5 cells compared to other mammalian cell lines is also not surprising, because the viruses were propagated and titered in BSR cells. The wtUUKV stock used has also been propagated in BHK-21 cells previously (Elliott *et al.*, 1992). Therefore, it is possible that the virus has adapted to rodent cell lines.

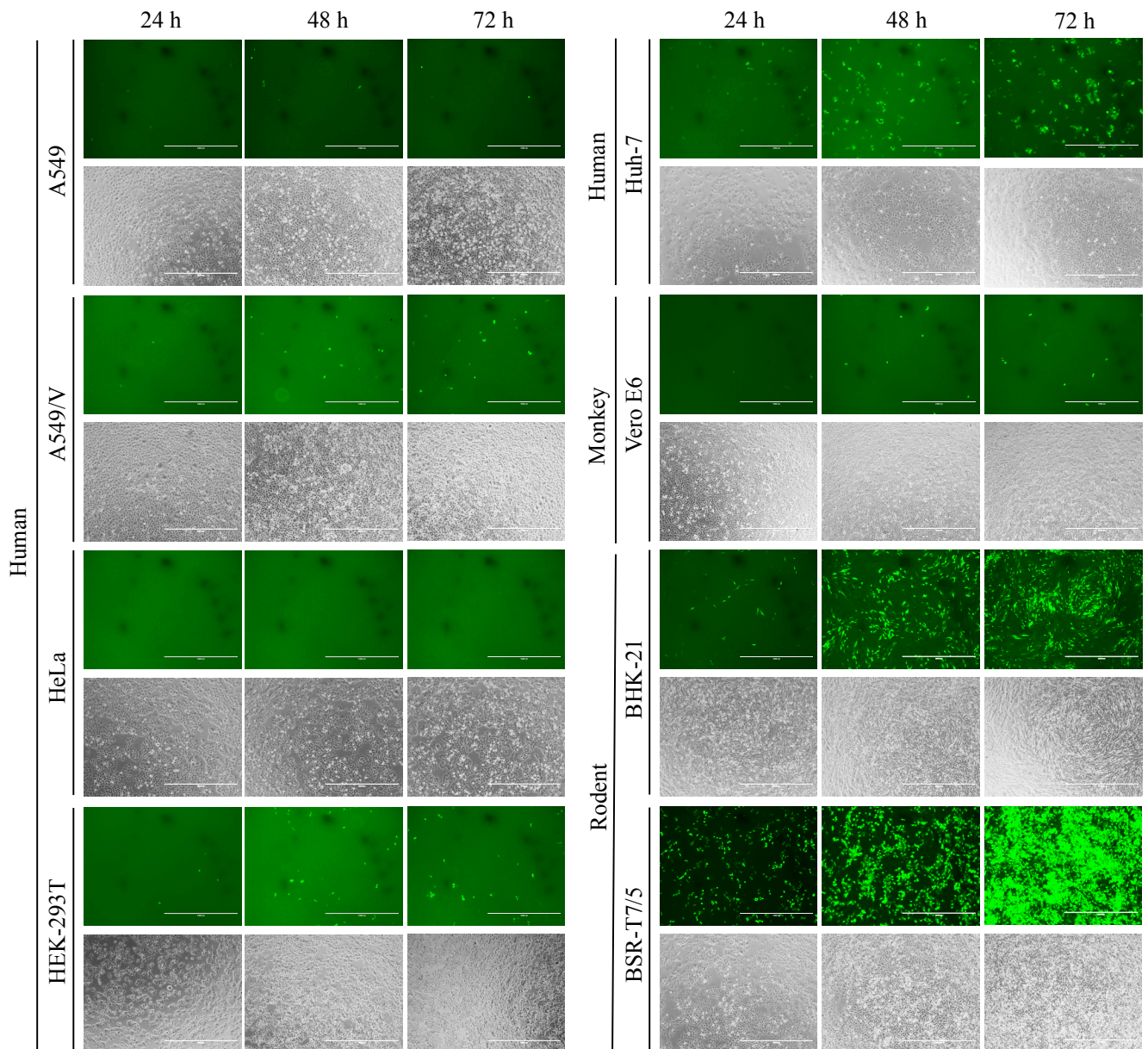


**Figure 5-9. eGFP expression in rUUKdelINSsGFP-infected cells.**

The indicated cell lines were infected with rUUKdelINSsGFP at an MOI 0.005 and eGFP expression monitored 24 h, 48 h and 72 h p.i. using an EVOS fluorescent microscope. Scale bars indicate 1000  $\mu\text{m}$ .

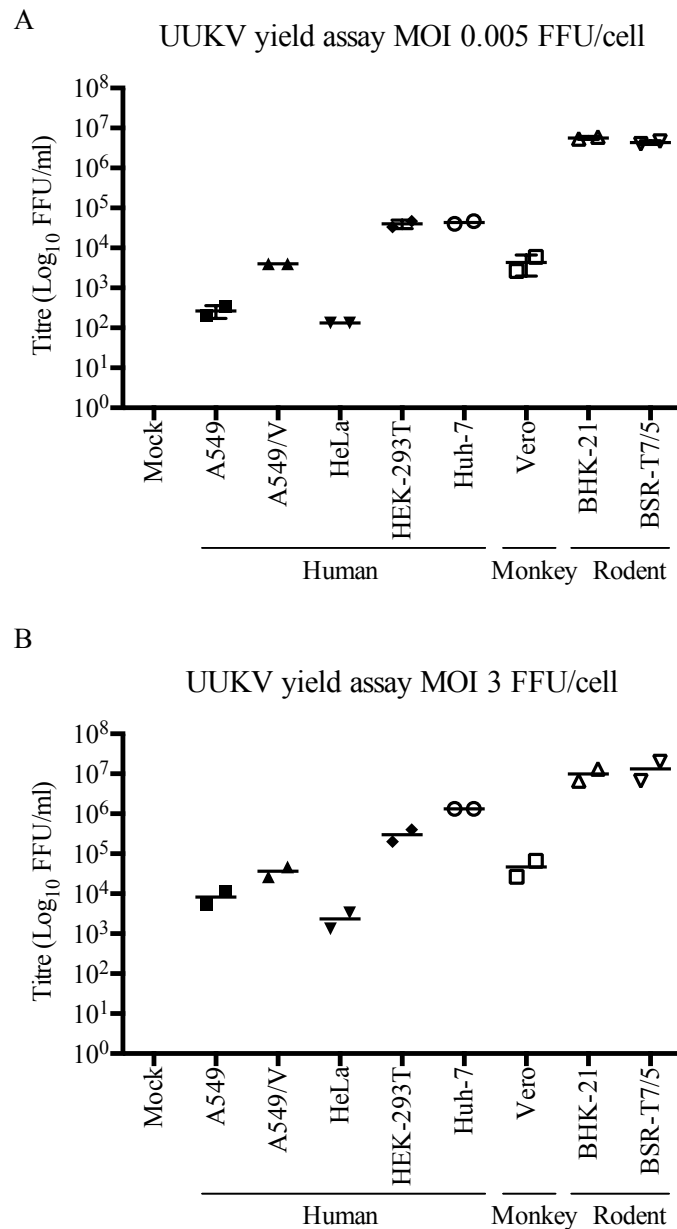


**Figure 5-10. wtUUKV yield assay in selected mammalian cell lines.**

The indicated cell lines were infected with wtUUKV at an MOI 0.005 or 3 FFU/cell and cell culture medium harvested 72 h p.i. Viral titres were determined by focus forming assays in BSR cells. The data presented are from a representative experiment of three, performed in duplicate with single data points plotted and with horizontal lines representing the mean.

### **5.3.8 Basic characterisation of rUUKV, rUUKdelNSs and rUUKdelNSsGFP in the chicken DF-1 fibroblast cell line.**

It was suggested migratory birds could play a role in the widespread distribution of tick-borne viruses in Europe (Hubálek and Rudolf, 2012). Therefore the growth properties of UUKV in an avian cell line were investigated. The growth kinetics of rUUKV and the recombinant viruses lacking NSs (rUUKdelNSs and rUUKdelNSsGFP) were compared by performing a growth curve at a MOI 0.1 FFU/cell on DF-1 cells, an immortalized cell line derived from chicken embryos (Himly *et al.*, 1998).

Interestingly, while rUUKV was able to reach titres as high as  $10^6$  FFU/mL by 48 h p.i., no increase in virus titre was observed for rUUKdelNSs or rUUKdelNSsGFP throughout the time course (Figure 5-11 A). These results suggested that UUKV NSs plays an essential role in virus replication in the DF-1 cell line. Western blotting analysis revealed that while in rUUKV-infected DF-1 cells NSs and N protein were detected by 48 h p.i. and 72 h p.i., respectively, N protein levels were undetectable for rUUKdelNSs and rUUKdelNSsGFP (Figure 5-11 B).

To confirm that the NSs-lacking recombinant viruses were able to enter and infect the cells, the availability of rUUKdelNSsGFP as a quick tool to monitor virus infection was exploited. Briefly, eGFP expression levels were monitored following rUUKdelNSsGFP infection at the MOI utilized for the DF-1 growth curve (MOI 0.1 FFU/cell). eGFP signal was detected following infection with rUUKdelNSsGFP at 12 and 24 h p.i. (Figure 5-12 A). This finding indicated that viruses lacking NSs are able to enter the cells and their genomes could undergo replication, in order for transcription of the eGFP subgenomic mRNA derived from the viral antigenome to occur. Because a decrease in the eGFP signal was detected in time points later than 24 h p.i., DF-1 cells were infected with rUUKdelNSsGFP at a higher MOI (5 FFU/cell) and the cell monolayer visualized at the indicated time points to examine DF-1 cell morphology. At 6 and 12 h p.i., most cells infected with rUUKdelNSsGFP appeared healthy, resembling uninfected cells, and only some cells rounded up, detached and floated (Figure 5-12 B). Within 24 h, most infected cells rounded up, detached and floated, showing severe cytopathicity. The eGFP signal decreased after 24h, and almost completely disappeared by 72h p.i., suggesting no infection of new cells. At 48 and 72 h p.i., the cell monolayer showed severe cytopathicity compared to the mock control (Figure 5-12 B, right panels).

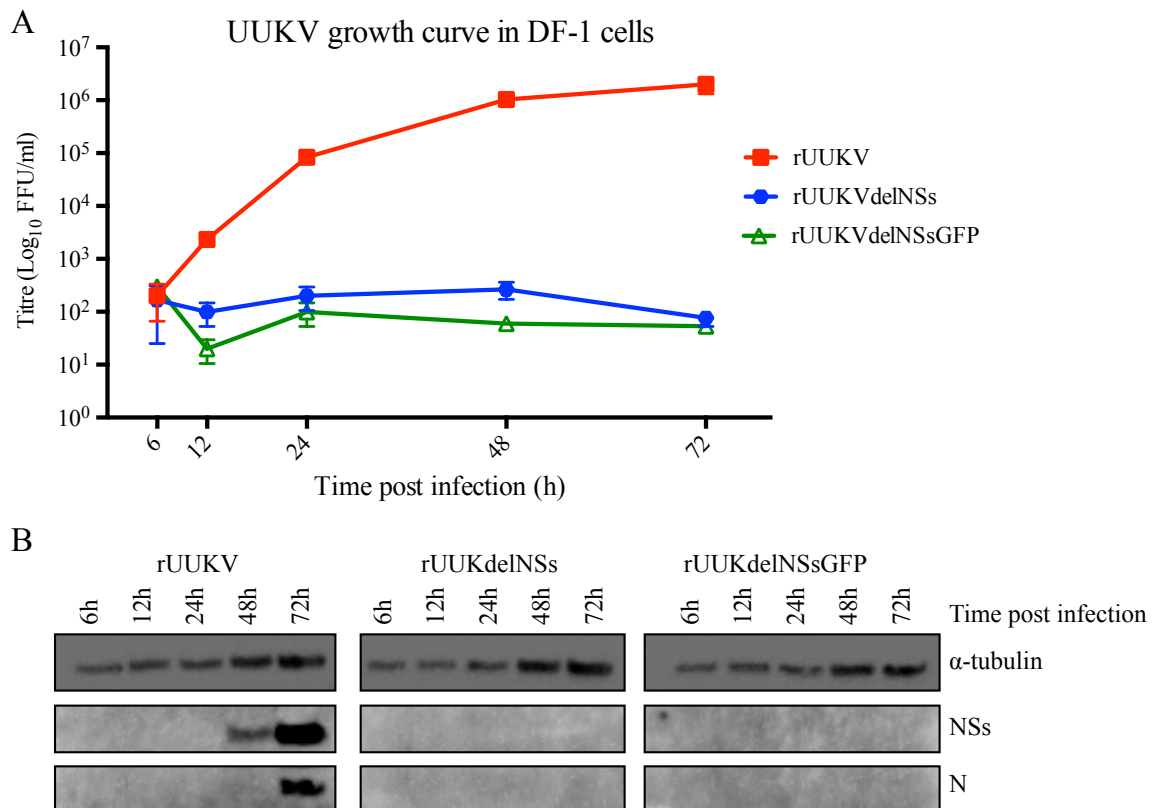


**Figure 5-11. Growth properties of recombinant UUKV in DF-1 cells.**

(A) Growth curves of recombinant viruses in DF-1 cells infected at an MOI 0.1 FFU/cell. Cell culture medium of duplicate samples was harvested at indicated time points and virus titres determined through focus-forming assays. Error bars represent the SD, for a representative experiment (n=2) performed in duplicate. (B) Analysis of viral protein synthesis in DF-1 cells. Cell lysates from the growth curve samples were harvested and western blots probed with anti- $\alpha$ -tubulin, anti-UUKV NSs and anti-UUKV N antibodies, as indicated. UUKV: Uukuniemi virus.

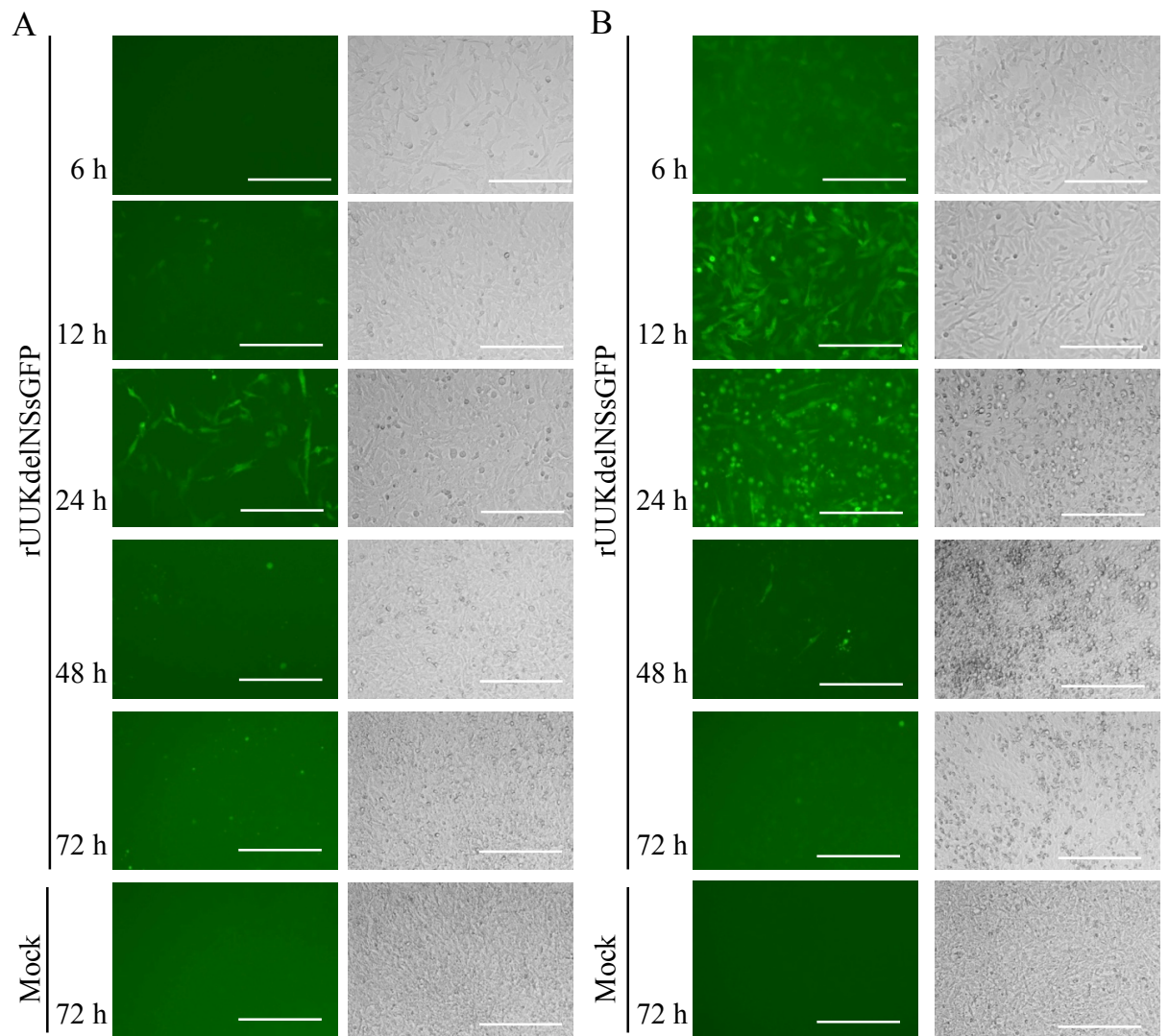


**Figure 5-12. DF-1 cell morphology following rUUKdelINSsGFP infection.**

(A) eGFP visualisation in DF-1 cells following infection with rUUKdelINSsGFP at an MOI 0.1 FFU/cell (B) eGFP visualisation in DF-1 cells following infection with rUUKdelINSsGFP at an MOI 5 FFU/cell. UUKV: Uukuniemi virus. Scale bars indicate 200 μm.

## **5.4 Discussion**

Minigenome and VLP assays based on UUKV cDNAs have already been described (K. Flick *et al.*, 2004; R. Flick *et al.*, 2002; Överby *et al.*, 2006), but are driven by Pol I. The aim of this chapter was to develop a reverse genetics system for UUKV driven by a T7 RNAP. T7 RNAP and Pol I -driven reverse genetics systems have been shown to be of similar efficiency for the rescue of RVFV (Billecocq *et al.*, 2008; Habjan *et al.*, 2008). However, some differences exist between these two systems. For instance, in a T7 RNAP driven reverse genetics system, the T7 RNAP must be provided *in trans*, commonly by cell lines stably expressing T7 RNAP such as BSR-T7/5 (Buchholz *et al.*, 1999). In addition, neither T7 RNAP nor Pol I can generate 5' capped or 3' poly-adenylated transcripts. Therefore, the T7 RNAP-driven systems use helper expression plasmids encoding the ORFs of the viral N and L proteins behind an (EMCV) IRES. This ensures that the uncapped T7 transcripts are efficiently translated. On the other hand, Pol I-driven systems commonly utilize helper plasmids which are under the control of Pol II or cytomegalovirus (CMV) promoters to generate capped and polyadenylated mRNA transcripts (Bouloy and Weber, 2010).

As bunyaviruses replicate exclusively in the cytoplasm (Elliott, 2013) and the cellular RNA polymerase I is found in the nucleus, T7 RNAP-driven reverse genetics systems for bunyaviruses are the favoured approach in our laboratory, due to the cytoplasmic localization of the T7 RNA polymerase (Elroy-Stein and B. Moss, 1990). The T7 RNAP-driven rescue system is based on three rescue plasmids encoding the full-length antigenomic cDNA copies of the viral S, M or L RNA segments, which are under the control of a T7 RNAP promoter. T7 RNAP can generate antigenome-sense RNA transcripts from the rescue plasmids. Leaky translation of the antigenome-sense RNA transcripts allows the generation of sufficient viral N and L proteins for the encapsidation of antigenome RNA. Subsequently, the antigenomic sense RNP can undergo replication, and genomic sense segments that can be packaged into viral particles are generated. Alternatively, N and L proteins can be supplied using T7 RNAP-driven expression plasmids (in a 5 plasmid system). It is important to note that, in the case of a 3 plasmid system, it is not well-understood why 'leakage' N and L expression from antigenome-sense transcripts generated by the T7 RNAP (which are not capped or polyadenylated) occurs (Billecocq *et al.*, 2008).

To initiate the development of a T7 RNAP-driven reverse genetics system for UUKV, a sensitive, luciferase- based minigenome system was developed. Addition of UUKV L protein to S, M, or L segment-based minigenome assays in BSR-T7/5 cells (constitutively expressing a T7 RNAP) resulted in an increase in reporter activity, compared to the negative control lacking the L protein (Figure 5-3). Importantly, in the M and L segment-based minigenome systems, the plasmids pT7UUKM $Ren(-)$  or pT7UUKL $Ren(-)$  encode a genome analogue that is in the genomic sense. Therefore, the increase in luciferase activity in the UUKV M and L segment-based minigenomes suggests that T7 RNAP can generate genomic sense reporter RNA transcripts from the minigenome plasmids, and that these transcripts are able to be encapsidated by the UUKV N protein, to form functional RNPs together with the L polymerase. Subsequently, the viral polymerase can replicate the genomic sense minigenome to generate antigenomic sense RNPs, which serve as a template for the transcription of the *Renilla* subgenomic mRNA, consequently resulting in an increase in *Renilla* luciferase activity. This is in comparison to the UUKV S segment-based minigenome, in which the antigenome-sense analogue transcript encoded by pT7UUKS $Ren(+)$  does not require to be replicated. Instead, the RNP formed by the antigenome analogue transcript generated by T7 RNAP and viral N and L proteins can serve directly for the transcription of the *Renilla* subgenomic mRNA. Thus, due to these inherent differences between the M or L segment-based minigenomes and the S segment-based minigenome, the promoter strengths are not comparable, as transcription of the *Renilla* subgenomic mRNA will be driven by different promoters (3' UTR promoters of the genomic or antigenomic RNA, respectively).

Interestingly, a dose-dependent decrease in the S and L segment-based minigenome activity was observed with increasing amounts of UUKV L-expressing plasmid, in comparison to the M segment –based minigenome activity, which showed a dose-dependent increase in minigenome activity with increasing amounts of UUKV L (Figure 5-3). The dose-dependent decrease in minigenome activity with increasing amounts of viral L protein has also been reported for the SFTSV M segment-based minigenome (Brennan *et al.*, 2015) and the LACV S, and L segment-based minigenomes (Blakqori *et al.*, 2003). It was suggested these observations could be attributed to a tight regulatory function of the L protein to switch from replication to cap-snatching activity (Blakqori *et al.*, 2003; Elliott and Schmaljohn, 2013). Another explanation could be that the UUKV L protein has an inhibitory effect on the generation of S and L RNA transcripts when found in high amounts, as a strategy to prevent the generation of 5'-triphosphorylated single-stranded

uncapped RNA, which can be detected by host cell helicases to induce an antiviral innate immune response.

Taken together, the minigenome assays developed allowed me to confirm that the viral UTRs, as well the UUKV N and L proteins used in this study were functional. These assays could now be used as a sensitive method to simulate viral transcription and replication processes, with RNA transcript synthesis taking place in the cytoplasm, the site of bunyavirus replication. This is in contrast to the Pol I-driven minigenome systems, where RNA transcripts are generated in the nucleus and exported to the cytoplasm for RNP assembly (R. Flick and Pettersson, 2001).

A luciferase-based system for the generation of UUKV VLPs was also developed, by supplementing the minigenome system with the UUKV glycoprotein precursor in the form of a T7 RNAP-driven expression plasmid. An increase in reporter activity was observed in recipient cells that were pre-transfected with N and L expression plasmids, in comparison to naïve recipient cells (Figure 5-4). This increase in efficiency can be attributed to the fact that transcription and replication processes in recipient cells pre-transfected with N and L will mostly be driven by these proteins, which are already expressed in the cells. In comparison, infection of naïve cells with VLPs will reflect primary transcription, carried out only by N and L proteins delivered by RNPs packaged in the VLPs. The latter system, although less efficient, serves to mirror more closely the first steps of the virus life cycle following infection of a naïve cell. Importantly, although VLPs are infectious and transcription and replication competent, they cannot mediate multi-cycle infections because not all genome segments required for virus replication are packaged in the VLPs. As they can only undergo a single-cycle infection, they remain a powerful tool to study highly pathogenic viruses outside of high containment laboratories. Therefore, the T7 RNAP-driven VLP system developed for UUKV could be applied to other tick-borne phleboviruses such as HRTV and SFTSV, in order to study virus packaging and budding processes, as well as virus morphogenesis.

The establishment of a working minigenome and VLP system allowed to confirm that all UUKV UTRs and N and L proteins were functional, and that the glycoprotein precursor could efficiently package RNPs and facilitate the delivery of minigenome analogues to naïve cells, an important prerequisite to enable rescue of UUKV from cDNA clones. Indeed, UUKV was successfully rescued entirely from cDNA clones, which exhibited similar properties to authentic wild-type UUKV, with similar focus size and phenotype,

and growth kinetics in BHK-21 cells (Figures 5-5 and 5-8). Comparison of a 3-plasmid rescue system and a 5-plasmid rescue system, where the rescue plasmids encoding the three antigenomic sense UUKV cDNA segments were supplemented with UUKV N- and L- expressing plasmids, resulted in no difference in virus yield.

Furthermore, two recombinant UUK viruses lacking NSs were generated: rUUKdelNSs, in which the NSs ORF was deleted from the genome, resulting in a virus with a shorter S segment, and rUUKdelNSsGFP, in which the NSs ORF was replaced with that of eGFP (Figure 5-6). Deletion of NSs from the UUKV genome resulted in the recombinant viruses forming significantly smaller foci (Figure 5-7 A). Additionally, the growth kinetics of rUUKdelNSs and rUUKdelNSsGFP in BHK-21 cells was slower compared to wtUUKV and rUUKV (Figure 5-8). BHK-21 cells lack a competent IFN system (Otsuki *et al.*, 1979). Therefore, the attenuation in growth kinetics of recombinant UUKV lacking NSs compared to wild-type UUKV is independent of the IFN status of the cell. This has been noted for other bunyaviruses such as BUNV (Bridgen *et al.*, 2001), OROV (Tilston-Lunel *et al.*, 2016) and SBV (Elliott *et al.*, 2013; Varela *et al.*, 2013), but intriguingly not for LACV (Blakqori and Weber, 2005). The attenuation in growth kinetics of viruses lacking NSs suggests that this protein could have some dispensable role in facilitating virus replication.

Interestingly, a one-log difference in virus titre was observed in the growth kinetics of rUUKdelNSsGFP compared to rUUKdelNSs in BHK-21 cells, with rUUKdelNSsGFP growing slightly better than rUUKdelNSs (Figure 5-8). It seems unlikely that GFP could itself contribute to the enhancement of virus replication. Rather, it is possible that this is due to the S segment of rUUKdelNSsGFP resembling more closely the S segment of wtUUKV (Figure 5-6 A). The S segment of rUUKdelNSs on the other hand, in which the NSs ORF was deleted, has an intergenic region that directly abuts the viral S 5' UTR, which could result in an impairment of antigenomic RNA synthesis. Investigating this hypothesis was beyond the scope of this study, however it would be interesting to examine virus RNA synthesis in all recombinant viruses, or to generate a recombinant UUKV where NSs expression is eliminated through for instance, the mutation of start codons, and comparing its growth kinetics to rUUKdelNSsGFP and rUUKdelNSs.

Nevertheless, the results in this chapter demonstrate that rUUKdelNSsGFP serves as a quick tool to visualise virus infection. Infection of various mammalian cell lines with rUUKdelNSsGFP enabled the examination of their permissibility to support UUKV

replication, through direct visualisation of eGFP (Figure 5-9). The results obtained by visualizing eGFP following rUUKdelNSsGFP infection are in agreement with yield assays performed using wtUUKV in the same cell lines (Figure 5-10). Briefly, rodent BHK-21 and BSR-T7/5 cells exhibited the highest permissibility to UUKV infection, which was not surprising since wtUUKV and the recombinant viruses were propagated in rodent cell lines in order to generate virus stocks. Of all the human cell lines tested, HEK-293T and Huh-7 cells yielded the highest UUKV titres and showed the most susceptibility to rUUKdelNSsGFP infection, whereas no eGFP expression and the lowest wtUUKV yields were observed in HeLa cells. A one-log increase in wtUUKV titre was observed in A549/V cells compared to its IFN-competent parental cell line A549, which was also reflected by increased eGFP expression following rUUKdelNSsGFP infection in A549/V cells compared to A549 cells (Figures 5-9 and 5-10). As A549/V cells are unable to respond to IFN, these results suggest that the IFN response may play a role in limiting UUKV infection.

Finally, various strains of UUKV, or UUKV-like viruses have been isolated from tick species collected in nesting areas of seabirds, passerine birds, or from tick nymphs collected on migrant birds (S. R. Moss, 1986; Nuttall *et al.*, 1984; 1981; Traavik and Mehl, 1977; Watret and Elliott, 1985). In 2012, Hubalek *et al.* suggested migratory birds could play a role in the widespread distribution of tick-borne viruses in Europe (Hubálek and Rudolf, 2012). A phylogenetic analysis of SFTSV and migratory bird routes in Asia proposed that migratory birds, well-known carriers of ticks, could be a potential source of the spread of SFTSV across countries (Yun *et al.*, 2015). Furthermore, antibodies against SFTSV were detected in two migratory bird species in China (Li *et al.*, 2016). Therefore, the growth properties of recombinant UUK viruses were also investigated in a cell line of avian origin, namely the chicken embryo DF-1 fibroblast cell line. Intriguingly, while rUUKV was able to reach titres of  $\sim 10^6$  FFU/mL, no increase in virus titre was observed for recombinant viruses lacking NSs (Figure 5-11 A). Additionally, no N or NSs protein could be detected in the time course by immunoblotting of rUUKdelNSsGFP or rUUKdelNSs –infected cell lysates, compared to rUUKV-infected cells (Figure 5-11 B). Taken together, these results suggest that NSs is essential for UUKV replication in DF-1 cells. Visualisation of eGFP in DF-1 cells following rUUKdelNSsGFP infection confirmed that rUUKdelNSsGFP is able to enter the cells and that the first steps of the viral cycle such as uncoating and genome replication must occur in order for the eGFP ORF, which is in the positive sense in the viral genome, to be transcribed and subgenomic eGFP mRNA

generated from antigenomic sense RNA (Figure 5-11 C and D). As DF-1 cells are IFN competent (Liniger *et al.*, 2012; H. Qu *et al.*, 2013), one possibility is that viruses lacking NSs induce an IFN response large enough to create an antiviral state in neighboring cells, rendering them resistant to virus infection. Alternatively, NSs could play an essential role in later stages of the viral life cycle, such as virus assembly and/or egress. As it stands, the finding that UUKV NSs has an essential role in the virus life cycle in DF-1 cells is an interesting finding, as the NSs protein of bunyaviruses is commonly regarded as a non-essential gene product.

To conclude, the T7 RNAP-driven minigenome assays developed and described in this chapter can be used in the future to resemble more closely the cytoplasmic transcriptional and replicational processes utilized by UUKV, in comparison to the established Pol I-driven UUKV minigenome system. The reverse genetics system described herein has allowed the successful rescue of UUKV entirely from cDNA clones, and enabled the targeted manipulation of the UUKV genome. The robustness of the T7 RNAP-driven UUKV reverse genetics system was highlighted by the generation of two viruses lacking NSs, rUUKdelNSs and rUUKdelNSsGFP. It was also demonstrated that rUUKdelNSsGFP can be used as a quick tool to monitor and visualize virus infection. Finally, the findings described in this chapter indicate that UUKV NSs has a dispensable role in facilitating virus replication in IFN-incompetent BHK-21 cells, whereas the presence of NSs seems to be essential for UUKV replication in chicken DF-1 cells.

## **5.5 Summary**

- A luciferase-based T7 RNAP-driven minigenome system for UUKV was developed, which showed that the UTR sequences as well as the N and L proteins used in this study are functional. The minigenome system will facilitate future studies on transcription and replication processes of UUKV.
- A VLP assay for UUKV was developed, which shows increased efficiency when recipient cells are pre-transfected with N and L.
- Recombinant UUKV was successfully rescued entirely from cDNA clones, and exhibited similar properties to authentic wild-type UUKV.
- Comparison of 3- and 5-plasmid rescue systems revealed no difference in virus yield.
- Two recombinant viruses lacking NSs were generated: rUUKdelNSs and rUUKdelNSsGFP.
- rUUKdelNSsGFP now serves as a tool to visualise and monitor virus infection.
- Attenuation in the growth kinetics of viruses lacking NSs compared to wild-type viruses in BHK-21 suggested that NSs could have a dispensable role in facilitating virus replication.
- In comparison to rUUKV, rUUKdelNSs and rUUKdelNSsGFP were unable to replicate in chicken DF-1 cells, indicating an essential role of UUKV NSs in virus replication in DF-1 cells.

## **6 Role of tick-borne phlebovirus NSs proteins in suppressing the human interferon system**

### **6.1 Introduction**

Vertebrate hosts rely on the innate immune system as a first line of defence upon exposure to pathogens. Following infection of a susceptible vertebrate host, viruses are confronted by the interferon (IFN) system. The IFN system plays an important role in the innate immune system to ‘interfere’ with and control virus replication (Randall and Goodbourn, 2008). Once an infected host cell detects ‘non-self’ products produced by viruses upon infection, intracellular signalling pathways are activated, which lead to the production and secretion of IFN. Secreted IFN can then signal neighbouring cells to begin the up-regulation of a number of IFN-stimulated genes (ISGs) that can have anti-viral activity, rendering the cells in an anti-viral state (Goodbourn *et al.*, 2000; Hoffmann *et al.*, 2015; Randall and Goodbourn, 2008; Schneider *et al.*, 2014). Viruses, in turn, utilise a plethora of countermeasures to overcome the IFN system. These countermeasures involve the modulation of IFN production or signalling, and/or the function of antiviral proteins induced by the IFN system (Haller *et al.*, 2007; Randall and Goodbourn, 2008; Wuerth and Weber, 2016).

The accessory protein of bunyaviruses NSs is known to act as an IFN antagonist that contributes to pathogenicity, a role first demonstrated for BUNV NSs (Bridgen *et al.*, 2001; Weber *et al.*, 2002). One of the first indications that the NSs protein of a member of the *Phlebovirus* genus had an IFN antagonistic activity was the finding that different strains of Rift Valley fever virus (RVFV) were differentially sensitive to the action of IFN (Bouloy *et al.*, 2001). Specifically, the virulent RVFV strain ZH548 failed to induce type I IFNs and replicated efficiently in both wild-type mice and mice lacking the type I IFN receptor. On the other hand, RVFV strains with mutations in the NSs gene (MP12 and clone 13) induced type I IFNs, and were highly virulent in mice lacking the type I IFN receptor but not in wild-type mice. These findings provided the first genetic evidence that RVFV NSs acts as an IFN antagonist. Indeed, the NSs protein of RVFV was later shown to act as an IFN antagonist by inhibiting transcription of IFN-induced genes (Billecocq *et al.*, 2004; Le May *et al.*, 2008). The IFN inhibitory activity of RVFV NSs was also confirmed by the generation of recombinant RVFV lacking its NSs protein, which induced IFN compared to wild-type RVFV (Ikegami *et al.*, 2006). Similar studies have also

demonstrated that other mosquito-borne phlebovirus NSs proteins have an IFN antagonist activity. TOSV NSs exhibits weak IFN antagonistic activity, which results in TOSV inducing IFN following infection of host cells (Gori-Savellini *et al.*, 2013; 2010). Additionally, using transient transfection assays and recombinant RVFV where the RVFV NSs ORF was replaced by that of PTV and SFSV NSs, it was demonstrated that PTV and SFSV NSs proteins act as antagonists of IFN production (Lihoradova *et al.*, 2013).

Until recently, the role of the NSs protein of tick-borne phleboviruses in modulating the host IFN response was poorly understood. It was the identification of the highly pathogenic tick-borne phlebovirus SFTSV in 2011 that prompted the need to understand the molecular biology and pathogenesis of tick-borne phleboviruses. Indeed, in 2014 a number of studies reported that the NSs protein of SFTSV acts as a potent antagonist of both IFN induction and IFN signalling (Ning *et al.*, 2015; 2014; Santiago *et al.*, 2014). Besides SFTSV, it remains unknown whether the NSs protein of other tick-borne phleboviruses play a role in blocking the human IFN response, and whether the efficiency of IFN antagonism by the NSs proteins contributes to viral pathogenicity. Such studies are urgently required, as tick-borne phleboviruses are continuously emerging and their movement into naïve geographical locations pose a risk to human and animal health (Elliott and Brennan, 2014). The development of a reverse genetics system for the apathogenic UUKV and the generation of NSs-lacking viruses are tools that can be used to assess the ability of UUKV NSs to antagonise the IFN response, and to compare its IFN antagonist activity to the NSs protein of more pathogenic tick-borne phleboviruses such as HRTV and SFTSV.

## **6.2 Aims**

The overall aim of this chapter was to determine whether the NSs protein of the tick-borne phleboviruses UUKV and HRTV exhibit an IFN antagonistic activity. Firstly, I aimed to exploit the established reverse genetics system for UUKV (described in Chapter 5), utilizing NSs-lacking viruses to evaluate whether UUKV NSs could inhibit the human IFN response in cell culture. Due to the lack of a working reverse genetics system for HRTV, I aimed to study the IFN antagonistic activity of its NSs protein using transient transfection assays. Furthermore, I intended to compare whether the NSs protein belonging to more pathogenic tick-borne phleboviruses (such as HRTV and SFTSV) could modulate the IFN system more efficiently than the NSs protein of the apathogenic UUKV. Finally, I aimed to investigate the sensitivity of UUKV, HRTV and SFTSV to IFN treatment.

## 6.3 Results

### 6.3.1 Evaluation of UUKV NSs as an IFN antagonist

With the aim of determining whether UUKV replication would be enhanced in cells lacking a functional IFN system, virus yields of wtUUKV, rUUKV and recombinant UUKV lacking NSs (rUUKdelNSs and rUUKdelNSsGFP) were compared following infection of IFN-competent A549 cells and of its IFN-incompetent derivative cell line A549/PIV5-V (henceforth referred to as A549/V). The A549/V cell line constitutively expresses the V protein of parainfluenza virus type 5, which blocks type I IFN signalling by targeting STAT1 for degradation (Killip *et al.*, 2013). Briefly, A549 and A549/V cells were infected at an MOI of 2 FFU/cell and the cell culture supernatant harvested 72 h p.i. Virus titres were determined in BSR cells. While wtUUKV and rUUKV achieved titres of  $\sim 10^6$  FFU/ml in A549 cells, a one-log increase in virus titre was observed in A549/V cells (Figure 6-1 A). rUUKdelNSs and rUUKdelNSs GFP reached titres of  $\sim 10^5$  FFU/ml in A549 cells, and titres were slightly higher in A549/V cells. Importantly, in IFN-incompetent A549/V cells, viruses lacking NSs did not reach the same titres as wild-type UUKV. If UUKV NSs only plays a role in IFN antagonism, then presumably UUKV lacking NSs should achieve similar titres as wild-type UUKV in IFN-incompetent cells. However, the lower titres achieved by NSs-lacking viruses in A549/V cells could be explained by a dispensable role NSs may be playing to facilitate virus replication, as it was noted in Chapter 5 (Section 5.3.6). Nonetheless, these results demonstrate that although UUKV is able to replicate in IFN-competent A549 cells, replication was enhanced in A549/V cells, which lack a functional IFN response.

To determine whether UUKV NSs plays a role in suppressing the human IFN system, a biological IFN protection assay was carried out to measure the production of IFN in the cell culture medium of virus-infected cells. Briefly, the cell culture medium was collected at 24 h p.i. from A549 cells infected with wtUUKV, rUUKV, rUUKdelNSs or rUUKdelNSsGFP at a high MOI (3 FFU/cell). Wild-type Bunyamwera virus (BUNV) and recombinant BUNV lacking its NSs protein (rBUNdelNSs2) (van Knippenberg *et al.*, 2010) were used as controls because it is well known that BUNV NSs is a potent IFN antagonist and the major virulence factor of BUNV (Bridgen *et al.*, 2001; Weber *et al.*, 2002). 24 h p.i. the cell culture medium was UV-inactivated and serially diluted to pre-treat A549/BVDV-Npro cells (Hale *et al.*, 2009) for 24 h, prior to infection with the IFN-sensitive encephalomyocarditis virus (EMCV). A549/BVDV-Npro cells constitutively

express the bovine viral diarrhea virus IFN antagonist NPro and therefore cannot produce IFN, but remain responsive to exogenously applied IFN (Hale *et al.*, 2009; Hilton *et al.*, 2006). While no protection was observed from mock- or BUNV-infected cells, cells treated with recombinant IFN- $\beta$  or with medium from rBUNdelNSs2-infected cells conferred protection from EMCV-induced cytopathic effect (CPE) (Figure 6-1 B). In contrast to cell culture medium from BUNV-infected cells, some protection (a mean of approximately 12 relative IFN units [RIU]) was provided by medium from cells infected with wtUUKV or rUUKV (Figure 6-1 B and C), suggesting that UUKV infection induces IFN production. However, a 10-fold increase in relative IFN production was observed in the cell culture medium of rUUKdelNSs or rUUKdelNSsGFP-infected cells compared to wtUUKV or rUUKV -infected cells. Taken together, these results demonstrate that UUKV viruses lacking NSs induce a larger IFN response than wild-type UUKV, as deletion of NSs leads to a 10-fold increase in IFN production during infection. The induction of IFN by wild-type UUKV suggests that UUKV is unable to fully ablate the IFN response induced by the virus, in comparison to BUNV, which induced no IFN.

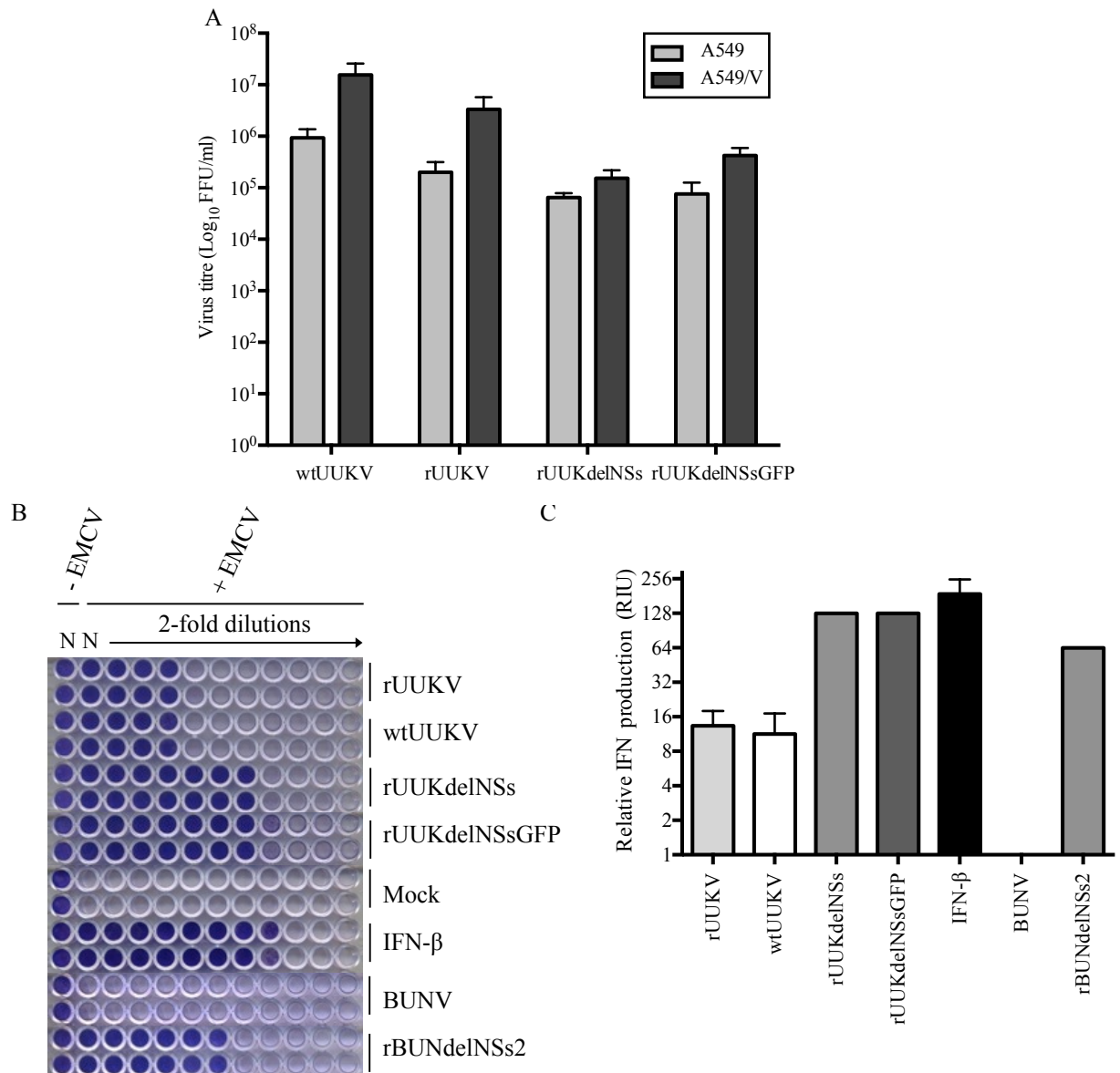


**Figure 6-1. Recombinant UUKV viruses lacking NSs are better inducers of IFN than wild-type UUKV.**

(A) Yield assay of indicated viruses in A549 or A549/V cells. Cell monolayers were infected at an MOI of 2 FFU/cell. The cell culture medium was harvested at 72 h p.i., and virus titre determined by focus-forming assays in BSR cells. Bars represent the mean virus titre of a representative experiment of two  $\pm$  SD ( $n=3$ ). (B-C) Biological interferon protection assays. A549 cells were infected at an MOI of 3 FFU/cell with the indicated viruses, or mock-infected. Cell culture medium was harvested 24 h p.i. and serial dilutions of the UV-inactivated medium (or 500 units of IFN- $\beta$ ) were used to pretreat A549-Npro cells prior to infection with EMCV. The cells were stained with crystal violet at 4 days p.i. (B) Assay plates. (C) Relative IFN units (RIU) produced, calculated as  $RIU = 2^N$ , where  $N$  represents the number of wells that are protected from EMCV infection. The bars indicate the mean RIU values calculated from a representative experiment of two performed in triplicate ( $n=3$ )  $\pm$  SD. UUKV: Uukuniemi virus, BUNV: Bunyamwera virus, IFN- $\beta$ : Interferon- $\beta$ .

### 6.3.2 Inhibition of IFN induction by tick-borne phlebovirus NSs proteins

Next, the role of UUKV and HRTV NSs proteins in modulating IFN induction was investigated. SFTSV NSs was used as a positive control, as it is a well-known potent antagonist of IFN induction. Firstly, the NSs proteins of UUKV, HRTV or SFTSV were cloned into a CMV-driven expression vector (pCMV) using restriction-free cloning. The NSs proteins were either left untagged, or tagged with a V5 tag at their C-terminus. The plasmids were called pCMV-XNSs or pCMV-XNSsV5, where X refers to the virus the NSs protein sequence was derived from, and V5 refers to the C-terminal V5-tagged NSs proteins. The reason for tagging the proteins with the V5 tag was to compare expression levels of the NSs proteins in subsequent assays by western blotting. The IFN induction assay was carried out by co-transfecting HEK293T cells with an inducer plasmid encoding the N-terminal 2CARD domain of RIG-I (pCMV-RIGI-N) along with increasing amounts of pCMVXNSs or pCMVXNSsV5. At 24 h post transfection, IFN production in the cell culture medium was quantified using a biological IFN protection assay (described in section 6.3.1). The percentage of induction was normalised against the induction control (RIG-I N plasmid alone), which was considered 100%.

A dose-dependent inhibitory effect of IFN induction was observed with increasing amounts of the untagged and V5-tagged NSs proteins of all three viruses (Figure 6-2 A). In agreement with the results presented in section 6.3.1, the inhibitory activity of UUKV NSs was distinctly weak compared to HRTV or SFTSV NSs. At the highest dose (250 ng) of NSs-expressing plasmid, UUKV NSs expression resulted in approximately 60% inhibition of IFN production, whereas that of HRTV and SFTSV NSs was 100% (Figure 6-2 A). A difference in the strength of IFN induction antagonism was observed between HRTV and SFTSV NSs proteins. While the lowest dose (10 ng) of HRTV NSs expression plasmids resulted in approximately a 50% decrease in IFN production, the same dose of SFTSV NSs expression plasmids led to almost a 95% decrease in IFN production (Figure 6-2 A). Transfected cell lysates were analysed by immunoblotting to visualise the expression levels of V5-tagged NSs proteins. Interestingly, visibly lower expression levels of V5-tagged HRTV NSs were detected in comparison to UUKV and SFTSV NSs proteins (Figure 6-2 B), which could account for the weaker inhibitory activity of HRTV NSs compared to SFTSV NSs. Indeed, 50 ng of V5-tagged HRTV NSs yielded similar protein expression levels to 10 ng of V5-tagged SFTSV NSs (Figure 6-2 B), and at these amounts similar inhibitory activity on IFN production was observed for the respective NSs proteins (Figure 6-2 A).

IRF-3 is a transcription factor that is ubiquitously expressed in cells. Upon activation of the IFN pathway, IRF-3 is phosphorylated by TBK1, which enables its homodimerization, prior to its translocation to the nucleus, where it acts as a transcription factor to enhance the activation of the IFN- $\beta$  promoter (Fitzgerald *et al.*, 2003; Lin *et al.*, 1998; Panne *et al.*, 2007; Yoneyama *et al.*, 1998). To investigate whether the inhibition of IFN production by tick-borne phlebovirus NSs proteins occurs by ultimately preventing the activation of IRF-3 and its translocation to the nucleus, the levels of phosphorylated and dimerized IRF-3 in the presence of UUKV, HRTV and SFTSV NSs proteins were assessed. HEK293Ts were transfected with RIG-I N-expressing plasmid, along with 250 ng of pCMVXNSs or pCMVXNSsV5 (the highest amount used in Figure 6-2). Transfected cell lysates were harvested for analysis of IRF-3 phosphorylation. IRF-3 phosphorylated at Ser386 could be readily detected in mock cells stimulated with RIG-I N-expressing plasmid. Whilst some IRF-3Ser386 was detected in cells transiently expressing UUKV NSs, almost undetectable levels of phosphorylated IRF-3 were observed in the presence of HRTV or SFTSV NSs (Figure 6-3 A). In all experimental conditions the levels of total IRF-3 remained unchanged (Figure 6-3 A). Similar results were obtained when cell lysates were analysed under non-denaturing conditions. Stimulation of mock cells with RIG-I N resulted in the dimerization of IRF-3, and although some dimerized IRF-3 could be detected in the presence of UUKV NSs, no dimeric IRF-3 could be detected in the presence of HRTV or SFTSV NSs (Figure 6-3 B). Of note, a shift in molecular weight was observed for the V5-tagged UUKV NSs under non-reducing conditions, presumably because the electrophoretic mobility of UUKV NSs under non-reducing conditions is affected by its charge and native conformation.

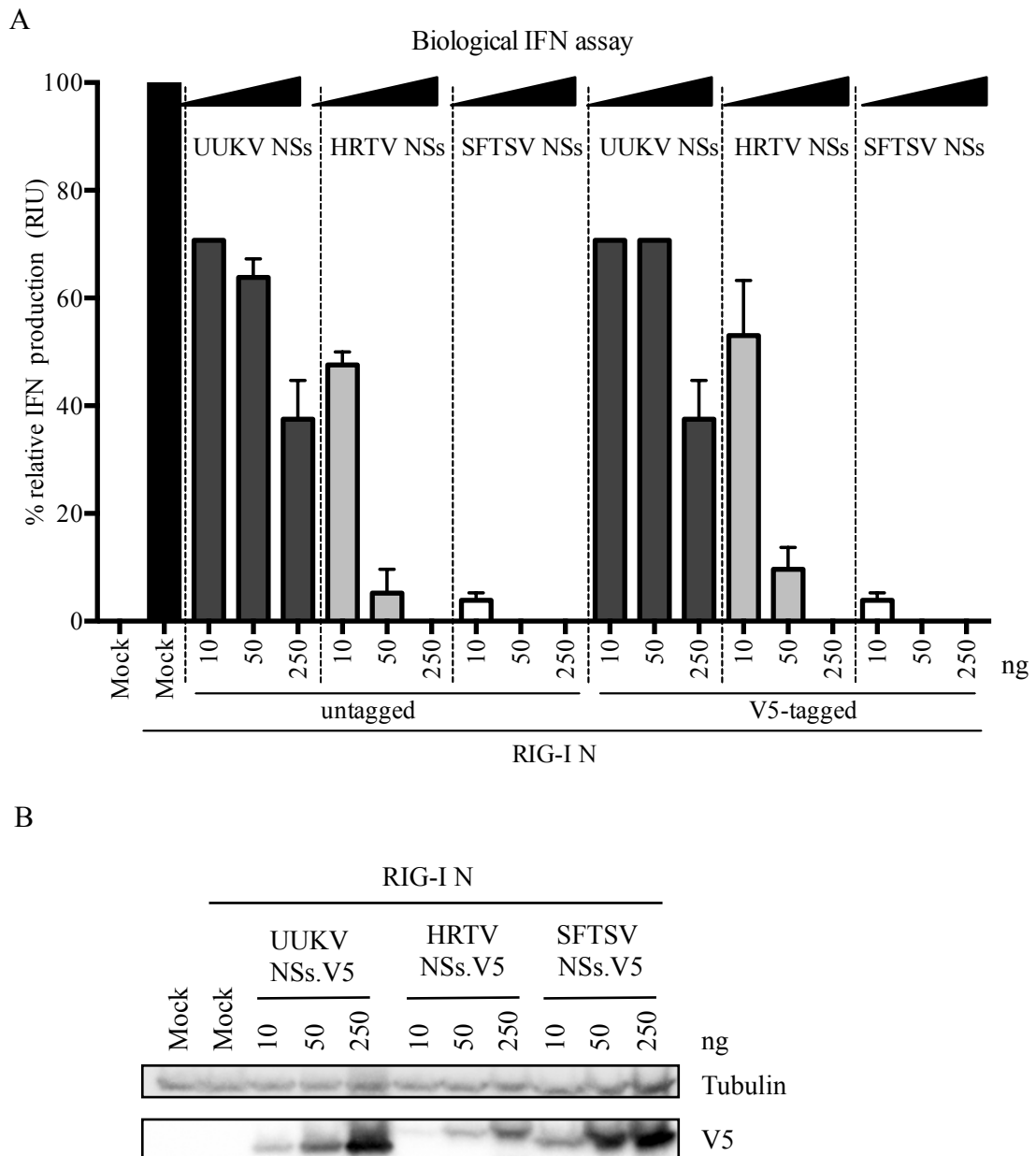


**Figure 6-2. Inhibition of IFN production by tick-borne phlebovirus NSs proteins.**

(A) The inhibitory effect of UUKV, HRTV and SFTSV NSs proteins on IFN induction was investigated by measuring induction of IFN production in HEK293T cells transfected with a plasmid encoding the N terminus of RIG-I in the presence of increasing amounts of untagged or V5-tagged NSs proteins. Cell culture medium was harvested 24 h post transfection and the relative IFN units assayed using a biological IFN protection assay in A549/BVDV-Npro cells. Percentage induction was normalised against the induction control (mock cells induced with RIG-I N only), which was considered 100%. Bars indicate the mean percentage IFN production from three independent experiments performed in duplicate  $\pm$  SEM ( $n=3$ ). (B) Immunoblot of V5-tagged NSs proteins in cell lysates belonging to the IFN induction assay described in (A). UUKV: Uukuniemi virus, HRTV: Heartland virus, SFTSV: Severe fever with thrombocytopenia syndrome virus.

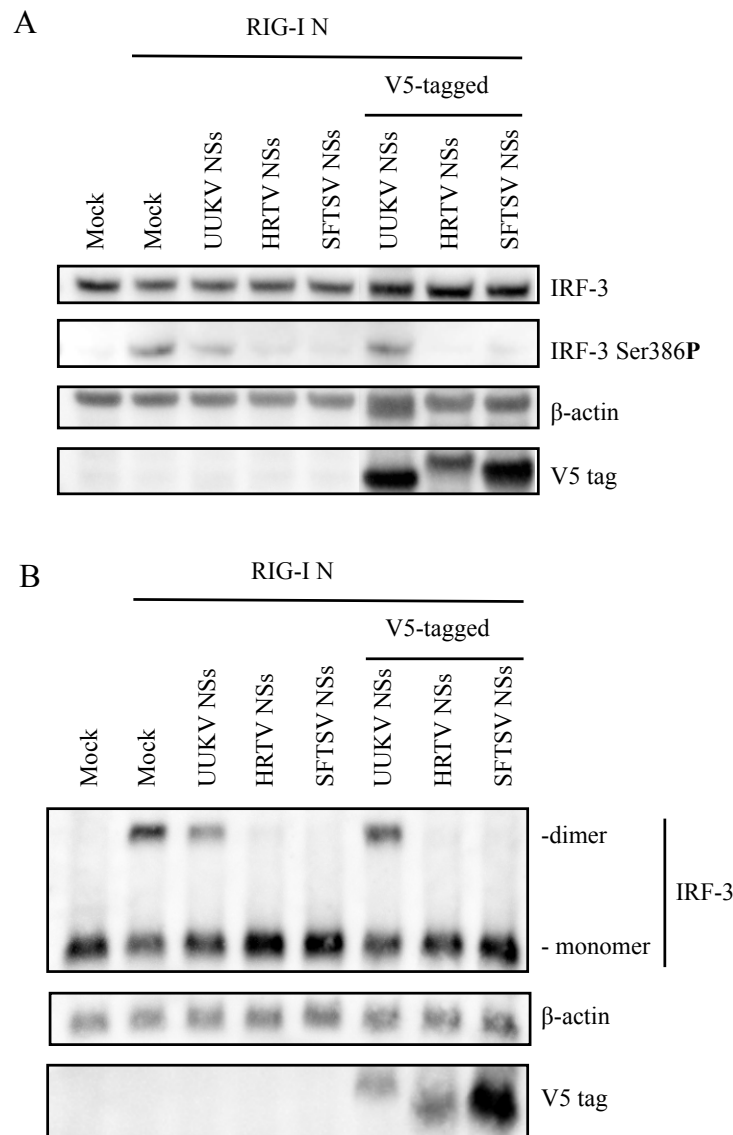


**Figure 6-3. Inhibition of IRF-3 phosphorylation and dimerization by tick-borne phlebovirus NSs proteins.**

(A) Western blot showing the phosphorylation status of IRF-3 at Ser386 in HEK293T cells transfected with 250 ng untagged or V5-tagged UUKV, HRTV or SFTSV NSs proteins and IFN- $\alpha$  induced by co-transfection of RIG-I N-expressing plasmid. (D) Western blot of monomeric and dimeric forms of IRF-3 in HEK293T cells co-transfected with 250 ng untagged or V5-tagged UUKV, HRTV or SFTSV NSs proteins and induced by co-transfection of RIG-I N-expressing plasmid. 24 h post transfection the cell monolayer was lysed with non-reducing lysis buffer and the proteins separated on a non-reducing gel before western blotting and probing with IRF-3, actin and V5 tag antibodies. UUKV: Uukuniemi virus, HRTV: Heartland virus, SFTSV: Severe fever with thrombocytopenia syndrome virus.

Furthermore, the translocation of IRF-3 upon induction by RIG-I N in the presence of the NSs proteins was investigated. Briefly, HEK293T cells transiently expressing the untagged, or tagged NSs proteins and induced with the RIG-I N-expressing plasmid were fixed, permeabilized and probed with anti-V5 and anti-IRF-3 antibodies 24 h post transfection, and visualized by confocal microscopy. While in un-induced cells IRF-3 remained cytoplasmic, nuclear translocation of IRF-3 was detected in 47% of mock cells transfected with the RIG-I N-expressing plasmid (Figure 6-4 A and B). In the presence of UUKV NSs, some nuclear IRF-3 could be observed, however the percentage of cells exhibiting nuclear translocation of IRF-3 was lower than in mock-transfected cells (nuclear IRF-3 was detected in 19% and 13% of cells in the presence of untagged, or V5-tagged UUKV NSs, respectively) (Figure 6-3 B). The presence of the V5 tag allowed me to confirm that in some (but not all) cells expressing UUKV NSs-V5, IRF-3 translocation was not inhibited (Figure 6-3 A). In contrast, in cells transiently expressing HRTV or SFTSV NSs proteins, the percentage of nuclear IRF-3 was similar to that in uninduced cells (Figure 6-3 B). A clear difference was observed in the subcellular localization of V5-tagged HRTV and SFTSV NSs proteins: whereas SFTSV NSs formed distinct cytoplasmic inclusion bodies (IBs) which sequestered IRF-3, IRF-3 remained diffused in the cytoplasm in the presence of HRTV NSs (Figure 6-3 A). Though overall this assay was informative, the quantification of nuclear translocation of IRF-3 was carried out blindly. Specifically, it was not possible to confirm that the counted cells had been transfected with the RIG I N-expressing plasmid, and thus perhaps not all counted cells have been induced. Tagging the N-terminus of RIG-I in the RIG-I N-expressing plasmid would certainly improve the reliability of this experiment.

Taken together, these data suggest that HRTV and SFTSV NSs proteins efficiently antagonize IFN induction by ultimately hindering the activation of IRF-3, thus inhibiting the activation of the IFN- $\beta$  promoter. On the other hand, UUKV NSs acts as a weak IFN antagonist, and is capable of blocking the activation of IRF-3 or the subsequent production of IFN, but with decreased efficiency compared to HRTV or SFTSV NSs proteins.

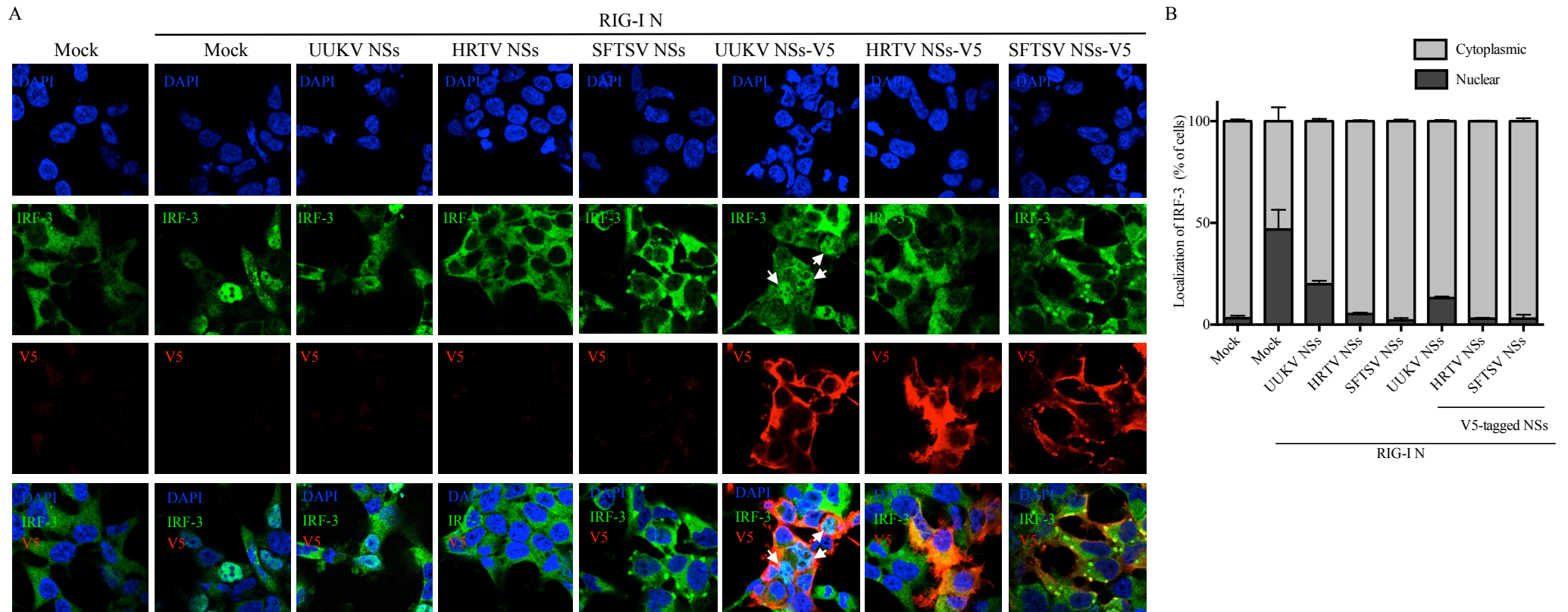


**Figure 6-4. RIG-I -induced nuclear translocation of IRF-3 in the presence of tick-borne phlebovirus NSs proteins.** (A) HEK293T cells were cotransfected with a RIG-I N-expressing plasmid, and untagged or V5-tagged UUKV, HRTV or SFTSV NSs proteins. 24 h post transfection, the cells were fixed, permeabilised and probed with IRF-3 and V5 antibodies to visualise the nuclear translocation of IRF-3 (green), V5-tagged NSs proteins (red), and DAPI-stained nuclei (blue) by confocal microscopy. The images shown are representative of one randomly selected area on a confocal slide, of two independent experiments. White arrows indicate nuclear translocation of IRF-3 in cells transiently expressing V5-tagged UUKV NSs. (B) Quantification of cells exhibiting nuclear or cytoplasmic staining IRF-3 in (A). Cells from two randomly selected areas were counted and the total number of counted cells in each image (n=43-95) considered 100%. Cells showing no nuclear staining of IRF-3 were considered cytoplasmic, whereas cells exhibiting only nuclear or nuclear and cytoplasmic IRF-3 staining were considered nuclear. The results shown indicate the mean percentage of cells with nuclear or cytoplasmic IRF-3 staining in two independent experiments  $\pm$  SD.

### ***6.3.3 Effect of tick-borne phlebovirus NSs proteins on NF- $\kappa$ B signalling***

The ability of UUKV, HRTV or SFTSV NSs proteins to inhibit NF- $\kappa$ B signalling was also investigated. Subconfluent HEK293T were transfected with 200 ng pNF- $\kappa$ Bluc and 5 ng of a plasmid encoding *Renilla* luciferase under the control of a CMV promoter (phRL), along with 150 ng pCMVXNSs or pCMVXNSsV5 (where X refers to UUKV, HRTV or SFTSV). pNF- $\kappa$ Bluc encodes firefly luciferase under the control of an NF- $\kappa$ B promoter containing five tandem copies of the canonical  $\kappa$ B elements. A plasmid encoding the I $\kappa$ B $\alpha$  super-repressor (pCMV-I $\kappa$ B $\alpha$ SR) was used as a positive control for the inhibition of NF- $\kappa$ B signalling. I $\kappa$ B $\alpha$ SR is a I $\kappa$ B $\alpha$  molecule that inhibits NF- $\kappa$ B signalling due to mutations at serine residues required for its phosphorylation and proteasomal degradation (Gupta *et al.*, 2010). In this way, NF- $\kappa$ B remains sequestered in the cytoplasm, thus the induction of NF- $\kappa$ B target genes is suppressed. 18 h post transfection the cells were mock-treated or treated with tumor necrosis factor (TNF)- $\alpha$ . 24 h post treatment, the cells were lysed and firefly and *Renilla* luciferase activities analysed. Firefly activity was normalised against the *Renilla* luciferase activity and fold induction was calculated relative to the uninduced control.

As expected, I $\kappa$ B $\alpha$ SR impeded NF- $\kappa$ B activation. However, no inhibition of NF- $\kappa$ B signalling by untagged or V5-tagged UUKV, HRTV or SFTSV NSs proteins was observed (Figure 6-5).

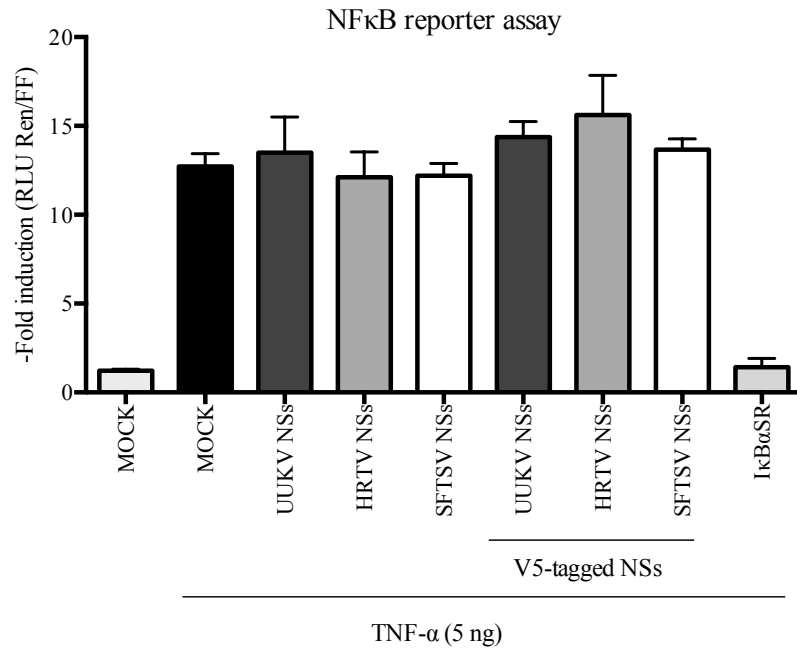


**Figure 6-5. The effect of tick-borne phlebovirus NSs proteins on NF- $\kappa$ B activation.**

HEK293T cells were transfected with a firefly luciferase reporter plasmid under the control of five tandem copies of the canonical  $\kappa$ B elements (pNF- $\kappa$ Bluc) and pRL in the presence of expression plasmids encoding untagged, or V5-tagged UUKV, HRTV or SFTSV NSs proteins, or I $\kappa$ B $\alpha$ SR. 18 h post transfection, the cells were mock-stimulated, or stimulated with TNF- $\alpha$  and lysed 24 h later. Firefly luciferase activity was normalised to *Renilla* luciferase and fold induction was calculated relative to the uninduced mock control. The data shown belongs to four experimental repeats performed in duplicate, and are shown as mean fold induction  $\pm$  SEM ( $n=4$ ). TNF: Tumor necrosis factor, RLU: Relative light Units, UUKV: Uukuniemi virus, HRTV: Heartland virus, SFTSV: Severe fever with thrombocytopenia syndrome virus, I $\kappa$ B $\alpha$ SR: I $\kappa$ B $\alpha$  super-repressor.

### 6.3.4 Effect of tick-borne phlebovirus NSs proteins on type I and type II IFN signalling

To determine whether UUKV and HRTV NSs could block IFN signalling, the ability of the NSs proteins to inhibit the activation of the Interferon-sensitive response element (ISRE) was analysed. SFTSV NSs was used as a control, as this protein is known to act as a strong antagonist of IFN signalling. ISRE acts as a promoter for the upregulation of type I IFNs (IFN- $\alpha/\beta$ ), which play an important role in inducing a large number of ISGs with anti-viral activity (Randall and Goodbourn, 2008). Briefly, subconfluent HEK293T cells were transfected with a *Renilla* luciferase-expressing plasmid (phRL) as a transfection control, increasing amounts of untagged, or V5-tagged UUKV, HRTV, or SFTSV NSs-expression plasmids, and a reporter plasmid encoding firefly luciferase under the control of an ISRE promoter (p[9-27]4tk $\Delta$ ]-39]lucifer, henceforth referred to as pISRE-luc) (King and Goodbourn, 1998). 24 h post transfection, cells were stimulated with IFN- $\beta$  and lysed 18 h later for analysis of firefly and *Renilla* luciferase activities. The firefly luciferase activity was normalised against the *Renilla* activity and percentage induction calculated relative to the mock induction control (i.e. mock cells treated with IFN- $\beta$ ), which was considered 100%.

UUKV NSs showed no inhibitory effect on the activation of the ISRE promoter following IFN treatment. In comparison, HRTV and SFTSV NSs proteins showed a potent, dose-dependent inhibitory activity on ISRE promoter activation (Figure 6-6 A). Although a stronger inhibitory effect on type I IFN signalling by SFTSV NSs (95% inhibition at the highest dose) was noted compared to HRTV NSs (80% inhibition at the highest dose), lower expression levels of V5-tagged HRTV NSs were detected in comparison to SFTSV NSs (Figure 6-6 B), as noted earlier.

A large number of cytokines which are regulated by type II IFN signalling have been shown to be elevated in the blood of SFTSV-infected patients (Deng *et al.*, 2012), and were correlated with SFTS severity (Liu *et al.*, 2017). Hence, the ability of the tick-borne phlebovirus NSs proteins to suppress type II IFN signalling was examined. HEK293T cells were transfected with the highest dose of NSs-encoding plasmids used in the ISRE reporter assay (100 ng). 24h post transfection, transfected cells were treated with IFN- $\gamma$  for a further 24 h, prior to isolation of total cellular RNA. mRNA levels of IRF-1 and CXCL10 (which are ISGs induced by IFN- $\gamma$  (Der *et al.*, 1998; Luster *et al.*, 1985)) relative to GAPDH mRNA levels (a housekeeping gene control) in the total cellular RNA were determined by

RT-pPCR. Curiously, none of the NSs proteins had an inhibitory effect on IRF-1 or CXCL10 mRNA levels following IFN- $\gamma$  treatment (Figure 6-7 A and B, respectively).

Thus, the results described in this section suggest that while the weak role of UUKV NSs as an IFN antagonist is mediated at the level of IFN induction only, HRTV and SFTSV NSs proteins antagonise both IFN induction and type I IFN signalling. Interestingly, while type I IFN signalling was potently inhibited by HRTV and SFTSV NSs proteins, these proteins did not exhibit antagonism of type II IFN signalling.

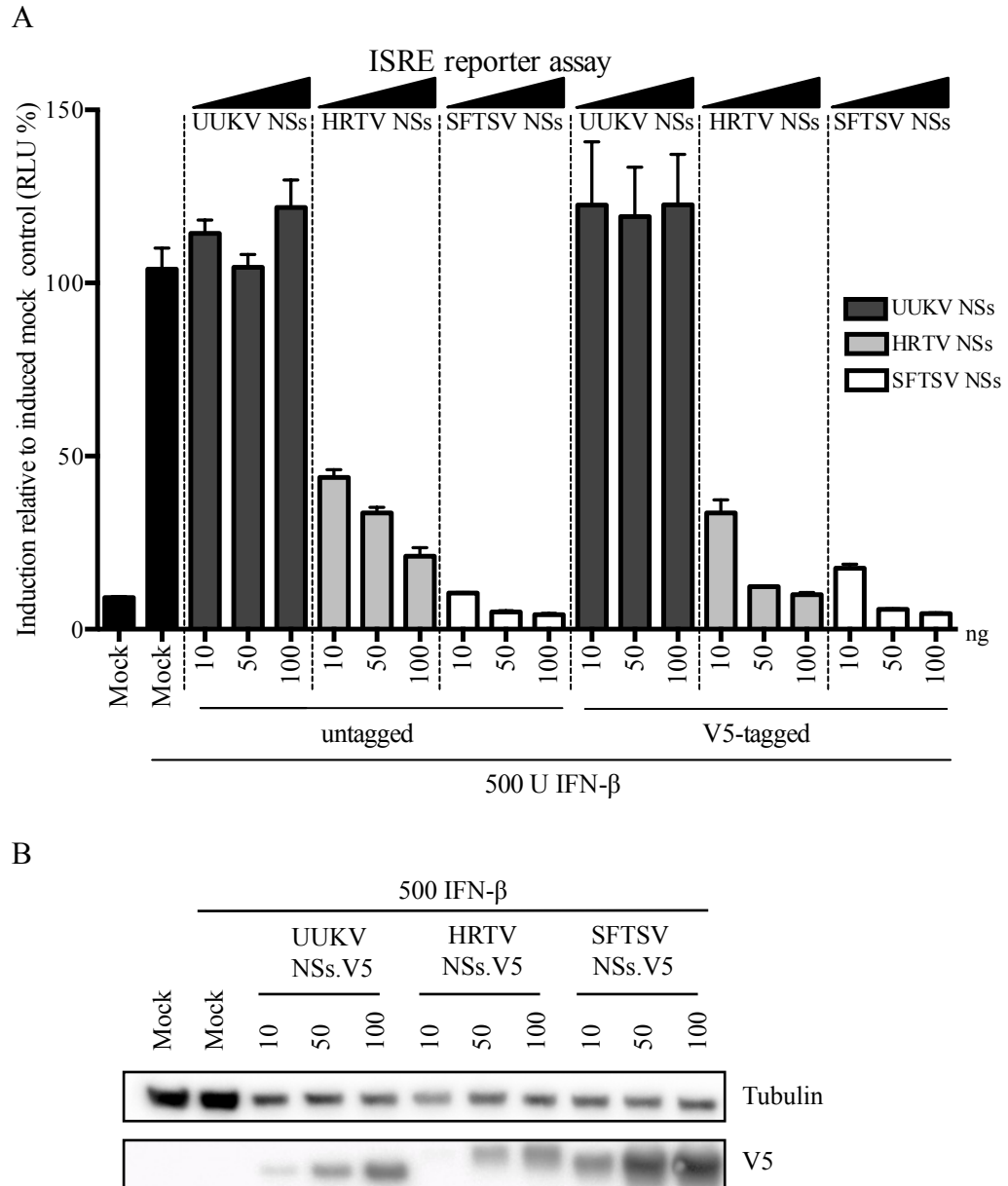


**Figure 6-6. Inhibition of type I IFN signalling by tick-borne phlebovirus NSs proteins.**

(A) ISRE reporter assay in the presence of tick-borne phlebovirus NSs proteins. HEK293T cells were transfected with a firefly luciferase reporter plasmid under the control of an ISRE promoter (pISREluc), and a control plasmid encoding *Renilla* luciferase (phRL) in the presence of the indicated amounts of pCMVXNSs or pCMVXNSsV5 expression plasmids. 24 h post transfection, transfected cells were stimulated with IFN- $\beta$  (500 U/mL) and lysed 18h later. Percentage induction was calculated by normalising the values to the mock induction control (mock cells treated with IFN- $\beta$ ), which was considered 100%. The data shown belong to three independent experiments performed in duplicate ( $n=3$ ), and are shown as mean induction  $\pm$  SEM. (B) Cell lysates from (A) were subjected to western blotting and probed with anti-tubulin and anti-V5 antibodies.

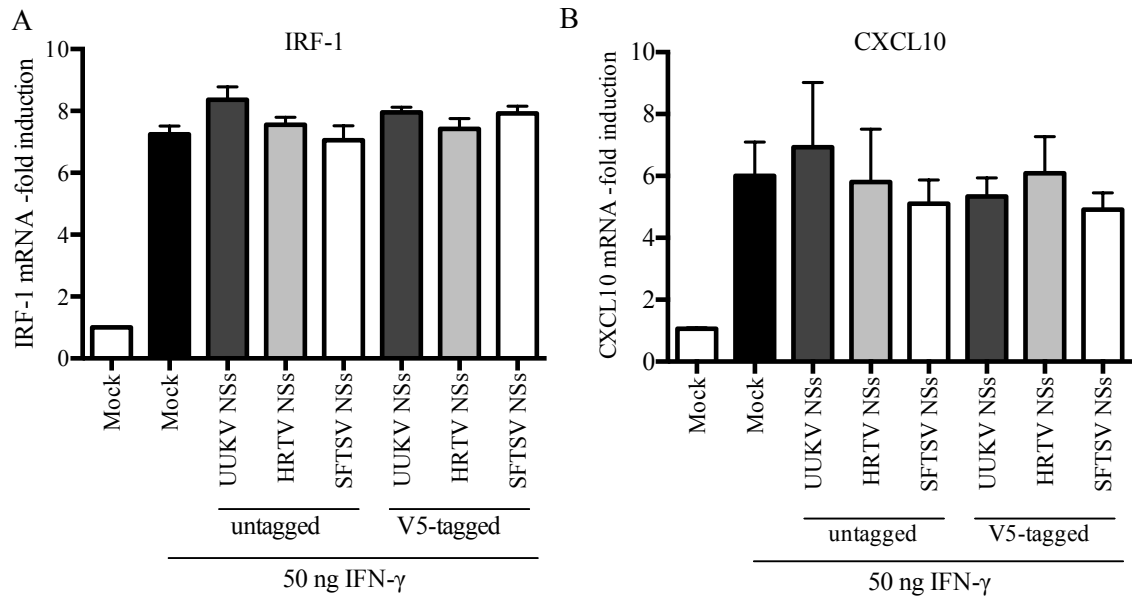


**Figure 6-7. Inhibition of type II IFN signalling by tick-borne phlebovirus NSs proteins.**

(A-B) HEK293T cells transiently expressing untagged or V5-tagged UUKV, HRTV or SFTSV NSs proteins were treated with 50 ng IFN- $\gamma$  24 h post transfection. 24 h post treatment, the total cellular RNA was isolated and subjected to RT-qPCR to determine mRNA levels of IRF-1 (A) or CXCL10 (B). Fold increase in mRNA levels was derived by normalising relative mRNA levels of the target genes to GAPDH mRNA, using a  $\Delta\Delta C_t$  method. Bar graphs represent the mean fold induction in relative mRNA levels of the target from three experimental repeats performed in triplicate ( $n=3$ )  $\pm$  SEM. ISRE: Interferon-Stimulated Response Element; IRF-1: Interferon regulatory factor-1; CXCL10: C-X-C motif chemokine 10.

### 6.3.5 IFN sensitivity of tick-borne phleboviruses

It has previously been shown that different strains of RVFV exhibit differential sensitivity to IFN treatment, depending on the capacity of the virus' NSs protein to efficiently block the type I IFN response (Bouloy *et al.*, 2001). Thus, the sensitivity of tick-borne phleboviruses relevant to this study (UUKV, HRTV and SFTSV) to IFN was also assessed.

First the sensitivity of UUKV, HRTV and SFTSV to exogenously applied type I IFN was assessed. Briefly, low MOI (0.1 FFU/cell) yield assays were carried out in A549/BVDV-Npro cells, which were pre-treated 24 h prior to infection with increasing amount of universal IFN- $\alpha$ . A549/BVDV-Npro cells were selected as they cannot produce IFN. This allows for a comparison of virus sensitivity to exogenously applied IFN without the contribution of IFN produced by cells in response to virus infection. The cell culture supernatant of infected cells was harvested 48 h p.i., and UUKV, HRTV and SFTSV titres determined by focus- or plaque-forming assays. While no infectious UUKV was detected by focus-forming assays upon pre-treatment of A549/BVDV-Npro cells with 10 IFN units, a 2-log and a 4-log reduction in HRTV and SFTSV titre was observed, respectively, compared to the virus yield in untreated cells. Infectious HRTV or SFTSV was undetectable in cells pre-treated with 100 IFN units or greater (Figure 6-8 A). These results demonstrate that UUKV, HRTV and SFTSV are highly sensitive to pre-treatment of cells with exogenously applied IFN.

A similar assay was carried out in A549/BVDV-Npro cells infected with UUKV, HRTV or SFTSV at a high MOI (3 FFU/cell). In this case the cells were infected prior to IFN treatment. Thus, presumably (and unlike in the previous assay) the cells were not in an IFN-induced antiviral state prior to infection. 100 IFN units were added at 0h, 1h, 2h, or 4h p.i. The cell culture supernatant of infected cells was harvested 48 h p.i., and the UUKV, HRTV and SFTSV titres determined by focus- or plaque-forming assays. Whereas a 5-fold decrease in UUKV titre was observed upon IFN treatment at all times post infection compared to mock-treated cells, HRTV or SFTSV replication was not hampered by IFN treatment following infection (Figure 6-8 B).

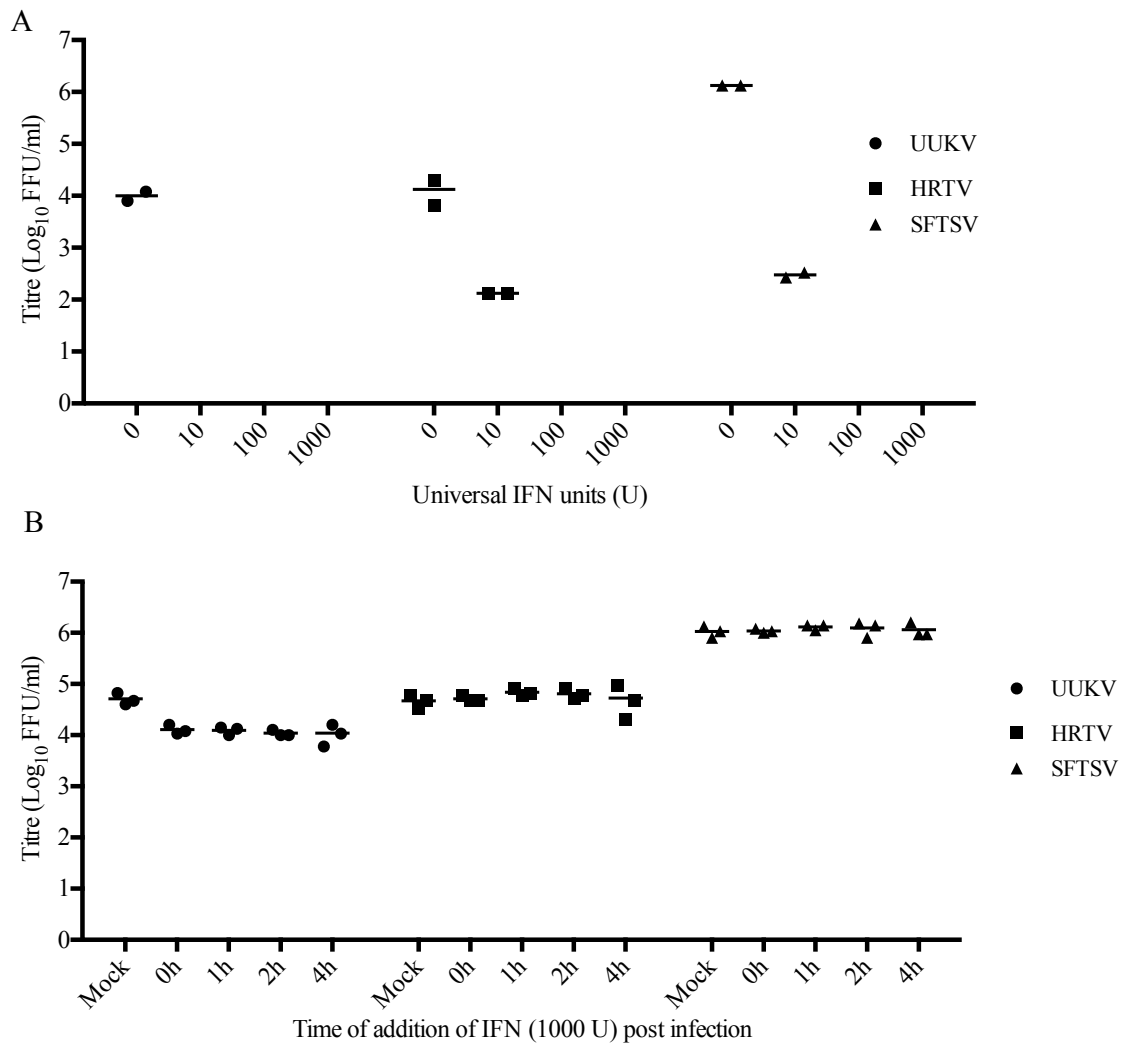


**Figure 6-8. Sensitivity of tick-borne phleboviruses to exogenous IFN.**

(A) A549/BVDV-Npro cells were pre-treated with the indicated amount of universal type I IFN- $\alpha$  for 24 h prior to infection with UUKV, HRTV or SFTSV (MOI 0.1 FFU/cell). (B) A549/BVDV-Npro cells were infected at a high MOI (3 FFU/cell) with UUKV, HRTV or SFTSV, and 100 universal IFN- $\alpha$  added to the cell culture medium at 0 h, 1 h, 2 h or 4 h p.i. At 48 h p.i. the cell culture medium of duplicate (A) or triplicate (B) wells was harvested and the virus titre determined by focus- or plaque-forming assay. The data presented are from a representative experiment of two, performed in triplicate with single data points plotted and with horizontal lines representing the mean. UUKV: Uukuniemi virus, HRTV: Heartland virus, SFTSV: Severe fever with thrombocytopenia syndrome virus.

The sensitivity of UUKV, HRTV and SFTSV to virus-induced IFN was also investigated by examining the effect of a JAK1/2 inhibitor (Ruxolitinib, previously described in (Stewart *et al.*, 2014)) on foci formation in IFN-competent A549 cells. In this assay the focus size is determined by the kinetics of the IFN response mounted to the pathogen-associated molecular patterns (PAMPs) associated with the infecting virion and the ability of the virus to circumvent this IFN response. Thus, the use of an inhibitor that can block IFN signalling in focus-forming assays is a convenient strategy to assess virus sensitivity to virus-induced IFN. While UUKV foci were undetectable in mock-treated A549 cells, Ruxolitinib treatment rescued the ability of UUKV to form foci in these cells. Comparatively, no significant increase in HRTV focus size was observed in Ruxolitinib-treated A549 cells in comparison to mock-treated cells, indicating that HRTV must have the capacity to evade IFN induction. Surprisingly, although SFTSV has evolved a potent IFN antagonist (NSs) that is able to suppress IFN induction and IFN signalling (Figures 6-2 and 6-6)(Chaudhary *et al.*, 2015; Ning *et al.*, 2015; 2014; Santiago *et al.*, 2014), a significant increase in SFTSV focus size was observed in A549 cells treated with Ruxolitinib (Figure 6-9 A and B). In order to ensure that this effect was not due to the presence of defective interfering particles in the laboratory SFTSV stock, the virus was plaque-purified. Four different newly plaque-purified SFTSV stocks yielded similar results to those obtained with the laboratory SFTSV stock (data not shown). Therefore, despite being equipped with a potent antagonist of the IFN system, SFTSV infection still results in IFN induction, which limits virus infection in neighboring cells.

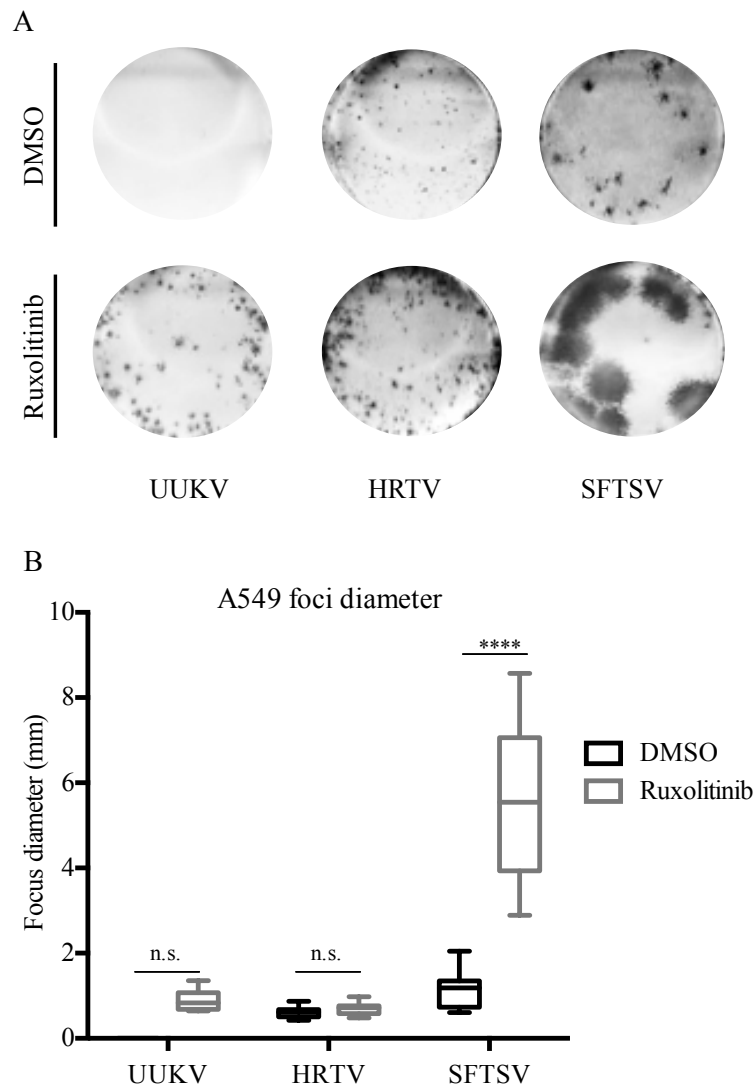


**Figure 6-9. Sensitivity of tick-borne phleboviruses to virus-induced IFN.**

(A) Focus-forming assays of UUKV, HRTV and SFTSV on A549 cells 6 days p.i. The overlay was supplemented with JAK/STAT inhibitor Ruxolitinib (0.4 $\mu$ M) or the equivalent volume of the vehicle control DMSO. Foci were detected using anti-UUKV, HRTV or SFTSV N antibodies. (B) Box plot for foci diameter of the focus-forming assays in (A) (n=10). Statistical significance for the comparison of means between groups was determined by two-way ANOVA followed by Tukey's multiple comparisons post-hoc test. n.s.= non-significant, \*\*\*\*  $p \leq 0.0001$ . UUKV: Uukuniemi virus; HRTV: Heartland virus; SFTSV: Sever Fever with Thrombocytopenia syndrome virus.

To corroborate the results obtained with Ruxolitinib treatment, the replication kinetics of UUKV, HRTV and SFTSV were compared in A549 cells infected at either low or high MOI (0.1 FFU/cell and 3 FFU/cell, respectively). At various time points throughout the time course, the cell culture medium was harvested, virus titre determined through focus- or plaque-forming assays, and the relative amount of IFN produced quantified by a biological IFN protection assay, as described in section 6.3.1. At a low MOI, the peak mean titres of UUKV and SFTSV were of  $2 \times 10^4$  FFU/ml and  $8.2 \times 10^5$  FFU/ml (at 72 h p.i.), approximately 1 log lower than the peak mean titre of these viruses following a high MOI infection (Figure 6-10 A and C). Using a high MOI infection, UUKV induced IFN by 24 h p.i., whereas no IFN could be detected at any point during the time course carried out at a low MOI (Figure 6-10 D). The lack of IFN production by UUKV at a low MOI could be explained by the slow replication kinetics of UUKV throughout the time course, with only a one-log increase in virus titre detected (Figure 6-10 A). On the other hand, the faster replication kinetics exhibited by SFTSV during the low MOI time course (a 3-log increase in virus titre) resulted in increased induction of IFN (Figure 6-10 C and F). In contrast to UUKV and SFTSV, HRTV infections at a high and low MOI yielded similar mean titres by 72 h p.i. (low MOI:  $1.7 \times 10^5$  FFU/ml and high MOI:  $3.3 \times 10^5$  FFU/ml) (Figure 6-10 B). Furthermore, even at a high MOI, HRTV infection resulted in very little induction of IFN (4 RIU) by 72 h p.i. (Figure 6-10 E).

Taken together, these results demonstrate that UUKV and SFTSV cannot efficiently inhibit IFN production following virus infection, which results in reduced spread of the virus to neighbouring cells. On the other hand, HRTV limits IFN production upon infection, as little IFN was induced throughout the time course.

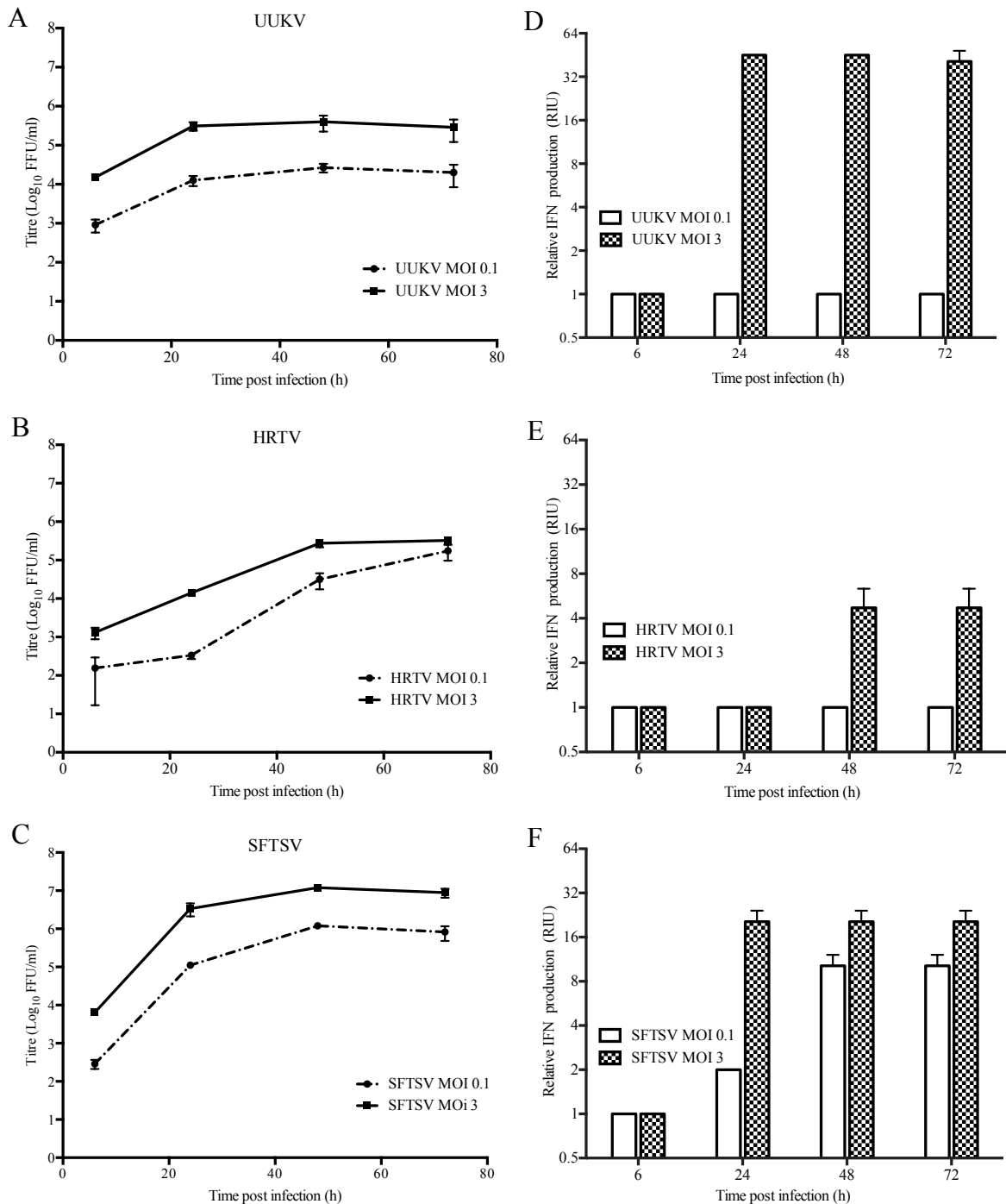


**Figure 6-10. Replication kinetics and IFN production following tick-borne phlebovirus infection.**

(A-C) Growth curves of UUKV (A), HRTV (B) or SFTSV (C) at low (0.1 FFU/cell) and high MOI (3 FFU/cell) in A549 cells. Cell culture supernatant of triplicate wells was collected at the indicated time points and virus titre determined through focus- or plaque-forming assays. (D-F) Samples from A-C were UV-inactivated and the relative IFN units measured through a biological IFN protection assay. Error bars indicate standard deviation (SD) of the mean ( $n=3$ ) of a representative experiment of two experimental repeats. UUKV: Uukuniemi virus; HRTV: Heartland virus; SFTSV: Sever fever with thrombocytopenia syndrome virus.

## **6.4 Discussion**

Viruses require mechanisms to antagonise the IFN response in order to replicate efficiently in host cells. The NSs protein of viruses within the *Bunyaviridae* family is best characterised by its IFN antagonist function. This role was shown to be of particular importance for the pathogenicity of BUNV (Bridgen *et al.*, 2001; Weber *et al.*, 2002). Within the mosquito-borne viruses of the *Phlebovirus* genus, RVFV, TOSV, PTV and SFSV NSs proteins were all shown to act as IFN antagonists (Billecocq *et al.*, 2004; Gori-Savellini *et al.*, 2013; 2010; Ikegami *et al.*, 2006; Lihoradova *et al.*, 2013). With the exception of SFTSV NSs (Ning *et al.*, 2015; 2014; Santiago *et al.*, 2014), no other tick-borne phlebovirus NSs protein has been shown to act as an IFN antagonist, and their role in modulating host immune responses remains poorly understood. The aim of this chapter was to investigate whether the NSs protein of the apathogenic UUKV and pathogenic HRTV block the human IFN response at the level of IFN induction and/or signalling. Additionally, the efficiency of their IFN antagonistic activities was compared to that of SFTSV NSs, which is a potent IFN antagonist.

The results in this chapter show that UUKV can replicate in a human IFN-competent cell line (A549), and thus must be able to overcome the human IFN response (Figure 6-1 A). The enhanced replication of UUKV in A549/V cells (in which the IFN response is lacking) suggested that IFN generated as a result of virus infection plays a role in inhibiting UUKV replication. The generation of NSs-lacking UUK viruses by reverse genetics in Chapter 5 provided the tools necessary to investigate the role of UUKV NSs as an IFN antagonist in the context of a virus infection. It has previously been shown that following infection, PTV and TOSV induce IFN in cell culture (Gori-Savellini *et al.*, 2010; Perrone *et al.*, 2007), which was also noted for UUKV in this Chapter (Figures 6-1 B and C). Similarly to PTV and TOSV, the NSs protein of UUKV also plays a role in antagonizing the host cell IFN response, as infection of A549 cells with NSs-lacking viruses (rUUKdelNSs and rUUKdelNSsGFP) yielded a 10-fold increase in IFN production compared to wild-type UUKV (Figures 6-1 B and C). These results indicate that UUKV NSs acts as an IFN antagonist in human cells. However, its antagonistic activity is weak because upon infection UUKV induces IFN (unlike the control BUNV which encodes an NSs protein with potent IFN antagonism characteristics). These results suggest that UUKV NSs is unable to completely inhibit the production of IFN mounted as a result of UUKV infection. This observation may provide an explanation for the inability of UUKV to cause disease in

humans. As various strains of UUKV (or UUKV-like viruses) have been isolated from ticks collected from passerine birds, migrant birds, or within nesting areas of seabirds (S. R. Moss, 1986; Nuttall *et al.*, 1984; 1981; Traavik and Mehl, 1977; Watret and Elliott, 1985), it would be interesting to investigate whether UUKV NSs has evolved to act as a potent antagonist of the avian IFN response.

The role of UUKV NSs as a regulator of the human innate immune system was compared to that of the NSs belonging to more pathogenic tick-borne phleboviruses HRTV and SFTSV. Transient transfection assays were carried out to investigate and compare at which stages of the IFN system the NSs proteins exerted an inhibitory activity. The weak IFN antagonistic activity of UUKV NSs reported in the context of a virus infection (Figure 6-1) was also reflected at the level of IFN induction in transient transfection assays. In comparison to HRTV and SFTSV NSs proteins, which potently inhibited RIG-I N-mediated IFN production, UUKV NSs exhibited lower efficiency in inhibiting RIG-I N-mediated IFN production (Figure 6-2 A). These findings were also reflected in RIG-I N-mediated IRF-3 phosphorylation (Figure 6-3 A), dimerization (Figure 6-3 B) and nuclear translocation (Figure 6-4). Thus, UUKV, HRTV and SFTSV NSs proteins are able to modulate the IFN system by suppressing RIG-I N-mediated IFN induction, albeit with different efficiencies, ultimately hindering the phosphorylation, dimerization and translocation of IRF-3 to the nucleus. The nuclear translocation of IRF-3 is important, as it is in the nucleus that IRF-3 can form part of the IFN enhanceosome complex to activate the transcription of the IFN- $\alpha/\beta$  gene (Wathelet *et al.*, 1998). Furthermore, the results presented in this chapter denote a correlation between the reported pathogenicity of the viruses in nature and the efficiency with which their respective NSs proteins antagonise the IFN response.

In comparison to the inhibitory effect of UUKV, HRTV and SFTSV NSs proteins on IFN induction, none of the proteins were able to inhibit NF $\kappa$ B signalling (Figure 6-4). NF $\kappa$ B signalling controls the expression of many inflammatory cytokines, chemokines and cell surface adhesion molecules, playing a major role in the regulation of inflammation (Lawrence, 2009; X. Li and Stark, 2003). The role of tick-borne phlebovirus NSs proteins in modulating NF $\kappa$ B signalling has only been investigated for SFTSV NSs, and some discrepancies exist in the literature. Initial reports indicated that although NF $\kappa$ B activation facilitated SFTSV replication, SFTSV NSs was capable of suppressing NF $\kappa$ B signalling in HEK293T cells (B. Qu *et al.*, 2012). This finding, in addition to the finding that SFTSV doesn't induce apoptosis (thus extending host cell survival), led the authors to suggest that

these strategies may be employed by SFTSV to reduce viral loads and therefore contribute to persistent infections. At odds with this report, another study showed no inhibitory activity of SFTSV NSs in similar experiments (Chaudhary *et al.*, 2015). The data presented in Figure 6-5 agrees with the latter report and, regardless of the disparity with the report suggesting an inhibitory role of SFTSV NSs on NF $\kappa$ B signalling, it is consistent with the upregulation of many NF- $\kappa$ B-regulated cytokines reported in SFTSV-infected humans and non-human primates (Deng *et al.*, 2012; Jin *et al.*, 2015; Y. Sun *et al.*, 2012).

Upon IFN induction, secreted IFNs engage with receptors on the cell surface of neighboring cells and activate intracellular signalling pathways that lead to the upregulation of a number of ISGs, consequently conferring an anti-viral state. Some redundancy exists between the signalling pathways activated by type I and type III IFNs, which converge in the regulation of the ISRE promoter by activation of both STAT1 and STAT2. The type II IFN signalling pathway differs slightly from type I and III, as it is majorly mediated by the activation of STAT1, and promotes the transcription of GAS promoter-regulated genes through STAT1 homodimers (known as GAF) (Figure 1-12) (Borden *et al.*, 2007; de Weerd and Nguyen, 2012; Platania, 2005). The findings in this chapter demonstrate that some tick-borne phlebovirus NSs proteins are capable of blocking IFN signalling in an IFN-specific manner to hamper the IFN response. Transient transfections assays indicated that unlike UUKV NSs, the NSs protein of pathogenic HRTV and SFTSV strongly inhibit the activation of the ISRE promoter following IFN treatment (Figure 6-6 A and B). In contrast, none of the tick-borne phlebovirus NSs proteins studied showed inhibitory activity on type II IFN signalling (Figure 6-7 C and D). Mechanistically, the ability of HRTV or SFTSV NSs to block the type I but not type II IFN signalling pathways could presumably lie within the inherent differences between these two pathways. For instance, it is possible that HRTV and/or SFTSV NSs proteins are able to interact with STAT2 or IRF-9, or inhibit STAT2 phosphorylation, thus preventing the formation of ISGF3 and blocking the major route of type I and III, but not type II IFN signalling. Alternatively, the NSs proteins may be able to block signalling at the level of the IFN receptors, thus providing an IFN-specific inhibitory action on IFN signalling. Further experiments are required to determine the molecular mechanism of IFN signalling inhibition of HRTV and SFTSV NSs proteins, which are discussed in Chapter 7. The activation of GAS elements by STAT1 homodimers in type II IFN signalling leads to the transcription of pro-inflammatory cytokines such as TNF, IL-6 and P40 (X. Hu and Ivashkiv, 2009). Therefore, it is possible that the inability of HRTV and SFTSV NSs

proteins to block type II IFN signalling enables the activation of pro-inflammatory responses that lead to severe disease following virus infection, as evidenced in SFTS mouse models and SFTSV-infected patients (Deng *et al.*, 2012; Jin *et al.*, 2012; Liu *et al.*, 2017). Of note, although to date there is no literature available relating to the upregulation of cytokines regulated by type II IFN signalling in HRTV-infected patients, HRTV-infected patients show identical symptoms to SFTSV-infected patients (McMullan *et al.*, 2012; Muehlenbachs *et al.*, 2014).

The first indication that the NSs protein of a phlebovirus had an IFN antagonist role was the finding that the virulent RVFV strain ZH548 failed to induce IFN following infection and replicated efficiently in wild-type mice and mice lacking the type I IFN receptor. This was in comparison to RVFV strains bearing mutations in the NSs gene (MP12 and clone 13), which induced IFN and were virulent in mice lacking the type I IFN receptor but not in wild-type mice (Bouloy *et al.*, 2001). The fact that the sensitivity of RVFV strains to IFN is dictated by the capacity of the virus to efficiently block IFN production upon infection led me to investigate the IFN sensitivity of the tick-borne phleboviruses relevant to this study. UUKV, HRTV and SFTSV were all shown to be sensitive to pre-treatment of human A549/BVDV-Npro cells with exogenous type I IFN (Figure 6-8 A), presumably because of their inability to replicate in cells that are in an IFN-induced anti-viral state prior to infection. While pre-treating the cells with the lowest dose of IFN resulted in a 2-log and 4-log decrease in HRTV and SFTSV titre respectively 48 h p.i., no infectious UUKV was detected under the same conditions, suggesting UUKV is more sensitive to IFN pre-treatment than HRTV and SFTSV. Furthermore, while UUKV replication was impaired when IFN was added upon virus infection, no effect was observed on HRTV or SFTSV replication (Figure 6-8 B). These findings are in agreement with the observation that UUKV NSs is unable to block type I IFN signalling, while HRTV and SFTSV NSs act as potent antagonists of type I IFN signalling. Presumably, in HRTV- and SFTSV-infected cells the NSs proteins encoded by the respective viruses can readily control IFN signalling pathways triggered by exogenously applied IFN after infection, and thus prevent the development of an antiviral state in these cells. In contrast, the lack of IFN signalling inhibitory activity by UUKV NSs could explain the impairment of UUKV replication in UUKV-infected cells treated with exogenous IFN.

In an attempt to assess the sensitivity of the tick-borne phleboviruses relevant to this study to virus-induced IFN, focus-forming assays in mock-treated and Ruxolitinib treated A549 cells were carried out. Ruxolitinib is a drug that inhibits IFN signalling (specifically

JAK1/2). Thus, in comparison to the assays where virus sensitivity to exogenous IFN was examined in cells that are unable to produce IFN, these focus-forming assays account for factors such as the kinetics of the IFN response mounted to virus-associated PAMPs and the ability of the viruses to circumvent the virus-induced IFN response only (Stewart *et al.*, 2014). In IFN-competent A549 cells, HRTV and SFTSV formed small foci, while UUKV did not form detectable foci. The addition of Ruxolitinib to the overlay rescued the ability of UUKV to form foci in these cells, and gave rise to significantly larger SFTSV foci (Figures 6-9 A and B). Therefore, these findings suggest that the IFN response mounted as a result of UUKV and SFTSV infection leads to the development of an antiviral state in neighbouring infected cells, which limits virus spread. In a similar manner, the sensitivity of UUKV and SFTSV to virus-induced IFN was demonstrated by the inability of both UUKV and SFTSV to reach similar peak titres during low and high MOI infections (Figure 6-10 A and C). In principle, if no IFN is produced during replication, or if the virus is able to efficiently block IFN signalling, infection at a low MOI would yield similar peak titres to a high MOI infection.

Notably, some differences were observed in the ability of UUKV and SFTSV to replicate in IFN-induced cells. UUKV exhibited poor replication kinetics, with low and high MOI infections showing a one-log increase in virus titre (Figure 6-10 A), which could explain the lack of IFN production by UUKV during the time course carried out at a low MOI (Figure 6-10 D). Comparatively, SFTSV exhibited faster replication kinetics than UUKV at a low MOI (with a 3-log increase in virus titre) and consequently induced more IFN throughout the time course (Figures 6-10 A, C, D and F). The induction of IFN following infection and the sensitivity of SFTSV to virus-induced IFN is surprising, as the NSs protein of SFTSV has very potent IFN induction and signalling suppressing activities (Ning *et al.*, 2015; 2014; Santiago *et al.*, 2014) (Figures 6-2 A and 6-6 A). The results described here suggest that despite encoding a potent and efficient IFN antagonist, the amount of IFN induced during SFTSV infection is not completely overcome by the action of its IFN antagonist NSs. During the writing of this chapter, a study emerged which claimed that sera from SFTSV-infected patients show high concentrations of IFN- $\alpha$  compared to sera from healthy patients. Additionally, the concentration of IFN- $\alpha$  in patients with severe SFTSV was significantly higher than that in patients with mild SFTS (Liu *et al.*, 2017). The authors speculated that perhaps the potent IFN induction antagonistic activity of SFTSV NSs suggested in *in vitro* studies (Ning *et al.*, 2014; Santiago *et al.*, 2014) may not play such an important role in inhibiting the production of type I IFNs *in vivo*. The

surprising high levels of IFN- $\alpha$  in SFTSV-infected patients is in agreement with the IFN induction detected in SFTSV-infected cells in this study (Figure 6-10 C). Perhaps, SFTSV has evolved such a potent antagonist of IFN induction because it generates a large amount of PAMPs during virus replication, resulting in the rapid induction of the IFN response; an interesting hypothesis and avenue for future studies.

Interestingly (and in contrast to UUKV and SFTSV), no significant difference was observed in HRTV focus size in A549 cells when comparing functional and non-functional IFN signalling responses (Figures 6-9 A and B). In agreement with these results, both low and high MOI HRTV infections resulted in similar peak titres with little IFN produced over the time course (Figures 6-10 B and E). Thus, despite encoding NSs proteins with similar efficiencies to block IFN induction and IFN signalling (Figures 6-2 and 6-4), HRTV (unlike SFTSV) is able to efficiently control IFN production upon infection, which presumably favours virus replication by preventing the development of an IFN-induced state, and allows HRTV to reach similar peak titres following low and high MOI infections. It is possible that this is due to HRTV generating less PAMPs than SFTSV, which allows HRTV NSs protein to control IFN production more efficiently than SFTSV NSs in the context of a virus infection.

Taken together, the data presented in this chapter shows that UUKV, HRTV and SFTSV are all sensitive to IFN pre-treatment, but only UUKV is sensitive to IFN treatment after virus infection presumably due to the lack of inhibitory activity of its NSs protein on IFN signalling. Additionally, whereas UUKV and SFTSV replication is limited by virus-induced IFN, HRTV infection produces such little IFN that it does not affect its replication, suggesting that the virus has acquired more efficient strategies than UUKV or SFTSV to hamper IFN production. The results in this chapter also show that UUKV NSs acts as an IFN antagonist at the level of IFN induction only. This is in comparison to HRTV and SFTSV NSs proteins, which antagonise both IFN induction and type I IFN signalling. Moreover, the antagonist activity of the NSs protein of apathogenic UUKV at the level IFN induction is weak, in comparison to the NSs protein belonging to highly pathogenic HRTV and SFTSV, indicating a correlation between the reported pathogenicity of the viruses in nature and the efficiency with which their respective NSs proteins antagonise the IFN response. Finally, while type I IFN signalling was potently inhibited by HRTV and SFTSV NSs proteins, these proteins did not exhibit antagonism of type II IFN signalling, which could serve as an explanation for the increased pro-inflammatory responses that lead to severe disease in HRTV and SFTSV patients (McMullan *et al.*,

2012; Muehlenbachs *et al.*, 2014). As the IFN antagonistic activities of UUKV NSs (at the level of IFN induction) and HRTV NSs (at the level of IFN induction and signalling) described in this chapter are novel, the molecular mechanism by which they exert their inhibition is unknown. These mechanisms are investigated further in Chapter 7.

## **6.5 Summary**

- Recombinant UUK viruses lacking NSs were utilized to show that the relative amount of IFN produced upon infection of A549 cells is greater than that produced by wtUUKV. Induction of IFN by wtUUKV suggests that its NSs protein is unable to completely abrogate virus-induced IFN production.
- Using transient transfection assays, a correlation was observed between the strength of IFN system inhibition by UUKV, HRTV and SFTSV NSs proteins and the pathogenicity exhibited by their cognate viruses in nature.
- UUKV, HRTV and SFTSV NSs proteins all inhibit IFN induction with different efficiencies, by ultimately preventing IRF-3 phosphorylation, dimerization and consequently its nuclear translocation. However, none of the NSs proteins hampered NF- $\kappa$ B signalling.
- While UUKV NSs is unable to inhibit type I or II IFN signalling, HRTV and SFTSV NSs proteins are potent antagonists of type I, but not II, IFN signalling.
- UUKV, HRTV and SFTSV are all sensitive to IFN pre-treatment, but only UUKV replication is impaired if IFN is applied 0-4 h after virus infection.
- UUKV and SFTSV induce IFN, which limits their replication and spread to neighboring cells. In contrast, HRTV produces little IFN upon infection and its replication is unaffected by the virus-induced IFN. This presumably is because HRTV employs more efficient strategies to inhibit IFN production than UUKV or SFTSV. The induction of IFN by SFTSV and its sensitivity to IFN in comparison to HRTV was surprising, since both viruses encode NSs proteins that exhibit similar efficiencies in inhibiting IFN induction and signalling in transient transfection assays. Perhaps SFTSV induces more PAMPs than HRTV and its NSs protein is unable to control the induction of IFN, unlike HRTV NSs.

# 7 Molecular mechanism of IFN antagonism by tick-borne phlebovirus NSs proteins

## 7.1 Introduction

The results presented in the previous chapter demonstrated that UUKV, HRTV and SFTSV NSs proteins are capable of suppressing IFN induction. In addition, whereas UUKV NSs showed no inhibition at the IFN signalling level, HRTV and SFTSV NSs proteins were potent antagonists of type I, but not type II IFN signalling.

The molecular mechanism employed by SFTSV NSs to subvert the human IFN system quickly became characterised following the emergence of SFTSV. Initial reports indicated that SFTSV NSs mediated the formation of NSs-containing cytoplasmic inclusion bodies (IBs), which have a granule-like appearance and are found in virus-infected cells, as well as in cells expressing SFTSV NSs in the absence of other viral proteins (Ning *et al.*, 2014; Santiago *et al.*, 2014). Ning *et al.* have showed that these structures are highly dynamic, and could undergo fusion to form larger aggregates, or fission to disperse into smaller IBs during their development (Ning *et al.*, 2014). In addition, Santiago *et al.* showed that the NSs-induced IBs colocalised with the early endosomal marker Rab5, but not with Golgi or Endoplasmic reticulum markers, indicating that the endosomal system is exploited for the formation of these IBs (Santiago *et al.*, 2014). The IBs were also found to co-localise with lipid droplets and viral dsRNA. As inhibition of fatty acid synthesis disrupted the formation of SFTSV NSs-induced IBs and hindered SFTSV replication, it was suggested that these structures may also function as virus replication factories (Santiago *et al.*, 2014). The studies described above also investigated the role of SFTSV NSs in suppressing the IFN system. Intriguingly, it was found that the NSs-induced IBs served to sequester and spatially isolate key components of IFN induction and signalling pathways, which was described as a novel and elegant strategy to modulate the IFN system. Specifically, SFTSV NSs was found to act as a potent antagonist of IFN induction by sequestering TRIM25 and RIG-I (Santiago *et al.*, 2014), TBK1 (Ning *et al.*, 2014; X. Wu *et al.*, 2014), and IRF-3 (Ning *et al.*, 2014; X. Wu *et al.*, 2014) into NSs-induced IBs, therefore depriving these signalling molecules from participation in the IFN induction cascade. Although the direct interaction between SFTSV NSs and TBK1 is a consistent finding in all reported studies (Ning *et al.*, 2014; Santiago *et al.*, 2014; X. Wu *et al.*, 2014), some discrepancies exist with regards to the interactions driving the imprisonment of other

IFN effector proteins into NSs-induced IBs. While Wu *et al* reported that the interaction between SFTSV NSs and IKK $\epsilon$  or IRF-3 is indirect and facilitated via the interaction of SFTSV NSs with TBK1 (X. Wu *et al.*, 2014), another study described a direct interaction with IKK $\epsilon$  (Ning *et al.*, 2014). Similarly, whereas no direct interaction was observed between SFTSV NSs and RIG-I by Ning *et al* (Ning *et al.*, 2014), another study reported a weak interaction between SFTSV NSs and RIG-I, which the authors indicated may be indirect and promoted via a direct interaction between SFTSV NSs and TRIM25 (Santiago *et al.*, 2014).

In addition to the IFN antagonist role at the level of IFN induction, SFTSV NSs was also shown to potently disrupt IFN signalling. This function was attributed to its interaction with and spatial isolation of STAT1 and STAT2, acting as an immunomodulator of the JAK/STAT signalling pathway (Chaudhary *et al.*, 2015; Ning *et al.*, 2015). Initially, a direct interaction between SFTSV NSs and the DNA-binding domain of STAT2 was reported only, which resulted in the inhibition of STAT2 phosphorylation and nuclear translocation of both STATs (Ning *et al.*, 2015). However, a later report indicated that the inhibitory activity of SFTSV NSs on IFN signalling was additionally mediated through a direct interaction between SFTSV NSs and STAT1, which inhibited STAT1 phosphorylation and its recruitment to IFN-stimulated promoters (Chaudhary *et al.*, 2015).

While the molecular mechanism utilized by SFTSV NSs protein to inhibit the IFN system has been extensively studied, that employed by UUKV and HRTV NSs proteins remain to be elucidated. Unfolding the mechanisms employed by the NSs proteins of tick-borne phleboviruses other than SFTSV to subvert the IFN system will serve to expand our knowledge on the viral immune evasion strategies utilized by these emerging pathogens.

## **7.2 Aims**

The overall aim of this chapter was to perform a comparative characterization of the mechanisms employed by tick-borne phlebovirus NSs proteins to antagonise the IFN response. I aimed to elucidate whether the strategies utilized by UUKV, HRTV and SFTSV NSs proteins to hamper the IFN response are conserved or divergent. In particular, I aimed to identify interacting partners of UUKV and HRTV NSs proteins within the IFN induction and signalling cascades, and to investigate their subcellular localization, utilizing the well-characterized SFTSV NSs as a control.

## 7.3 Results

### 7.3.1 Subcellular localization of UUKV, HRTV and SFTSV NSs

In comparison to other viral proteins, the NSs proteins of bunyaviruses exhibit notoriously low conservation at the amino acid level (Elliott, 2014; Yu *et al.*, 2011). To begin the characterization of tick-borne phlebovirus NSs proteins, the amino acid identity of UUKV (AAA47959.1), HRTV (AFP33392.1) and SFTSV (AJD86041.1) NSs proteins was compared using CLUSTAL Omega (McWilliam *et al.*, 2013; Sievers *et al.*, 2011) (Table 6-1). While UUKV NSs shares a low amino acid sequence identity with HRTV (22.73%) and SFTSV (22.22%) NSs proteins, the identity between the NSs protein of the closely related HRTV and SFTSV is higher (62.76%) (Table 6-1).

**Table 6-1. Percentage amino acid identity of the tick-borne phlebovirus NSs proteins used in this study.**

| Virus | Amino acid identity (%)* |       |       |
|-------|--------------------------|-------|-------|
|       | UUKV                     | HRTV  | SFTSV |
| UUKV  | 100                      |       |       |
| HRTV  | 22.73                    | 100   |       |
| SFTSV | 22.22                    | 62.67 | 100   |

\* Based on accession numbers AAA47959.1, AFP33392.1 and AJD86041.1 for UUKV, HRTV and SFTSV NSs proteins, respectively. Generated using Clustal Omega.

An alignment of the amino acid sequences of the three NSs proteins is shown in Figure 7-1. Interestingly, a PxxP motif (P refers to Proline and x to any amino acid) which was identified in SFTSV NSs as a motif required for IB formation and its IFN antagonist activity (Ning *et al.*, 2014) was conserved in HRTV NSs (Figure 7-1, highlighted in red).

```

UUKV_NSs      MSYFTIQNEDLPQG-----FTFRPHDKIYDSL
HRTV_NSs      MSLSKASQPSVKSACVRLPIVVLEPNLAELSTSYVGLVSCKCSVLTCMMRKMKAFTNTV
SFTSV_NSs     MSLSKCSNVDLKSVMANANTVRLEPSLGEYPTLRRDLVECSVLTLSMVKRMGKMTNTV
** . .: .: . .: .: .:

UUKV_NSs      WEMMDDGYFPSTIPLKTTINGVDMPSVGWLEVDEGLYDILIDGLDVLRLPTDEEMIVSATG
HRTV_NSs      WLFGNP-----NNP-----HALEPA-----VEQLLDEYSGLGS----YSQEKSLR
SFTSV_NSs     WLFGNP-----KNP-----HQLEPG-----LEQLLDMYYKDMRC----YSQRELSALR
* : : . ** : . * * * : .: **

UUKV_NSs      WPLEKNRALILNFFRNLRMDIIGTYTLQRSFITIMSIVLFGDQNPRLRRKKRSRVSLGKM
HRTV_NSs      WPSGKPSVHFLQAA-HLFFSLKNTWAVETGQ-----ENWRGFFHRIT-SGKKYKFEGDM
SFTSV_NSs     WPSGKPSVWFLQAA-HMFFSIKNSWAMETGR-----ENWRGLFHRIT-KGQKYLFEEDM
** * . :*: .: .: : : : . : * : . : . *.*

UUKV_NSs      LFDLALRMRSKIRRMKLTVEVQVTGQNLVKDLCLLHILDQLKRLVTRGTIAEKRFFTAIEQ
HRTV_NSs      VIDSCYKIDERRRRMGLPDTFITGLNPIMDVALLQIESLLR---VRGLTLNYHLFTSPFL
SFTSV_NSs     ILDSLEAIEKRRRLRLGLPEILITGLSPILDVALLQIESLAR---LRGMSLNHHLFTSPSL
: : * : .: * : * : : ** . : * : * : * . * : * * : : : : :

UUKV_NSs      A----PCNYEPKRYGMKKKHMMFM-FESDRKNLTVHP-----TL-----VNL
HRTV_NSs      DKPLLDSLYFAIWRDKKKDDGSYSQDEGARQDDPLNPLDELlyLSGLPKPLAHYLNKCP
SFTSV_NSs     RKPLLDCWDFIPVRKKKTGDSYSLDED-----DEPGVLHGYPHMAHYLNRCPP
. * * . : : : : : :

UUKV_NSs      EEHWITFESARERLLDFTTKDWPVVGSL----
HRTV_NSs      HNIIMHDEEVREAYLNPIWGKDWALSSSP---
SFTSV_NSs     HNLIRFDEELRTAALNTIWGRDWPALGDLPEV
.: * . * * : : : * * . : .

```

**Figure 7-1. Amino acid sequence alignment of UUKV, HRTV and SFTSV NSs proteins.**

UUKV (AAA47959.1), HRTV (AFP33392.1) and SFTSV (AJD86041.1) NSs amino acid sequences were aligned using CLUSTAL Omega. “\*” depicts conserved amino acids, “:” amino acids with similar properties, and “.” amino acids with weakly similar properties. The PxxP motif found in HRTV and SFTSV NSs is highlighted in red. UUKV: Uukuniemi virus; HRTV: Heartland virus; SFTSV: Sever fever with thrombocytopenia syndrome virus.

Given that the characteristic IBs formed by SFTSV NSs are key for its IFN antagonist activity, the subcellular localization of UUKV or HRTV NSs proteins was compared to that of SFTSV NSs. As well as IFN competent human A549 cells, cell lines which are IFN incompetent but can be readily infected by each of the viruses (namely BHK-21 cells for UUKV and Vero E6 for HRTV and SFTSV) were also used. Subconfluent cell monolayers were infected at a high MOI (3 FFU/cell), fixed at 24 h p.i. and probed with the appropriate anti-NSs antibodies prior to analysis by confocal microscopy. In agreement with a previous study (Simons *et al.*, 1992), UUKV NSs showed cytoplasmic distribution, with small punctate staining in A549 and BHK-21 cell lines (Figure 7-2 A). Despite the higher amino acid conservation between HRTV and SFTSV NSs proteins, HRTV NSs was diffused in the cytoplasm of both A549 and Vero E6 cells (Figure 7-2 B). This is in comparison to SFTSV NSs, which formed characteristic cytoplasmic IBs (Figure 7-2 C). Because SFTSV NSs-induced IBs play an important role in the suppression of the IFN response via the sequestration of various components of the IFN pathways (Ning *et al.*, 2015; 2014; Santiago *et al.*, 2014), the divergent subcellular localization of UUKV and HRTV NSs proteins in comparison to SFTSV NSs indicated that these proteins may utilise a disparate mechanism to that of SFTSV NSs to circumvent the IFN response.

As detailed in chapter 6, C-terminal V5-tags were added to UUKV, HRTV and SFTSV NSs-expressing plasmids to be utilized in the transient expression assays. The aim of tagging the NSs proteins was to compare their expression levels by western blotting. To ensure that the subcellular localization of V5-tagged NSs proteins in the cell line used for transient transfection assays was similar to that of native NSs proteins upon virus infection, HEK293T cells were transfected with expression plasmids encoding the V5-tagged UUKV, HRTV or SFTSV NSs proteins. 24 h post transfection the transfected cells were fixed, permeabilized and probed with an anti-V5 antibody. Analysis by confocal microscopy revealed that the subcellular localization of V5-tagged UUKV, HRTV or SFTSV NSs proteins in HEK293T cells was similar to that described for the wild-type protein in other cell lines infected with the cognate viruses (Figure 7-3 and 7-2).

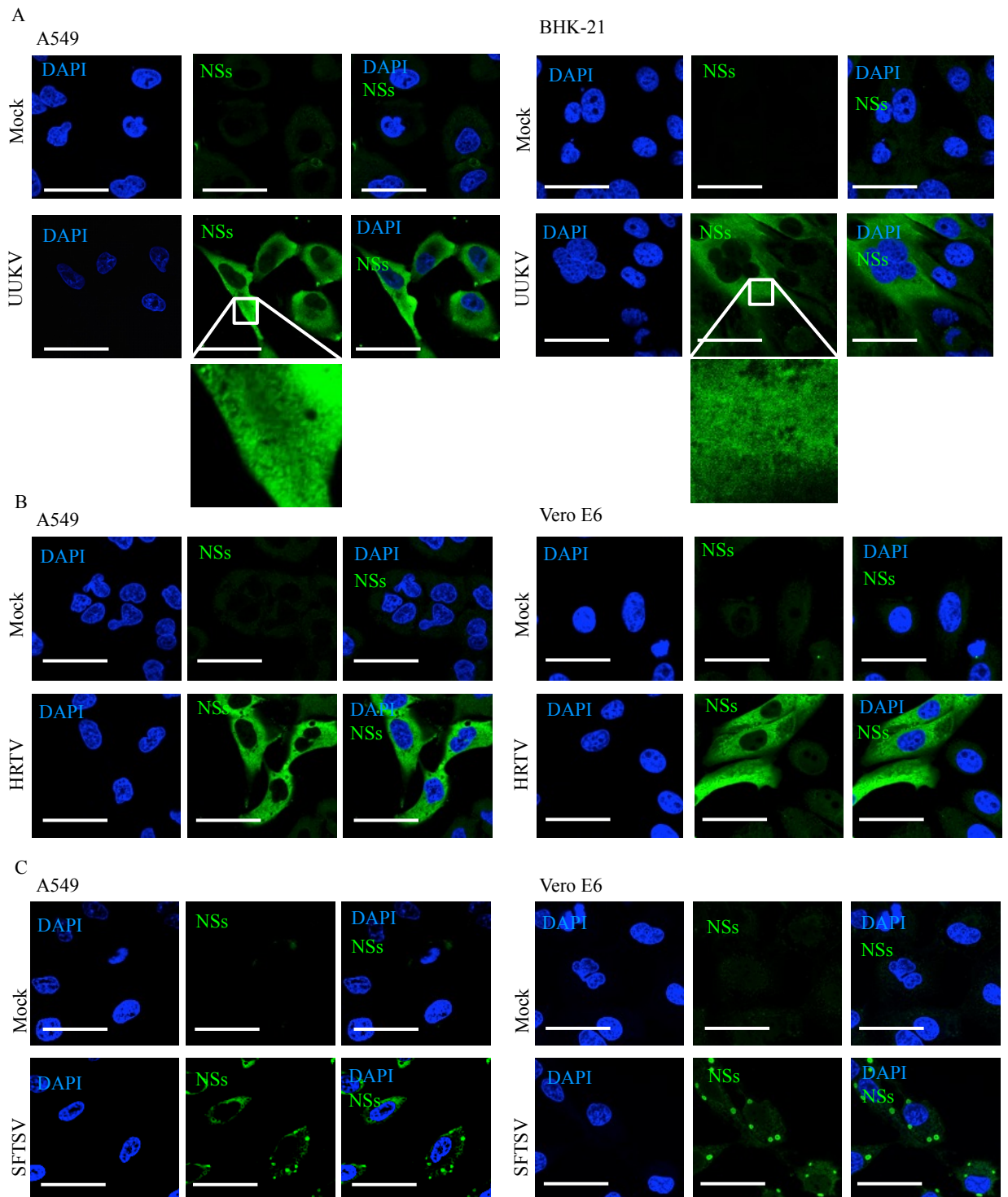


**Figure 7-2. Subcellular localization of UUKV, HRTV and SFTSV NSs proteins.**

The subcellular localization of UUKV (A), HRTV (B) and SFTSV (C) was analysed by confocal microscopy following virus infection. The indicated cell lines were infected at a high MOI (3 FFU/cell), or mock-infected. 24 h p.i. Cells were fixed, permeabilised and probed with the appropriate anti-NSs antibody. NSs proteins (green) and cell nuclei (blue) were visualized by confocal microscopy. Scale bars indicate 20  $\mu$ m. UUKV: Uukuniemi virus; HRTV: Heartland virus; SFTSV: Sever Fever with Thrombocytopenia syndrome virus.

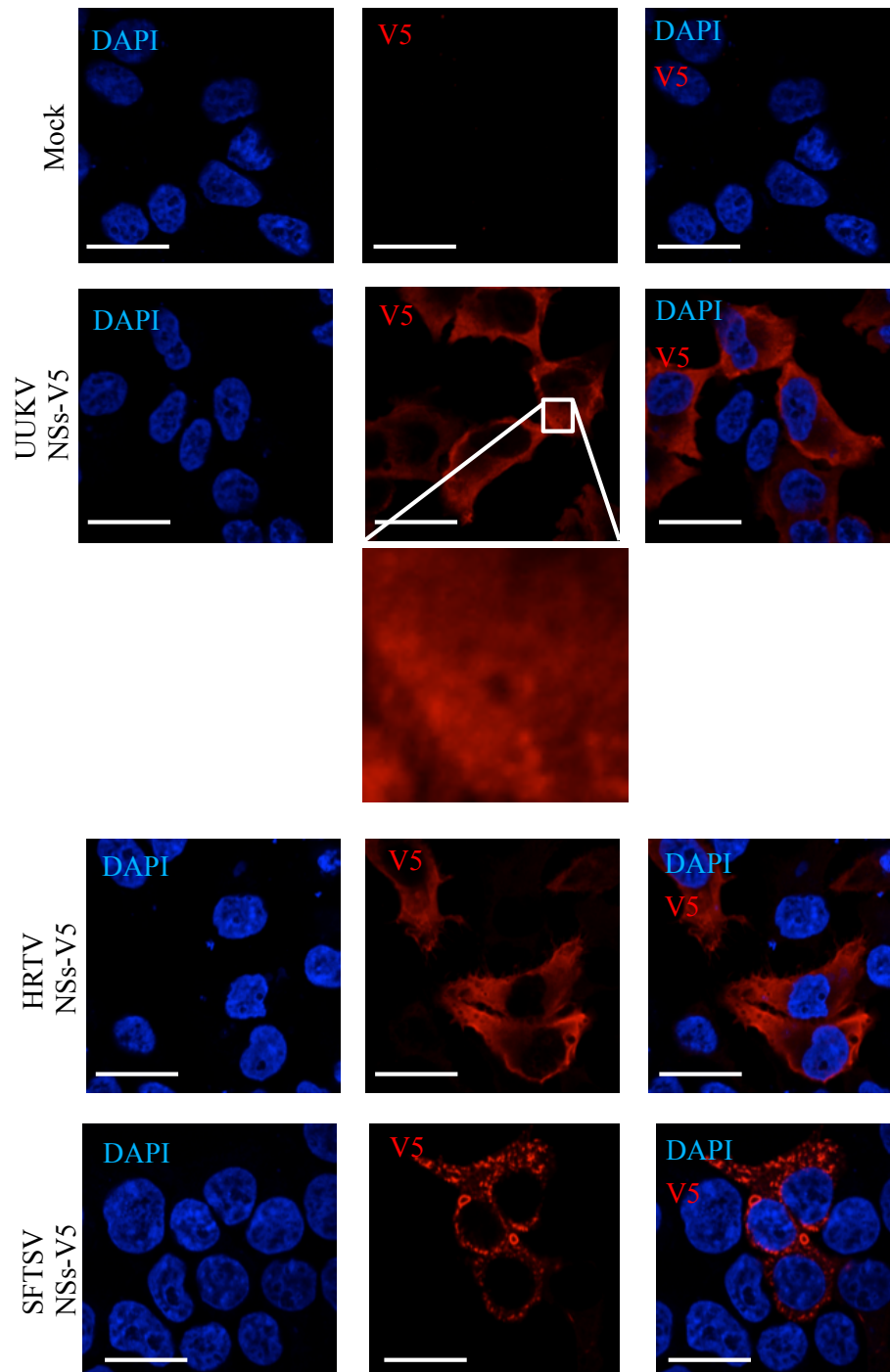


**Figure 7-3. Subcellular localization of V5-tagged UUKV, HRTV and SFTSV NSs proteins.**

The subcellular localization of V5-tagged UUKV, HRTV and SFTSV NSs was investigated by confocal microscopy. HEK293T cells were transfected with plasmids encoding UUKV, HRTV or SFTSV NSs proteins tagged at their C terminus with a V5 tag (pCMVUUKNSsV5, pCMVHRTNSsV5 and pCMVSFTSNSsV5, respectively). 24 h post transfection cells were fixed, permeabilised and probed with an anti-V5 antibody. DAPI-stained nuclei (blue) and the V5-tagged NSs proteins (red) were visualized by confocal microscopy. Scale bars indicate 20  $\mu$ m. UUKV: Uukuniemi virus; HRTV: Heartland virus; SFTSV: Sever fever with thrombocytopenia syndrome virus.

### ***7.3.2 Dissection of the IFN induction pathway to study the inhibitory effect of UUKV, HRTV and SFTSV NSs proteins.***

To examine at which stage of IFN induction UUKV and HRTV NSs proteins exerted their IFN antagonist function, an IFN- $\beta$  reporter assay was performed. In this assay a firefly luciferase reporter gene under the control of a murine IFN- $\beta$  promoter is activated by the overexpression of various effectors of the IFN induction pathway (in this case constitutively active RIG-I N terminus [RIG-I N], MAVS, TBK1, IKK $\epsilon$ , or a phosphomimetic, active form of IRF-3 [IRF-3 5D]). Similar assays have been commonly used to study the IFN antagonistic properties of the Ebola virus VP35 protein (Prins *et al.*, 2009), influenza virus PB1-F2 protein (Varga *et al.*, 2011), the Nipah virus matrix protein (Bharaj *et al.*, 2016), and the V protein of paramyxoviruses (Andrejeva *et al.*, 2004).

Firstly, the assay was optimised by examining the activation of the IFN- $\beta$  promoter by various IFN induction effectors. Briefly, HEK293T cells were transfected with increasing amounts of expression plasmids encoding FLAG-tagged RIG-I N, MAVS, TBK1, IKK $\epsilon$ , or untagged IRF-3 5D (kindly provided by Mirko Schmölke, University of Geneva), as well as a plasmid encoding firefly luciferase under the control of a murine IFN- $\beta$  promoter (p[125]luc), and the transfection control plasmid encoding for *Renilla* luciferase under a CMV promoter (phRL). 18 h post transfection, the firefly and *Renilla* activities were measured, and firefly activity normalised against the *Renilla* control. Fold induction was expressed as the fold increase in normalised luciferase activity, relative to the non-stimulated mock control that was transfected without any IFN induction effector expression plasmid. Overexpression of RIG-I N, MAVS, TBK1, IKK $\epsilon$ , or IRF-3 5D resulted in transactivation of the IFN- $\beta$  promoter. TBK1 exhibited the highest efficiency, resulting in a mean 1278-fold increase relative to the mock-transfected cells when the highest amount (100 ng) of TBK1 expression plasmid was added (Figure 7-4). Overall, at least a 100-fold increase in IFN- $\beta$  promoter activation relative to the mock-transfected cells was detected when the lowest dose of all IFN induction effector expression plasmids was used (5 ng), indicating that the assay was functional with the overexpression all IFN induction effector components.

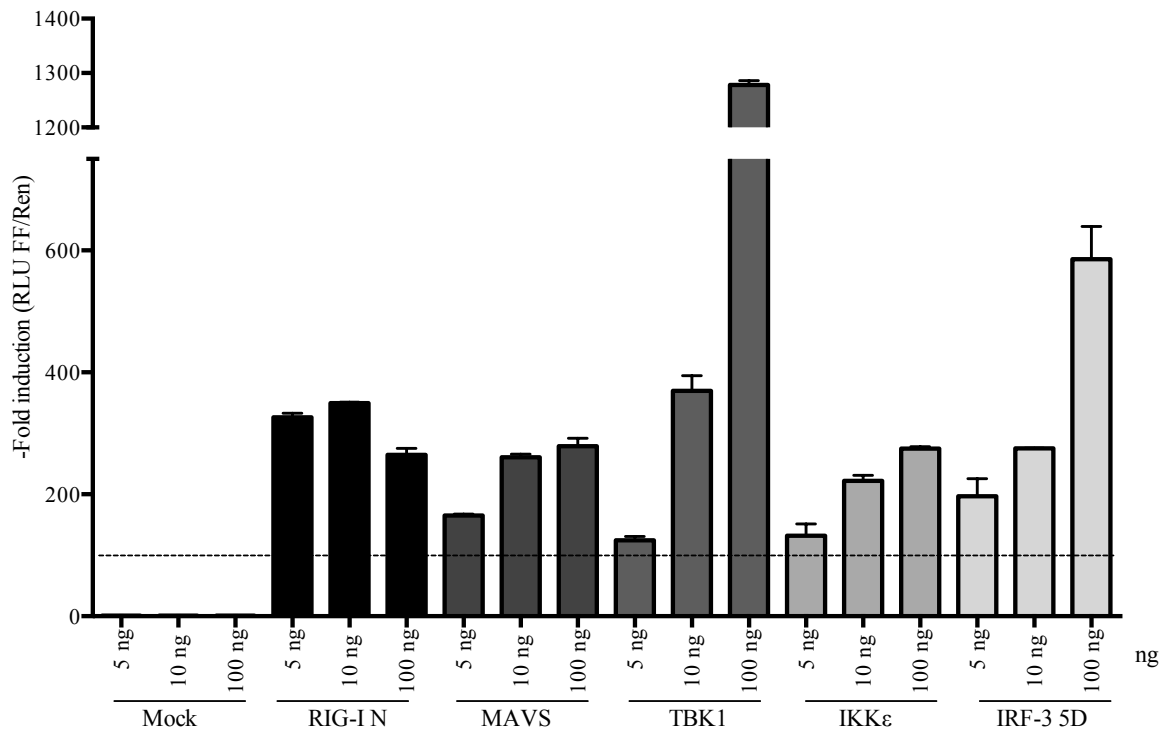


**Figure 7-4. IFN- $\beta$  promoter activation by effectors of the IFN induction pathway.**

HEK293T cells were transfected with the indicated amounts of IFN induction effector expression plasmids or with empty plasmid, along with a plasmid encoding firefly luciferase under the control of an IFN- $\beta$  promoter (p[125]luc), and a control CMV-driven expression plasmid encoding *Renilla* luciferase (phRL). The total amount of plasmid DNA in all reactions was kept constant by the addition of empty control plasmid to the DNA mix. 18 h post transfection the cell lysates were harvested, firefly and *Renilla* luciferase activities measured and firefly activity normalised against *Renilla* activity. Fold induction of the IFN- $\beta$  promoter was calculated as the fold increase in normalised luciferase activity relative to the non-stimulated mock control. Dashed line indicates 100-fold induction. The bars indicate mean fold induction in normalised luciferase activity ( $\pm$  SD) from a single experiment performed in duplicate ( $n=2$ ).

Next, the effect of untagged or V5-tagged UUKV or HRTV NSs on the activation of the murine IFN- $\beta$  promoter by overexpression of RIG-I N, MAVS, TBK1, IKK $\epsilon$ , or IRF-3 5D was examined, utilizing SFTSV NSs as a control. Assays were performed in HEK293T cells as described above, utilizing 50 ng of IFN induction effector expression plasmids, to allow detection of the effector proteins by western blotting. Additionally, 250 ng of untagged or V5-tagged NSs protein-expressing plasmids were co-transfected (the highest dose of plasmid utilised in Section 6.3.3).

While no inhibition by UUKV NSs was observed in RIG-I N, TBK1, IKK $\epsilon$ , or IRF-3 5D-induced IFN- $\beta$  reporter assays, the presence of untagged or V5-tagged UUKV NSs resulted in a mean 55% or 45% inhibition of the MAVS-induced IFN- $\beta$  promoter activation, respectively (Figure 7-5 A-E). Although a difference of 10% inhibition was observed between untagged and V5-tagged UUKV NSs at the level of MAVS, this difference was not statistically significant. Given that the N terminus of RIG-I is implicated in the subsequent activation of MAVS for signalling in the IFN induction pathway and that UUKV NSs impaired MAVS-induced IFN- $\beta$  promoter activation, the lack of inhibition of RIG-I N-induced IFN- $\beta$  promoter activation by UUKV NSs was surprising (Figure 7-5 A). However, the results presented in chapter 6 showed that UUKV NSs weakly inhibited the RIG-I N-induced production of IFN in a dose-dependent manner (Figure 6-4). Therefore, it is possible that transactivation of the murine IFN- $\beta$  promoter via the overexpression of RIG-I N allows for the detection of an inhibitory effect by UUKV NSs when IFN production is measured by a biological IFN assay (Figure 6-4), whereas measuring IFN- $\beta$  promoter-driven luciferase activity upon RIG-I N induction saturates the weak inhibitory effect of UUKV NSs at the level of RIG-I N (Figure 7-5 A).

In comparison to UUKV NSs, the NSs protein of HRTV and SFTSV impaired RIG-I N, MAVS and TBK1 (Figure 7-5 A-C), but not IKK $\epsilon$ , or IRF-3 5D -induced activation of the IFN- $\beta$  promoter (Figure 7-5 D-E). Notably, whereas SFTSV NSs yielded 99.7% inhibition of TBK1-induced IFN- $\beta$  promoter activation, only ~ 45% inhibition was observed by untagged and V5-tagged HRTV NSs (Figure 7-5 C). Nevertheless, the difference in inhibitory efficiency by SFTSV and HRTV NSs proteins on TBK1-induced IFN- $\beta$  promoter activation may be due to the lower expression levels of HRTV NSs compared to SFTSV NSs, as detected by immunoblotting of the transfected cell lysates (Figure 7-5 C).

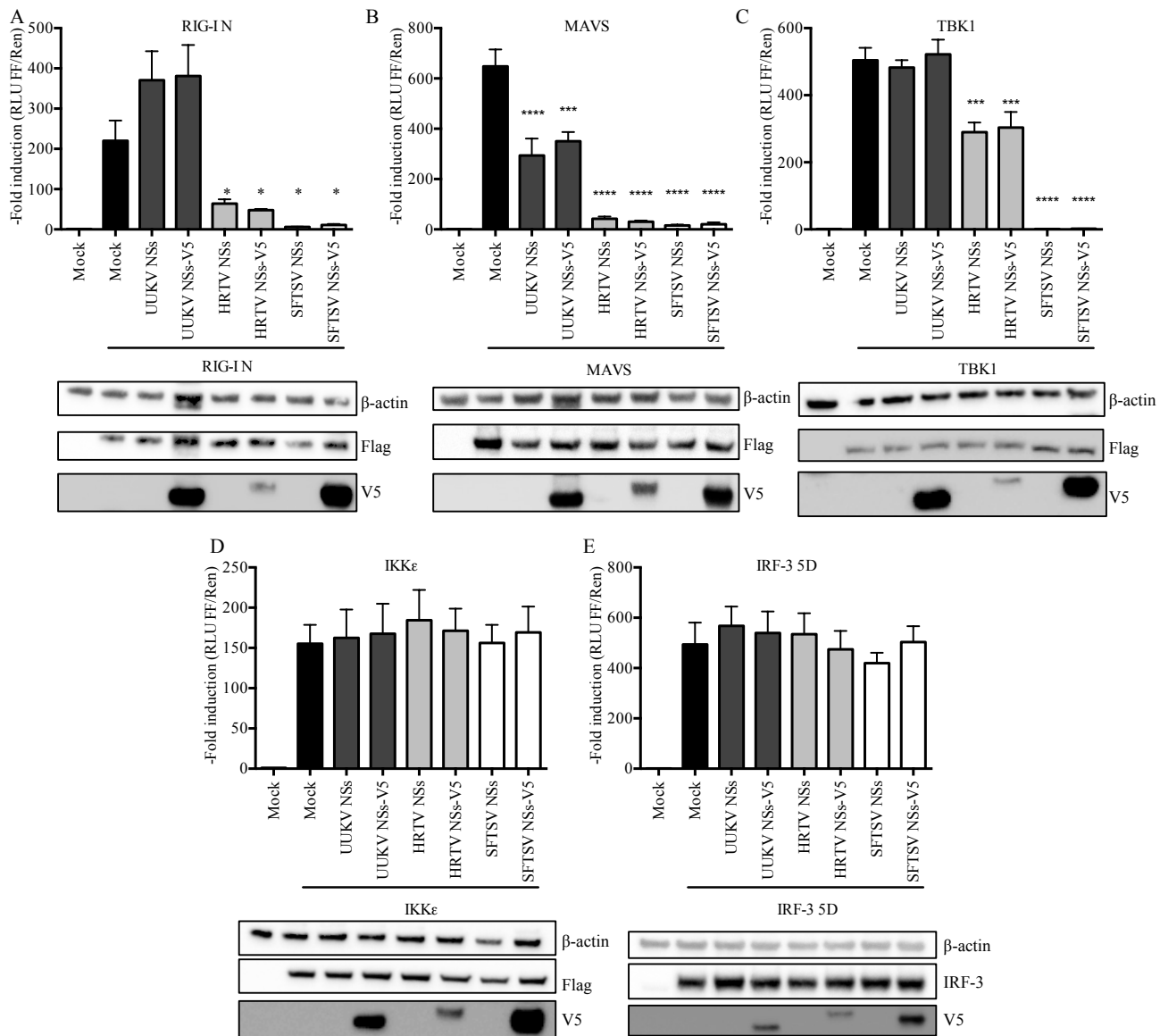


**Figure 7-5. UUKV NSs protein inhibits IFN- $\beta$  induction at the level of MAVS, whereas HRTV NSs antagonises at the level of TBK1.**

HEK293T cells were transfected with p(125)luc and phRL plasmid in the presence of untagged or V5-tagged UUKV, HRTV or SFTSV NSs proteins. The IFN- $\beta$  promoter was stimulated by co-transfection of FLAG-tagged inducer plasmids RIG-I N (A), MAVS (B), TBK1 (C), IKK $\epsilon$  (D) or a plasmid expressing untagged IRF-3 5D (E). 18 h post transfection the cell lysates were harvested, firefly and *Renilla* luciferase activities measured and firefly activity normalised against *Renilla* activity. Fold induction of the IFN- $\beta$  promoter was calculated as the fold increase in normalised luciferase activity relative to the non-stimulated mock control. Western blots for cell lysates of the transfected samples are shown in the lower panels. Data depicts three independent experiments performed in duplicate (n=3), presented as mean fold induction  $\pm$  SEM. Statistical significance for the comparison of means between groups was determined by one-way ANOVA followed by Dunnet multiple comparisons post-hoc test. \*\*\*\*,  $p \leq 0.0001$ ; \*\*\*,  $p \leq 0.001$ ; \*\*,  $p \leq 0.01$ ; \*,  $p \leq 0.05$ .

### ***7.3.3 Interaction between UUKV, HRTV and SFTSV NSs proteins and the IFN induction pathway***

The dissection of the IFN induction pathway enabled to pinpoint at which stage of the IFN induction pathway the tick-borne phlebovirus NSs proteins exhibited an inhibitory activity. In order to corroborate whether the inhibitory activity was due to direct interactions between the NSs proteins with individual effectors of the IFN induction pathway, immunoprecipitation (IP) studies were carried out. Briefly, HEK293T cells were transfected with each of the FLAG-tagged effectors of the IFN induction pathway or untagged IRF-3 5D individually, in the presence of the V5-tagged UUKV, HRTV or SFTSV NSs proteins. 18 h post transfection, the cell lysates were subjected to co-IP using FLAG-conjugated beads. Immunoprecipitated eluates as well as whole cell lysate samples (included to confirm that the transfected proteins were expressed) were analysed by western blotting.

V5-tagged UUKV NSs could only be precipitated with FLAG-tagged RIG-I N and MAVS, but not with TBK1, IKK $\epsilon$ , or IRF-3 5D (Figure 7-6 A). This is in comparison to HRTV NSs, which behaved similarly to SFTSV NSs, as both the NSs proteins could be pulled down only with FLAG-tagged TBK1, but not RIG-I N, MAVS, IKK $\epsilon$ , or IRF-3 5D. (Figure 7-6 B and C). No V5-tagged NSs proteins could be pulled down when cell lysates of cells transiently expressing only the individual V5-tagged proteins NSs proteins were subjected to IP with anti-FLAG beads, or using the anti-IRF-3 antibody (used for the aforementioned co-IPs) (Figure 7-6 D).

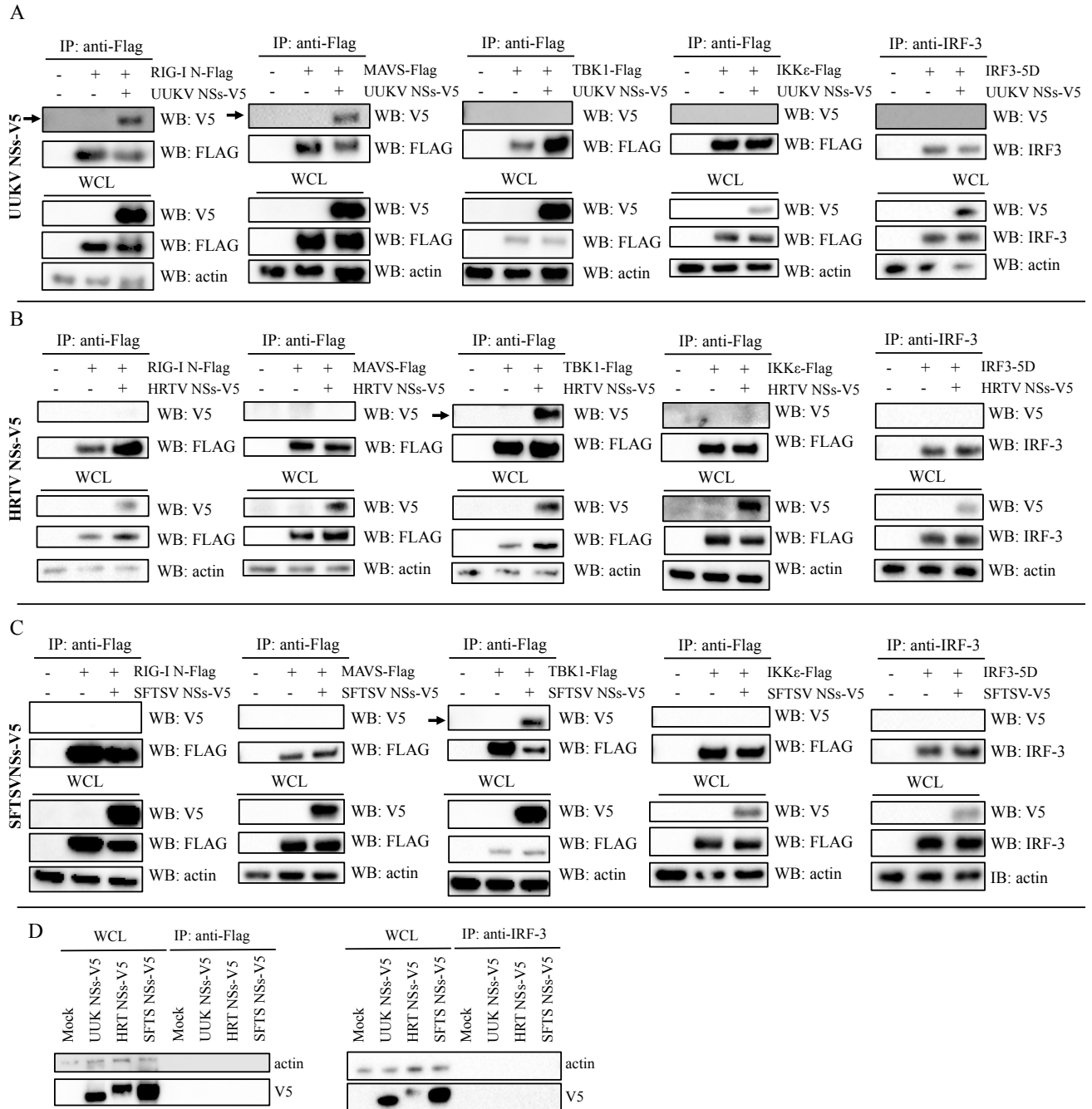


**Figure 7-6. UUKV NSs interacts with RIG-I N and MAVS, whereas HRTV and SFTSV NSs interact with TBK1 in a transient overexpression system.**

HEK293T cells were co-transfected with V5-tagged UUKV (A), HRTV (B) or SFTSV (C) NSs proteins along with FLAG-tagged RIG-I N, MAVS, TBK1, IKKε or untagged IRF-3 5D. Cell lysates were subjected to co-IP with beads conjugated to FLAG or IRF-3 antibodies. V5-tagged UUKV, HRTV and SFTSV NSs proteins in the co-IP eluates (indicated with a black arrow) were detected by western blot using an anti-V5 antibody. (D) Control IP for V5-tagged NSs proteins pull-down. HEK293T cells were transfected with V5-tagged UUKV, HRTV or SFTSV NSs proteins only, and the cell lysates subjected to IP with beads conjugated to FLAG or IRF-3 antibodies. IP eluates were analysed by western blot with an anti-V5 antibody. The results shown are representative of two independent experiments. IP: immunoprecipitation; WB: Western blotting; WCL: whole cell lysate.

### ***7.3.4 UUKV NSs protein interacts with MAVS.***

In a transient overexpression system, V5-tagged UUKV NSs showed a direct interaction with the N terminus of RIG-I and MAVS (Figure 7-6 A). However, UUKV NSs blocked the MAVS- but not RIG-I N-induced activation of the IFN- $\beta$  promoter in reporter assays (Figure 7-5 A and B), despite showing the dose-dependent inhibition of RIG-I N-mediated IFN production (chapter 6, Figure 6-4 A). To clarify these observations further and to confirm the interaction observed in a transient overexpression system between V5-tagged UUKV NSs and RIG-I N or MAVS, a reverse immunoprecipitation of UUKV NSs in the context of a virus infection was performed.

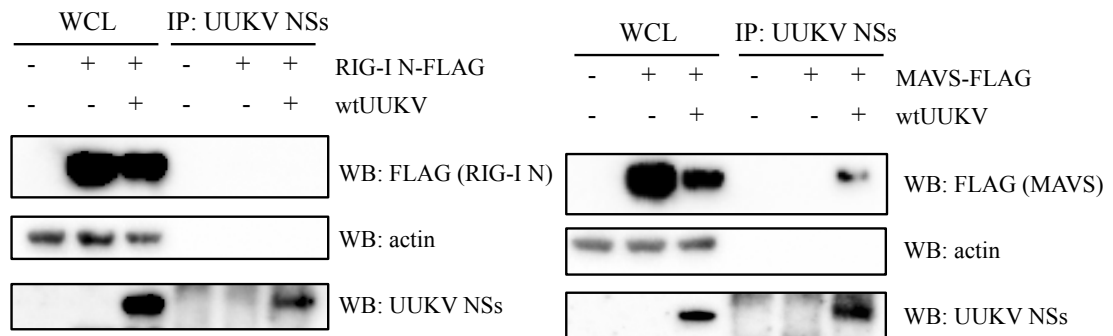
Briefly, HEK293T cells were infected with UUKV at a high MOI (20 FFU/cell). Rather than aiming to detect endogenous RIG-I or MAVS, UUKV-infected cells were transfected with FLAG-tagged RIG-I N and MAVS 8 h p.i, because their overexpression allows for a more convenient approach for detection by western blotting. 30 h p.i. the cell lysates were subjected to co-IP using a rabbit polyclonal anti-UUKV NSs antibody (kindly provided by Anna Överby, Umeå University), followed by western blotting. While no RIG-I N could be detected in the IP eluates from UUKV-infected cells (Figure 7-7 A, left panel), FLAG-tagged MAVS was precipitated in the IP eluates from UUKV-infected cells (Figure 7-7 A, right panel). The band detected belonging to FLAG-tagged MAVS was only visible upon long exposure of the membrane, and was weak relative to the expression levels observed in the whole cell lysate, suggesting a weak interaction (Figure 7-7, right panel). These findings are at odds with the results obtained when both UUKV NSs and the FLAG-tagged IFN induction effector proteins were overexpressed and FLAG-tagged MAVS or RIG-I N subjected to IP. Under the latter conditions, a direct interaction was found between V5-tagged UUKV NSs and both FLAG-tagged RIG-I N or MAVS (Figure 7-6 A). One explanation for such discrepancy could be that MAVS and RIG-I interact with each other through their 2CARD domains. Thus, the detection of UUKV NSs in IP eluates following immunoprecipitation of FLAG-tagged RIG-I N (which is in excess) could be a result of the direct interaction between UUKV NSs and endogenous MAVS, but not with overexpressed RIG-I N. On the other hand, immunoprecipitation UUKV NSs may result in undetectable amounts of FLAG-tagged RIG-I N pulled down as a result of the direct interaction of FLAG-tagged RIG-I N and endogenous MAVS.

In order to corroborate these results, a reverse co-IP was also carried out under the same conditions as in the previous section (7.3.3) (i.e. HEK293T cells transiently expressing

both V5-tagged UUKV NSs and FLAG-tagged RIG I N or MAVS). 24 h post transfection, the cell lysates of transfected cells were utilized for co-IP using an anti-V5 antibody for the pull-down of V5-tagged UUKV NSs instead of immunoprecipitation of FLAG-tagged RIG-I N or MAVS. As observed in the context of UUKV infection (Figure 7-7 A), no FLAG-tagged RIG-I N could be detected in the IP eluate containing V5-tagged UUKV NSs (Figure 7-7 B, left panel) but a weak band corresponding to FLAG-tagged MAVS was detected (Figure 7-7 B, right panel). Therefore, these results suggest that UUKV NSs exhibits a weak, direct interaction with MAVS, but not with RIG-I N. This finding is in agreement with the weak inhibition of the MAVS-induced IFN- $\beta$  reporter activity by UUKV NSs reported in section 7.3.2 (Figure 7-5).

To confirm whether UUKV NSs could co-localise with MAVS, their subcellular localization was examined in HEK293T cells transiently expressing FLAG-tagged MAVS and V5-tagged UUKV NSs. Upon its activation, MAVS has been reported to adopt a speckled-like staining pattern (Onoguchi *et al.*, 2010). Overexpression of FLAG-tagged MAVS in HEK293T cells resulted in the speckled-like staining characteristic of the active form of MAVS (Figure 7-8 C). V5-tagged UUKV NSs showed the distinct cytoplasmic, punctate staining described earlier (Figures 7-2 A, 7-3 and 7-8 B). Although in some HEK293T cells transiently expressing V5-tagged UUKV NSs and FLAG-tagged MAVS co-localization of UUKV NSs and MAVS was not obvious, close examination revealed partial co-localization of the small punctate UUKV NSs staining with MAVS speckles (Figure 7-8 D). The partial co-localization of UUKV NSs with MAVS is in agreement with the aforementioned hypothesis that the interaction between these two proteins is weak, and could explain the weak IFN antagonistic activity of UUKV NSs.

A



B

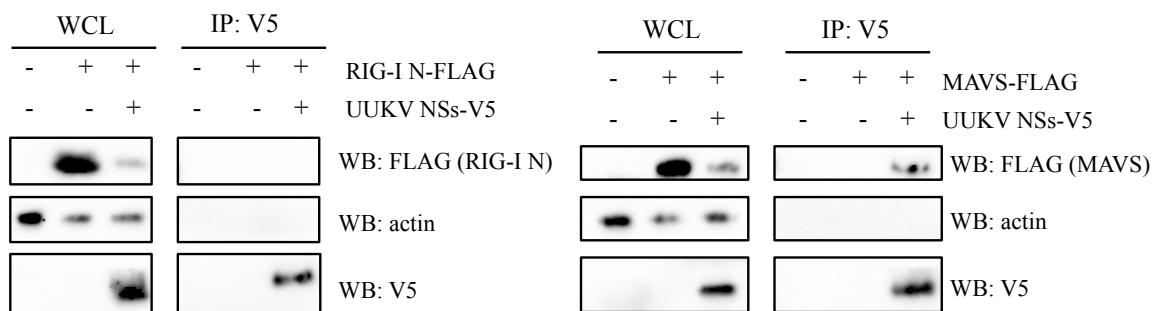


**Figure 7-7. Interaction between UUKV NSs and MAVS detected by immunoprecipitation.**

(A) Co-IP of UUKV NSs protein upon UUKV infection in the presence of FLAG-RIG-I N or FLAG-MAVS. HEK293T cells were mock infected or infected with UUKV at a high MOI (20 FFU/cell) for 8h, followed by a mock-transfection or transfection of FLAG-tagged RIG-I N (left panel) or MAVS-encoding plasmids (right panel). At 30 h p.i., the cell lysates were subjected to co-IP using an anti-UUKV NSs antibody, followed by detection of FLAG-tagged RIG-I N or MAVS and UUKV NSs by western blotting. (B) Co-IP of V5-tagged UUKV NSs in the presence of FLAG-RIG-I N or FLAG-MAVS. HEK293T cells were mock transfected, or transfected with V5-tagged UUKV NSs and FLAG-tagged RIG-I N (left panel) or MAVS (right panel). Cell lysates were subjected to co-IP with an anti-V5 antibody. FLAG-tagged RIG-I N and MAVS in the co-IP eluates were detected by western blotting with an anti-FLAG antibody. The results shown in this figure are representative of two experimental repeats. IP: immunoprecipitation, WB: Western blotting, WCL: whole cell lysate.

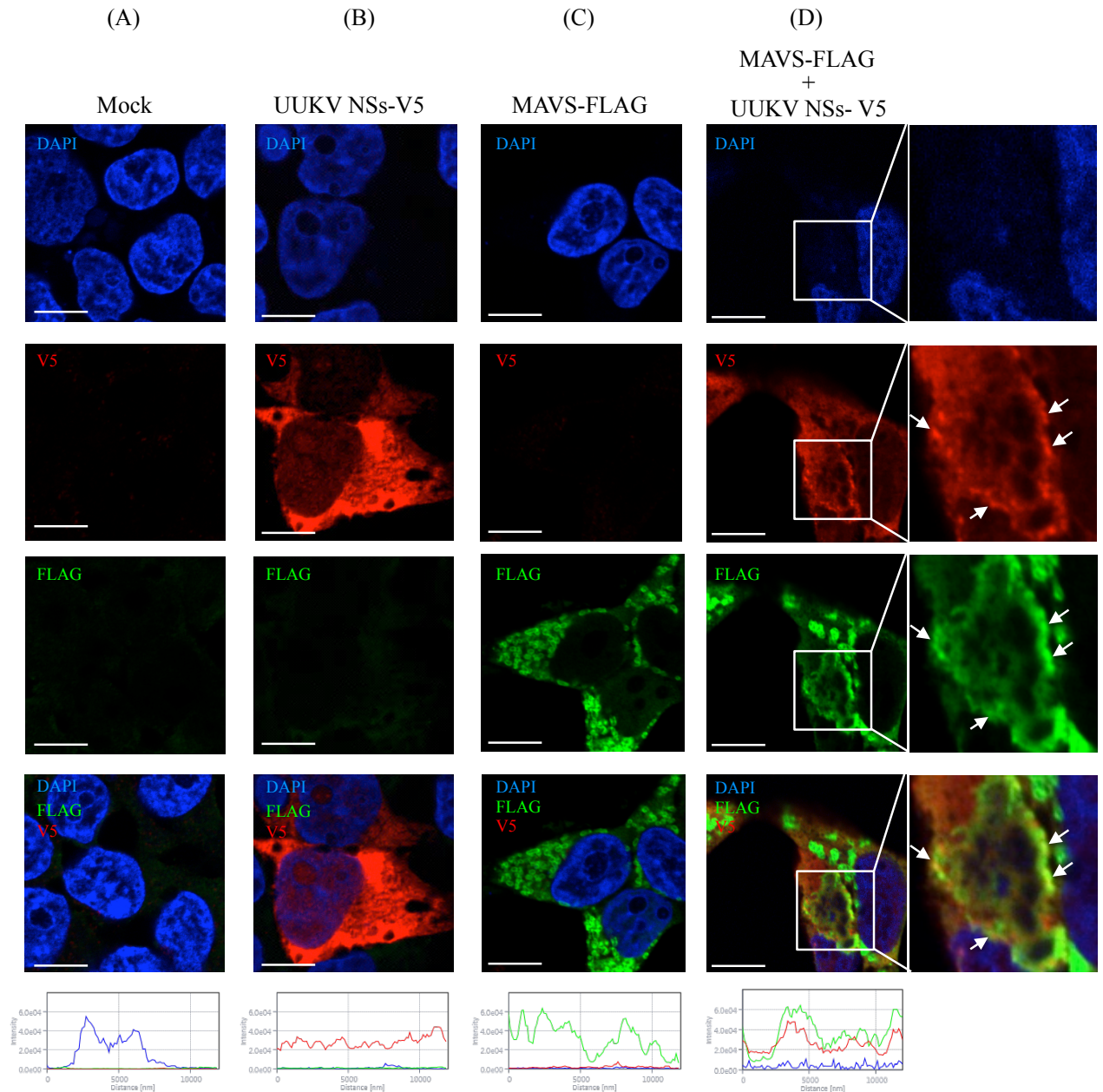


**Figure 7-8. Subcellular localization of V5-tagged UUKV NSs and FLAG-tagged MAVS.**

Subcellular localization of UUKV NSs-V5 and MAVS-FLAG. HEK293T cells were mock-transfected (A), or transfected with UUKV NSs-V5 (B), MAVS-FLAG (C) or both (D). 24 h post transfection the cells were fixed, permeabilised and probed with V5 (red) and FLAG (green) antibodies. DAPI-stained nuclei (blue) and subcellular localization of the proteins was analysed by confocal microscopy. Intensity profile graphs are shown at the bottom of the images. Scale bars indicate 10  $\mu$ m. The results shown in this figure are representative of two experimental repeats.

### 7.3.5 *HRTV NSs protein interacts with TBK1.*

Whereas the interaction between SFTSV NSs and TBK1 is well characterised, that of HRTV NSs with TBK1 is novel. To confirm the interaction observed between HRTV NSs and TBK1 in the context of HRTV infection, A549 cells were infected with HRTV at a high MOI (10 FFU/cell). 48 h p.i. the cell lysates were subjected to co-IP using an anti-HRTV NSs antibody and immunoblotting. Endogenous TBK1 could be pulled down in HRTV-infected cells, when the NSs protein was immunoprecipitated (Figure 7-9 A). These data, along with the interaction observed between HRTV and TBK1 when overexpressed in immunoprecipitation studies (Figure 7-6 B), is in agreement with the inhibitory activity of HRTV NSs in TBK1-induced activation of the IFN- $\beta$  promoter (Figure 7-5 C).

In order to compare the interaction between HRTV NSs and TBK1 to that between SFTSV NSs and TBK1, the subcellular localization of TBK1 in the presence or absence of HRTV or SFTSV NSs proteins in HEK293T cells was examined. Briefly, HEK293T cells transiently expressing FLAG-tagged TBK1 and either V5-tagged HRTV or SFTSV NSs proteins were fixed, permeabilised and probed with anti-TBK1 and anti-V5 antibodies 24 h post transfection. Of note, an anti-TBK1 antibody rather than an anti-FLAG antibody was utilized, due to issues in detecting FLAG-tagged TBK1 by immunofluorescence using the latter antibody (data not shown). Whereas TBK1 showed diffused cytoplasmic staining on its own, TBK1 was clearly sequestered into IBs formed by SFTSV NSs in cells transiently expressing SFTSV NSs, as it has been previously described (Ning *et al.*, 2014; Santiago *et al.*, 2014; X. Wu *et al.*, 2014). In contrast, in cells transfected with HRTV NSs, TBK1 remained diffused in the cytoplasm, but co-localised with the HRTV NSs signal (Figure 7-8 B).

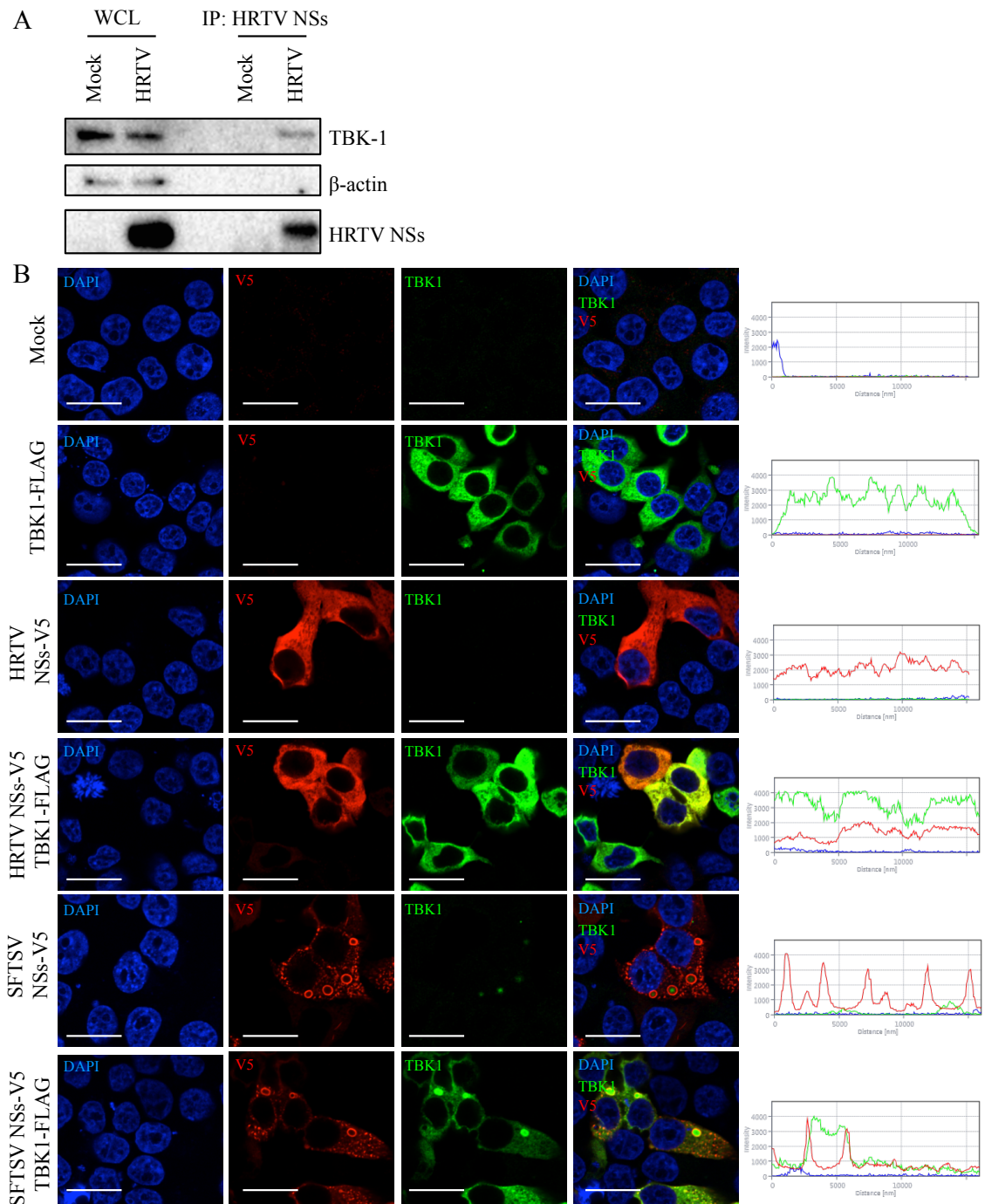


**Figure 7-9. Interaction between HRTV NSs and TBK1.**

(A) co-IP of HRTV NSs in HRTV infected cells. Cell lysates of HRTV-infected A549 cells (MOI 10 FFU/cell) were subjected to co-IP with an anti-HRTV NSs antibody. Western blotting was performed on eluates in order to detect endogenous TBK1 and HRTV NSs in infected cells. (B) Immunofluorescence studies of HEK293T cells transiently expressing TBK1-FLAG and V5-tagged HRTV or SFTSV NSs. HEK293T cells were fixed and permeabilised 24 h post transfection and probed with anti-TBK1 and anti-V5 antibodies. The subcellular localization of NSs proteins (red), TBK1 (green) and nuclei stained with DAPI (blue) were analysed by confocal microscopy. Intensity profile graphs are shown to the right of the image. Scale bars indicate 20  $\mu$ m. The results shown are representative of at least two experimental repeats. IP: immunoprecipitation, WB: Western blotting, WCL: whole cell lysate.

### 7.3.6 Interaction between HRTV or SFTSV NSs and the IFN signalling pathway

The results in chapter 6 indicated that while UUKV NSs was unable to inhibit type I and type II IFN signalling, HRTV and SFTSV NSs strongly blocked type I, but not type II IFN signalling. Other groups have shown that the mechanism by which SFTSV NSs blocks type I IFN signalling is by interacting with and sequestering STAT1 and STAT2 into IBs (Chaudhary *et al.*, 2015; Ning *et al.*, 2015). To elucidate whether HRTV and SFTSV NSs have conserved the same interacting partners of the JAK/STAT signalling pathway, immunoprecipitation of V5-tagged tick-borne phlebovirus NSs proteins in HEK293T cells was carried out. The co-immunoprecipitation of endogenous STAT1 and STAT2 in the presence of HRTV and SFTSV NSs proteins was assessed, utilizing UUKV NSs as a negative control, as UUKV NSs does not block IFN signalling (Figure 6-6 and 6-7). In agreement with previous assays that showed no inhibition of IFN signalling by UUKV NSs (Figure 6-6 and 6-7), no STAT1 or STAT2 was co-immunoprecipitated in the presence of UUKV NSs (Figure 7-10 A). In contrast, endogenous STAT1 and STAT2 were co-immunoprecipitated in the presence of V5-tagged HRTV or SFTSV NSs proteins (Figure 7-10 A), suggesting the IFN signalling interacting partners of HRTV and SFTSV NSs proteins are conserved. Intriguingly, STAT2 levels in IP eluates were visibly higher than those of STAT1 (relative to the respective expression levels in the whole cell lysates). Indeed, long exposure was required in order to detect STAT1 in IP samples.

STAT3 is a pleiotropic STAT that has been implicated in modulating inflammatory responses (Oh *et al.*, 2011; Takeda *et al.*, 1998; Yu *et al.*, 2013). With this in mind, the ability of tick-borne phlebovirus NSs proteins to interact with STAT3 was investigated using an assay similar to the one described in the previous paragraph. No STAT-3 was co-immunoprecipitated along with the tick-borne phlebovirus V5-tagged NSs proteins (Figure 7-10 B).

One study has reported that only STAT2 (but not STAT1) phosphorylation is inhibited by SFTSV NSs (Ning *et al.*, 2015). Another study has shown that the phosphorylation of STAT2 as well as STAT1 at position Ser727 is blocked by SFTSV NSs (Chaudhary *et al.*, 2015). The ability of HRTV or SFTSV NSs proteins to hamper STAT1 or STAT2 phosphorylation was examined utilizing UUKV NSs as a negative control. Briefly, HEK293T cells transiently expressing untagged, or V5-tagged UUKV, HRTV or SFTSV NSs proteins were treated with recombinant IFN- $\beta$  for 30 min, and the cell lysates harvested for immunoblotting analysis 24 h post transfection. At odds with the findings by

Chaudhary *et al* (Chaudhary *et al.*, 2015), no difference in phosphorylated STAT1 (at positions Ser727 or Tyr701) or STAT1 levels was observed in the presence of UUKV, HRTV or SFTSV NSs proteins, compared to the mock control (Figure 7-10 C). While in the presence of the tick-borne phlebovirus NSs proteins STAT2 levels also remained unchanged compared to the mock control, the presence of HRTV and SFTSV NSs proteins resulted in a reduction of STAT2 phosphorylation at position Tyr690, compared to the levels found in the mock control and the UUKV NSs-transfected controls (Figure 7-10 C).

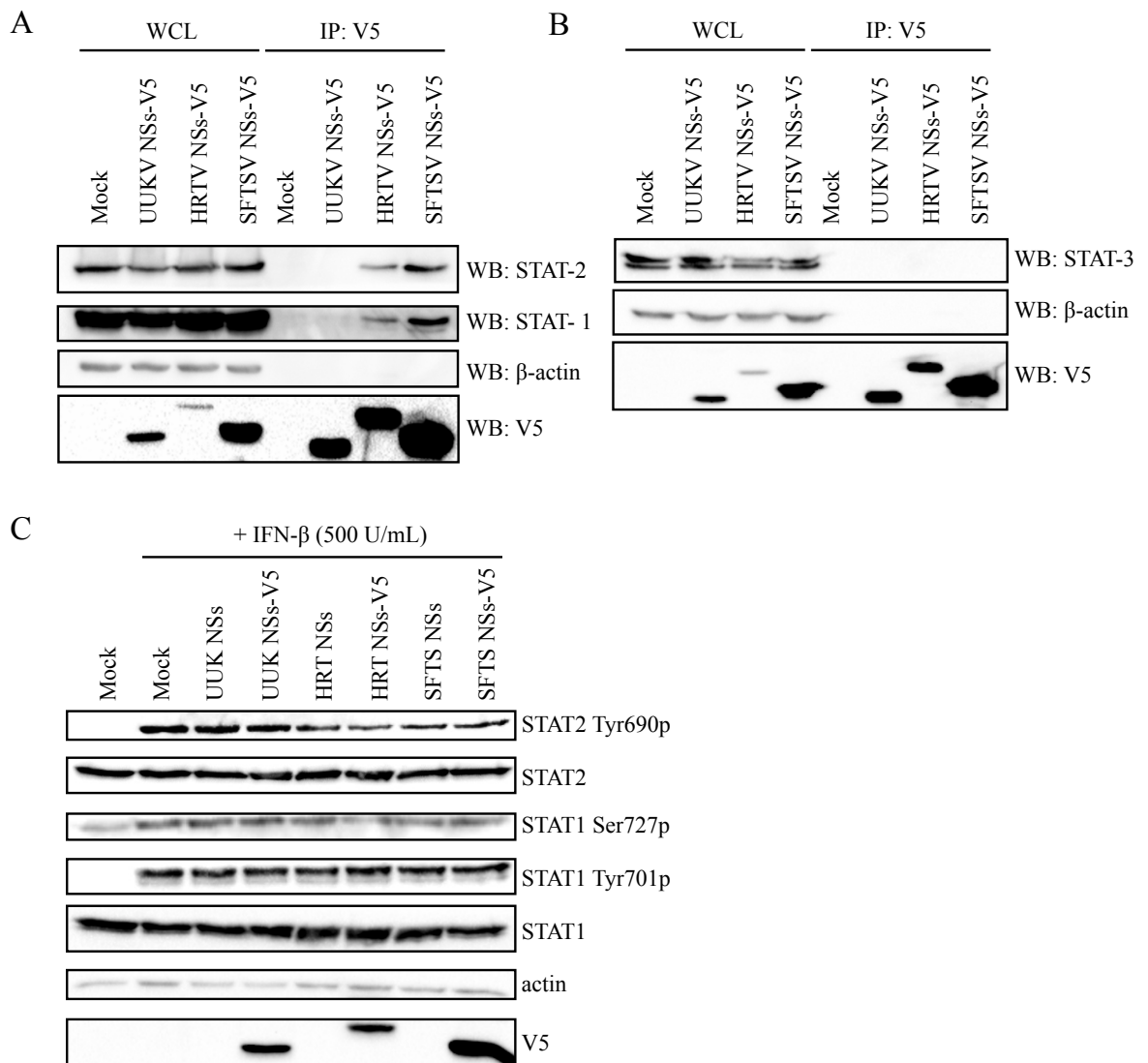


**Figure 7-10. Interaction between UUKV, HRTV or SFTSV NSs and STAT proteins.**

Cell lysates from HEK293T cells transiently expressing V5-tagged UUKV, HRTV or SFTSV NSs were immunoprecipitated with an anti-V5 antibody and analysed by western blot with STAT1 and STAT2 antibodies (A), or a STAT3 antibody (B). (C) Phosphorylation of STAT1 and STAT2 in HEK293T cells upon treatment with recombinant IFN- $\beta$ . HEK293T cells transiently expressing untagged or V5-tagged UUKV, HRTV or SFTSV NSs were treated with recombinant IFN- $\beta$  24 h post transfection. Upon 30 min of IFN- $\beta$  treatment, cell lysates were harvested and utilised for immunoblotting of STAT2, STAT2 phosphorylated at Tyr690, STAT1, STAT1 phosphorylated at Ser727 and Tyr701, actin and V5 with the appropriate antibodies. The results shown are representative of at least two experimental repeats. IP: immunoprecipitation, WB: Western blotting, WCL: whole cell lysate.

### ***7.3.7 The effect of HRTV and SFTSV NSs proteins on STAT1 and STAT2 nuclear translocation.***

In this section, the ability of HRTV and SFTSV NSs proteins to inhibit the IFN-induced nuclear translocation of STAT1 and STAT2 were compared. As HeLa cells have been previously utilised to visualise the sequestration of STAT1 and STAT2 into SFTSV NSs-formed IBs (Chaudhary *et al.*, 2015), and because this cell line was commonly used for similar studies in Prof Jin Dong-Yan's laboratory (University of Hong Kong, where these assays were carried out), the HeLa cell line was chosen for this part of the study. Briefly, HeLa cells transiently expressing V5-tagged HRTV or SFTSV NSs proteins were treated with recombinant IFN- $\beta$  for 30 min 24 h post transfection, prior to immunofluorescence using anti-V5 and anti- STAT1 or STAT2 antibodies. As expected, in untransfected cells STAT1 remained cytoplasmic (Figure 7-11 A), whereas nuclear translocation of STAT1 was observed following IFN- $\beta$  treatment (Figure 7-11 B). Although in cells transiently expressing SFTSV NSs STAT1 was sequestered into the characteristic IBs, its translocation to the nucleus as a result of IFN- $\beta$  stimulation was not completely inhibited, as nuclear STAT1 could also be detected (Figure 7-11 C). Expression of HRTV NSs did not result in an accumulation of STAT1 into IBs as noted for SFTSV NSs, but instead STAT1 appeared diffused throughout the cytoplasm, as well as in the nucleus (Figure 7-11 D). In contrast to STAT1, no nuclear translocation of STAT2 was observed following IFN- $\beta$  stimulation in cells transiently expressing HRTV or SFTSV NSs proteins (Figure 7-12 B-C). As observed with TBK1 (Figure 7-8 B) and STAT1 (Figure 7-11 C), STAT2 remained diffused in the cytoplasm in the presence of HRTV NSs, whereas a clear sequestration of STAT2 into IBs formed by SFTSV NSs was observed (Figure 7-12 B-C). Thus, these results indicate that the interaction between HRTV or SFTSV NSs proteins with STAT2 (but not STAT1) results in the efficient inhibition of IFN- $\beta$  induced STAT2 (but not STAT1) nuclear translocation.

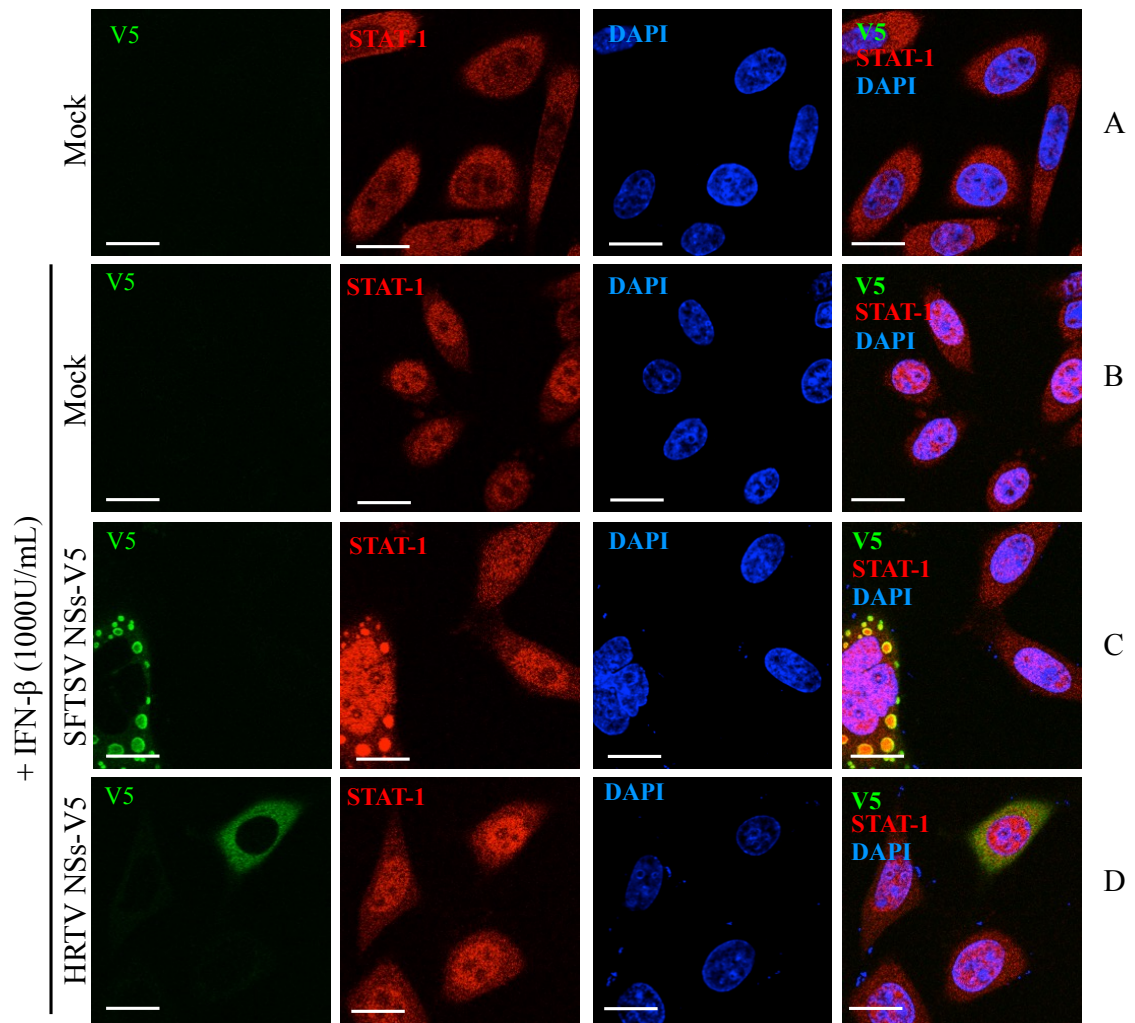


**Figure 7-11. Inhibition of IFN- $\beta$ -induced STAT1 nuclear translocation by HRTV and SFTSV NSs proteins.**

Mock HeLa cells (A-B) or HeLa cells transiently expressing V5-tagged SFTSV (C) or HRTV NSs (D) proteins were treated with IFN- $\beta$  (1000 U/mL) for 30 min, or left untreated 24 h post transfection. Upon IFN treatment, the cells were fixed, permeabilized and probed with V5 and STAT1 antibodies. The subcellular localization of endogenous STAT1 (red), V5-tagged NSs proteins (green) and DAPI-stained nuclei (blue) was analysed by confocal microscopy. Scale bars indicate 20  $\mu$ m. The results shown are representative of at least two experimental repeats.

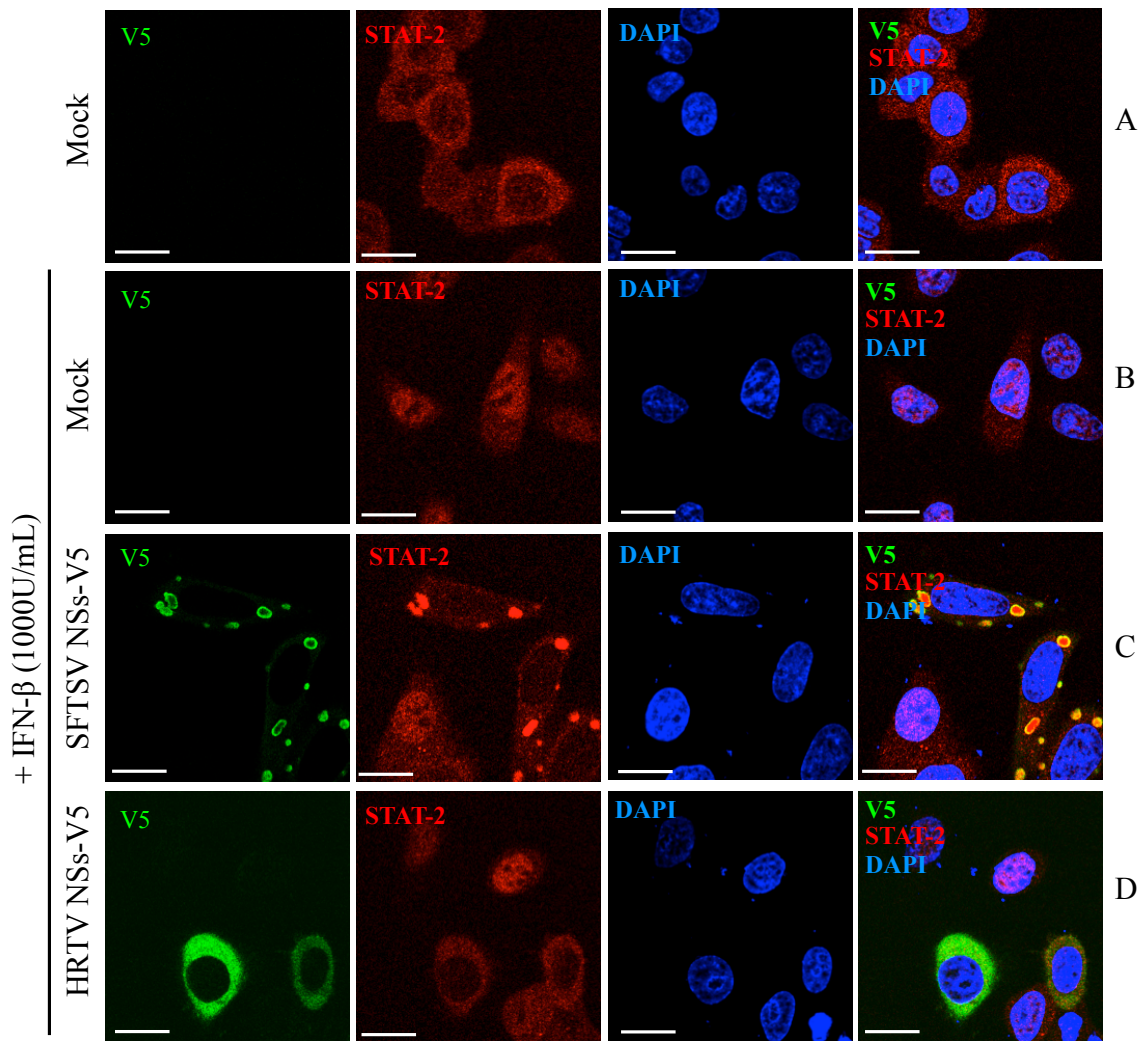


**Figure 7-12. Inhibition of IFN- $\beta$ -induced STAT2 nuclear translocation by HRTV and SFTSV NSs proteins.**

Mock HeLa cells (A-B) or HeLa cells transiently expressing V5-tagged SFTSV (C) or HRTV NSs (D) proteins were treated with IFN- $\beta$  (1000 U/mL) for 30 min, or left untreated 24 h post transfection. Upon IFN treatment, the cells were fixed, permeabilized and probed with V5 and STAT2 antibodies. The subcellular localization of endogenous STAT2 (red), V5-tagged NSs proteins (green) and DAPI-stained nuclei (blue) was analysed by confocal microscopy. Scale bars indicate 20  $\mu$ m. The results shown are representative of at least two experimental repeats.

The results in chapter 6 showed that none of the tick-borne phlebovirus NSs proteins concerning this study are able to inhibit type II IFN signalling (Figure 6-7 A and B). Type II IFN signalling is majorly mediated by STAT1 homodimers. Thus, I aimed to investigate whether the lack of inhibitory activity of HRTV and SFTSV NSs proteins on type II IFN signalling was due to their inability to hinder the nuclear translocation of STAT1 following IFN- $\gamma$  treatment. In mock-transfected, mock-treated cells STAT1 remained cytoplasmic (Figure 7-13 A), and IFN- $\gamma$  stimulation resulted in its nuclear translocation (Figure 7-13 B). As observed upon IFN- $\beta$  stimulation, nuclear translocation of STAT1 was also detected in cells transiently expressing V5-tagged HRTV or SFTSV NSs proteins when stimulated with IFN- $\gamma$  (Figure 7-13 C and D). Additionally, some STAT1 was sequestered in SFTSV NSs-formed IBs, which were absent in HRTV NSs-expressing cells (Figure 7-13 C and D). Taken together, these findings suggest that the weak interaction of HRTV or SFTSV NSs proteins with STAT1 (Figure 7-10 A) does not lead to the inhibition of type II IFN signalling (described in Chapter 6, Section 6.3.4, Figure 6-7). Presumably, this is due to their inability to efficiently block the translocation of STAT1 homodimers to the nucleus, the major route of IFN- $\gamma$  signalling utilized to activate the transcription of GAS elements.

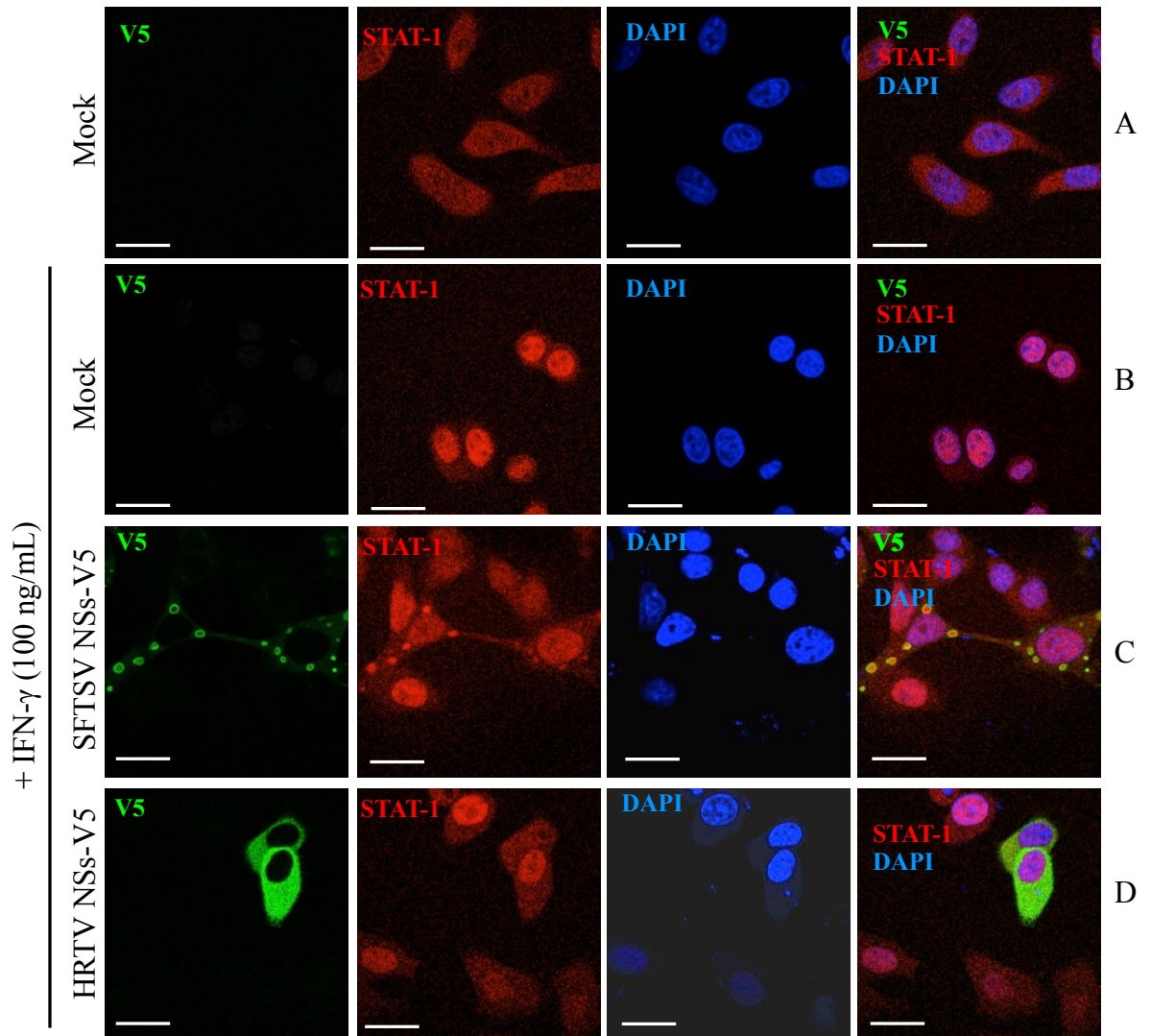


**Figure 7-13. Inhibition of IFN- $\gamma$ -induced STAT1 nuclear translocation by HRTV and SFTSV NSs proteins.**

Mock HeLa cells (A-B) HeLa cells transiently expressing V5-tagged SFTSV (C) or HRTV (D) NSs proteins were treated with IFN- $\gamma$  (100 ng) for 30 min, or left untreated 24 h post transfection. Upon IFN treatment, the cells were fixed, permeabilized and probed with V5 and STAT1 antibodies. The subcellular localization of endogenous STAT1 (red), V5-tagged NSs proteins (green) and DAPI-stained nuclei (blue) was analysed by confocal microscopy. Scale bars indicate 20  $\mu$ m. The results shown are representative of at least two experimental repeats.

## **7.4 Discussion**

In this chapter, a comparative study was carried out to characterize the molecular mechanisms employed by tick-borne phlebovirus NSs proteins to block the human IFN response. The results in chapter 6 indicated that UUKV, HRTV and SFTSV NSs proteins are able to suppress IFN induction. However, HRTV and SFTSV NSs, but not UUKV NSs, are capable of blocking type I IFN signalling. In addition, none of the tick-borne phlebovirus NSs proteins relevant to this study were able to suppress type II IFN signalling. Understanding the approaches employed by UUKV and HRTV NSs proteins to hinder IFN induction and/or signalling serves to expand our knowledge on the viral immune evasion strategies utilised by emerging tick-borne phleboviruses.

The NSs proteins of bunyaviruses show notoriously low conservation at the amino acid level in comparison to other viral proteins (Elliott, 2014; Yu *et al.*, 2011). In fact, among the NSs proteins relevant to this study, UUKV NSs shares only 23% amino acid sequence identity with HRTV and SFTSV NSs proteins (Table 6-1). The amino acid sequence identity of the NSs proteins belonging to the more closely related HRTV and SFTSV is higher (62.76%) (Table 6-1). However, the higher conservation between the latter two is not reflected in their subcellular localization. In UUKV-infected cells and cells expressing only V5-tagged UUKV NSs in the absence of other viral proteins, UUKV NSs showed small, punctate cytoplasmic staining, which is in agreement with previous studies (Simons *et al.*, 1992) (Figure 7-2 A). While SFTSV NSs formed distinct round, cytoplasmic IBs (Ning *et al.*, 2015; 2014; Santiago *et al.*, 2014), the subcellular localization of HRTV NSs resembled more closely that of UUKV NSs, exhibiting diffused cytoplasmic distribution (7-2 B and C). A PxxP motif located at the N terminus (amino acid residues 66-69) of SFTSV NSs was suggested to be required for the formation of SFTSV NSs-induced IBs, and for its IFN antagonistic function (Ning *et al.*, 2014). In fact, simultaneous substitution of SFTSV NSs P66 and P69 resulted in the cytoplasmic localization of SFTSV NSs and the loss of its IFN inhibitory activity in transient transfection assays. Curiously, the PxxP motif was conserved in the HRTV NSs amino acid sequence (Figure 7-1) despite the diffused cytoplasmic distribution of HRTV NSs. It should be considered that prolines are unique amino acids with a cyclic structure that gives the amino acid conformational rigidity. The biochemical properties of proline residues play a key role in determining a protein's secondary and tertiary structure, commonly introducing kinks and turns. Therefore, it is possible that the mere presence of the PxxP motif in SFTSV NSs may be

required but not sufficient for IB formation, as HRTV NSs is unable to form IBs despite the conservation of the PxxP motif. However, this motif may be one of the contributing factors in the overall protein structure required for IB formation for SFTSV NSs. Determining the structure of these two NSs proteins could provide insights into the relevance of the PxxP motif in the formation of SFTSV NSs IBs in comparison to HRTV NSs.

Collectively, given that the IBs formed by SFTSV NSs play a key role in its IFN antagonist activity (Ning *et al.*, 2014; Santiago *et al.*, 2014), the low amino acid sequence identity and the divergent subcellular localization between UUKV or HRTV NSs and that of SFTSV NSs led me to hypothesize that these proteins may have acquired disparate strategies to that of SFTSV NSs to circumvent the IFN response. The findings presented in this chapter provide an insight into the diverse strategies tick-borne phleboviruses utilise to suppress IFN induction and IFN signalling.

Firstly, transient transfection assays indicated that UUKV NSs weakly inhibits MAVS-induced IFN- $\beta$  promoter activation (Figure 7-5 B). These results correlate with the interaction detected in co-IP experiments between UUKV NSs and MAVS in the context of overexpression assays (Figures 7-6 A and 7-7 B) and virus infection (Figure 7-7 A). In addition, this interaction was examined using confocal microscopy, which revealed that some of the punctate cytoplasmic UUKV NSs staining co-localised with the speckle-like structures formed by MAVS (Figure 7-8). These findings suggest that the weak IFN antagonistic activity of UUKV NSs at the level of IFN induction (described in Chapter 6) occurs through a weak interaction with MAVS. TOSV NSs protein, similarly to UUKV NSs, also inhibits the induction of type I IFN at early stages of the IFN induction pathway, but targets RIG-I for proteasomal degradation (Gori-Savellini *et al.*, 2013). As it stands, targeting MAVS is a novel strategy described for phlebovirus NSs proteins to block the IFN response. Other viruses such as Influenza A virus can also block MAVS-mediated IFN induction. Specifically, the Influenza A virus PB1-F2 protein inhibits IFN synthesis by binding to MAVS and altering the mitochondrial membrane potential (Varga *et al.*, 2011; 2012), which is known to mediate IFN induction through the rearrangement of MAVS (Koshiba *et al.*, 2011). It would be interesting to investigate whether UUKV NSs utilizes similar mechanisms to that of Influenza virus PB1-F2 protein to block MAVS-mediated IFN induction.

The data presented herein also indicates that the IFN induction and signalling interacting partners of HRTV NSs and SFTSV NSs are conserved, despite exhibiting contrasting subcellular localization and sharing 63% amino acid identity. Co-IP studies demonstrated that, similarly to SFTSV NSs, HRTV NSs interacts with TBK1 in overexpression assays (Figure 7-6 B) as well as in the context of a virus infection (Figure 7-9 A). These results correlate with the inhibition of the RIG-I N, MAVS, and TBK1-induced IFN- $\beta$  promoter activation by HRTV NSs (Figure 7-5). While in the presence of SFTSV NSs TBK1 was clearly sequestered into NSs-formed IBs, TBK1 exhibited diffused cytoplasmic staining in the presence of HRTV NSs, but co-localised with HRTV NSs signal (Figure 7-9 B). Taken together, these findings suggest that some key characteristics between HRTV and SFTSV NSs are conserved, such as their ability to interact with TBK1. However, the strategy used by HRTV NSs to exert its antagonistic function is not identical to that of SFTSV NSs, which sequesters TBK1 into NSs-formed IBs. It is possible that HRTV NSs prevents the activation of TBK1 by hindering its phosphorylation by IKK $\beta$ , *trans*-autophosphorylation or K63-linked polyubiquitination, all of which have been proposed to contribute to TBK1 activation (Kishore *et al.*, 2002; Ma *et al.*, 2012; Tu *et al.*, 2013). Whether any of these mechanisms are utilized by HRTV NSs to inhibit TBK1-mediated signalling pathways remains to be elucidated.

In addition to IFN induction, the findings in this chapter provide insights into the mechanism of IFN signalling inhibition by HRTV NSs. Co-IP experiments showed that STAT1 and STAT2, but not STAT3 could be immunoprecipitated with HRTV and SFTSV NSs proteins (Figure 7-10 A and B). This finding suggested that the IFN signalling inhibitory activity of HRTV NSs protein is mediated by its interactions with STAT1 and STAT2, as it has already been demonstrated for SFTSV NSs (Chaudhary *et al.*, 2015; Ning *et al.*, 2015). STAT3 is known to play a role in regulating inflammatory responses by regulating T cell proliferation by preventing apoptosis (Takeda *et al.*, 1998), and CD4<sup>+</sup> and CD8<sup>+</sup> T cell survival and differentiation (Oh *et al.*, 2011; Yu *et al.*, 2013). Therefore, the lack of interaction between the NSs proteins and STAT3 (Figure 7-10 B) may be a contributing factor to the strong inflammatory responses that could play a role in HRTV or SFTSV –infected patients.

Importantly, a stronger interaction between HRTV or SFTSV NSs and STAT2 than that between the NSs proteins and STAT1 was observed in co-IP assays (Figure 7-10 A), which could explain the ability of these NSs proteins to block type I but not type II IFN signalling. While type I IFN signalling is mediated majorly through the activation of ISRE

elements by STAT1-STAT2 heterodimers, type II IFN signalling is mediated via the activation of GAS elements by STAT1 homodimers. Therefore, the interaction of HRTV and SFTSV NSs proteins with STAT2 may result in inhibition of type I IFN signalling, while the weak interaction with STAT1 may explain the lack of type II IFN signalling inhibitory activity by the NSs proteins. However, it remains a possibility that, in the presence of HRTV or SFTSV NSs proteins, STAT1-STAT2 heterodimers are precipitated, and therefore the STAT1 detected in the IP eluates is not a result of a direct interaction with the NSs proteins, but rather an indirect interaction mediated via an interaction with STAT2 and pulldown of STAT1-STAT2 heterodimers.

Additionally, the results described in this chapter show that the IFN- $\beta$ -induced STAT2 (but not STAT1) phosphorylation appears to be reduced in the presence of HRTV and SFTSV NSs proteins (Figure 7-10 C). These results are in agreement with previous reports which showed that SFTSV inhibits STAT2, but not STAT1 phosphorylation (Ning *et al.*, 2015). The ability of HRTV NSs to hamper the IFN-induced nuclear translocation of STAT1 and STAT2 in a similar manner to SFTSV NSs was also examined. In the presence of SFTSV NSs, both STAT1 and STAT2 were sequestered into SFTSV NSs-induced IBs. However, while no IFN- $\beta$ -induced nuclear translocation of STAT2 was detected in cells expressing SFTSV NSs, the IFN- $\beta$  and IFN- $\gamma$  -induced nuclear translocation of STAT1 was not efficiently inhibited (Figures 7-11, 7-12, and 7-13). Similarly, only the IFN- $\beta$ -induced nuclear translocation of STAT2, but not the IFN- $\beta$  or IFN- $\gamma$  -induced nuclear translocation of STAT1 was efficiently inhibited in the presence of HRTV NSs (Figures 7-11, 7-12, and 7-13). The ability of both NSs proteins to block IFN-induced STAT2 nuclear translocation more efficiently than STAT1 nuclear translocation is consistent with the finding that the NSs proteins can partially inhibit STAT2 but not STAT1 phosphorylation (Figure 7-10 C). Perhaps the ability of STAT1 to translocate to the nucleus upon IFN stimulation in the presence of HRTV or SFTSV NSs proteins (in contrast to STAT2) is a result of the weak or indirect interaction between STAT1 and the NSs proteins, as noted above. Additionally, it has also been shown that STAT1-STAT1 homodimers can also form and play a role in the transcriptional activation of ISGs during type I IFN signalling, albeit a less critical role than STAT1-STAT2 heterodimers (Li *et al.*, 1996; Ramana *et al.*, 2000). Therefore, if the interaction between the NSs proteins and STAT1 is indirect (facilitated by the interaction of the NSs proteins with STAT2 in STAT1-STAT2 heterodimers), the detection of nuclear STAT1 may result due to the inability of the NSs proteins to directly interact with STAT1 and inhibit the nuclear translocation of STAT1 homodimers. On the other hand, the

cytoplasmic localization of STAT1 may be a result of the ability of the NSs proteins to interact with and efficiently inhibit the nuclear translocation of STAT1-STAT2 heterodimers.

In comparison to SFTSV NSs, HRTV NSs did not result in the sequestration of STAT1 or STAT2 to IBs, but instead the proteins remained diffused in the cytoplasm (Figures 7-11, 7-12 and 7-13). Thus, in contrast to SFTSV NSs, STAT1 and STAT2 are not sequestered into IBs by HRTV NSs, but instead simply an interaction between STAT2 and HRTV NSs may inhibit STAT2 phosphorylation and thus the translocation of STAT1-STAT2 heterodimers to the nucleus, consequently resulting in abrogation of type I IFN signalling.

Taken together, the findings presented in this chapter expand our knowledge of the plethora of immune evasion strategies that tick-borne phleboviruses have acquired to suppress the IFN response. The proposed model of the tick-borne phlebovirus NSs antagonist role is summarised in Figure 7-14. Whereas UUKV NSs inhibits IFN induction through a direct interaction with MAVS, the NSs protein of HRTV and SFTSV target the immunomodulatory kinase TBK1 to suppress the production of IFN. HRTV and SFTSV NSs proteins have an additional IFN signalling inhibitory role, which occurs mainly in a STAT2-dependent manner. As it stands, the weak or indirect interaction between HRTV or SFTSV NSs and STAT1, in addition to the direct interaction with STAT2 may play a role in the differential regulation of type I and type II IFN signalling: it is possible that the NSs proteins inhibit the STAT1-STAT2 heterodimer-dependent activation of the ISRE promoter through a direct interaction with STAT2, but not that of the STAT1 homodimer-dependent activation of the GAS promoter. However, further experiments such as chromatin immunoprecipitation studies are required to confirm this hypothesis.

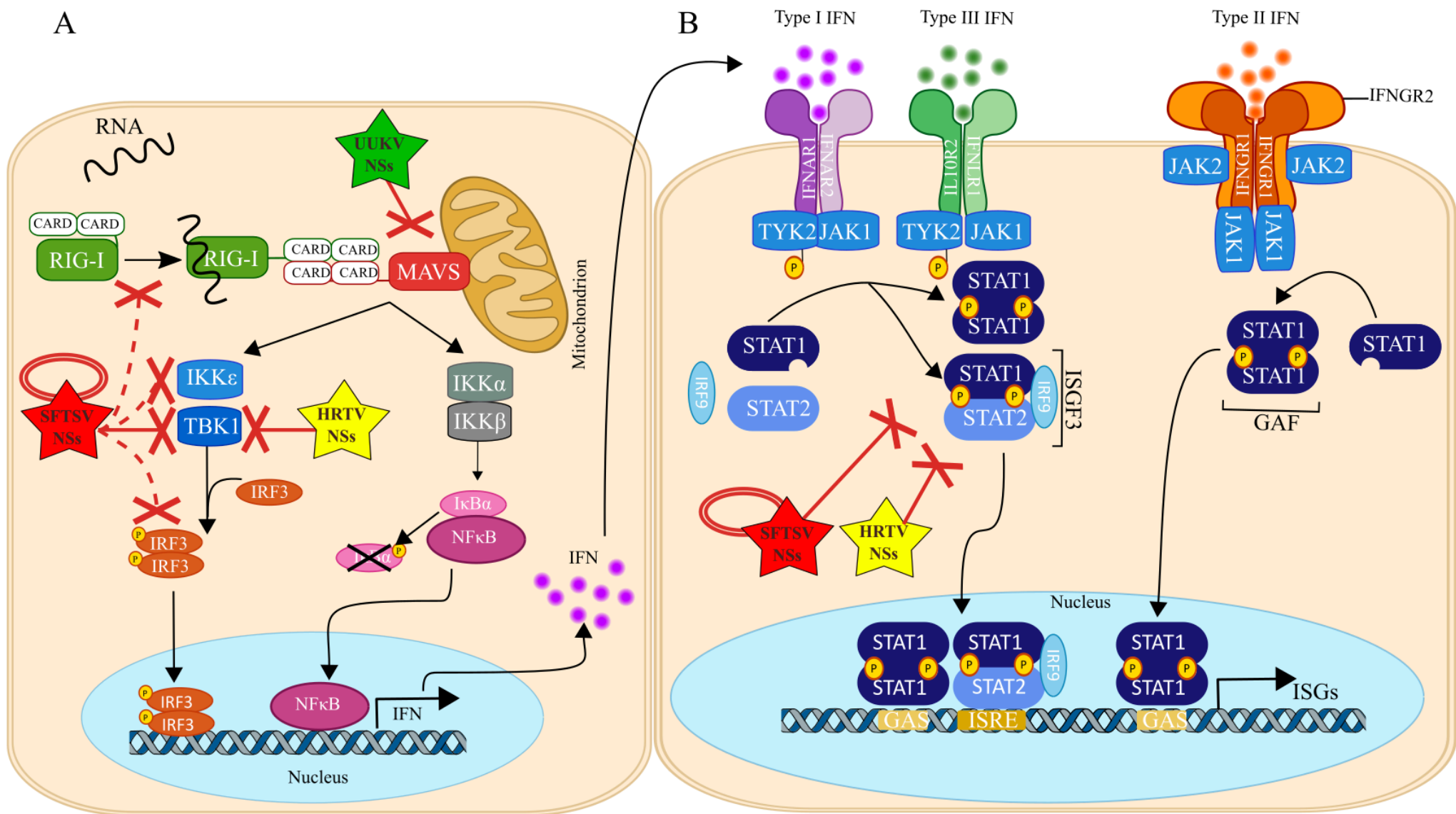


**Figure 7-14. Schematic summary of the mechanisms utilized by tick-borne phlebovirus NSs proteins to inhibit the canonical IFN induction and signalling pathways.**

(A) Following bunyavirus infection, the generation of single stranded RNA (ssRNA) with uncapped 5' triphosphate ends during uncoating, transcription or replication results in ssRNA binding to the RNA helicase RIG-I. RIG-I is in turn activated and exposure of its associated CARD domains allows the recruitment of the adaptor MAVS through CARD-CARD interactions. Activation of MAVS leads to the subsequent activation of kinases TBK1 and/or IKK $\epsilon$ , which concomitantly phosphorylate IRF-3 or IRF-7 at specific serine residues. Phosphorylation of IRF-3 or IRF-7 leads to their dimerization and translocation to the nucleus, where they ultimately stimulate transcription of genes under the control of the IFN  $\alpha/\beta$  promoter, resulting in the secretion of IFN  $\alpha/\beta$ . The kinase IKK $\beta$  can also be ultimately activated in the signalling pathway, which leads to the phosphorylation of I $\kappa$ B. I $\kappa$ B phosphorylation results in its ubiquitination and proteasomal degradation, freeing NF- $\kappa$ B for translocation to the nucleus, where it can also assemble on the IFN  $\alpha/\beta$  promoter. (B) Signal transduction of type I, II and III IFNs initiates through the binding of secreted IFN to the respective IFN receptors and the activation of multiple downstream signalling pathways. Type I and type III IFN signalling pathways are majorly mediated via STAT1-STAT2 heterodimers. Receptor-associated kinases JAK1 and TYK2 become activated and phosphorylate STAT1 and STAT2, respectively, on specific tyrosine and/or serine residues. Phosphorylated STATs can heterodimerise and recruit IRF9 for the assembly of the heterotrimer complex ISGF3. ISGF3 translocates to the nucleus and binds to ISRE, leading to the induction of many IFN stimulated genes (ISG). Type III IFN signalling is more commonly associated with signalling by homodimerization of STAT1, which can translocate to the nucleus and activate GAS promoters, also initiating ISG transcription. Tick-borne phlebovirus NSs proteins have evolved a number of countermeasures to block the IFN pathway. SFTSV NSs directly interacts with and sequesters TBK1, and STAT2 into inclusion bodies, in order to spatially isolate these elements. Additionally, through its interaction with TBK1 and STAT2, SFTSV NSs can also indirectly sequester IKK $\epsilon$ , IRF-3 and STAT1 into the inclusion bodies. An interaction between SFTSV NSs and TRIM-25 also facilitates the spatial isolation of RIG-I, in an indirect manner. HRTV NSs can also block IFN induction through a direct interaction with TBK1 and IFN signalling by a direct interaction with STAT2. However, as HRTV NSs does not form inclusion bodies as SFTSV NSs does, its mechanism of antagonism is different to that of SFTSV NSs. UUKV NSs block IFN induction only, targeting MAVS. For references, see text. Dashed red lines indicate indirect interactions. Solid red lines indicate direct interactions. CARD: caspase recruitment domain; GAS:  $\gamma$ -activated sequence; IFNAR: interferon- $\alpha/\beta$  receptor; IKK $\epsilon$ : I $\kappa$ B kinase- $\epsilon$ ; IRF: IFN-regulatory factor; ISGF3: IFN-stimulated gene factor 3; ISGs: IFN-stimulated genes; ISRE: IFN-stimulated response element; JAK: janus kinase; MAVS: mitochondrial antiviral signalling protein; RIG-I: retinoic acid-inducible gene I; STAT: signal transducer and activator of transcription; TBK1: TANK-binding kinase 1; TYK: tyrosine kinase.

## **7.5 Summary**

- Although HRTV NSs is more highly conserved in amino acid sequence with SFTSV NSs (sharing 63% amino acid identity) than with UUKV NSs (sharing 23% amino acid identity), the subcellular localization of HRTV NSs in infected cells and in cells transiently expressing HRTV NSs resembles that of UUKV NSs more closely, displaying diffused cytoplasmic staining. This is in comparison to SFTSV NSs, which forms characteristic round, cytoplasmic IBs, which are important for the sequestration of effectors of the innate immune signalling pathways
- While UUKV NSs inhibited MAVS-induced IFN- $\beta$  reporter activity in transient transfection assays, both HRTV and SFTSV NSs proteins blocked RIG-I N, MAVS and TBK1-induced IFN- $\beta$  reporter activity.
- UUKV NSs is able to weakly interact with MAVS in overexpression assays and in the context of a virus infection. Small, punctate structures formed by UUKV NSs partially co-localized with characteristic speckles formed by MAVS. The weak interaction between UUKV NSs and MAVS may serve as an explanation for the weak IFN antagonistic activity of UUKV NSs.
- Similar to the NSs protein of SFTSV, HRTV NSs can interact with TBK1 to inhibit IFN induction. However, while the mechanism of inhibition by SFTSV NSs occurs through the spatial isolation of TBK1 into IBs, these structures are not formed by HRTV NSs. Instead, in the presence of HRTV NSs TBK1 remains diffused in the cytoplasm, but colocalises with HRTV NSs signal.
- HRTV and SFTSV NSs proteins can interact with STAT1 and STAT2, but not STAT3. Co-IP experiments showed a stronger interaction between the NSs proteins and STAT2 than with STAT1, suggesting that the interaction of the NSs proteins with STAT1 may be indirect, facilitated by their direct interaction with STAT2. This observation was also reflected in the ability of the NSs proteins to efficiently block the nuclear translocation of STAT2 upon IFN- $\beta$  treatment, but not that of STAT1 following IFN- $\beta$  or IFN- $\gamma$  treatment. These results may indicate why HRTV and SFTSV NSs proteins are able to inhibit type I, but not type II IFN signalling.

## 8 Development of a HRTV minigenome system to assess tick-borne phlebovirus genome reassortment

### 8.1 Introduction

Like other bunyaviruses, tick-borne phleboviruses have a tri-segmented genome of negative- or ambi-sense. Their S segment utilizes an ambi-sense coding strategy, where the nucleocapsid protein N is translated from subgenomic mRNA transcribed from the genomic RNA, and non-structural protein NSs is translated from subgenomic mRNA transcribed from antigenomic RNA (Figure 1-4 B) (Bouloy and Weber, 2010). The M and L segments utilize a negative-sense coding strategy. While the M segment encodes the glycoprotein precursor, which is cleaved for the generation of the glycoproteins Gn and Gc, the L segment encodes the viral RNA-dependent RNA polymerase (RdRp, or L protein). Because of the segmented nature of these viruses, if closely related viruses co-infect the same host or vector cell, it is possible that RNA segments from either of the parental viruses are incorporated into progeny virions, and thus the genome of the reassortant progeny virions will be composed of a mixture of RNA segments belonging to the parental viruses.

This genetic exchange phenomenon, known as genome reassortment, plays an important role in the evolution of segmented viruses. Genome reassortment can accelerate the rate of acquisition of markers that can alter virus phenotype, tropism, transmissibility, and host range, as well as introducing new immunogenic characteristics that could enable reassortant viruses to escape immune surveillance (Briese *et al.*, 2013; Elliott, 2014).

Within the *Phlebovirus* genus, genome analyses have suggested that a number of mosquito-borne viruses are reassortants of existing or unidentified viruses (Bird *et al.*, 2007; Collao *et al.*, 2010; Palacios *et al.*, 2011). Homologous recombination of the L segment of the recently emerged tick-borne Severe fever with thrombocytopenia syndrome virus (SFTSV) was suggested to play a role in the evolution of this virus (Lam *et al.*, 2013). Homologous recombination is a different form of genetic reassortment, driven by a template switch mechanism in which the replicating RdRp can dissociate from one genome and continue replication using the genome of a co-infecting virus as the template, resulting in a new mosaic-like genome (Vijaykrishna *et al.*, 2015).

Little is known about the possibility of reassortment between tick-borne phleboviruses. In addition, no experimental evidence exists to support the above-mentioned phylogenetic studies that suggest that certain members of the *Phlebovirus* genus are reassortant progeny. The availability of phlebovirus reverse genetics systems could aid to understand the potential of genome reassortment under experimental conditions, by assessing the compatibility of viral proteins of one virus with another to form viable progeny. So far, reverse genetics systems for the tick-borne phleboviruses Uukuniemi virus (UUKV) (described in Chapter 5), and SFTSV (Brennan *et al.*, 2015) have been described. Apart from UUKV and SFTSV, Heartland virus (HRTV) is another tick-borne phlebovirus available in our laboratory. HRTV is closely related to SFTSV but was isolated in the United States and was associated with two deaths (McMullan *et al.*, 2012; Muehlenbachs *et al.*, 2014; Williams, 2014). The availability of a reverse genetics system for HRTV could provide an additional tool to investigate the molecular biology of tick-borne phleboviruses. Additionally, in conjunction with the reverse genetics systems developed for UUKV and SFTSV, the ability of tick-borne phlebovirus proteins to replicate, transcribe and package the genome of related viruses could be tested. These tools could help to understand whether genome reassortment acts as a force to drive the evolution of these emerging viruses, and to predict possible outcomes of reassortant viruses in nature under an experimental setting. Such studies could enable better preparedness for the emergence of new reassortant tick-borne phleboviruses with the timely development of vaccines.

## **8.2 Aims**

The aims of this chapter were to: (i) sequence the HRTV laboratory stock, (ii) develop a HRTV minigenome system, (iii) attempt to rescue infectious HRTV entirely from cDNA clones, and (iv) utilise the HRTV minigenome in combination with the minigenomes available for other tick borne phleboviruses. The aim of the latter experiment was to examine the compatibility of the N and L proteins of a particular tick-borne phlebovirus with the UTRs from a different tick-borne phlebovirus at the molecular level, in order to assess the potential for reassortment to take place.

## 8.3 Results

### 8.3.1 Sequencing of the laboratory HRTV stock

The HRTV strain used in this study was a patient-derived isolate (MO-4), provided by Dr Robert Tesh (World Reference Center for Emerging Viruses and Arboviruses, Galveston, TX). The patient, referred to as ‘patient two’ in (McMullan *et al.*, 2012), was a 67 year old man from northern Missouri who received approximately 20 daily tick bites for a period of two weeks and was hospitalised for twelve days, presenting with fatigue, myalgia, severe thrombocytopenia and leukopenia. The genome of the patient-derived HRTV was sequenced and published (McMullan *et al.*, 2012). The working stock of HRTV available for this project was generated by Dr Benjamin Brennan (MRC-Centre for Virus Research, University of Glasgow, UK), by passaging HRTV at a low MOI (0.001 PFU/cell) in Vero E6 cells, and harvesting the medium 7 days p.i. (personal communication).

When developing a reverse genetics system for a particular virus, it is important to determine the correct full-genome sequence of that virus in order to generate cDNA clones that reflect the virus’ genome (Acrani *et al.*, 2015; Brennan *et al.*, 2015). In order to determine whether the HRTV stock available in our laboratory had any cell culture adapted mutations, and to confirm its genome sequence in comparison to the published sequence, full genome sequencing of the HRTV laboratory stock was carried out. Briefly, total cellular RNA from duplicate HRTV-infected Vero E6 cells (MOI 5 PFU/cell) was extracted, and used for RT-PCR to sequence the entire S, M and L segments, except their termini. To sequence the 3’ and 5’ termini of all segments, 3’ rapid amplification of cDNA ends (RACE) analysis was performed on the extracted RNA (which contained genomic and antigenomic segments) using sequence-specific primers. The amplified products were sequenced using conventional Sanger sequencing and the results compared to the database entries with GenBank accession numbers JX005843, JX005845 and JX005847, for the HRTV S, M and L segments, respectively.

In total, 3 mutations in the HRTV laboratory stock genome were identified (Figure 8-1). One mutation was present in the genomic-sense 5’ UTR of the S segment, at position 1751 (A→G). The other two mutations, found in the ORF of the M and L segments resulted in amino acid changes. In the M segment, a C→U mutation at the nucleotide position 1764 (genomic sense) results in a His→Tyr amino acid change at the N terminus of Gc. In the L segment, the A→U mutation at nucleotide position 3309 (genomic sense) results in a

Tyr→Phe amino acid change in the viral polymerase. Of note, while in the S and M segment the mutations were identified as clear peaks in the sequencing chromatogram corresponding to the nucleotide change, two peaks were observed in the L segment A3309U mutation, with the more predominant peak corresponding to T (U in RNA) signal, and the smaller peak corresponding to A signal (Figure 8-1), suggesting a mixed population of the virus genome. The mutations identified from duplicate infections were confirmed using primers annealing to the complementary strand for all samples.

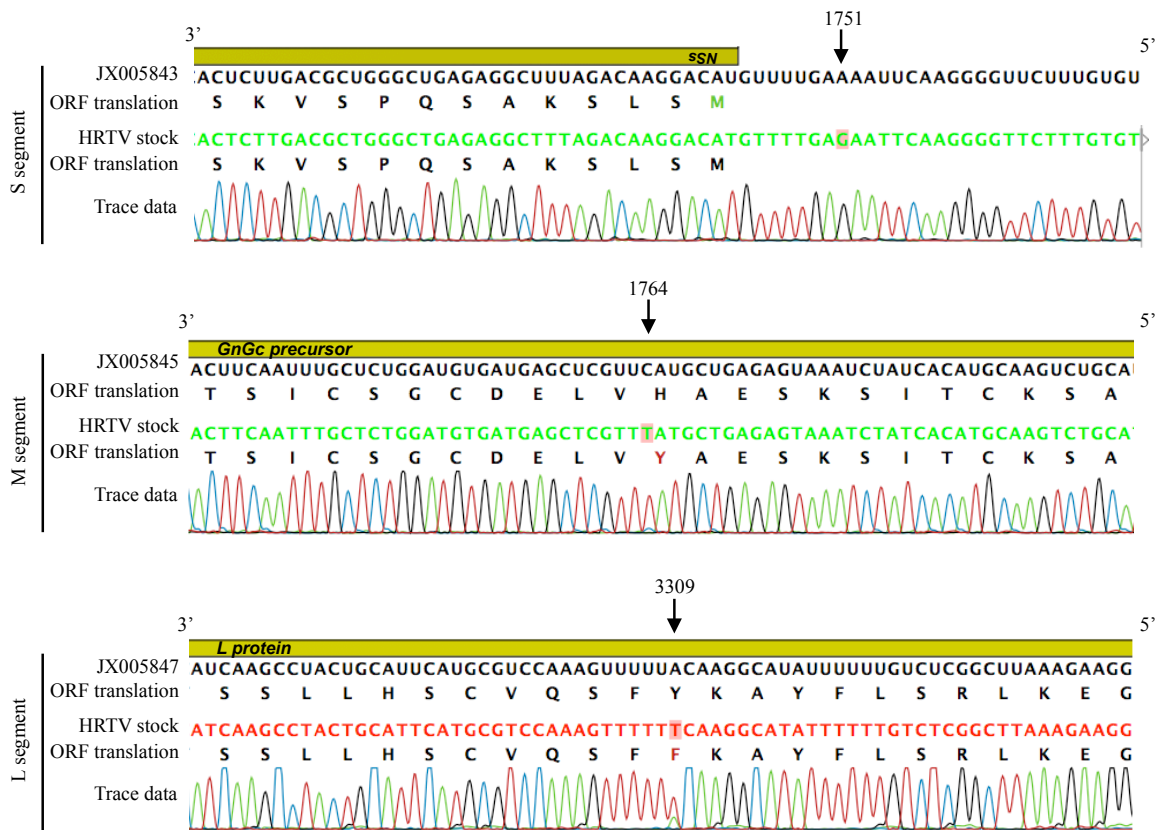


**Figure 8-1. Differences in the sequence of the HRTV laboratory stock compared to the published HRTV sequence.**

Alignment showing the chromatograph of S, M and L segment RACE and RT-PCR cDNA sequencing results of the HRTV laboratory stock, in comparison to RNA published sequences (GenBank accession numbers: S: JX005843; M: JX005845; L: JX005847). Arrows denote identified mutations (highlighted) and their nucleotide position. Sequences are shown in the genomic sense, and the ORF translation indicated below the DNA or RNA sequences. Adenine (A): green; Thymine (T): red; Cytosine (C): Blue; Guanine (G): Black.

### 8.3.2 Development of a minigenome system for HRTV

Next, a minigenome system for HRTV was developed to: (i) enable the basic molecular characterization of the HRTV UTR sequences as promoters of replication and transcription, and to (ii) assess the functionality of the HRTV N and L proteins. As described in chapter 5, the minigenome system of bunyaviruses comprises an analogue of the virus genome under the control of a T7 RNAP promoter, in which a reporter gene (such as *Renilla*) in the negative sense replaces the ORF of a particular segment such that it is flanked by the viral 3' and 5' UTRs. In this way, transcription of a genome analogue by T7 RNAP and co-expression of viral N and L proteins enables the subsequent formation of RNP complexes that, if functional, lead to reporter gene activity.

T7 RNAP promoter-driven minigenome plasmids for the HRTV S, M and L segments were generated based on the published HRTV sequence, and named pT7HRTSren(+), pT7HRTMren(-) and pT7HRTLren(-) respectively. The templates used for generating the HRTV minigenome clones were kindly provided by Dr Benjamin Brennan (MRC Centre for Virus Research, University of Glasgow), and involved HRTV rescue plasmids in which the full-length antigenomic-sense cDNA copies of the published HRTV S, M and L RNA segment sequences were cloned into pTVT7 (0,0) (Johnson *et al.*, 2000) (pT7HRTS(+), pT7HRTM(+) and pT7HRTL(+), respectively). The HRTV minigenome clones were generated as described in chapter 5 (section 5.3.2) for UUKV, using restriction-free cloning. Briefly, the viral coding sequence in pT7HRTM(+) and pT7HRTL(+) was replaced by that of humanised *Renilla* (hereafter referred to as *Renilla*), in the same (positive) sense. Next, the cassette containing the *Renilla* ORF flanked by the viral UTRs was amplified for its inversion in pTVT7 (0,0), such that the transcripts generated by the T7RNAP would be in the viral genomic sense. Therefore, pT7HRTMren(-) and pT7HRTLren(-) constructs contain the *Renilla* ORF sequence in the negative sense, flanked by the viral UTR in the genomic sense. On the other hand, pT7HRTSren(+) was generated by replacing the NSs ORF in pT7HRTS(+), with *Renilla*, in the same (negative) orientation. Of note, whereas in the plasmids pT7HRTMren(-) and pT7HRTLren(-) the minigenome analogues are encoded in the genomic sense, the minigenome analogue in pT7HRTS(+) is encoded in the antigenomic sense. Therefore, in the M and L segment-based minigenomes, T7 RNAP generates genomic sense RNA that can be encapsidated by the N protein, and together with the L protein RNPs are formed. Subsequently, the viral proteins N and L can replicate the minigenome into an antigenomic sense minigenome,

which serves as a template for the transcription of *Renilla* mRNA. In contrast, in the S segment -based minigenome is in the antigenomic sense. Thus, the antigenome-sense minigenome generated from pT7UUKS<sup>Ren(+)</sup> can serve for the transcription of the *Renilla* subgenomic mRNA without the need of a replication step. Therefore, due to these inherent differences between the M and L segment-based minigenomes and the S segment-based minigenome, the UTR promoter strengths are not comparable, as transcription of the *Renilla* subgenomic mRNA will be driven by different promoters (3' UTR promoters of the genomic or antigenomic RNA, respectively). To ensure that the sequence of the generated plasmids was correct, the sequence of all constructs was confirmed by Sanger sequencing.

Helper plasmids expressing HRTV N and L proteins in the T7 RNAP-driven expression vector pTM1 (Moss *et al.*, 1990) were also provided by Dr Benjamin Brennan and are called pTM1HRTN and pTM1HRTL. In addition to the minigenome constructs derived from the published HRTV sequence, constructs containing the mutations identified in the HRTV laboratory stock were also generated (Section 8.3.1). Briefly, site-directed mutagenesis was used to introduce the A1751G and A3309U mutations in the 5' UTR region (genomic sense) and in the L ORF of pT7HRTS<sup>Ren(+)</sup> and pTM1HRTL, respectively. These plasmids were named pT7HRTS<sup>Ren(+)</sup>A1751G and pTM1HRTLA3309U, respectively.

In order to determine whether the published sequences would allow the generation of functional RNPs that are transcription and replication competent, a minigenome assay using the plasmids corresponding to the published HRTV sequences was carried out. Briefly, sub-confluent monolayers of BSR-T7/5 cells (a BHK-21 clone which constitutively express a T7 RNAP) (Buchholz *et al.*, 1999) were transfected with constant amounts of pT7HRTS<sup>Ren(+)</sup>, pT7HRTM<sup>Ren(-)</sup> or pT7HRTL<sup>Ren(-)</sup>, pTM1HRTN, a plasmid expressing firefly luciferase (pTMFFluc) as an internal control for transfection efficiency, and increasing amounts (0-375 ng) of pTMHRTL. The total amount of DNA per well was kept constant by supplementing the DNA reactions with empty pTM1. 18 h post transfection, the cells were harvested and *Renilla* and firefly activities measured. The *Renilla* values were normalised to firefly values and minigenome activity expressed as fold increase of normalised luciferase units relative to the background control (absence of L protein).

---

Collectively, all minigenome constructs resulted in a dose-dependent increase in normalised luciferase activity when pTM1HRTL was provided (Figure 8-2). The highest fold increase in normalised luciferase activity was observed for the HRTV M segment-based minigenome, which resulted in a mean 10241-fold increase when 375 ng of pTM1HRTL was supplied, relative to the background control. This is in comparison to the S and L segment based-minigenomes, which yielded a peak mean 76- and 155-fold increase in luciferase activities, respectively (Figure 8-2). These results confirmed that the cDNA clones of the N and L proteins, as well as the viral UTRs belonging to the three segments in the published HRTV sequences are functional and enable replication and transcription processes to occur.

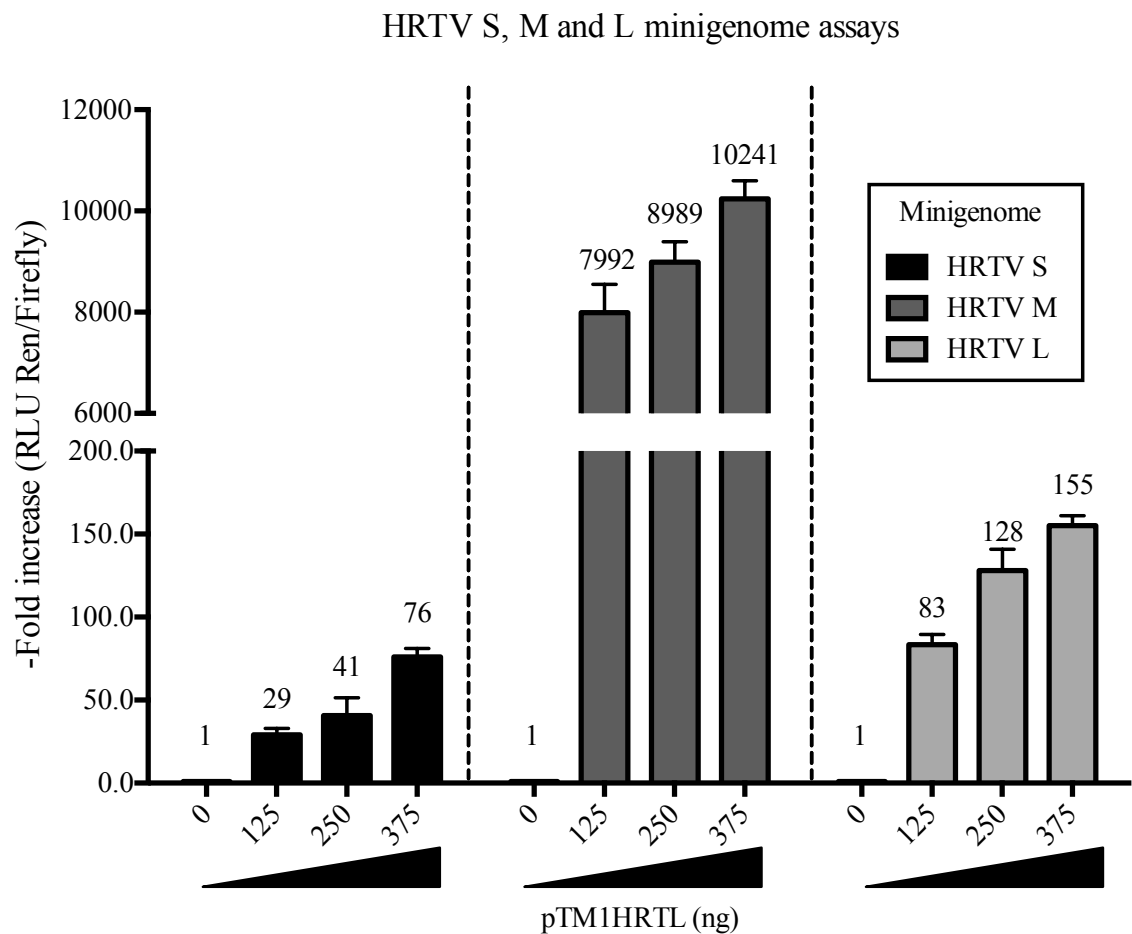


**Figure 8-2. HRTV S, M and L minigenome assays using constructs based on published HRTV sequences.**

BSR-T7/5 cells were transfected with constant amounts of pT7HRTS<sub>Ren(+)</sub> (black), pT7HRTM<sub>Ren(-)</sub> (dark grey) or pT7HRTL<sub>Ren(-)</sub> (light grey), pTM1HRTN, pTMFFluc and increasing amounts (0-375 ng) of pTMHRTL. The total amount of plasmid DNA in all reactions was kept constant by the addition of empty control plasmid pTM1 to the DNA mix. Cells were lysed 18 h post transfection and the *Renilla* and firefly luciferase units measured. Minigenome activity is expressed as the fold induction of normalised luciferase units relative to the background control (no pTM1HRTL). The mean minigenome activities calculated are shown above the bars. Error bars represent the standard deviation (SD) from the mean of one representative experiment of three, performed in triplicate ( $n = 3$ ). HRTV: Heartland virus; RLU: Relative light units.

To investigate whether the mutations identified in the HRTV stock could have an effect on the efficiency of replication and transcription of the viral genome, a S segment-based minigenome assay comparing pT7HRTS<sub>Ren(+)</sub> and pT7HRTS<sub>Ren(+)</sub>A1751G minigenome constructs was carried out. In addition, the minigenome assays were performed utilising helper expression plasmids encoding either the published sequence-based L protein, or that with the A3309U mutation identified in the HRTV laboratory stock (pTM1HRTL and pTM1HRTLA3309U, respectively). In comparison to the published sequence-based L protein, the A3309U mutation in the HRTV L protein did not confer any difference in minigenome activity when using either pT7HRTS<sub>Ren(+)</sub> and pT7HRTS<sub>Ren(+)</sub>A1751G minigenome constructs (Figure 8-3). The constructs containing the A1751G mutation identified in the 5' UTR of the S segment belonging to the HRTV laboratory stock resulted in a slight decrease in S segment minigenome activity, compared to the S segment minigenome activity of the plasmids encoding the published sequence UTRs (Figure 8-3). However, it must be noted that the 5' UTR mutation identified still resulted in an increase in reporter gene activity when the viral polymerase was provided, suggesting that although the mutation leads to a decrease in minigenome activity, the 5' UTR of the HRTV laboratory stock is still able to act as a functional promoter of transcription and replication.

## Analysis of HRTV laboratory stock S and L mutations

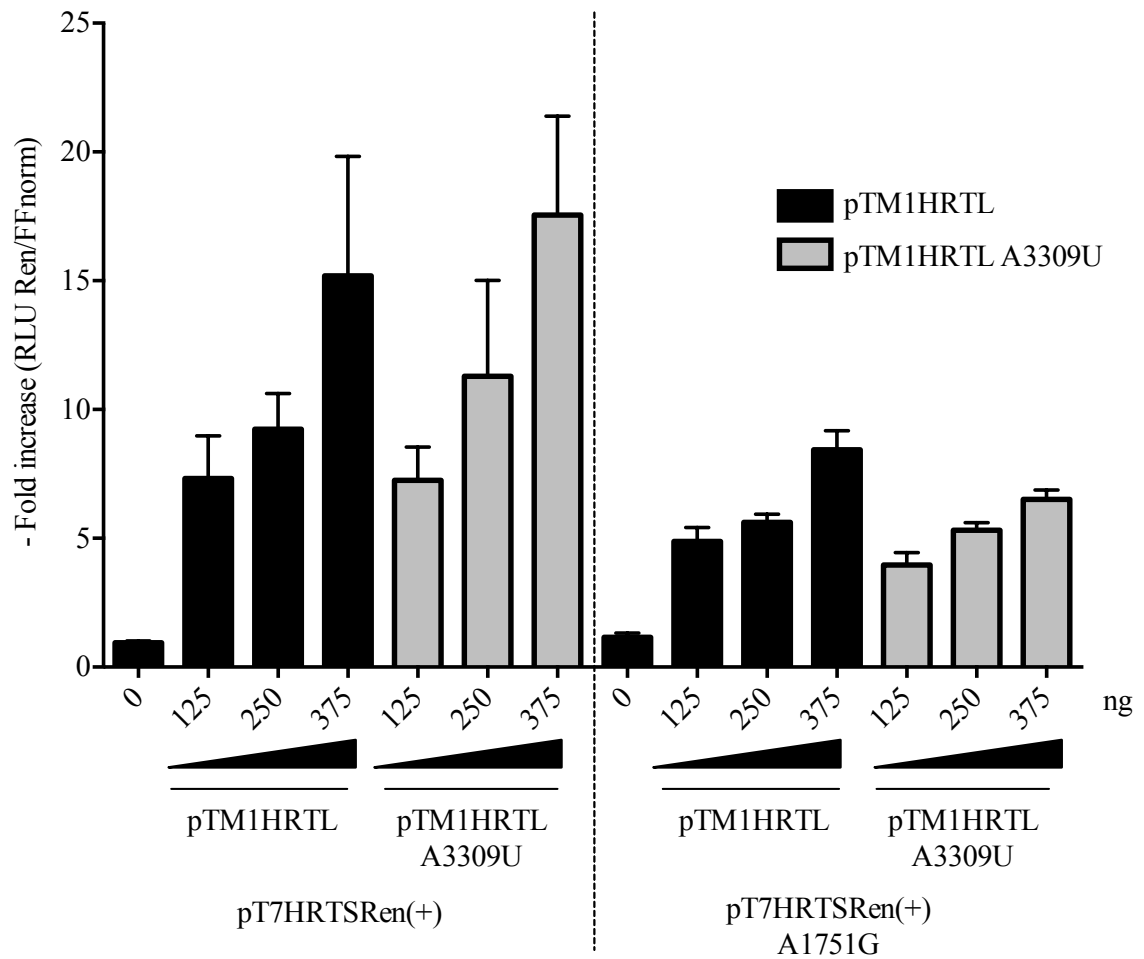


**Figure 8-3. HRTV S segment minigenome assay using constructs based on published and newly identified sequences.**

BSR-T7/5 cells were transfected with constant amounts of pT7HRTSren(+) or pT7HRTSrenA1751G(+), pTM1HRTL, pTMFFluc and increasing amounts (0-375 ng) of pTMHRTL or pTM1HRTLA3309U. The total amount of plasmid DNA in all reactions was kept constant by the addition of empty control plasmid pTM1 to the DNA mix. Cells were lysed 18 h post transfection and the *Renilla* and firefly luciferase units measured. Minigenome activity is expressed as the fold induction of normalised luciferase units relative to the background control. Bars represent the mean fold induction  $\pm$ SEM of three experiments performed in duplicate or triplicate (n=3). HRTV: Heartland virus; RLU: Relative light units.

### ***8.3.3 Investigating the ability of UUKV, HRTV and SFTSV N and L proteins to utilize the M segment minigenome of heterologous tick-borne phleboviruses.***

Minigenome systems serve as a useful tool to investigate transcription and replication processes. The ability of N and L proteins of a particular virus to recognize the viral UTRs as promoters of transcription and replication will determine the functionality of a minigenome. Therefore, the availability of working tick-borne phlebovirus minigenome systems was exploited to investigate whether the N and L protein of a particular virus could transcribe and replicate the M segment genome analogue of other tick-borne phleboviruses. These studies would enable to assess under an experimental setting the potential of reassortment between tick-borne phleboviruses. For the purpose of this study, activity of the M-segment based minigenome of a particular virus was considered as an indication of potential of reassortment between the viruses tested. The M segment-based minigenome system was chosen because reassortant viruses with a novel M segment are of major concern. This is because the gene products of reassortant viruses with a novel M segment (the surface envelope glycoproteins Gn and Gc) can introduce new immunogenic characteristics, alter tropism and host range, and can allow escape from immune surveillance (Briese *et al.*, 2013; Elliott, 2014). The available tick-borne phlebovirus M segment-based minigenome systems include that of UUKV (described in chapter 5), HRTV (present study, Section 8-3), and SFTSV (Brennan *et al.*, 2015).

Compatible viral components (such as the ability of N and L proteins of a particular virus to recognize the viral UTRs of a segment belonging to a heterologous virus) are a key requirement that favour reassortment between closely related viruses. Therefore, the amino acid identity of UUKV, HRTV and SFTSV N and L protein was compared, to assess the relatedness between these proteins. While UUKV N shares 27% and 28.3% amino acid identity with HRTV and SFTSV N proteins (respectively), the amino acid identity between HRTV and SFTSV N proteins is of 61.6% (Table 8-1). Similarly, UUKV L shares only 34.2% and 35.4 % amino acid identity with HRTV and SFTSV L proteins (respectively), whereas the L protein of HRTV and SFTSV share 73.3% amino acid identity (Table 8-2). Therefore, the amino acid identity shared between HRTV and SFTSV N and L proteins is noticeably higher than that shared between HRTV or SFTSV and UUKV N and L. An amino acid alignment of the N and L proteins used in this study is shown in Figures 10-1 and 10-2 (Appendices).

**Table 8-1. Percentage amino acid identity of UUKV, HRTV and SFTSV N proteins.**

| Virus | N amino acid identity (%)* |       |       |
|-------|----------------------------|-------|-------|
|       | UUKV                       | HRTV  | SFTSV |
| UUKV  | 100                        |       |       |
| HRTV  | 27.05                      | 100   |       |
| RVFV  | 28.28                      | 61.63 | 100   |

\* Based on the GenBank accession numbers AAA47958.1, AFP33391.1 and AJD86040.1 for UUKV, HRTV and SFTSV N proteins, respectively. Generated using Clustal Omega (Sievers *et al.*, 2011).

**Table 8-2. Percentage amino acid identity of UUKV, HRTV and SFTSV L proteins.**

| Virus | L amino acid identity (%)* |       |       |
|-------|----------------------------|-------|-------|
|       | UUKV                       | HRTV  | SFTSV |
| UUKV  | 100                        |       |       |
| HRTV  | 35.36                      | 100   |       |
| SFTSV | 34.24                      | 73.32 | 100   |

\* Based on the GenBank accession numbers BAA01590.1, AFP33396.1 and AJD86038.1 for UUKV, HRTV and SFTSV L proteins, respectively. Generated using Clustal Omega (Sievers *et al.*, 2011).

The UTR sequences of bunyaviral segments also play a key role in transcription and replication. Particularly, specific sequences found at the terminal ends of the 5' and 3' UTRs act as promoters of transcription, and contain *cis*-acting RNA replication signals (Schmaljohn and Nichol, 2007). Phleboviral 3' and 5' UTR of all three segments contain 8 terminal nucleotides that are complementary to each other, and were initially thought to be strictly conserved in all three segments across the *Phlebovirus* genus (3'-ACACAAAG...CUUUGUGU-5') (Elliott and Blakqori, 2011; Freiberg and Flick, 2013). To analyse the conservation and diversity in nucleotide sequence which may determine M segment promoter activity or recognition by the N and L proteins, a nucleotide sequence alignment of the M segment 3' and 5' UTR of UUKV, HRTV and SFTSV was carried out.

Hereafter 3' and 5' UTR refer to the genomic sense UTRs. Whereas the UUKV M segment 3' and 5' UTRs contain the consensus 8-nucleotide long terminal sequences that are complementary to each other, the HRTV and SFTSV M segment 3' UTR contain a G at position 6 instead of an A, deviating from the consensus sequence. The inter-segment variations at this position have been described for the 3' UTR of HRTV S and M segments, SFTSV M and L segments, Bhanja virus (BHAV) L segment and the 5' UTR of Lone Star Virus (LSV) S segment (Elliott and Brennan, 2014). Thus, it appears that the nucleotide identity at this position of the 3' and 5' UTR termini of tick-borne phlebovirus S, M and L segments is not strictly conserved.

Importantly, the M segment 5' UTR terminal sequences of HRTV and SFTSV do not deviate from the consensus sequence (Figures 8-4 and 8-5). This would result in a 'mismatch' in complementarity at this position (3'-ACACAGAG...CUUUGUGU-5'; mismatched nucleotides in bold) in the HRTV and SFTSV, but not UUKV M segment UTR termini. In addition, whereas the UUKV and SFTSV 3' UTRs are relatively short (17 and 18 nt, respectively), that of HRTV was significantly longer (50 nt) (Figure 8-4). Despite high conservation of the 10 terminal residues of the 5' UTR between UUKV, HRTV and SFTSV M segments, little conservation of the rest of the 5' UTRs was noted (Figure 8-5). Finally, while the 5' UTR of the UUKV M segment is 185 nt in length, HRTV and SFTSV have shorter M segment 5' UTRs of 146 nt and 138 nt, respectively (Figure 8-5).



**Figure 8-4. Sequence alignment of the M segment 3' UTR of three tick-borne phleboviruses.** The M segment 3' UTR sequences of UUKV, HRTV and SFTSV are presented in the RNA genomic sense. GenBank accession numbers used: M17417.1, JX005845.1 and KP202164, respectively. Adenine (A) residues are highlighted in green, Uracil (U) in green, Cytosine (C) in blue and Guanine (G) in red. The consensus sequence is in black. '-' denotes gaps and 'N' denotes absence of consensus. Generated with CLC Genomics Workbench 7. The dashed line denotes 3' UTR termini, which were thought to be strictly conserved within the S, M and L segments of all phleboviruses.

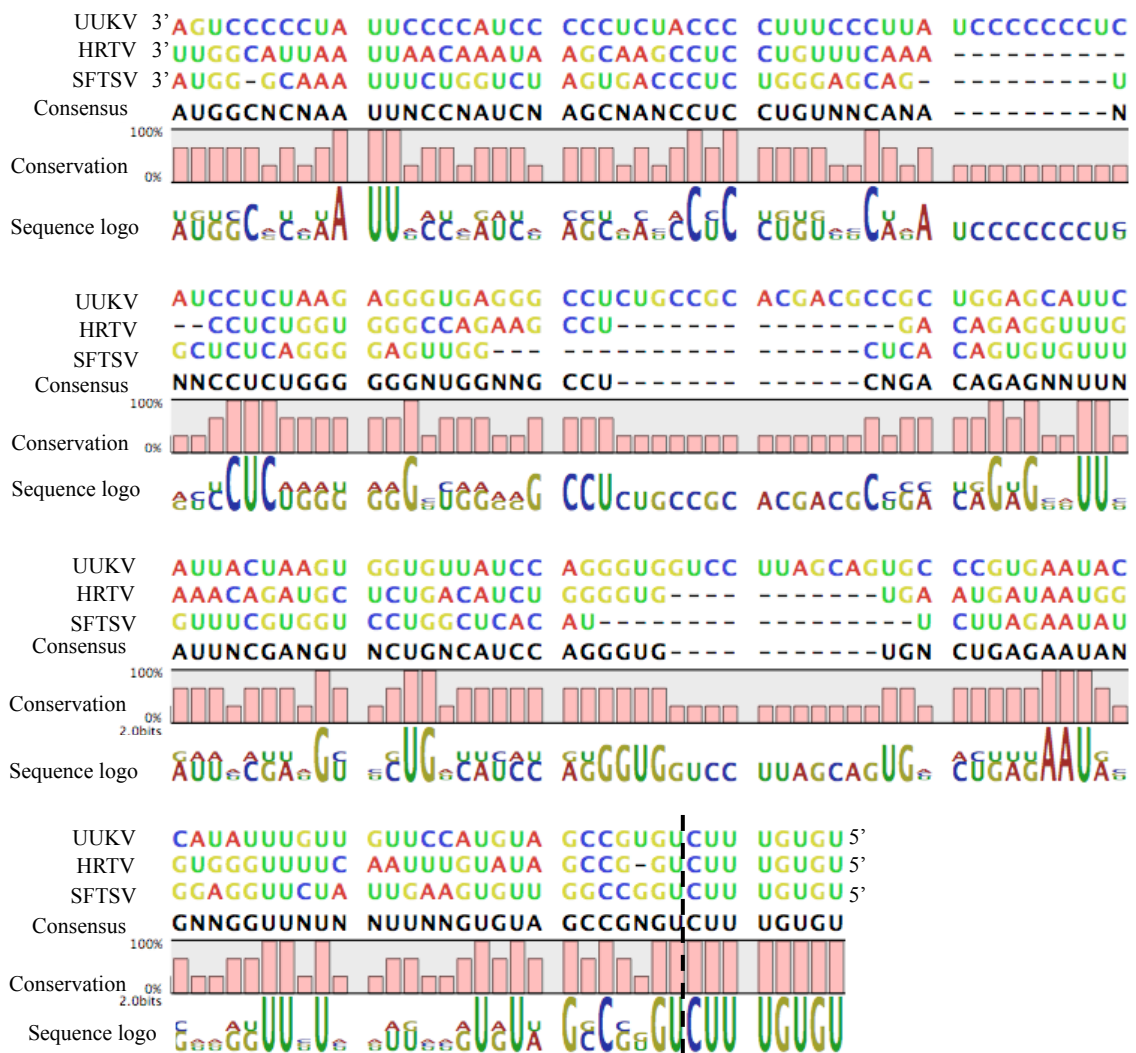


**Figure 8-5. Sequence alignment of the M segment 5' UTR of three tick-borne phleboviruses.**

The M segment 5' UTR sequences of UUKV, HRTV and SFTSV are presented in the RNA genomic sense. GenBank accession numbers used are M17417.1, JX005845.1 and KP202164, respectively. Adenine (A) residues are highlighted in green, Uracil (U) in green, Cytosine (C) in blue and Guanine (G) in red. The consensus sequence is in black. '-' denotes gaps and 'N' denotes absence of consensus. Generated with CLC Genomics Workbench 7. The dashed line denotes 3' UTR termini, which were thought to be strictly conserved within the S, M and L segments of all phleboviruses.

The ability of the N and L proteins of UUKV, HRTV or SFTSV to replicate and transcribe the M segment-based minigenome belonging to heterologous viruses was tested, using the minigenome of homologous viruses as a control. Most bunyavirus reassortants identified to date possess the S and L segments derived from one virus, and the M segment derived from another virus, indicating that reassortment may be restricted to the M segment (Briese *et al.*, 2013). In addition, similar studies with viruses belonging to the *Orthobunyavirus* genus were carried out previously by Dr Natasha Tilston-Lunel (Boston University), and showed that N and L proteins belonging to different orthobunyaviruses were unable to function together in the context of a minigenome setting, therefore suggesting that the sole determinant of orthobunyavirus reassortment capacity lies in the recognition of the M segment UTRs of virus ‘Y’ by the N and L proteins of virus ‘X’ (unpublished). Therefore, for simplicity the assays were carried out utilizing N and L from homologous viruses only and the ability of N and L proteins from different viruses to collectively recognize, replicate and transcribe a particular minigenome was not tested.

The SFTSV M segment-based minigenome construct (pTVT7HB29M:hRen), as well SFTSV N- and L- expression plasmids (pTM1HB29N and pTM1HB29L, respectively) which are under the control of a T7RNAP promoter and EMCV IRES have been previously described and were provided by Dr Benjamin Brennan (Brennan *et al.*, 2015). Briefly, BSR-T7/5 (constitutively expressing T7 RNAP) (Buchholz *et al.*, 1999) were transfected with constant amounts of each of the M segment-based minigenomes (pT7XMRen(-) or pTVT7HB29M:hRen; [X= UUKV or HRTV]), the firefly luciferase expression plasmid pTMFFluc and 125 ng of the indicated N- and L-expressing plasmids (pTM1XN and pTM1XL, [X= UUKV, HRTV or SFTSV strain HB29]). Control wells lacked L-expressing plasmids and the DNA reactions were supplemented with empty pTM1 to keep the total amount of DNA constant in all conditions. 18 h post transfection, the cells were harvested and *Renilla* and firefly values measured. *Renilla* values were normalised to firefly values and minigenome activity expressed as the normalised luciferase activity relative to the background control (absence of L-expressing plasmid). As expected, the M segment-based minigenomes of UUKV, HRTV and SFTSV exhibited the highest activity when each minigenome system was supplied with the N and L proteins of the cognate viruses (Figure 8-6 A-C). Interestingly, HRTV and SFTSV N and L proteins were able to recognize the UUKV M segment UTRs as a promoter for transcription and replication. Whereas a mean 72-fold increase in UUKV M minigenome activity was observed in the presence of UUKV N and L proteins, HRTV or SFTSV N and L proteins

resulted in a mean 24- or 14- fold increase in UUKV M minigenome activity, respectively (Figure 8-6 A). UUKV and SFTSV N and L proteins were also able to promote HRTV M minigenome activity, resulting in a mean 507- and 1491-fold increase in minigenome activity, respectively. This is in comparison to the mean 7569-fold increase detected in HRTV M minigenome activity in the presence of HRTV N and L (Figure 8-6 B). Finally, SFTSV N and L proteins yielded a mean 2157-fold increase in SFTSV M minigenome activity, and only HRTV N and L (but not UUKV N and L) proteins promoted SFTSV M minigenome activity, with a mean 30-fold increase detected, relative to the background (Figure 8-6 C).

Taken together, these results demonstrate that UUKV N and L proteins are able to recognize and utilize the HRTV M UTRs but not the SFTSV M UTRs as a promoter, whereas HRTV N and L can recognize both UUKV and SFTSV M UTRs and that SFTSV N and L proteins can recognize UUKV and HRTV M UTRs for the transcription and replication of M segment-based minigenomes (summarized in Table 8-3).

**Table 8-3. Summary of UUKV, HRTV and SFTSV M-segment based minigenome activities detected in the presence of N and L proteins from cognate or heterologous viruses.**

| <b>N+ L proteins</b><br><b>M minigenome</b> | UUKV    | HRTV     | SFTSV    |
|---|---------|----------|----------|
| UUKV  | ✓ (72)  | ✓ (24)   | ✓ (14)   |
| HRTV  | ✓ (507) | ✓ (7569) | ✓ (1491) |
| SFTSV                                       | ✗       | ✓ (30)   | ✓ (2157) |

Note: Ticks depict an increase in minigenome activity for the indicated M segment-based minigenome in the presence of the indicated N and L proteins. Crosses depict no increase in minigenome activity. The numbers shown between brackets depict the fold increase in minigenome activity (relative to the background control in the absence of L protein).

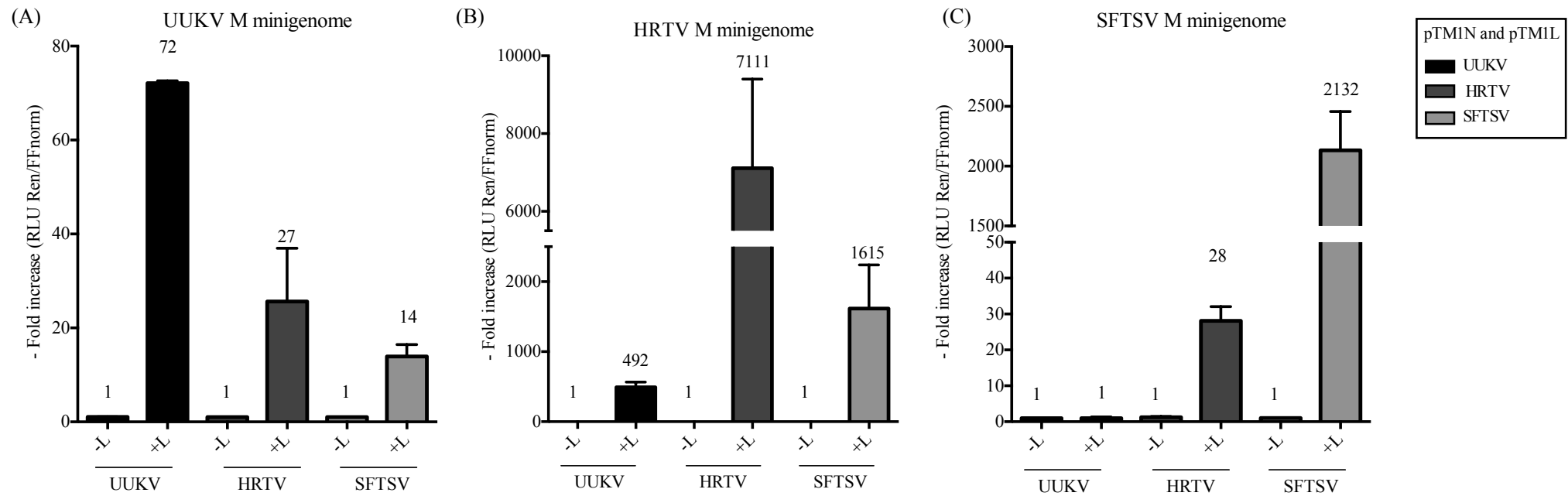


**Figure 8-6. Activity of the UUKV, HRTV and SFTSV M segment-based minigenomes using UUKV, HRTV or SFTSV N and L proteins.**

BSR-T7/5 cells were transfected with pT7UUKMren(-), pT7HRTMren(-) or pTVT7HB29M:hRen, pTMFFluc, pTM1XN and pTM1XL, where X refers to UUKV, HRTV or SFTSV. Cells were lysed 18 h post transfection and the *Renilla* and firefly luciferase units measured. Minigenome activity is expressed as the fold induction of normalised luciferase units relative to the background control (absence of L-expressing plasmid). Bars and the number above represent the mean fold induction  $\pm$ SEM of two experiments performed in duplicate or triplicate (n=2). UUKV: Uukuniemi virus; HRTV: Heartland virus; SFTSV: Severe Fever with Thrombocytopenia Syndrome virus; RLU: Relative light units.

### 8.3.4 Efforts to generate cDNA clones of the HRTV M segment

Previous attempts to rescue HRTV entirely from cDNA clones taking the T7 RNAP-driven approach routinely used in our laboratory have failed (personal communication, Dr Benjamin Brennan). However, the results in Section 8.3.2 indicated that HRTV UTRs, as well as the N and L proteins were functional, leading to measurable minigenome activity and suggesting successful replication and transcription of the HRTV minigenomes. In order to revisit the failure to rescue HRTV from cDNA clones, HRTV rescue plasmids pT7HRMS(+), pT7HRM(+), and pT7HRTL(+), were utilized as templates to introduce the mutations identified in the full genome sequencing of the HRTV laboratory stock (Section 8.3.1).

While the S and L segment mutations were successfully introduced by site-directed mutagenesis in pT7HRMS(+) and pT7HRTL(+) (respectively) to generate pT7HRMSA1751G(+) and pT7HRTLA3309U(+), problems were encountered when attempting to generate the correct HRTV M segment clone. Initially, an approximately 1.4 kbp insertion corresponding to an *E. coli* sequence was identified within the HRTV M segment ORF in the pT7HRM(+) template. This finding provided an explanation for the inability to rescue HRTV entirely from cDNA clones at first. In an attempt to generate the correct pT7HRM(+) clone, (i) the foreign *E. coli* sequence were removed by excision PCR, followed by ligation, and (ii) the full-length antigenome cDNA of the HRTV laboratory stock was cloned into into pTVT7 (0,0) (Johnson *et al.*, 2000). However, despite successfully removing foreign *E. coli* sequences and cloning the full length cDNA of the HRTV M segment into the pTVT7 plasmid in the antigenome sense, all clones sequenced had either insertions, deletions and/or multiple mutations within the M segment ORF, which would result in a frame-shift or amino acid mutations within the glycoprotein precursor (data not shown). These findings indicated that presumably, the clone was toxic to bacteria. Therefore, several methods were tested to successfully clone the construct. These included the incubation of transformed *E. coli* at either 37 °C, 30 °C or at room temperature, in combination with using the following *E. coli* strains for generation of the plasmid: JM109, SURE2, BL21(DE3), Stellar™ and CopyCutter™ EPI400™. All bacterial strains generated pT7HRM(+) clones with insertions, deletions and/or multiple mutations. However, altering the manufacturer's protocol for the growth of CopyCutter™ EPI400™ yielded the correct pT7HRM(+) sequence. These cells contain a gene that controls the vector copy number under an inducible promoter (*pcnB* [plasmid copy number

B]). Therefore, the plasmid is kept at a low copy number to enhance plasmid stability following transformation, and a short incubation with induction solution provided by the manufacturer leads to the subsequent raise in copy number, enhancing plasmid yields for DNA recovery. Because induction to raise the plasmid copy number in CopyCutter™ *EPI400*™ bacteria gave rise to mutations in pT7HRTM(+), the transformed uninduced bacteria were incubated at 37° for 30 h without induction, which resulted in low plasmid yield. However, most pT7HRTM(+) clones isolated carried the correct HRTV sequence.

The recovery of infectious, recombinant HRTV using plasmids derived from the published sequences was attempted in BSR-T7/5 cells (Buchholz *et al.*, 1999) and Huh-Lunet-T7 cells (Kaul *et al.*, 2007), both of which constitutively express a T7 RNAP. Huh-Lunet-T7 cells were used in addition to the routinely used BSR-T7/5 cells because HRTV replicates more efficiently in Huh-7 cells than BHK-21 cells (cell line which the BSR-T7/5 cell line is derived from; personal communication with Dr Benjamin Brennan). Briefly, subconfluent cells in 6 well plates were transfected with 1µg of pT7HRTS(+), pT7HRTM(+) and pT7HRTL(+) in a 3-plasmid rescue system, or supplemented with 250 ng pTM1HR TN and pTM1HRTL in a 5-plasmid rescue system. The supernatant was harvested 7 days post transfection and plaque assays carried out in Vero E6. None of the conditions tested yielded infectious HRTV. However, it must be mentioned that due to time constraints, the rescue was attempted once, using plasmids based on the HRTV published sequences only. It is worth repeating the rescue under different experimental conditions, such as varying plasmid amounts to optimise transfection conditions, or attempting the rescue using plasmids containing the mutations identified in the HRTV laboratory stock.

## **8.4 Discussion**

The tick-borne phlebovirus reverse genetics systems developed so far include that of UUKV (Chapter 5) and SFTSV (Brennan *et al.*, 2015). Developing a reverse genetics system for another tick-borne phlebovirus available in our laboratory, such as HRTV, would provide the tools to take a comparative approach for investigating further the molecular biology of these viruses. Moreover, as tick-borne phleboviruses continue to emerge in naïve geographical locations with increasing host range (Elliott and Brennan, 2014), there is a need to understand the viral determinants that contribute to the evolution of these viruses and their escape from immune surveillance. Genome reassortment (or antigenic shift) has long been acknowledged as a key force driving the evolution of the *Bunyaviridae* (Weber and Elliott, 2002) and other segmented viruses. In fact, Briese *et al.*, hypothesised that it is possible that all known bunyaviruses represent reassortants of existing or extinct viruses (Briese *et al.*, 2013). This hypothesis emphasizes the need of working reverse genetics systems for emerging bunyaviruses, as such tools could allow to assess the potential of genome reassortment under experimental conditions.

In order to develop a reverse genetics system for HRTV, the stock of HRTV available in the laboratory was sequenced to confirm that the sequences available in the database were correct, and to identify possible mutations that may have arisen while passaging the virus in cell culture. Compared to the published sequence for the HRTV patient isolate number 2 (McMullan *et al.*, 2012), three mutations present in the laboratory HRTV stock were identified, one in each of the viral segments (Figure 8-1). The S segment contained a A1751G mutation in the 5' UTR (genomic-sense), the M segment contained a C1764U mutation which results in a His→Tyr amino acid change in the Gc glycoprotein, and the L segment contained an A3309U mutation which results in a Tyr→Phe amino acid change in the viral RNA-dependent RNA polymerase (RdRp, or L protein) (Figure 8-1). Minigenome analysis revealed that while the mutation in the viral polymerase had no effect in minigenome activity, the mutation in the genomic 5' UTR of the S segment led to a decrease in minigenome activity compared to the published sequences. However, although less efficient, the S segment-based minigenome containing the mutation identified in the genomic 5' UTR still resulted in a functional minigenome (Figure 8-3). These results suggested that under the experimental conditions used in this study, the mutations identified in the S and L segments of our HRTV laboratory stock did not confer any advantage in terms of replication and transcription of the viral genome. Due to time

constraints, it remains to be determined whether the mutations could grant advantages in the cell line used to propagate HRTV (Vero E6), or if the mutation identified in the M segment could aid in other stages of the virus life cycle, such as entry, packaging or egress. Such studies could be carried out using virus-like particle (VLP) assays, or by introducing the mutations in the viral genome by reverse genetics to examine their effect on virus phenotype.

In this Chapter, the development of a minigenome system for HRTV is described. A dose-dependent increase in S, M and L minigenome activities with increasing amount of HRTV L-expressing plasmid was observed. This is in contrast to the dose-dependent decrease in UUKV S and L (but not M) minigenome activities with increasing amount of UUKV L-expressing plasmid described in Chapter 5 (Figure 5-3), and the reported dose-dependent decrease in SFTSV M minigenome activity with increasing SFTSV L-expressing plasmid (Brennan *et al.*, 2015). These differences may be attributed to the fact that the optimal L protein levels required for efficient minigenome activity may differ between UTR sequences. Similar results have been observed for other bunyaviruses, and were attributed to a tight regulatory function of the L protein to switch from replication to cap-snatching activity (Blakqori *et al.*, 2003; Elliott and Schmaljohn, 2013). Nevertheless, the HRTV N and L –encoding plasmids used in this study were shown to be functional and driving reporter gene expression from minigenomes. The developed HRTV minigenome system will serve as a useful tool for future studies to facilitate functional studies of the HRTV UTR sequences, N and L proteins and other transcriptional and replication processes.

Because bunyaviruses have a tripartite segmented genome, infection of the same host cell by two closely related bunyaviruses can in theory result in eight potential progeny viruses, with different genome combinations: AAA, ABA, BAA, AAB, BBA, ABB, BAB and BBB (where A and B refer to parental viruses with genomes  $S_A$ ,  $M_A$ ,  $L_A$  and  $S_B$ ,  $M_B$ ,  $L_B$ , respectively) (Briese *et al.*, 2013). Perhaps the most well known example of natural genome reassortment occurrence within the *Bunyaviridae* is that of Ngari virus, which emerged in 1997 and caused a large outbreak of hemorrhagic fever in East Africa. The virus was later reported to be a reassortant virus, progeny of two closely related orthobunyaviruses: BUNV (S and L segment donor) and Batai virus (M segment donor) (Briese *et al.*, 2006). Intriguingly, two years before the outbreak, Dunn *et al.* had predicted that BUNV and Batai virus could reassort, a hypothesis based on experimental evidence showing that BUNV and Batai viral proteins were compatible for the transcription of RNA

template minigenome assays (Dunn *et al.*, 1995). Another orthobunyavirus, named Schmallenberg virus, emerged in 2012 and was reported to cause congenital defects in newborn calves, goats and lambs (Hoffmann *et al.*, 2012). It was later found that Schmallenberg virus was a reassortant of two other orthobunyaviruses, namely Sathuperi virus (M segment donor) and Shamonda virus (S and L segment donor) (Yanase *et al.*, 2012). Within the *Phlebovirus* genus, a genome analysis of RVFV strains indicated that reassortment events among RVFV lineages occurred over the evolutionary history of these virus strains (Bird *et al.*, 2007). Additionally, Aguacate virus has been suggested to be a natural reassortant from an as-yet unknown virus (Palacios *et al.*, 2011), and Granada virus is likely a reassortant of Massilia virus (S and L segment donor) and a yet unidentified phlebovirus (M segment donor) (Collao *et al.*, 2010).

Briese *et al.* also suggested that the intricate play between the viral polymerase, nucleocapsid protein and the viral RNA may explain why most recognized bunyavirus reassortants possess the S and L segments derived from one virus, and the M segment derived from another virus (Briese *et al.*, 2013). With this in mind, the newly developed HRTV minigenome system, as well as the already developed UUKV (Chapter 5) and SFTSV (Brennan *et al.*, 2015) minigenome systems were utilized as a first step to assess whether the N and L proteins of UUKV, HRTV or SFTSV could recognize, transcribe and replicate the M segment-based minigenome of each of these tick-borne phleboviruses. As expected, the highest minigenome activity was detected when the N and L proteins UUKV, HRTV or SFTSV were used in combination with the M segment-based minigenome of the respective viruses, demonstrating that utilizing N and L proteins and the M segment UTRs from homologous viruses results in optimal minigenome activity. Despite the fact that the N and L proteins of UUKV were less closely related in amino acid identity to HRTV and SFTSV N and L (Tables 8-1 and 8-2), the latter two were able to utilize UUKV M UTRs as a functional promoter (Figure 8-6 A). Interestingly, the results from this work revealed that UUKV N and L proteins are able to recognize HRTV M UTRs but not SFTSV M UTRs as a functional promoter (Figures 8-6 B and C). These results indicate that possibly, sequence differences or secondary structure differences found within the HRTV and SFTSV M UTRs could allow recognition, transcription and replication of the HRTV M UTRs but not SFTSV M UTRs by UUKV N and L. Finally, the higher conservation in amino acid identity between HRTV and SFTSV N and L was reflected in their ability to recognize each others' M segment UTRs as functional promoters (Figure 8-6 B and C). The ability of the N and L proteins of virus 'X' to recognize the M segment UTRs of virus

‘Y’ for subsequent transcription and replication indicates that, provided that the glycoproteins from virus ‘Y’ are able to package the S and L segments of virus ‘X’, a new reassortant virus with the S and L segments of virus ‘X’ and the M segment of virus ‘Y’ could be generated upon co-infection of the same host cell. Therefore, the findings described here show that from the six possible reassortment outcomes examined (UM/HS/HL, UM/SS/SL, HM/US/UL, HM/SS/SL, SM/US/UL and SM/HS/HL; where the first letter refers to UUKV, HRTV or SFTSV and the second letter refers to the segment S, M or L), five reassortment combinations (UM/HS/HL, UM/SS/SL, HM/US/UL, HM/SS/SL and SM/HS/HL) could be possible amongst the tick-borne phleboviruses tested. However, further studies are required to confirm this hypothesis, such as utilizing virus-like particle assays to assess whether the M segment of a particular virus is capable of packaging the S and L segments of other tick-borne phleboviruses to produce viable progeny. Additionally, attempting to rescue reassortant viruses using reverse genetics under the appropriate biosafety conditions could help in predicting possible outcomes of natural reassortant viruses, as has previously been demonstrated for Ngari virus emergence (Dunn *et al.*, 1995), and could allow the timely development of vaccines for these emerging viruses that can escape immune surveillance. It must be noted that factors such as geographic and ecological conditions should also be taken into account when assessing the possibility of reassortment between tick-borne phleboviruses. For instance, the two potential donor viruses must be circulating in close proximity to each other in order to infect the same vector or host cell. Although it appears that the distribution of the tick-borne phleboviruses analysed in this study are distinct (UUKV = northern Europe, HRTV = United States, SFTSV = China, Japan, South Korea), the geographic distribution of tick-borne phleboviruses in general is global (Matsuno *et al.*, 2015), and climate change may induce alterations in the distribution of the vector tick species of these viruses, or routes of migratory birds carrying the vector ticks (Elliott, 2009). Donor viruses must also be able to infect the same vector or host species. While UUKV has been isolated from *Ixodes ricinus* tick species (Oker-Blom *et al.*, 1964), the primary tick vector of HRTV and SFTSV are believed to be *Amblyomma americanum* (lone star tick) (Savage *et al.*, 2013) and *Haemaphysalis longicornis* (Yu *et al.*, 2011; Zhang *et al.*, 2012b), respectively. Despite the differences in vector species carrying the three viruses relevant to this study, the vertebrate hosts of these viruses remain unclear. Although a number of serological surveys were reported, which examined the distribution of UUKV-, HRTV-, or SFTSV- specific antibodies in a number of different species

(Bosco-Lauth *et al.*, 2015; Hubálek and Rudolf, 2012; Li *et al.*, 2016; 2014; Ni *et al.*, 2015; Niu *et al.*, 2013; Riemersma and Komar, 2015; Saikku and Brummer-Korvenkontio, 1973), there is a need for further surveillance of animal and human populations to assess the risks of genome reassortment to occur.

Finally, the findings described in this chapter indicate that the HRTV M segment clone pT7HRTM(+) is unstable. The availability of this clone is crucial for enabling the rescue of HRTV entirely from cDNA clones using the T7 RNAP-driven system routinely used in our laboratory, which has enabled the rescue of many other bunyaviruses (Brennan *et al.*, 2015; Tilston-Lunel *et al.*, 2016) (Bergeron *et al.*, 2015; Elliott *et al.*, 2013; Lowen *et al.*, 2004; Varela *et al.*, 2013). The conditions required to generate a pT7HRTM(+) clone with the correct sequence was optimized after 18 months of failed attempts. However, a single attempt at rescuing HRTV entirely from cDNA clones derived from published HRTV sequences using either a 3-plasmid or 5-plasmid rescue system failed. Further experimental repeats are required to (i) optimise transfection conditions, and (ii) to attempt to rescue HRTV utilizing plasmids containing the mutations identified in the HRTV laboratory stock. Developing a reverse genetics system for HRTV that allows the rescue of infectious virus entirely from cDNA clones will prove invaluable for advancing our understanding of the molecular biology of tick-borne phleboviruses.

## **8.5 Summary**

- The laboratory HRTV stock was sequenced. Three mutations were identified in the HRTV genome: A1751G in the S segment 5' UTR, C1764U in the M segment, and A3309U in the L segment (nucleotide positions in the genomic sense).
- A minigenome system for HRTV was developed, which will facilitate future studies on transcription and replicational processes of HRTV.
- Using available tick-borne phlebovirus minigenome systems, the results in this chapter demonstrate that the UUKV M UTRs act as a functional promoter in the presence of HRTV and SFTSV N and L proteins and that the HRTV M UTRs act as a functional promoter for UUKV and SFTSV N and L proteins. In contrast, SFTSV M UTRs can be recognized and used for transcription and replication of reporter RNA by HRTV N and L, but not by UUKV N and L. These findings can be used to predict the capability of tick-borne phleboviruses to undergo genome reassortment.

- pT7HRTM(+) is an unstable clone and the conditions to recover the correct clone in *E. coli* were optimized. The correct pT7HRTM(+) clone can be utilized for further attempts to recover infectious HRTV entirely from cDNA clones.

---

Chapter 9

CONCLUSIONS

---

## 9 Conclusions

### 9.1 Fulfilment of the project aims

The primary aim of this project was to carry out a molecular characterization of the NSs proteins belonging to the tick-borne phleboviruses UUKV and HRTV, and utilize reverse genetics systems to aid with these investigations.

The availability of a reverse genetics system for tick-borne phleboviruses was key to this project, as it would enable the genetic manipulation of the virus' genome and could therefore be utilized to investigate the phenotype of viruses engineered to lack their NSs protein. Using molecular tools that have enabled the establishment of reverse genetics systems for other bunyaviruses, I developed a T7 RNAP-driven minigenome system for UUKV, which could also be used for the generation of virus-like particles in the presence of UUKV glycoproteins (Chapter 5). These assays were of great value before attempting the rescue of UUKV, because they confirmed that the cDNA clones of the nucleocapsid (N) and RNA-dependent RNA polymerase (L) proteins, as well as the viral UTRs and glycoproteins were functional. Indeed, I successfully rescued recombinant UUKV entirely from cDNA clones (which exhibited similar properties to the authentic wild-type UUKV) (Chapter 5). The reverse genetics system also enabled the generation of recombinant viruses lacking NSs: rUUKdelNSs and rUUKdelNSsGFP, which highlighted the robustness of the system to recover mutant viruses. In addition, the results presented indicated that rUUKdelNSsGFP can serve as a tool to visualize and monitor virus infection (Chapter 5).

Although UUKV or UUKV-like antibodies have been found in humans, there is no association of UUKV with human disease. Taking advantage of the established reverse genetics system, I demonstrated that UUKV acts as a weak antagonist of the human IFN response in cell culture, as upon infection UUKV lacking NSs induced more IFN than wild-type viruses, although wild-type UUKV still induced IFN (Chapter 6). These results raised the question whether the NSs protein belonging to more pathogenic tick-borne phleboviruses have evolved a more efficient IFN antagonistic function to facilitate replication in the host upon infection. Using transient transfection assays, I showed that in general, the NSs protein of apathogenic UUKV is a weaker IFN antagonist than that belonging to the pathogenic HRTV and SFTSV. Additionally, similar assays allowed me to demonstrate that while UUKV, HRTV and SFTSV NSs proteins were able to inhibit

IFN induction with different efficiencies, none of the proteins were able to hinder NFκB signalling. Furthermore, while UUKV NSs was unable to inhibit type I or type II IFN signalling, HRTV and SFTSV NSs proteins were potent antagonists of type I, but not type II IFN signalling (Chapter 6).

The molecular mechanisms by which SFTSV NSs blocks IFN induction and signalling pathways are well characterized, whereas that of UUKV and HRTV NSs proteins remain unknown. Reporter assays, immunoprecipitation and immunofluorescence studies allowed me to elucidate the signalling proteins targeted by UUKV and HRTV NSs proteins to facilitate their IFN antagonistic activity. I showed that while UUKV interacts with MAVS to inhibit IFN induction, HRTV NSs behaves in a similar manner to SFTSV NSs and interacts with TBK1 to inhibit IFN induction and STAT2 to inhibit type I IFN signalling (Chapter 7).

Finally, developing a reverse genetics system for HRTV would benefit comparative studies that entail genetic engineering of the genomes of tick-borne phleboviruses. In this study, I sequenced the full genome of the HRTV stock available in our laboratory and identified three mutations compared to the published sequences (McMullan *et al.*, 2012): A1751G in the S segment 5' UTR, C1764U in the M segment, and A3309U in the L segment (nucleotide positions in the genomic sense). Using minigenome assays, I showed that while the mutation found in the S segment UTR resulted in a decrease in minigenome efficiency, the mutation in the L segment conferred no difference in minigenome activity compared to the wild-type sequences. Unfortunately, the aim of recovering infectious HRTV entirely from cDNA clones remained unfulfilled. This is due to time constraints and major hurdles encountered while attempting to generate the HRTV M segment cDNA clone, which was found to be unstable. Nevertheless, the extensive optimization carried out to obtain the correct HRTV M segment cDNA clones will provide a basis for the continuation of this work. The successful development of a minigenome system for HRTV allowed me to utilize this tool in combination with the minigenome systems available for UUKV and SFTSV to assess the ability of the N and L proteins from a particular tick-borne phlebovirus to recognize, replicate and transcribe the M-segment based minigenome of heterologous tick-borne phleboviruses. These assays were informative and enabled me to shed light on possible outcomes of genome reassortment between tick-borne phleboviruses under experimental conditions (Chapter 8).

## **9.2 Future directions**

Tick-borne phleboviruses have become recognized as a public health threat only recently due to the emergence of SFTSV, which caused significant morbidity and mortality in China, Japan, and South Korea. Understanding how SFTSV and other related tick-borne phleboviruses cause disease is of great importance as these viruses continue to emerge worldwide.

The studies described in this thesis have enabled to advance our understanding of how the NSs protein of the tick-borne phleboviruses UUKV, HRTV and SFTSV can counteract a key component of the first line of defence against viral infections: the interferon system. Initial transient transfection assays indicated that the NSs protein of UUKV is a weak IFN antagonist compared to the NSs belonging to HRTV and SFTSV (Chapter 6). Because HRTV and SFTSV can cause severe disease in humans and UUKV is apathogenic, these results indicated that the NSs protein of these tick-borne phleboviruses could act as an important virulence factor that contribute to pathogenicity. The results were confirmed in the context of a virus infection for UUKV, by using reverse genetics to generate recombinant UUKV lacking NSs (chapter 6). However, there is a need to develop similar NSs-lacking viruses for HRTV and SFTSV to confirm the results observed in transient transfection assays, as in these assays the NSs proteins were overexpressed and the IFN system induced artificially. In the context of a virus infection, factors that differ between viruses and may contribute to the evasion of antiviral immunity can be taken into account. These factors include differences in the half-life of NSs proteins expressed exclusively from S segment-specific promoters, or the ability to minimize the detection of PAMPs associated with the respective virus. Thus, a comparison of the ability of each particular virus to utilize the NSs protein to block the IFN response induced by the virus itself would be a more informative approach to understand the relevance of the NSs proteins in the context of a virus infection. This is highlighted by the observation that although transient transfection assays indicated that SFTSV NSs potently inhibits type I IFN induction, SFTSV infection induced IFN, which limited viral replication (chapter 6). The latter finding is in agreement with a recent study that found significantly higher levels of IFN- $\alpha$  in sera from SFTSV-infected patients compared to healthy patients (Liu *et al.*, 2017). In fact, the authors suggested that perhaps the ability of SFTSV NSs to potently block type I IFN production *in vitro* may not play such an important role *in vivo*. Therefore, the kinetics between induction of IFN by the PAMPs associated with the viruses and the ability of their

NSs proteins to block such induction would be an interesting follow-up study stemming from this work, and could be aided by the generation of NSs-lacking viruses using reverse genetics.

The development of a reverse genetics system for UUKV (chapter 5) can now facilitate a vast number of studies that require the manipulation of the UUKV genome, and serves as a starting point for the generation of, and comparison with other NSs-lacking tick-borne phleboviruses. Unfortunately, time constraints prevented further attempts to rescue HRTV from cDNA clones to genetically manipulate its genome. Additionally, although a reverse genetics system for SFTSV was described (Brennan *et al.*, 2015), the generation of NSs-lacking SFTSV has not yet been reported. As well as serving as convenient tools to understand the molecular basis for virulence and pathogenicity, developing a reverse genetics system that allows the recovery of infectious HRTV from cDNA and the generation of NSs-lacking HRTV and SFTSV could also be further explored as an avenue for the design of recombinant live-attenuated vaccines, as it has been described for RVFV (Bird *et al.*, 2011).

During the progress of this PhD study, *in vivo* models of SFTSV infection have become available, which demonstrated that whilst mice engineered to lack  $\alpha/\beta$  IFN receptors or STAT2 are highly susceptible to SFTSV infection, wild-type mice do not become ill (Gowen *et al.*, 2016; Liu *et al.*, 2014). This suggests that the type I IFN response plays a key role in determining disease outcome. The results in this thesis indicate that the NSs protein of HRTV and SFTSV have the ability to block type I but not type II IFN signalling (Chapter 7). HRTV and SFTSV engineered to lack their NSs proteins and rUUKdelNSs could be used in combination with these *in vivo* models. Such projects would serve as an excellent resource to understand the role that the NSs protein of tick-borne phleboviruses and type II IFN signalling play during disease progression *in vivo*, and to evaluate live attenuated vaccines which could be generated using reverse genetics tools.

In addition, studies to identify additional roles of tick-borne phlebovirus NSs proteins are worthy of further investigation. For instance, findings from this thesis suggested that UUKV NSs could have a dispensable role in facilitating virus replication, as UUK viruses lacking NSs exhibited slower replication kinetics than wild-type UUKV (Chapter 5). Moreover, SFTSV NSs has been implicated to act as a scaffold for the formation of characteristic inclusion bodies, which are thought to function as virus replication factories (Bird *et al.*, 2011). Therefore, SFTSV NSs could also play a role in facilitating replication.

Mass spectrometry-based analyses to map the interaction between viral and host proteins (interactome studies) could facilitate the identification of unknown host or viral interacting partners of tick-borne phlebovirus NSs proteins, and could give an insight into unknown roles of these proteins.

An interesting area of research outwith the scope of this study would be investigating whether tick-borne phlebovirus NSs proteins play any role in tick cells. Persistence of RVFV in mosquito cells was suggested to be mediated by antiviral RNA interference by downregulating the expression of RVFV NSs upon virus infection, which would otherwise inhibit host cell transcription (Léger *et al.*, 2013). Little is known about antiviral responses in tick cells, and studies have suggested that the RNA interference system in ticks is different and more complex than that in mosquitoes (Schnettler *et al.*, 2013). Future projects focused on understanding whether NSs proteins play a role in tick cells, whether tick-borne phleboviruses can establish persistence in tick cells, and if similar mechanisms to that described for RVFV NSs in mosquitoes enable persistence of tick-borne phleboviruses to occur in ticks would be beneficial for the better understanding of the replication of tick-transmitted viruses in their vectors. Indeed, studies investigating UUKV entry, replication and and persistence in tick cells have recently begun (Mazelier *et al.*, 2016).

The research I carried out during my PhD project enabled me to characterize at the molecular level how the NSs protein of UUKV and HRTV can block IFN induction only or IFN induction and IFN signalling, respectively, in comparison to the well-characterized SFTSV NSs. UUKV NSs was able weakly inhibit IFN induction through a direct interaction with MAVS, whereas HRTV and SFTSV NSs proteins inhibited IFN induction and type I IFN signalling via an interaction with TBK1 and STAT2, respectively (Chapter 7). The molecular basis for IFN induction or signalling inhibition by these interactions deserves further investigation. The Influenza virus PB1-F2 protein was shown to inhibit IFN synthesis by binding to MAVS, altering mitochondrial membrane potential levels (Varga *et al.*, 2012; 2011), which are known to mediate antiviral signalling via the rearrangement of MAVS (Koshiba *et al.*, 2011). Whether the weak antagonistic activity of UUKV NSs observed at the level of IFN induction and shown to be mediated through a direct interaction with MAVS could have similar consequences to those described for Influenza PB1-F2 is a hypothesis worth pursuing. Work from this project also suggested that, in order to inhibit IFN induction and type I IFN signalling, HRTV NSs has conserved the same interacting partners as SFTSV NSs: TBK1 and STAT2, respectively (Chapter 7).

However, the strategy employed by HRTV NSs to exert its antagonistic activity must be divergent to the one used by SFTSV, because HRTV NSs is unable to form inclusion bodies which are used by SFTSV NSs to spatially isolate these two proteins. In this PhD project, I showed that in the presence of HRTV NSs, STAT2 nuclear translocation was inhibited (chapter 7). However, the effect of HRTV NSs on TBK1 activation needs to be explored further. TBK1 serves as an integrator of multiple signalling pathways that are activated upon pathogen recognition, and therefore plays a key role in innate immunity. To date, the mechanisms of TBK1 activation are not clearly understood, although *trans*-autophosphorylation, K63-linked polyubiquitination and phosphorylation at position serine 172 by IKK $\beta$  have all been suggested to be required for its activation (Kishore *et al.*, 2002; Ma *et al.*, 2012; Tu *et al.*, 2013). Therefore, it would be worth exploring whether HRTV NSs inhibits TBK1-mediated IFN production by hindering any of the proposed models of TBK1 activation. Efforts to understand in more detail the molecular basis of the IFN antagonistic properties of UUKV and HRTV NSs proteins could unveil not only novel mechanisms evolved by viruses to counteract the IFN response, but also to provide insight into how these signalling molecules work. After all, viruses are the best cell biologists and thus can be utilized to uncover unknown cellular processes that are naked to our eyes.

Some evidence suggests that birds may play a role in the widespread distribution of some tick-borne phleboviruses (Hubálek and Rudolf, 2012). For instance, various strains of UUKV (or UUKV-like viruses) have been isolated from ticks collected from passerine birds, migrant birds, or within nesting areas of seabirds (S. R. Moss, 1986; Nuttall *et al.*, 1984; 1981; Traavik and Mehl, 1977; Watret and Elliott, 1985). Furthermore, a study proposed that migratory birds are responsible for the spread of SFTSV across countries (Yun *et al.*, 2015), and antibodies against SFTSV (or SFTSV-like viruses) were detected in migratory birds in China in another study (Li *et al.*, 2016). Preliminary data in this PhD project showed that, while UUKV was able to achieve high viral titres in the chicken embryo fibroblast cell line DF-1, UUK viruses lacking NSs were unable to replicate in this cell line (Chapter 5). These results suggested that perhaps, unlike in the mammalian cells that have been used in this study (BHK-21 and A549), UUKV NSs plays an essential role in virus replication in avian cells. NSs proteins of bunyaviruses are believed to be non-essential gene products. Therefore, the inability of UUK viruses lacking NSs to replicate in DF-1 cells is an interesting finding worth pursuing that could change our views on the canonical accessory role that bunyaviral NSs proteins are attributed. Furthermore, this finding raised the question whether the NSs protein of UUKV, which has a weak IFN

antagonistic role in human cells (Chapter 6), may act as a potent antagonist of the avian IFN response. It is possible that the inability of UUK viruses lacking NSs to replicate in DF-1 cells is due to large amounts of IFN produced following infection, which may be efficiently counteracted by its NSs protein. Therefore, follow up studies stemming from the work described in this thesis could involve comparing the antagonist activity of the tick-borne phlebovirus NSs proteins in the human IFN system (this PhD project) to the avian IFN system. Such studies would be interesting because they would allow a comprehensive analysis of the molecular adaptations of different viruses to their hosts in order to replicate efficiently.

Finally, despite interesting reports suggesting that it is possible that all known bunyaviruses represent reassortants of existing or extinct viruses (Briese *et al.*, 2013), *Phlebovirus* reassortment is an area of research that remains largely unexplored. In an attempt to shed light on the possibility of reassortment between tick-borne phleboviruses, minigenome results showed that except UUKV N and L and SFTSV M segment UTRs, the N and L proteins of each of the viruses (UUKV, HRTV or SFTSV) were compatible with M segment-based minigenome belonging to heterologous viruses (Chapter 8). The preliminary results from this assay highlighted the plasticity of interactions between the N and L proteins and UTR sequences from heterologous tick-borne phleboviruses, and allowed me to assess the possibility of genome reassortment between tick-borne phleboviruses. Although the significance of the potential reassortants were not confirmed due to time constraints, this assay can now be easily adapted for the use with other bunyaviruses. Future work could involve utilizing virus-like particles and reverse genetics to attempt to rescue potential reassortant viruses (under the appropriate biosafety conditions). Such studies would be beneficial to predict outcomes of genome reassortment under an experimental setting, and could help to develop better immune surveillance strategies.

Collectively, work from this PhD study provided significant progress towards the molecular characterization of tick-borne phlebovirus NSs proteins (other than SFTSV) as IFN antagonists, and expanded our knowledge on the plethora of immune evasion strategies acquired by tick-borne phleboviruses to suppress the IFN response. In addition, the reverse genetics system described for UUKV and the minigenome system described for HRTV provide a basis for advancing our understanding of the molecular biology of these important pathogens that continue to emerge and pose a public health threat.

---

Chapter **10**

APPENDICES

---

# 10 Appendices

## 10.1 Oligonucleotide primers used in this study

**Table 10-1. Common oligonucleotide primers used throughout this study.**

| Primer             | Sequence (5' → 3')                                   | Purpose                                  |
|--------------------|--|--|
| pT7exi1<br>pT7exi2 | gggtcggcatggcatctccacctc<br>ctatagtgagtcgtattaatttcg | Linearization of the pTVT7 plasmid (0,0) |
| pUC118F            | agcgccaataacgcaaac                                   | Forward sequencing of pTVT7 plasmids     |
| pTM1 fwd           | ggtgcacatgctttacatgtg                                | Forward sequencing of pTM1 plasmids      |
| pTM1 Rev           | caactcagcttcttctgggc                                 | Reverse sequencing of pTM1 plasmids      |
| PCR anchor primer  | gaccacgcgatcgcgatgcgac                               | 3' RACE                                  |
| Oligod(T)-Anchor   | gaccacgcgatcgcgacttttttttttttv                       | 3' RACE                                  |

**Table 10-2. Oligonucleotide primers used for the generation of UUKV reverse genetics plasmids.**

| Primer   | Sequence (5' → 3')  | Purpose   |
|--|---|---|
| UUK ST7F<br>UUK ST7R<br>UUK MT7F<br>UUKMT7R<br>UUK LT7F<br>UUKLT7R                                 | tacgactactatagacacaaagacctcca<br>atgccatgccgacccacacaaagacctcc<br>tacgactactatagacacaaagacggcta<br>atgccatgccgacccacacaaagacacggc<br>tacgactactatagacacaaagacgccaag<br>atgccatgccgacccacacaaagtccgcca | Amplification of full-length segments for insertion into pTVT7 plasmid in the antigenomic sense   |
| UUKSdelNSs:eGFPexi1<br>UUKSdelNSs:eGFPexi2   | ttagggccgaagcccttttagagtc<br>gcttaatgttgagggtctttgtgtgg   | Amplification of pT7-UUKS lacking NSs for eGFP insertion  |
| UUK GFPexi1<br>UUK GFPexi2   | ggcttcggcccaaattactgtacagc<br>ccaacattaagcatggtgagcaagg   | Amplification of eGFP for insertion in pT7UUKS lacking NSs  |
| UUK SdelNSsexi1<br>UUK SdelNSsexi2   | ttagggccgaagcccttttagagtc<br>cggcccaaagcttaatgttgagggg  | Amplification of pT7-UUKS lacking NSs, followed by religation   |
| UUK SF1<br>UUK SR1   | acacaaagacctccaacattaagc<br>acacaaagacctccaacttagc  | RT-PCR for full S segment amplification   |
| UUK NpTM1F<br>UUK NpTM1R<br>UUK LpTM1F<br>UUK LpTM1R   | gaaaaacacgataataccatggetatgceggag<br>attaggcctctcgagtcagatcaatgatct<br>gaaaaacacgataataccatgcttttagcgatt<br>attaggcctctcgagtcaccaaacatgctc  | UUKV N and L ORF amplification for insertion into pTM1 expression plasmid   |
| UUK SNSs:hRenF<br>UUK SNSs:hRenR<br>UUK MhRenF<br>UUK MhRenR<br>UUK LhRenF<br>UUK LhRenR           | ggcttcggcccaaattactgctcgtcttc<br>cctccaacattaagcatggctccaaggtg<br>gggaataggggactttactgctcgtctt<br>cacaagacggctaccatggctccaaggt<br>ccaagaaaagtcactactgctcgtt<br>acacaaagacgccaagatggctccaaggtg         | Amplification of humanised <i>Renilla</i> for the generation of UUK S, M and L minigenome plasmids.   |
| UUK ShRenexi1<br>UUK ShRenexi2<br>UUK MhRenexi1<br>UUK MhRenexi2<br>UUK LhRenexi1<br>UUK LhRenexi2 | gcttaatgttgagggtctttgtgtgg<br>ttagggccgaagcccttttagagtc<br>agtcccctattcccaccccctcta<br>ggtagccgtctttgtgtgggtcgg<br>cttgcgctctttgtgtgggtcggcatgg<br>gtgactttctttgggttgatgctgg                          | Excision of NSs, GnGc and L ORFs from UUK pT7S (+), M (-) and L(-) for recombination with hRen amplicons for the generation of minigenome plasmids. |
| UUK GnGcpTM1F<br>UUK GnGcpTM1R   | gaaaaacacgataataccatgtaaggacatat<br>attaggcctctcgagtcacgatttttaac   | Amplification of GnGc ORF for insertion into pTM1.  |

**Table 10-3. Oligonucleotide primers used for sequencing the UUKV genome and plasmids.**

| Primer*      | Sequence (5' → 3')        | Purpose   |
|--------------|---------------------------|---|
| UUK S Fwd 1  | acacaaagaccctccaacattaagc | Sequencing the S segment of UUKV                |
| UUK S Fwd 2  | ataaggagaatgaagctcactg    |   |
| UUK S Fwd 3  | gctcagcaggtaagctctctctg   |   |
| UUK S Fwd 4  | atgtccctcagcatctggccc     |   |
| UUK S Rev 1  | acacaaagaccctccaacttagc   |   |
| UUK S Rev 2  | ccagcaggctgcaactgtcctc    |   |
| UUK S Rev 3  | cccttgtagctagctctttctgg   |   |
| UUK M Fwd 1  | acacaaagacacggctacatgg    | Sequencing the M segment of UUKV                |
| UUK M Fwd 2  | gactttcaagcgtgttcttcac    |   |
| UUK M Fwd 3  | gaaactttgtccgtgtagatcc    |   |
| UUK M Fwd 4  | gatcctaataagagtcactgctg   |   |
| UUK M Fwd 5  | gacctcactgcaactagattag    |   |
| UUK M Fwd 6  | gcatgtgaattctgtgcaaac     |   |
| UUK M Fwd 7  | gtgattgacactgactcatcaatg  |   |
| UUK M Rev 1  | acacaaagacggctaccatggaag  |   |
| UUK L Fwd 1  | acacaaagtccgccaagatggaag  | Sequencing the L segment of UUKV                |
| UUK L Fwd 2  | ctctgctgagaccatccagcatc   |   |
| UUK L Fwd 3  | gaaggacgcttttgagaatctc    |   |
| UUK L Fwd 4  | cagaatgcctgctgcttcaatc    |   |
| UUK L Fwd 5  | cagctgtgccggagtcaacctgg   |   |
| UUK L Fwd 6  | gtacttgaatcctgatagaccag   |   |
| UUK L Fwd 7  | ctgagctctgcaagacatccac    |   |
| UUK L Fwd 7  | gaatggccagttttgctttgg     |   |
| UUK L Fwd 8  | catcactaggagggtccccaag    |   |
| UUK L Fwd 9  | ctcattcccagcccagaagggtac  |   |
| UUK L Fwd 10 | gtgctcattgttgaacatcaagtc  |   |
| UUK L Fwd 11 | ccttaacctgttcaagctctcc    |   |
| UUK L Fwd 12 | gagattgttctgtgctgaccgg    |   |
| UUK L Rev 1  | acacaaagacgccaagatgcttta  |   |
| UUK S Rev 1  | acacaaagaccctccaacttagc   | Generation of UUKV S segment cDNA               |
| UUK S Fwd 1  | acacaaagaccctccaacattaagc | PCR of the full-length UUKV S segment from cDNA |
| UUK S Rev 1  | acacaaagaccctccaacttagc   |   |

\* Primers used in chapter 5 for the full-genome sequencing of recombinant UUKV by 3' RACE and RT-PCR, as well as for sequencing reverse genetics plasmids are shown.

**Table 10-4. Oligonucleotide primers used in Chapter 6.**

| Primer*                            | Sequence (5' → 3')   | Purpose  |
|------------------------------------|--|--|
| pCMVexi1<br>pCMVexi2               | ttctagagcggccgcttcgagcagacatgataag<br>ggtggctagcctatagtgagtcgtattaagtactc                        | Linearization of pCMV for restriction-free cloning                           |
| pCMV-UUKNSsFwd<br>pCMV-UUKNSsRev   | gcgccgctctagaactacagtgatcctacgactggcc<br>ctataggctagccaccatgtcttactcactatccagaac                 | Amplification of UUKV NSs for insertion in into pCMV                         |
| pCMV-HRTNSsFwd<br>pCMV-HRTNSsRev   | ctataggctagccaccatgtccttctctaaagcctcagcccagcgtc<br>gcgccgctctagaactagggggagctggaaagtgctggccagtcc | Amplification of HRTV NSs for insertion in into pCMV                         |
| pCMV-SFTSNSsFwd<br>pCMV-SFTSNSsRev | gcgccgctctagaattagacctccttcgggaggtc<br>ctataggctagccaccatgtcgtctagcaaatgctccaac                  | Amplification of SFTSV NSs for insertion in into pCMV                        |
| UUKNSsV5Fwd<br>UUKNSsV5Rev         | gcagtgggtagggatgggcttcccagtgatcctacgactggcc<br>taggttagacagcacctaatagttctagagcggccgcttcgagc      | PCR for ligation of pCMVUUKNSs with V5 at C terminus                         |
| HRTNSsV5Fwd<br>HRTNSsV5Rev         | gcagtgggtagggatgggcttcccggggagctggaaagtgctgg<br>taggttagacagcacctaatagttctagagcggccgcttcgagc     | PCR for ligation of pCMVHRTNSs with V5 at C terminus                         |
| SFTSNSsV5Fwd<br>SFTSNSsV5Rev       | gcagtgggtagggatgggcttccgacctccttcgggaggtcacc<br>taggttagacagcacctaatagttctagagcggccgcttcgagc     | PCR for ligation of pCMVSFTSNSs with V5 at C terminus                        |
| CXCL10Fwd<br>CXCL10Rev             | ccattctgatttgcctt<br>ttccttgctaactgctttcagta   | Real-time qPCR for determination of CXCL10 mRNA levels in total cellular RNA |
| IRF1Fwd<br>IRF1Rev                 | ctgtgcgagtgaccggatg<br>atccccacatgacttctctt  | Real-time qPCR for determination of IRF-1 mRNA levels in total cellular RNA  |
| GAPDHFwd<br>GAPDHRev               | ggagcgagatccctccaaaat<br>ggctgtgtcatacttctcatgg  | Real-time qPCR for determination of GAPDH mRNA levels in total cellular RNA  |

\* Primers used for the generation of pCMVXNSs and pCMVXNSsV5 (where X refers to UUKV, HRTV or SFTSV), and for real-time qPCR are shown.

**Table 10-5. Oligonucleotide primers used for the full-genome sequencing of the HRTV laboratory stock.**

| Primer*      | Sequence (5' → 3')           | Purpose  |
|--------------|------------------------------|--|
| HRT S 5'     | cataaactctagccagattgtc       | Sequencing the genomic 3' and 5' UTR of HRTV S, M and L segments by 3' RACE following cDNA synthesis |
| HRT S 3'     | gagcagcctgcaggaatggac        |  |
| HRT M 5'     | aggaaacacttggcctccccttc      |  |
| HRT M 3'     | gccattcatcaaagctgttgcttaag   |  |
| HRT L 5'     | ctagtcttgtgtatcacatc         |  |
| HRT L 3'     | ggaaatgggagaagctatgg         |  |
| HRT S seq 1  | acacagagaaccccttgaatc        | Full-length sequencing of the HRTV S segment by RT-PCR   |
| HRT S seq 2  | cataaactctagccagattgtc       |  |
| HRT S seq 3  | gtctcaattgaagtcataaaggac     |  |
| HRT S seq 4  | aatttggcgccaaattcaaatattc    |  |
| HRT S seq 5  | tccaaggggttgagagggtcatcc     |  |
| HRT S seq 6  | cgagggggacatggtcattgac       |  |
| HRT S seq 7  | gagcagcctgcaggaatggac        |  |
| HRT S seq 8  | acacaaagaaccccttgaatttcaa    |  |
| HRT M seq 1  | acacagagacggctatacattaagg    | Full-length sequencing of the HRTV M segment by RT-PCR   |
| HRT M seq 2  | aggaaacacttggcctccccttc      |  |
| HRT M seq 3  | ctaagccactctggcacatattg      |  |
| HRT M seq 4  | catggcagttgcccttactc         |  |
| HRT M seq 5  | tgtgaattatggaggcgtctctgtaag  |  |
| HRT M seq 6  | gtaacattgtgggttctcagg        |  |
| HRT M seq 7  | catgggttttgcctcaataaag       |  |
| HRT M seq 8  | atgcagactgcatgtgatag         |  |
| HRT M seq 9  | gtaagaagggtgcaggtgggcaggtgac |  |
| HRT M seq 10 | tagagtcttaacctctctgatggc     |  |
| HRT M seq 11 | aagcgcaaagcacatcagatctgatgg  |  |
| HRT M seq 12 | atctgaatcacatttaagatg        |  |
| HRT M seq 13 | gccattcatcaaagctgttgcttaag   |  |
| HRT M seq 14 | acacaaagaccggctatacaaaattg   |  |
| HRT L seq 1  | acacaaagacgtccagatg          | Full-length sequencing of the HRTV L segment by RT-PCR   |
| HRT L seq 2  | cgaataagagcacagtgaag         |  |
| HRT L seq 3  | gagcttgttactctcacgag         |  |
| HRT L seq 4  | tacaaccaagttggccatgg         |  |
| HRT L seq 5  | gatgcaacaactggtggaac         |  |
| HRT L seq 6  | atgctgctgagggttggaag         |  |
| HRT L seq 7  | ggaaatgggagaagctatgg         |  |
| HRT L seq 8  | acccttaagaagacctatc          |  |
| HRT L seq 9  | tctgctttgactatgtcc           |  |
| HRT L seq 10 | tgccaaagagcgggttatg          |  |
| HRT L seq 11 | acacagagacggctatacattaagg    |  |
| HRT L seq 12 | ctctctctccaagctttgc          |  |
| HRT L seq 13 | ttgataagccattttggtgc         |  |
| HRT L seq 14 | ttgatgcatcaggcattatg         |  |
| HRT L seq 15 | gatatctgggacggtctttgtgt      |  |

\* 3' RACE, RT-PCR and sequencing primers used in Chapter 8 are shown.

**Table 10-6. Oligonucleotide primers utilised for the generation of HRTV minigenome constructs.**

| Primer*        | Sequence (5' → 3')                                  | Purpose  |
|----------------|---|--|
| HRT ShRenexi1  | ttgaattttcaaacatggcttccaaggt                        | Amplification of humanised <i>Renilla</i> for the generation of HRTV S, M and L minigenome constructs.       |
| HRT ShRenexi2  | gttttgaaaattcaaggggtctttgtgt                        |  |
| HRT MhRenexi1  | ctcagtggttacggtttacctctacctta                       |  |
| HRT MhRenexi2  | ttggcattaattaacaataagcaagcctc                       |  |
| HRT LhRenexi1  | accaaccaggactggggctcgggttga                         |  |
| HRT LhRenexi2  | ctggacgtctttgtgtctatagtgagtcgt                      |  |
| HRT SexiRen1   | ggggagctaatttagatcgaattcatttg                       | Excision of NSs, GnGc and L ORFs from UUK pT7HRTS (+), M (+) and L(+) for recombination with hRen amplicons. |
| HRT SexiRen2   | gttttgagaattcaaggggtctttgtgt                        |  |
| HRT MexiRen1   | ccgtaatcactgagatggcttccaaggtg                       |  |
| HRT MexiRen2   | gttaattaatgccaataactgctcgttcttc                     |  |
| HRT LexiRen1   | cacaaagacgtccagatggcttccaaggtg                      |  |
| HRT LexiRen2   | cccagtctggttggttactgctcgttc                         |  |
| HRTMFlip1      | tacgactactatagacacaaagaccggctatacaaatgaaaaccacc     | Amplification of minigenome cassette in genomic sense to flip in antigenomic sense into pTVT7.               |
| HRTMFlip2      | atgcatgccgaccacacagagacggctatacattaaggtagaggtaaaccg |  |
| HRTLFlip1      | tacgactactatagacacaaagaccgtccagatatcaacctttagg      |  |
| HRTLFlip2      | gccatgccgaccacacaaagacgtccagatggcttccaaggtgtacg     |  |
| HRT S A1751G F | cacacaaagaaccctgaaatctcaa                           | Site-directed mutagenesis of the HRTV S and L segments.  |
| HRT S A1751G R | ttagacaaggacatgtttgagaattca                         |  |
| HRT L A3309T F | caaaaaatagccttgaaaaacttggacgcatgaatgcagtag          |  |
| HRT L A3309T R | ctactgcattcatgcgtccaaagtttttcaagcatatttttg          |  |

\* Primers used for the generation of S, M and L segment-based minigenome constructs, and for the introduction of mutations identified in the HRTV laboratory stock in chapter 8 are shown.

## 10.2 Amino acid alignments of UUKV, HRTV and SFTSV N and L proteins

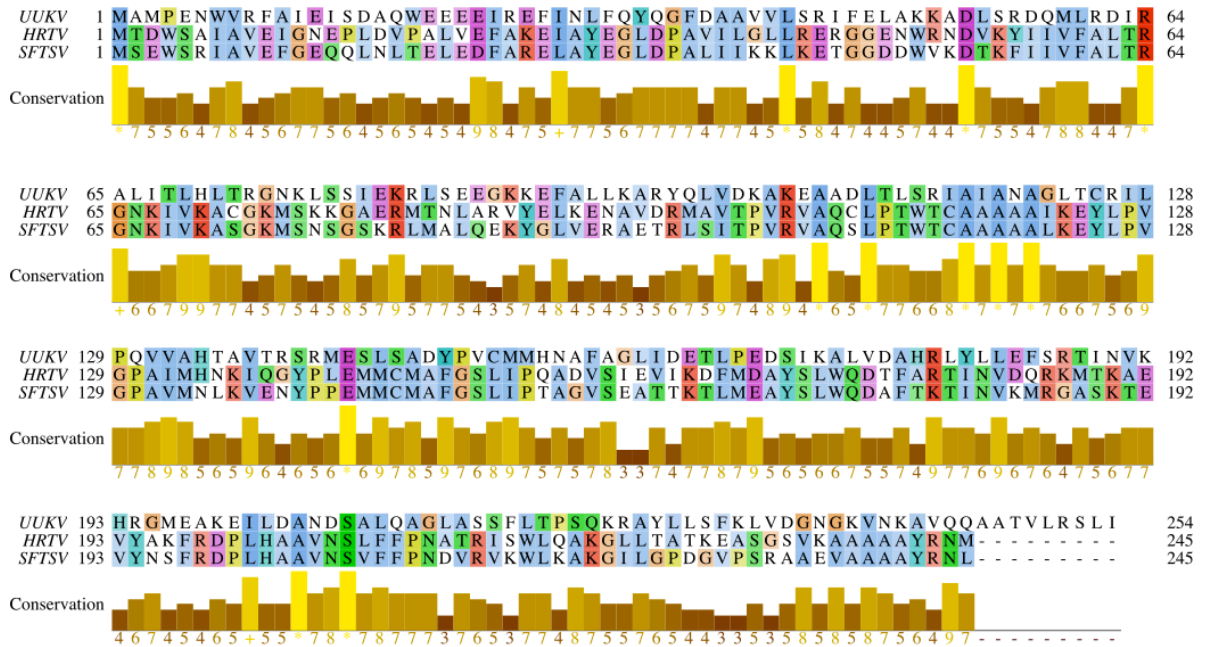
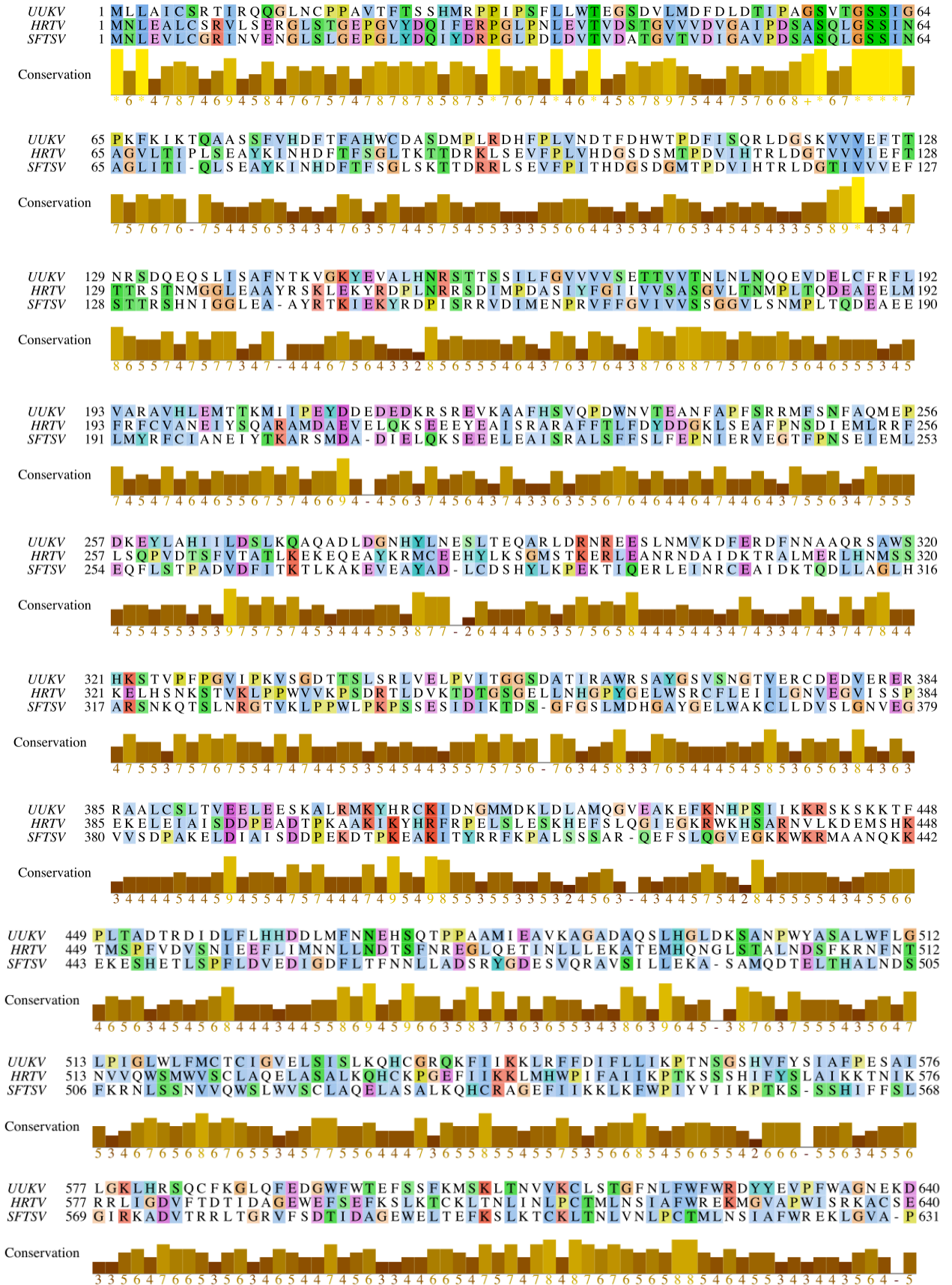


**Figure 10-1. Amino acid sequence alignment for UUKV, HRTV and SFTSV N proteins.**

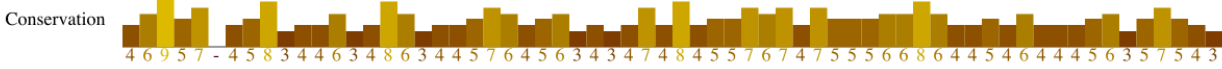
UUKV, HRTV and SFTSV N amino acid sequences (GenBank accession numbers AAA47958.1, AFP33391.1 and AJD86040.1, respectively) were aligned using Jalview 2 (Waterhouse *et al.*, 2009). Residues are highlighted using the ClustalX colour scheme such that the colour of a particular residue depends on the residue type and its conservation (Thompson *et al.*, 1994). Blue: hydrophobic; Magenta: negative charge; Red: positive charge; Green: polar; Pink: cysteine; Orange: glycine; Yellow: proline; Cyan: hydrophobic. The conservation histogram below the alignment depicts conservation scores for each position (0-10, '\*' refers to a score of 11, indicating conserved amino acids).



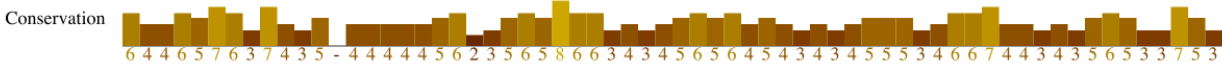
UUKV 641 FQTGKQRANKMFKFCLLMLEEDKARTEEIAATLSRYVMMEGFVSPPCIPKPKQKMIKELPNLARTK 704  
 HRTV 641 LREQVAITFLMSLEDKSTTEELVTLTRYSQMEGFVSPPLLPKPKQKMQVEKLEVPVLRRTKLQVFLFR 704  
 SFTSV 632 WLVRKPCSELRREQVGLTFLVLSLEDKSKTEEIIITLTRYTQMEGFVSPPLPKPKQKMLGKLDGGLR 695



UUKV 705 FQVWLI SRMLQTIIRVSDYPFK I TAGHKSANWTGMFNWVTGEP I ESTOKLISLFLYLGYLK NKEE 768  
 HRTV 705 RHLDAIVRVAASPFPIVARDGRV EWTGTFNALITGRSTGLENMNVNWI GYYKNKEESTELNALG 768  
 SFTSV 696 TKLQV - YLLRKHLD CMVRIASQP FNLI PREGRVEWGGTFHAISGRS T NLENMNVNSWY I GY YKNK 758



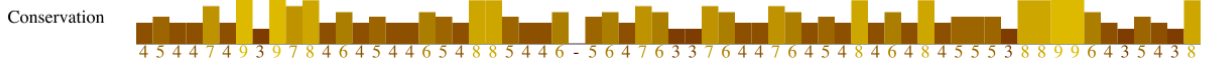
UUKV 769 SPERNASISGMYYKILEYEDKHPGRYTYLGLGDPSPDTRFHEYSISLKLHLCIHAEHDLRRNWG 832  
 HRTV 769 EMYKKIIVEIEAEKPASS EYLGWGD TSSPKRHEFSR SFLKSACISLEKEIEMRHGKSWKQSLER 832  
 SFTSV 759 EESTELNALGEM - YKKIVEMEEDK P S S P E F L G W G D T D S P K K H E F S R S F L R A A C S S L E R E I A Q R H 821



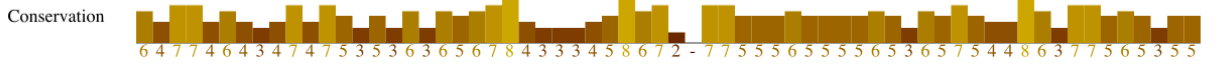
UUKV 833 ESFKAMISRDIVDAIASLDLRLATLTKASSNFNEEWYQKRGDGKTYHR SKVLEKVS KYVKKSSS 896  
 HRTV 833 VLKELGSKNLLDLATMKATS N F S K E W E A F S E V R T K E Y H R S K L L E K M A E L I E H G L M W Y V D A A G H A 896  
 SFTSV 822 GRQWKQNLERVLKEIGTK - NILDLASMKATSN F S K D W E L Y S E V Q T K E Y H R S K L L E K M A T L I E K 884



UUKV 897 HVHHIMEECLRKVESQGC M H V C L F E K K P O H G G L R E I Y V L G F E E R V V O L V I E T I A R Q I C K R F K S E T 960  
 HRTV 897 WKAVLDDKCMR I C L F K K N Q H G G L R E I Y V T N A N A R L V Q F G V E T M A R C V C E L S P H E T I A N P R L K S 960  
 SFTSV 885 GVMWYI DAVGQAWKAVLDDGCMR I C L - F K K N Q H G G L R E I Y V M D A N A R L V Q F G V E T M A R C V C E L 947



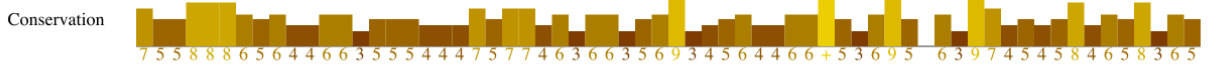
UUKV 961 LTNPKOKLAIPE THGLRAVKT CGIHHETVATSSDDAAKWNQCHHVTKFALMLCHF TDPLFHGF I 1024  
 HRTV 961 I I E N H G L K S A R Q L G Q G T I N V N S S N D A K K W S Q G H Y T T K L A M V L C W F M P A K F H R F I W A G I S M F R C K 1024  
 SFTSV 948 P H E T V A N P R L K N S I I E N H G L K S A R S L G P G S I N I - N S N D A K K W N Q G H Y T T K L A L V L C W F M P A K F 1010



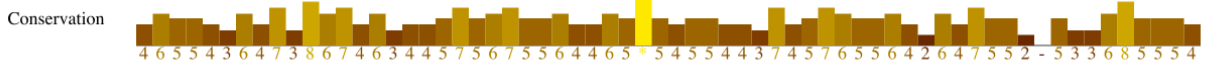
UUKV 1025 RGC SMFMKKRIMIDQSLIDIIDSHTTLETSDAYLQKIHRG YHGS LDDQPRWISRGGAFVQTE TEG 1088  
 HRTV 1025 KMMMDLRFLEKLS T K A N Q K T D D F R K D L A G A F H G N S D E V P W M T Q G A T Y L Q T E T G M M Q G I L H F T S 1088  
 SFTSV 1011 H R F I W A A I S M F R R K K M M V D L R F L A H L S T K S E R S S D P F R E - A M T D A F H G N R E V S W M D K G R T Y I K 1073



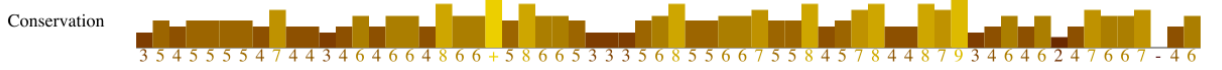
UUKV 1089 MMQGI LHYTSSLLHTLLQEWLRTFSQR FIRTRVSVDQRPDVLVDV LQS S D S G M M I S F P S T D K G 1152  
 HRTV 1089 LLHSCVQSFYKAYFLSRLKEGIAGKTIKAAIDVLEGSDDSAIMI SLKPASDNEEAMARFLTANL 1152  
 SFTSV 1074 TETGMMQGI LHF TSSLLHSCVQSFYKSYFVSKLKEGYMGESISGVVD - VI E G S D S A I M I S I R P 1136

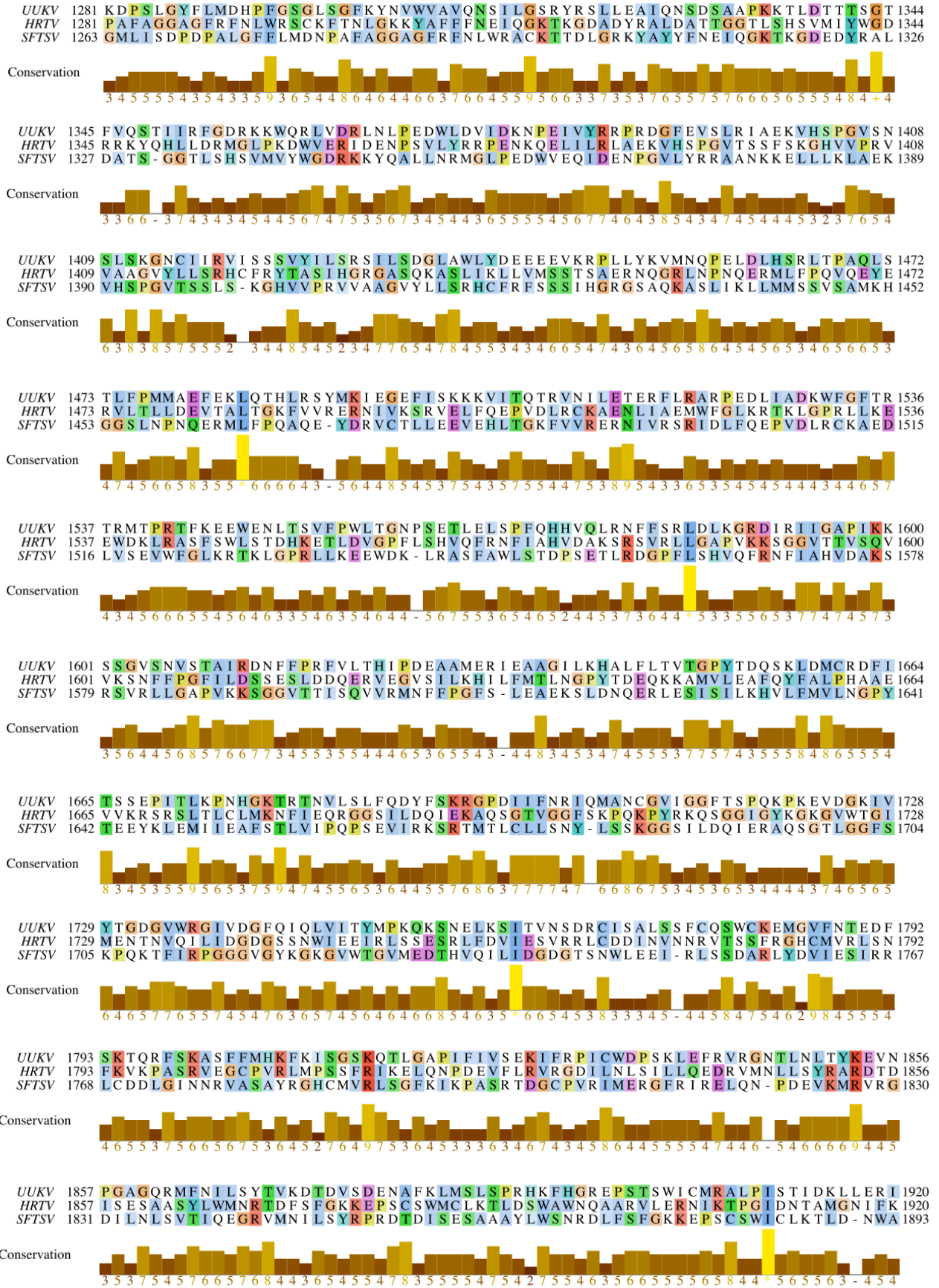


UUKV 1153 ATGKYR YLSALIFKYKVI GKYLGIYSVKS T N N T L H L L E F N S E F F F H I N H N R P L L R W I T A C D T 1216  
 HRTV 1153 LYSVRVINPLFGIYSSEKSTVN T L F C V E Y N S E F H F H K H L V R P T I R W V A A S H Q I S E S E A L A S R Q E 1216  
 SFTSV 1137 KSDMDEVRSRFFVANLLHSVKFLNPLFGIYSSSEKSTVNTVYCV EYNS E F H F H R H - L V R P T L R W I 1199



UUKV 1217 ISEQESLASRQEEMYNNTSVLEGGGSFSLVSVFCQFGQLLLHYTLLGMTVSPFLFLEYIKLVSEI 1280  
 HRTV 1217 DYANLLTQCLGGSSFS LTYLIQCAQLVHHYMLLGLCLHPLFGTFVGM L I E D P D P A L G F F I M D N 1280  
 SFTSV 1200 AASHQISETEALASRQEDYSNLLTQCLEGGASFS LTYLIQCAQLLHHYMLLGLCLHPLFGT - FM 1262





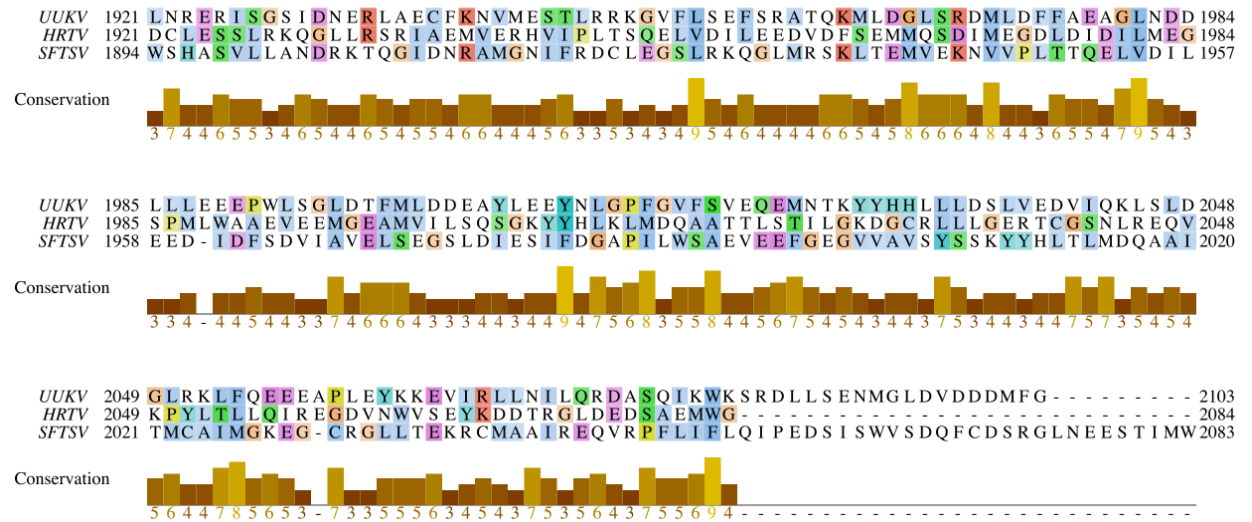


**Figure 10-2. Amino acid sequence alignment for UUKV, HRTV and SFTSV L proteins.**

UUKV, HRTV and SFTSV N amino acid sequences (GenBank accession numbers BAA01590.1, AFP33396.1 and AJD86038.1, respectively) were aligned using Jalview 2 (Waterhouse *et al.*, 2009). Residues are highlighted using the ClustalX colour scheme such that the colour of a particular residue depends on the residue type and its conservation (Thompson *et al.*, 1994). Blue: hydrophobic; Magenta: negative charge; Red: positive charge; Green: polar; Pink: cysteine; Orange: glycine; Yellow: proline; Cyan: hydrophobic. The conservation histogram below the alignment depicts conservation scores for each position (0-10, ‘\*’ refers to a score of 11, indicating conserved amino acids).

---

Chapter **11**

REFERENCES

---

# 11 References

- Acrani, G.O., Tilston-Lunel, N.L., Spiegel, M., Weidmann, M., Dilcher, M., Andrade da Silva, D.E., Nunes, M.R.T., Elliott, R.M.**, 2015. Establishment of a minigenome system for Oropouche virus reveals the S genome segment to be significantly longer than reported previously. *J Gen Virol* 96, 513–523. doi:10.1099/jgv.0.000005
- Albariño, C.G., Bird, B.H., Nichol, S.T.**, 2007. A shared transcription termination signal on negative and ambisense RNA genome segments of Rift Valley fever, sandfly fever Sicilian, and Toscana viruses. *J Virol* 81, 5246–5256. doi:10.1128/JVI.02778-06
- Alberts, B., Johnson, A., Lewis, J., Morgan, D., Raff, M., Roberts, K., Walter, P.**, 2014. **The Adaptive Immune System**, in: *Molecular Biology of the Cell*. New York.
- Albornoz, A., Hoffmann, A.B., Lozach, P.-Y., Tischler, N.D.**, 2016. Early Bunyavirus-Host Cell Interactions. *Viruses* 8, 143. doi:10.3390/v8050143
- Anderson, G.W., Smith, J.F.**, 1987. Immunoelectron microscopy of Rift Valley fever viral morphogenesis in primary rat hepatocytes. *Virology* 161, 91–100.
- Andrejeva, J., Childs, K.S., Young, D.F., Carlos, T.S., Stock, N., Goodbourn, S., Randall, R.E.**, 2004. The V proteins of paramyxoviruses bind the IFN-inducible RNA helicase, mda-5, and inhibit its activation of the IFN-beta promoter. *PNAS* 101, 17264–17269. doi:10.1073/pnas.0407639101
- Andrejeva, J., Young, D.F., Goodbourn, S., Randall, R.E.**, 2002. Degradation of STAT1 and STAT2 by the V proteins of simian virus 5 and human parainfluenza virus type 2, respectively: consequences for virus replication in the presence of alpha/beta and gamma interferons. *J Virol* 76, 2159–2167.
- Aquino, V.H., Moreli, M.L., Moraes Figueiredo, L.T.**, 2003. Analysis of oropouche virus L protein amino acid sequence showed the presence of an additional conserved region that could harbour an important role for the polymerase activity. *Arch. Virol.* 148, 19–28. doi:10.1007/s00705-002-0913-4
- Banninger, G., Reich, N.C.**, 2004. STAT2 nuclear trafficking. *J. Biol. Chem.* 279, 39199–39206. doi:10.1074/jbc.M400815200
- Bao, C.-J., Guo, X.-L., Qi, X., Hu, J.-L., Zhou, M.-H., Varma, J.K., Cui, L.-B., Yang, H.-T., Jiao, Y.-J., Klena, J.D., Li, L.-X., Tao, W.-Y., Li, X., Chen, Y., Zhu, Z., Xu, K., Shen, A.-H., Wu, T., Peng, H.-Y., Li, Z.-F., Shan, J., Shi, Z.-Y., Wang, H.**, 2011. A family cluster of infections by a newly recognized bunyavirus in eastern China, 2007: further evidence of person-to-person transmission. *Clin Infect Dis.* 53, 1208–1214. doi:10.1093/cid/cir732
- Barnwal, B., Karlberg, H., Mirazimi, A., Tan, Y.-J.**, 2016. The Non-structural Protein of Crimean-Congo Hemorrhagic Fever Virus Disrupts the Mitochondrial Membrane Potential and Induces Apoptosis. *J. Biol. Chem.* 291, 582–592. doi:10.1074/jbc.M115.667436

- Barr, J.N.**, 2007. Bunyavirus mRNA synthesis is coupled to translation to prevent premature transcription termination. *RNA* 13, 731–736. doi:10.1261/rna.436607
- Barr, J.N., Rodgers, J.W., Wertz, G.W.**, 2006. Identification of the Bunyamwera bunyavirus transcription termination signal. *J Gen Virol* 87, 189–198. doi:10.1099/vir.0.81355-0
- Bergeron, E., Zivcec, M., Chakrabarti, A.K., Nichol, S.T., Albariño, C.G., Spiropoulou, C.F.**, 2015. Recovery of Recombinant Crimean Congo Hemorrhagic Fever Virus Reveals a Function for Non-structural Glycoproteins Cleavage by Furin. *PLoS Pathogens* 11, e1004879. doi:10.1371/journal.ppat.1004879
- Bharaj, P., Wang, Y.E., Dawes, B.E., Yun, T.E., Park, A., Yen, B., Basler, C.F., Freiberg, A.N., Lee, B., Rajsbaum, R.**, 2016. The Matrix Protein of Nipah Virus Targets the E3-Ubiquitin Ligase TRIM6 to Inhibit the IKK $\epsilon$  Kinase-Mediated Type-I IFN Antiviral Response. *PLoS Pathogens* 12, e1005880. doi:10.1371/journal.ppat.1005880
- Billecocq, A., Gaudiard, N., Le May, N., Elliott, R.M., Flick, R., Bouloy, M.**, 2008. RNA polymerase I-mediated expression of viral RNA for the rescue of infectious virulent and avirulent Rift Valley fever viruses. *Virology* 378, 377–384. doi:10.1016/j.virol.2008.05.033
- Billecocq, A., Spiegel, M., Vialat, P., Kohl, A., Weber, F., Bouloy, M., Haller, O.**, 2004. NSs protein of Rift Valley fever virus blocks interferon production by inhibiting host gene transcription. *J Virol* 78, 9798–9806. doi:10.1128/JVI.78.18.9798-9806.2004
- Bird, B.H., Khristova, M.L., Rollin, P.E., Ksiazek, T.G., Nichol, S.T.**, 2007. Complete Genome Analysis of 33 Ecologically and Biologically Diverse Rift Valley Fever Virus Strains Reveals Widespread Virus Movement and Low Genetic Diversity due to Recent Common Ancestry. *J Virol* 81, 2805–2816. doi:10.1128/JVI.02095-06
- Bird, B.H., Maartens, L.H., Campbell, S., Erasmus, B.J., Erickson, B.R., Dodd, K.A., Spiropoulou, C.F., Cannon, D., Drew, C.P., Knust, B., McElroy, A.K., Khristova, M.L., Albariño, C.G., Nichol, S.T.**, 2011. Rift Valley fever virus vaccine lacking the NSs and NSm genes is safe, nonteratogenic, and confers protection from viremia, pyrexia, and abortion following challenge in adult and pregnant sheep. *J Virol* 85, 12901–12909. doi:10.1128/JVI.06046-11
- Bishop, D.H., Gay, M.E., Matsuoko, Y.**, 1983. Nonviral heterogeneous sequences are present at the 5' ends of one species of snowshoe hare bunyavirus S complementary RNA. *Nucleic Acids Research* 11, 6409–6418.
- Blakqori, G., Kochs, G., Haller, O., Weber, F.**, 2003. Functional L polymerase of La Crosse virus allows in vivo reconstitution of recombinant nucleocapsids. *J Gen Virol* 84, 1207–1214. doi:10.1099/vir.0.18876-0
- Blakqori, G., Weber, F.**, 2005. Efficient cDNA-Based Rescue of La Crosse Bunyaviruses Expressing or Lacking the Nonstructural Protein NSs. *J Virol* 79, 10420–10428. doi:10.1128/JVI.79.16.10420-10428.2005

- Borden, E.C., Sen, G.C., Uzé, G., Silverman, R.H., Ransohoff, R.M., Foster, G.R., Stark, G.R.,** 2007. Interferons at age 50: past, current and future impact on biomedicine. *Nat Rev Drug Discov* 6, 975–990. doi:10.1038/nrd2422
- Bosco-Lauth, A.M., Calvert, A.E., Root, J.J., Gidlewski, T., Bird, B.H., Bowen, R.A., Muehlenbachs, A., Zaki, S.R., Brault, A.C.,** 2016. Vertebrate Host Susceptibility to Heartland Virus. *Emerg. Infect. Dis.* 22, 2070–2077. doi:10.3201/eid2212.160472
- Bosco-Lauth, A.M., Panella, N.A., Root, J.J., Gidlewski, T., Lash, R.R., Harmon, J.R., Burkhalter, K.L., Godsey, M.S., Savage, H.M., Nicholson, W.L., Komar, N., Brault, A.C.,** 2015. Serological investigation of heartland virus (Bunyaviridae: Phlebovirus) exposure in wild and domestic animals adjacent to human case sites in Missouri 2012-2013. *Am. J. Trop. Med. Hyg.* 92, 1163–1167. doi:10.4269/ajtmh.14-0702
- Bouloy, M.,** 2011. Molecular biology of phleboviruses, in: *Bunyaviridae Molecular and Cellular Biology*. Caister Academic Press.
- Bouloy, M., Flick, R.,** 2009. Reverse genetics technology for Rift Valley fever virus: current and future applications for the development of therapeutics and vaccines. *Antiviral Res.* 84, 101–118. doi:10.1016/j.antiviral.2009.08.002
- Bouloy, M., Janzen, C., Vialat, P., Khun, H., Pavlovic, J., Huerre, M., Haller, O.,** 2001. Genetic evidence for an interferon-antagonistic function of rift valley fever virus nonstructural protein NSs. *J Virol* 75, 1371–1377. doi:10.1128/JVI.75.3.1371-1377.2001
- Bouloy, M., Pardigon, N., Vialat, P., Gerbaud, S., Girard, M.,** 1990. Characterization of the 5' and 3' ends of viral messenger RNAs isolated from BHK21 cells infected with Germiston virus (Bunyavirus). *Virology* 175, 50–58.
- Bouloy, M., Weber, F.,** 2010. Molecular Biology of Rift Valley Fever Virus. *The Open Virology Journal* 4, 8–14. doi:10.2174/1874357901004010008
- Bowden, T.A., Bitto, D., McLees, A., Yeromonahos, C., Elliott, R.M., Huiskonen, J.T.,** 2013. Orthobunyavirus ultrastructure and the curious tripodal glycoprotein spike. *PLoS Pathogens* 9, e1003374. doi:10.1371/journal.ppat.1003374
- Brennan, B., Li, P., Elliott, R.M.,** 2011a. Generation and characterization of a recombinant Rift Valley fever virus expressing a V5 epitope-tagged RNA-dependent RNA polymerase. *J Gen Virol* 92, 2906–2913. doi:10.1099/vir.0.036749-0
- Brennan, B., Li, P., Zhang, S., Li, A., Liang, M., Li, D., Elliott, R.M.,** 2015. Reverse genetics system for severe fever with thrombocytopenia syndrome virus. *J Virol* 89, 3026–3037. doi:10.1128/JVI.03432-14
- Brennan, B., Welch, S.R., Elliott, R.M.,** 2014. The Consequences of Reconfiguring the Ambisense S Genome Segment of Rift Valley Fever Virus on Viral Replication in Mammalian and Mosquito Cells and for Genome Packaging. *PLoS Pathogens* 10, e1003922. doi:10.1371/journal.ppat.1003922
- Brennan, B., Welch, S.R., McLees, A., Elliott, R.M.,** 2011b. Creation of a recombinant

- Rift Valley fever virus with a two-segmented genome. *J Virol*.
- Bridgen, A., Elliott, R.M.**, 1996. Rescue of a segmented negative-strand RNA virus entirely from cloned complementary DNAs. *PNAS* 93, 15400–15404.
- Bridgen, A., Weber, F., Fazakerley, J.K., Elliott, R.M.**, 2001. Bunyamwera bunyavirus nonstructural protein NSs is a nonessential gene product that contributes to viral pathogenesis. *PNAS* 98, 664–669. doi:10.1073/pnas.98.2.664
- Briese, T., Bird, B., Kapoor, V., Nichol, S.T., Lipkin, W.I.**, 2006. Batai and Ngari viruses: M segment reassortment and association with severe febrile disease outbreaks in East Africa. *J Virol* 80, 5627–5630. doi:10.1128/JVI.02448-05
- Briese, T., Calisher, C.H., Higgs, S.**, 2013. Viruses of the family Bunyaviridae: are all available isolates reassortants? *Virology* 446, 207–216. doi:10.1016/j.virol.2013.07.030
- Buchholz, U.J., Finke, S., Conzelmann, K.K.**, 1999. Generation of bovine respiratory syncytial virus (BRSV) from cDNA: BRSV NS2 is not essential for virus replication in tissue culture, and the human RSV leader region acts as a functional BRSV genome promoter. *J Virol* 73, 251–259.
- Calisher, C.H., Goodpasture, H.C.**, 1975. Human infection with Bhanja virus. *Am. J. Trop. Med. Hyg.* 24, 1040–1042.
- Chaudhary, V., Zhang, S., Yuen, K.-S., Li, C., Lui, P.-Y., Fung, S.-Y., Wang, P.-H., Chan, C.-P., Li, D., Kok, K.-H., Liang, M., Jin, D.-Y.**, 2015. Suppression of type I and type III IFN signalling by NSs protein of severe fever with thrombocytopenia syndrome virus through inhibition of STAT1 phosphorylation and activation. *J Gen Virol* 96, 3204–3211. doi:10.1099/jgv.0.000280
- Chen, J., Baig, E., Fish, E.N.**, 2004. Diversity and Relatedness Among the Type I Interferons. *Journal of Interferon & Cytokine Research* 24, 687–698. doi:10.1089/1079990042722891
- Chevalier, V., Pépin, M., Plée, L., Lancelot, R.**, 2010. Rift Valley fever--a threat for Europe? *Euro Surveill.* 15, 19506.
- Choi, Y., Kwon, Y.-C., Kim, S.-I., Park, J.-M., Lee, K.-H., Ahn, B.-Y.**, 2008. A hantavirus causing hemorrhagic fever with renal syndrome requires gC1qR/p32 for efficient cell binding and infection. *Virology* 381, 178–183. doi:10.1016/j.virol.2008.08.035
- Chung, H.C., Nguyen, V.G., Goede, D., Park, C.H., Kim, A.R., Moon, H.J., Park, S.J., Kim, H.K., Park, B.K.**, 2014. Gouleako and Herbert viruses in pigs, Republic of Korea, 2013. *Emerg. Infect. Dis.* 20, 2072–2075. doi:10.3201/eid2012.131742
- Collao, X., Palacios, G., de Ory, F., Sanbonmatsu, S., Pérez-Ruiz, M., Navarro, J.M., Molina, R., Hutchison, S.K., Lipkin, W.I., Tenorio, A., Sánchez-Seco, M.P.**, 2010. Granada virus: a natural phlebovirus reassortant of the sandfly fever Naples serocomplex with low seroprevalence in humans. *Am. J. Trop. Med. Hyg.* 83, 760–765. doi:10.4269/ajtmh.2010.09-0697

- Crabtree, M.B., Kent Crockett, R.J., Bird, B.H., Nichol, S.T., Erickson, B.R., Biggerstaff, B.J., Horiuchi, K., Miller, B.R.,** 2012. Infection and transmission of Rift Valley fever viruses lacking the NSs and/or NSm genes in mosquitoes: potential role for NSm in mosquito infection. *PLoS Negl Trop Dis* 6, e1639. doi:10.1371/journal.pntd.0001639
- Crispin, M., Harvey, D.J., Bitto, D., Halldorsson, S., Bonomelli, C., Edgeworth, M., Scrivens, J.H., Huiskonen, J.T., Bowden, T.A.,** 2014. Uukuniemi Phlebovirus assembly and secretion leave a functional imprint on the virion glycome. *J Virol* 88, 10244–10251. doi:10.1128/JVI.01662-14
- Cusi, M.,** 2010. Toscana Virus Epidemiology: From Italy to Beyond. *The Open Virology Journal* 4, 22–28. doi:10.2174/1874357901004010022
- Cyr, N., la Fuente, de, C., Lecoq, L., Guendel, I., Chabot, P.R., Kehn-Hall, K., Omichinski, J.G.,** 2015. A  $\Omega$ XaV motif in the Rift Valley fever virus NSs protein is essential for degrading p62, forming nuclear filaments and virulence. *Proc. Natl. Acad. Sci. U.S.A.* 112, 6021–6026. doi:10.1073/pnas.1503688112
- Darnell, J.E., Kerr, I.M., Stark, G.R.,** 1994. Jak-STAT pathways and transcriptional activation in response to IFNs and other extracellular signaling proteins. *Science* 264, 1415–1421.
- de Boer, S.M., Kortekaas, J., de Haan, C.A.M., Rottier, P.J.M., Moormann, R.J.M., Bosch, B.J.,** 2012a. Heparan sulfate facilitates Rift Valley fever virus entry into the cell. *J Virol* 86, 13767–13771. doi:10.1128/JVI.01364-12
- de Boer, S.M., Kortekaas, J., Spel, L., Rottier, P.J.M., Moormann, R.J.M., Bosch, B.J.,** 2012b. Acid-activated structural reorganization of the Rift Valley fever virus Gc fusion protein. *J Virol* 86, 13642–13652. doi:10.1128/JVI.01973-12
- de Haro, C., Méndez, R., Santoyo, J.,** 1996. The eIF-2 $\alpha$  kinases and the control of protein synthesis. *The FASEB Journal* 10, 1378–1387.
- de Weerd, N.A., Nguyen, T.,** 2012. The interferons and their receptors--distribution and regulation. *Immunol. Cell Biol.* 90, 483–491. doi:10.1038/icb.2012.9
- Deng, B., Zhang, S., Geng, Y., Zhang, Y., Wang, Y., Yao, W., Wen, Y., Cui, W., Zhou, Y., Gu, Q., Wang, W., Wang, Y., Shao, Z., Wang, Y., Li, C., Wang, D., Zhao, Y., Liu, P.,** 2012. Cytokine and Chemokine Levels in Patients with Severe Fever with Thrombocytopenia Syndrome Virus. *PLoS ONE* 7, e41365. doi:10.1371/journal.pone.0041365
- Der, S.D., Zhou, A., Williams, B.R., Silverman, R.H.,** 1998. Identification of genes differentially regulated by interferon alpha, beta, or gamma using oligonucleotide arrays. *PNAS* 95, 15623–15628.
- Dessau, M., Modis, Y.,** 2013. Crystal structure of glycoprotein C from Rift Valley fever virus. *Proc. Natl. Acad. Sci. U.S.A.* 110, 1696–1701. doi:10.1073/pnas.1217780110
- Devignot, S., Bergeron, E., Nichol, S., Mirazimi, A., Weber, F.,** 2015. A virus-like particle system identifies the endonuclease domain of Crimean-Congo hemorrhagic

- fever virus. *J Virol* 89, 5957–5967. doi:10.1128/JVI.03691-14
- Di Bonito, P., Nicoletti, L., Mochi, S., Accardi, L., Marchi, A., Giorgi, C.,** 1999. Immunological characterization of Toscana virus proteins. *Arch. Virol.* 144, 1947–1960.
- Dong, H., Li, P., Elliott, R.M., Dong, C.,** 2013. Structure of Schmallenberg orthobunyavirus nucleoprotein suggests a novel mechanism of genome encapsidation. *J Virol* 87, 5593–5601. doi:10.1128/JVI.00223-13
- Dragan, A.I., Hargreaves, V.V., Makeyeva, E.N., Privalov, P.L.,** 2007. Mechanisms of activation of interferon regulator factor 3: the role of C-terminal domain phosphorylation in IRF-3 dimerization and DNA binding. *Nucleic Acids Research* 35, 3525–3534. doi:10.1093/nar/gkm142
- Dunn, E.F., Pritlove, D.C., Jin, H., Elliott, R.M.,** 1995. Transcription of a recombinant bunyavirus RNA template by transiently expressed bunyavirus proteins. *Virology* 211, 133–143. doi:10.1006/viro.1995.1386
- Eifan, S.A., Elliott, R.M.,** 2009. Mutational Analysis of the Bunyamwera Orthobunyavirus Nucleocapsid Protein Gene. *J Virol* 83, 11307–11317. doi:10.1128/JVI.01460-09
- Elliott, R.M.,** 2014. Orthobunyaviruses: recent genetic and structural insights. *Nat. Rev. Microbiol.* 12, 673–685. doi:10.1038/nrmicro3332
- Elliott, R.M.,** 2013. *The Bunyaviridae*. Springer Science & Business Media, Boston, MA. doi:10.1007/978-1-4899-1364-7
- Elliott, R.M.,** 2009. Bunyaviruses and climate change. *Clin. Microbiol. Infect.* 15, 510–517. doi:10.1111/j.1469-0691.2009.02849.x
- Elliott, R.M., Blakqori, G.,** 2012. Molecular Biology of Orthobunyaviruses., in: Plyusnin, A., Elliott, R.M. (Eds.), *Bunyaviridae Molecular and Cellular Biology*. Norfolk, UK, pp. 200–223.
- Elliott, R.M., Blakqori, G.,** 2011. Molecular and Cellular Biology, in: Plyusnin, A., Elliott, R.M. (Eds.), *Bunyaviridae*. Horizon Scientific Press, pp. 1–39.
- Elliott, R.M., Blakqori, G., van Knippenberg, I.C., Koudriakova, E., Li, P., McLees, A., Shi, X., Szemiel, A.M.,** 2013. Establishment of a reverse genetics system for Schmallenberg virus, a newly emerged orthobunyavirus in Europe. *J Gen Virol* 94, 851–859. doi:10.1099/vir.0.049981-0
- Elliott, R.M., Brennan, B.,** 2014. Emerging phleboviruses. *Curr Opin Virol* 5, 50–57. doi:10.1016/j.coviro.2014.01.011
- Elliott, R.M., Dunn, E., Simons, J.F., Pettersson, R.F.,** 1992. Nucleotide sequence and coding strategy of the Uukuniemi virus L RNA segment. *J Gen Virol* 73 ( Pt 7), 1745–1752. doi:10.1099/0022-1317-73-7-1745
- Elliott, R.M., Schmaljohn, C.S.,** 2013. *Bunyaviridae*, in: Knipe, D.E., Howley, P.M. (Eds.), *Fields Virology*. Philadelphia, USA, pp. 1244–1282.

- Elroy-Stein, O., Moss, B.**, 1990. Cytoplasmic expression system based on constitutive synthesis of bacteriophage T7 RNA polymerase in mammalian cells. *PNAS* 87, 6743–6747. doi:10.1073/pnas.87.17.6743
- Fagerlund, R., Mélen, K., Kinnunen, L., Julkunen, I.**, 2002. Arginine/lysine-rich nuclear localization signals mediate interactions between dimeric STATs and importin alpha 5. *J. Biol. Chem.* 277, 30072–30078. doi:10.1074/jbc.M202943200
- Ferron, F., Li, Z., Danek, E.I., Luo, D., Wong, Y., Coutard, B., Lantéz, V., Charrel, R., Canard, B., Walz, T., Lescar, J.**, 2011. The hexamer structure of Rift Valley fever virus nucleoprotein suggests a mechanism for its assembly into ribonucleoprotein complexes. *PLoS Pathogens* 7, e1002030. doi:10.1371/journal.ppat.1002030
- Fitzgerald, K.A., McWhirter, S.M., Faia, K.L., Rowe, D.C., Latz, E., Golenbock, D.T., Coyle, A.J., Liao, S.-M., Maniatis, T.**, 2003. IKKepsilon and TBK1 are essential components of the IRF3 signaling pathway. *Nat. Immunol.* 4, 491–496. doi:10.1038/ni921
- Flick, K., Katz, A., Overby, A., Feldmann, H., Pettersson, R.F., Flick, R.**, 2004. Functional analysis of the noncoding regions of the Uukuniemi virus (Bunyaviridae) RNA segments. *J Virol* 78, 11726–11738. doi:10.1128/JVI.78.21.11726-11738.2004
- Flick, R., Elgh, F., Pettersson, R.F.**, 2002. Mutational analysis of the Uukuniemi virus (Bunyaviridae family) promoter reveals two elements of functional importance. *J Virol* 76, 10849–10860. doi:10.1128/JVI.76.21.10849-10860.2002
- Flick, R., Pettersson, R.F.**, 2001. Reverse genetics system for Uukuniemi virus (Bunyaviridae): RNA polymerase I-catalyzed expression of chimeric viral RNAs. *J Virol* 75, 1643–1655. doi:10.1128/JVI.75.4.1643-1655.2001
- Fodor, E., Devenish, L., Engelhardt, O.G., Palese, P., Brownlee, G.G., Garcia-Sastre, A.**, 1999. Rescue of influenza A virus from recombinant DNA. *J Virol* 73, 9679–9682.
- Foster, D.N.**, 1998. Development of a spontaneously immortalized chicken embryo fibroblastic cell line. *Virology*.
- Freiberg, A., Flick, R.**, 2013. Rift Valley Fever Virus and Hemorrhagic Fever, in: *Viral Hemorrhagic Fevers*. CRC Press, pp. 379–404. doi:10.1201/b15172-24
- Freiberg, A.N., Sherman, M.B., Morais, M.C., Holbrook, M.R., Watowich, S.J.**, 2008. Three-dimensional organization of Rift Valley fever virus revealed by cryoelectron tomography. *J Virol* 82, 10341–10348. doi:10.1128/JVI.01191-08
- Gack, M.U., Shin, Y.C., Joo, C.-H., Urano, T., Liang, C., Sun, L., Takeuchi, O., Akira, S., Chen, Z., Inoue, S., Jung, J.U.**, 2007. TRIM25 RING-finger E3 ubiquitin ligase is essential for RIG-I-mediated antiviral activity. *Nature* 446, 916–920. doi:10.1038/nature05732
- Gahmberg, N.**, 1984. Characterization of Two Recombination-Complementation Groups of Uukuniemi Virus Temperature-sensitive Mutants. *J Gen Virol* 65, 1079–1090. doi:10.1099/0022-1317-65-6-1079

- García-Sastre, A., Biron, C.A.**, 2006. Type 1 interferons and the virus-host relationship: a lesson in détente. *Science* 312, 879–882. doi:10.1126/science.1125676
- Gauci, P.J., McAllister, J., Mitchell, I.R., St George, T.D., Cybinski, D.H., Davis, S.S., Gubala, A.J.**, 2015. Hunter Island Group Phlebovirus in Ticks, Australia. *Emerg. Infect. Dis.* 21, 2246–2248. doi:10.3201/eid2112.141303
- Gauliard, N., Billecocq, A., Flick, R., Bouloy, M.**, 2006. Rift Valley fever virus noncoding regions of L, M and S segments regulate RNA synthesis. *Virology* 351, 170–179. doi:10.1016/j.virol.2006.03.018
- Gavrilovskaya, I.N., Brown, E.J., Ginsberg, M.H., Mackow, E.R.**, 1999. Cellular entry of hantaviruses which cause hemorrhagic fever with renal syndrome is mediated by beta3 integrins. *J Virol* 73, 3951–3959.
- Gavrilovskaya, I.N., Shepley, M., Shaw, R., Ginsberg, M.H., Mackow, E.R.**, 1998. beta3 Integrins mediate the cellular entry of hantaviruses that cause respiratory failure. *PNAS* 95, 7074–7079.
- Gerdes, G.H.**, 2004. Rift Valley fever. *Rev. - Off. Int. Epizoot.* 23, 613–623.
- Gerlach, P., Malet, H., Cusack, S., Reguera, J.**, 2015. Structural Insights into Bunyavirus Replication and Its Regulation by the vRNA Promoter. *Cell* 161, 1267–1279. doi:10.1016/j.cell.2015.05.006
- Gey, G.O., Coffman, W.D.**, 1952. Tissue culture studies of the proliferative capacity of cervical carcinoma and normal epithelium. *Cancer* .... doi:10.1002/ar.1090010503/abstract
- Goldsmith, C.S., Elliott, L.H., Peters, C.J., Zaki, S.R.**, 1995. Ultrastructural characteristics of Sin Nombre virus, causative agent of hantavirus pulmonary syndrome. *Arch. Virol.* 140, 2107–2122.
- Goodbourn, S., Didcock, L., Randall, R.E.**, 2000. Interferons: cell signalling, immune modulation, antiviral response and virus countermeasures. *J Gen Virol* 81, 2341–2364. doi:10.1099/0022-1317-81-10-2341
- Gori-Savellini, G., Valentini, M., Cusi, M.G.**, 2013. Toscana Virus NSs Protein Inhibits the Induction of Type I Interferon by Interacting with RIG-I. *J Virol* 87, 6660–6667. doi:10.1128/JVI.03129-12
- Gori-Savellini, G., Weber, F., Terrosi, C., Habjan, M., Martorelli, B., Cusi, M.G.**, 2010. Toscana virus induces interferon although its NSs protein reveals antagonistic activity. *J Gen Virol* 92, 71–79. doi:10.1099/vir.0.025999-0
- Gowen, B.B., Westover, J.B., Miao, J., Van Wettere, A.J., Rigas, J.D., Hickerson, B.T., Jung, K.-H., Li, R., Conrad, B.L., Nielson, S., Furuta, Y., Wang, Z.**, 2016. Modeling severe fever with thrombocytopenia syndrome virus infection in golden Syrian hamsters: Importance of STAT2 in preventing disease and effective treatment with favipiravir. *J Virol* 91, e01942–16. doi:10.1128/JVI.01942-16
- Gupta, S.C., Sundaram, C., Reuter, S., Aggarwal, B.B.**, 2010. Inhibiting NF-κB activation by small molecules as a therapeutic strategy. *Biochim. Biophys. Acta* 1799,

775–787. doi:10.1016/j.bbagr.2010.05.004

- Habjan, M., Penski, N., Spiegel, M., Weber, F.,** 2008. T7 RNA polymerase-dependent and -independent systems for cDNA-based rescue of Rift Valley fever virus. *J Gen Virol* 89, 2157–2166. doi:10.1099/vir.0.2008/002097-0
- Habjan, M., Penski, N., Wagner, V., Spiegel, M., Överby, A.K., Kochs, G., Huiskonen, J.T., Weber, F.,** 2009a. Efficient production of Rift Valley fever virus-like particles: The antiviral protein MxA can inhibit primary transcription of bunyaviruses. *Virology* 385, 400–408. doi:10.1016/j.virol.2008.12.011
- Habjan, M., Pichlmair, A., Elliott, R.M., Överby, A.K., Glatter, T., Gstaiger, M., Superti-Furga, G., Unger, H., Weber, F.,** 2009b. NSs protein of rift valley fever virus induces the specific degradation of the double-stranded RNA-dependent protein kinase. *J Virol* 83, 4365–4375. doi:10.1128/JVI.02148-08
- Hale, B.G., Knebel, A., Botting, C.H., Galloway, C.S., Precious, B.L., Jackson, D., Elliott, R.M., Randall, R.E.,** 2009. CDK/ERK-mediated phosphorylation of the human influenza A virus NS1 protein at threonine-215. *Virology* 383, 6–11. doi:10.1016/j.virol.2008.10.002
- Halldorsson, S., Behrens, A.-J., Harlos, K., Huiskonen, J.T., Elliott, R.M., Crispin, M., Brennan, B., Bowden, T.A.,** 2016. Structure of a phleboviral envelope glycoprotein reveals a consolidated model of membrane fusion. *Proc. Natl. Acad. Sci. U.S.A.* 113, 7154–7159. doi:10.1073/pnas.1603827113
- Haller, O., Kochs, G., Weber, F.,** 2007. Interferon, Mx, and viral countermeasures. *Cytokine Growth Factor Rev.* 18, 425–433. doi:10.1016/j.cytogfr.2007.06.001
- Hart, T.J., Kohl, A., Elliott, R.M.,** 2009. Role of the NSs protein in the zoonotic capacity of Orthobunyaviruses. *Zoonoses Public Health* 56, 285–296. doi:10.1111/j.1863-2378.2008.01166.x
- Hemmersbach-Miller, M., Parola, P., Charrel, R.N., Paul Durand, J., Brouqui, P.,** 2004. Sandfly fever due to Toscana virus: an emerging infection in southern France. *Eur. J. Intern. Med.* 15, 316–317. doi:10.1016/j.ejim.2004.05.006
- Hepojoki, J., Strandin, T., Vaheri, A., Lankinen, H.,** 2010. Interactions and oligomerization of hantavirus glycoproteins. *J Virol* 84, 227–242. doi:10.1128/JVI.00481-09
- Hewlett, M.J., Pettersson, R.F., Baltimore, D.,** 1977. Circular forms of Uukuniemi virion RNA: an electron microscopic study. *J Virol* 21, 1085–1093.
- Hilton, L., Moganeradj, K., Zhang, G., Chen, Y.-H., Randall, R.E., McCauley, J.W., Goodbourn, S.,** 2006. The NPro product of bovine viral diarrhea virus inhibits DNA binding by interferon regulatory factor 3 and targets it for proteasomal degradation. *J Virol* 80, 11723–11732. doi:10.1128/JVI.01145-06
- Himly, M., Foster, D.N., Bottoli, I., Iacovoni, J.S., Vogt, P.K.,** 1998. The DF-1 Chicken Fibroblast Cell Line: Transformation Induced by Diverse Oncogenes and Cell Death Resulting from Infection by Avian Leukosis Viruses. *Virology* 248, 295–304.

doi:10.1006/viro.1998.9290

- Hoffmann, B., Scheuch, M., Höper, D., Jungblut, R., Holsteg, M., Schirrmeier, H., Eschbaumer, M., Goller, K.V., Wernike, K., Fischer, M., Breithaupt, A., Mettenleiter, T.C., Beer, M.,** 2012. Novel orthobunyavirus in Cattle, Europe, 2011. *Emerg. Infect. Dis.* 18, 469–472. doi:10.3201/eid1803.111905
- Hoffmann, H.-H., Schneider, W.M., Rice, C.M.,** 2015. Interferons and viruses: an evolutionary arms race of molecular interactions. *Trends Immunol.* 36, 124–138. doi:10.1016/j.it.2015.01.004
- Hofmann, H., Li, X., Zhang, X., Liu, W., Köhl, A., Kaup, F., Soldan, S.S., González-Scarano, F., Weber, F., He, Y., Pöhlmann, S.,** 2013. Severe fever with thrombocytopenia virus glycoproteins are targeted by neutralizing antibodies and can use DC-SIGN as a receptor for pH-dependent entry into human and animal cell lines. *J Virol* 87, 4384–4394. doi:10.1128/JVI.02628-12
- Hollidge, B.S., Nedelsky, N.B., Salzano, M.-V., Fraser, J.W., González-Scarano, F., Soldan, S.S.,** 2012. Orthobunyavirus entry into neurons and other mammalian cells occurs via clathrin-mediated endocytosis and requires trafficking into early endosomes. *J Virol* 86, 7988–8001. doi:10.1128/JVI.00140-12
- Honda, K., Taniguchi, T.,** 2006. IRFs: master regulators of signalling by Toll-like receptors and cytosolic pattern-recognition receptors. *Nat. Rev. Immunol.* 6, 644–658. doi:10.1038/nri1900
- Hoogstraal, H., Roberts, F.H., Kohls, G.M., Tipton, V.J.,** 1968. Review of *Haemaphysalis (kaiseriana) Longicornis Neumann (resurrected)* of Australia, New Zealand, New Caledonia, Fiji, Japan, Korea, and Northeastern China and USSR, and its parthenogenetic and bisexual populations (Ixodoidea, Ixodidae). *J. Parasitol.* 54, 1197–1213.
- Hornung, V., Ellegast, J., Kim, S., Brzózka, K., Jung, A., Kato, H., Poeck, H., Akira, S., Conzelmann, K.-K., Schlee, M., Endres, S., Hartmann, G.,** 2006. 5'-Triphosphate RNA Is the Ligand for RIG-I. *Science* 314, 994–997. doi:10.1126/science.1132505
- Hou, F., Sun, L., Zheng, H., Skaug, B., Jiang, Q.-X., Chen, Z.J.,** 2011. MAVS Forms Functional Prion-like Aggregates to Activate and Propagate Antiviral Innate Immune Response. *Cell* 146, 841. doi:10.1016/j.cell.2011.08.013
- Hu, J., Haseebuddin, M., Young, M., Colburn, N.H.,** 2005. Suppression of p65 phosphorylation coincides with inhibition of I $\kappa$ B $\alpha$  polyubiquitination and degradation. *Molecular Carcinogenesis* 44, 274–284. doi:10.1002/mc.20142
- Hu, X., Ivashkiv, L.B.,** 2009. Cross-regulation of signaling pathways by interferon-gamma: implications for immune responses and autoimmune diseases. *Immunity* 31, 539–550. doi:10.1016/j.immuni.2009.09.002
- Hubálek, Z.,** 2009. Biogeography of tick-borne bhanja virus (bunyaviridae) in europe. *Interdiscip Perspect Infect Dis* 2009, 372691–11. doi:10.1155/2009/372691

- Hubálek, Z., Rudolf, I.**, 2012. Tick-borne viruses in Europe. *Parasitol. Res.* 111, 9–36. doi:10.1007/s00436-012-2910-1
- Huiskonen, J.T., Hepojoki, J., Laurinmäki, P., Vaheri, A., Lankinen, H., Butcher, S.J., Grunewald, K.**, 2010. Electron cryotomography of Tula hantavirus suggests a unique assembly paradigm for enveloped viruses. *J Virol* 84, 4889–4897. doi:10.1128/JVI.00057-10
- Huiskonen, J.T., Överby, A.K., Weber, F., Grunewald, K.**, 2009. Electron cryo-microscopy and single-particle averaging of Rift Valley fever virus: evidence for GN-GC glycoprotein heterodimers. *J Virol* 83, 3762–3769. doi:10.1128/JVI.02483-08
- Ihara, T., Smith, J., Dalrymple, J.M., Bishop, D.H.**, 1985. Complete sequences of the glycoproteins and M RNA of Punta Toro phlebovirus compared to those of Rift Valley fever virus. *Virology* 144, 246–259.
- Ikegami, T., Makino, S.**, 2011. The pathogenesis of Rift Valley fever. *Viruses* 3, 493–519. doi:10.3390/v3050493
- Ikegami, T., Narayanan, K., Won, S., Kamitani, W., Peters, C.J., Makino, S.**, 2009a. Dual functions of Rift Valley fever virus NSs protein: inhibition of host mRNA transcription and post-transcriptional downregulation of protein kinase PKR. *Ann. N. Y. Acad. Sci.* 1171 Suppl 1, E75–85. doi:10.1111/j.1749-6632.2009.05054.x
- Ikegami, T., Narayanan, K., Won, S., Kamitani, W., Peters, C.J., Makino, S.**, 2009b. Rift Valley fever virus NSs protein promotes post-transcriptional downregulation of protein kinase PKR and inhibits eIF2 $\alpha$  phosphorylation. *PLoS Pathogens* 5, e1000287. doi:10.1371/journal.ppat.1000287
- Ikegami, T., Peters, C.J., Makino, S.**, 2005a. Rift valley fever virus nonstructural protein NSs promotes viral RNA replication and transcription in a minigenome system. *J Virol* 79, 5606–5615. doi:10.1128/JVI.79.9.5606-5615.2005
- Ikegami, T., Won, S., Peters, C.J., Makino, S.**, 2007. Characterization of Rift Valley fever virus transcriptional terminations. *J Virol* 81, 8421–8438. doi:10.1128/JVI.02641-06
- Ikegami, T., Won, S., Peters, C.J., Makino, S.**, 2006. Rescue of infectious rift valley fever virus entirely from cDNA, analysis of virus lacking the NSs gene, and expression of a foreign gene. *J Virol* 80, 2933–2940. doi:10.1128/JVI.80.6.2933-2940.2006
- Ikegami, T., Won, S., Peters, C.J., Makino, S.**, 2005b. Rift Valley fever virus NSs mRNA is transcribed from an incoming anti-viral-sense S RNA segment. *J Virol* 79, 12106–12111. doi:10.1128/JVI.79.18.12106-12111.2005
- Isaacs, A., Lindenmann, J.**, 1957. Virus interference. I. The interferon. *Proc. R. Soc. Lond., B, Biol. Sci.* 147, 258–267.
- Jääskeläinen, K.M., Kaukinen, P., Minskaya, E.S., Plyusnina, A., Vapalahti, O., Elliott, R.M., Weber, F., Vaheri, A., Plyusnin, A.**, 2007. Tula and Puumala hantavirus NSs ORFs are functional and the products inhibit activation of the interferon-beta promoter. *J. Med. Virol.* 79, 1527–1536. doi:10.1002/jmv.20948

- Jiang, X.L., Zhang, S., Jiang, M., Bi, Z.Q., Liang, M.F., Ding, S.J., Wang, S.W., Liu, J.Y., Zhou, S.Q., Zhang, X.M., Li, D.X., Xu, A.Q.**, 2015. A cluster of person-to-person transmission cases caused by SFTS virus in Penglai, China. *Clin. Microbiol. Infect.* 21, 274–279. doi:10.1016/j.cmi.2014.10.006
- Jin, C., Jiang, H., Liang, M., Han, Y., Gu, W., Zhang, F., Zhu, H., Wu, W., Chen, T., Li, C., Zhang, W., Zhang, Q., Qu, J., Wei, Q., Qin, C., Li, D.**, 2015. SFTS virus infection in nonhuman primates. *J Infect Dis.* 211, 915–925. doi:10.1093/infdis/jiu564
- Jin, C., Liang, M., Ning, J., Gu, W., Jiang, H., Wu, W., Zhang, F., Li, C., Zhang, Q., Zhu, H., Chen, T., Han, Y., Zhang, W., Zhang, S., Wang, Q., Sun, L., Liu, Q., Li, J., Wang, T., Wei, Q., Wang, S., Deng, Y., Qin, C., Li, D.**, 2012. Pathogenesis of emerging severe fever with thrombocytopenia syndrome virus in C57/BL6 mouse model. *Proc. Natl. Acad. Sci. U.S.A.* 109, 10053–10058. doi:10.1073/pnas.1120246109
- Jin, H., Elliott, R.M.**, 1993a. Characterization of Bunyamwera virus S RNA that is transcribed and replicated by the L protein expressed from recombinant vaccinia virus. *J Virol* 67, 1396–1404.
- Jin, H., Elliott, R.M.**, 1993b. Non-viral sequences at the 5' ends of Dugbe nairovirus S mRNAs. *J Gen Virol* 74 ( Pt 10), 2293–2297. doi:10.1099/0022-1317-74-10-2293
- Jin, H., Elliott, R.M.**, 1991. Expression of functional Bunyamwera virus L protein by recombinant vaccinia viruses. *J Virol* 65, 4182–4189.
- Jin, M., Park, J., Lee, S., Park, B., Shin, J., Song, K.-J., Ahn, T.-I., Hwang, S.-Y., Ahn, B.-Y., Ahn, K.**, 2002. Hantaan virus enters cells by clathrin-dependent receptor-mediated endocytosis. *Virology* 294, 60–69. doi:10.1006/viro.2001.1303
- Johnson, K.N., Zeddam, J.L., Ball, L.A.**, 2000. Characterization and construction of functional cDNA clones of Pariacoto virus, the first Alphanodavirus isolated outside Australasia. *J Virol* 74, 5123–5132.
- Kading, R.C., Crabtree, M.B., Bird, B.H., Nichol, S.T., Erickson, B.R., Horiuchi, K., Biggerstaff, B.J., Miller, B.R.**, 2014. Deletion of the NSm virulence gene of Rift Valley fever virus inhibits virus replication in and dissemination from the midgut of *Aedes aegypti* mosquitoes. *PLoS Negl Trop Dis* 8, e2670. doi:10.1371/journal.pntd.0002670
- Kainulainen, M., Habjan, M., Hubel, P., Busch, L., Lau, S., Colinge, J., Superti-Furga, G., Pichlmair, A., Weber, F.**, 2014. Virulence factor NSs of rift valley fever virus recruits the F-box protein FBXO3 to degrade subunit p62 of general transcription factor TFIIF. *J Virol* 88, 3464–3473. doi:10.1128/JVI.02914-13
- Kainulainen, M., Lau, S., Samuel, C.E., Hornung, V., Weber, F.**, 2016. NSs Virulence Factor of Rift Valley Fever Virus Engages the F-Box Proteins FBXW11 and  $\beta$ -TRCP1 To Degrade the Antiviral Protein Kinase PKR. *J Virol* 90, 6140–6147. doi:10.1128/JVI.00016-16
- Kalveram, B., Ikegami, T.**, 2013. Toscana virus NSs protein promotes degradation of double-stranded RNA-dependent protein kinase. *J Virol* 87, 3710–3718.

doi:10.1128/JVI.02506-12

- Kalveram, B., Lihoradova, O., Ikegami, T.**, 2011. NSs protein of rift valley fever virus promotes posttranslational downregulation of the TFIIF subunit p62. *J Virol* 85, 6234–6243. doi:10.1128/JVI.02255-10
- Karl S, Pritschow Y, Volcic M, Häcker S, Baumann B, Wiesmüller L, Debatin KM, Fulda S.**, 2009. Identification of a novel pro-apoptotic function of NF- $\kappa$ B in the DNA damage response. *J Cell Mol Med* 13, 4239–4256. doi: 10.1111/j.1582-4934.2009.00888.x
- Kato, H., Takeuchi, O., Mikamo-Satoh, E., Hirai, R., Kawai, T., Matsushita, K., Hiiragi, A., Dermody, T.S., Fujita, T., Akira, S.**, 2008. Length-dependent recognition of double-stranded ribonucleic acids by retinoic acid-inducible gene-I and melanoma differentiation-associated gene 5. *J Exp Med* 205, 1601–1610. doi:10.1084/jem.20080091
- Kato, H., Takeuchi, O., Sato, S., Yoneyama, M., Yamamoto, M., Matsui, K., Uematsu, S., Jung, A., Kawai, T., Ishii, K.J., Yamaguchi, O., Otsu, K., Tsujimura, T., Koh, C.-S., Reis e Sousa, C., Matsuura, Y., Fujita, T., Akira, S.**, 2006. Differential roles of MDA5 and RIG-I helicases in the recognition of RNA viruses. *Nature* 441, 101–105. doi:10.1038/nature04734
- Katz, A., Freiberg, A.N., Backström, V., Schulz, A.R., Mateos, A., Holm, L., Pettersson, R.F., Vaheri, A., Flick, R., Plyusnin, A.**, 2010. Oligomerization of Uukuniemi virus nucleocapsid protein. *Virol. J.* 7, 187. doi:10.1186/1743-422X-7-187
- Kaul, A., Woerz, I., Meuleman, P., Leroux-Roels, G., Bartenschlager, R.**, 2007. Cell Culture Adaptation of Hepatitis C Virus and In Vivo Viability of an Adapted Variant. *J Virol* 81, 13168–13179. doi:10.1128/JVI.01362-07
- Killip, M.J., Young, D.F., Gatherer, D., Ross, C.S., Short, J.A.L., Davison, A.J., Goodbourn, S., Randall, R.E.**, 2013. Deep sequencing analysis of defective genomes of parainfluenza virus 5 and their role in interferon induction. *J Virol* 87, 4798–4807. doi:10.1128/JVI.03383-12
- Kim, K.-H., Yi, J., Kim, G., Choi, S.J., Jun, K.I., Kim, N.-H., Choe, P.G., Kim, N.-J., Lee, J.-K., Oh, M.-D.**, 2013. Severe Fever with Thrombocytopenia Syndrome, South Korea, 2012. *Emerg. Infect. Dis.* 19. doi:10.3201/eid1911.130792
- King, P. and Goodbourn, S.**, 1998. STAT1 is inactivated by a caspase. *J. Biol. Chem.* 273, 8699–8704. doi: 10.1074/jbc.273.15.8699
- Kishore, N., Huynh, Q.K., Mathialagan, S., Hall, T., Rouw, S., Creely, D., Lange, G., Carroll, J., Reitz, B., Donnelly, A., Boddupalli, H., Combs, R.G., Kretzmer, K., Tripp, C.S.**, 2002. IKK-i and TBK-1 are enzymatically distinct from the homologous enzyme IKK-2: comparative analysis of recombinant human IKK-i, TBK-1, and IKK-2. *J. Biol. Chem.* 277, 13840–13847. doi:10.1074/jbc.M110474200
- Kohl, A., Lowen, A.C., Léonard, V.H.J., Elliott, R.M.**, 2006. Genetic elements regulating packaging of the Bunyamwera orthobunyavirus genome. *J Gen Virol* 87, 177–187. doi:10.1099/vir.0.81227-0

- Kolakofsky, D., Lamb, R.A.**, 2001. Paramyxoviridae: the viruses and their replication., in: Howley, P.M., Knipe, D.E. (Eds.), *Fields Virology*. Lippincott Williams & Wilkins, Philadelphia, PA.
- Kormelink, R., van Poelwijk, F., Peters, D., Goldbach, R.**, 1992. Non-viral heterogeneous sequences at the 5' ends of tomato spotted wilt virus mRNAs. *J Gen Virol* 73 ( Pt 8), 2125–2128. doi:10.1099/0022-1317-73-8-2125
- Koshiba, T., Yasukawa, K., Yanagi, Y., Kawabata, S.-I.**, 2011. Mitochondrial membrane potential is required for MAVS-mediated antiviral signaling. *Science Signaling* 4, ra7–ra7. doi:10.1126/scisignal.2001147
- Kotenko, S.V., Gallagher, G., Baurin, V.V., Lewis-Antes, A., Shen, M., Shah, N.K., Langer, J.A., Sheikh, F., Dickensheets, H., Donnelly, R.P.**, 2003. IFN-lambdas mediate antiviral protection through a distinct class II cytokine receptor complex. *Nat. Immunol.* 4, 69–77. doi:10.1038/ni875
- Krautkrämer, E., Zeier, M.**, 2008. Hantavirus causing hemorrhagic fever with renal syndrome enters from the apical surface and requires decay-accelerating factor (DAF/CD55). *J Virol* 82, 4257–4264. doi:10.1128/JVI.02210-07
- Kreher, F., Tamietti, C., Gomet, C., Guillemot, L., Ermonval, M., Failloux, A.-B., Panthier, J.-J., Bouloy, M., Flamand, M.**, 2014. The Rift Valley fever accessory proteins NSm and P78/NSm-GN are distinct determinants of virus propagation in vertebrate and invertebrate hosts. *Emerg Microbes Infect* 3, e71. doi:10.1038/emi.2014.71
- Kuismanen, E., Bång, B., Hurme, M., Pettersson, R.F.**, 1984. Uukuniemi virus maturation: immunofluorescence microscopy with monoclonal glycoprotein-specific antibodies. *J Virol* 51, 137–146.
- Kuismanen, E., Hedman, K., Saraste, J., Pettersson, R.F.**, 1982. Uukuniemi virus maturation: accumulation of virus particles and viral antigens in the Golgi complex. *Mol. Cell. Biol.* 2, 1444–1458.
- Kukkonen, S.K.J., Vaheri, A., Plyusnin, A.**, 2004. Tula hantavirus L protein is a 250 kDa perinuclear membrane-associated protein. *J Gen Virol* 85, 1181–1189. doi:10.1099/vir.0.19748-0
- Lam, T.T.-Y., Liu, W., Bowden, T.A., Cui, N., Zhuang, L., Liu, K., Zhang, Y.-Y., Cao, W.-C., Pybus, O.G.**, 2013. Evolutionary and molecular analysis of the emergent severe fever with thrombocytopenia syndrome virus. *Epidemics* 5, 1–10. doi:10.1016/j.epidem.2012.09.002
- Lara, E., Billecocq, A., Léger, P., Bouloy, M.**, 2011. Characterization of wild-type and alternate transcription termination signals in the Rift Valley fever virus genome. *J Virol* 85, 12134–12145. doi:10.1128/JVI.05322-11
- Lawrence, T.**, 2009. The nuclear factor NF-kappaB pathway in inflammation. *Cold Spring Harbor Perspectives in Biology* 1, a001651–a001651. doi:10.1101/cshperspect.a001651

- Le May, N., Dubaele, S., Proietti De Santis, L., Billecocq, A., Bouloy, M., Egly, J.-M.**, 2004. TFIIF transcription factor, a target for the Rift Valley hemorrhagic fever virus. *Cell* 116, 541–550.
- Le May, N., Gaudiard, N., Billecocq, A., Bouloy, M.**, 2005. The N terminus of Rift Valley fever virus nucleoprotein is essential for dimerization. *J Virol* 79, 11974–11980. doi:10.1128/JVI.79.18.11974-11980.2005
- Le May, N., Mansuroglu, Z., Léger, P., Josse, T., Blot, G., Billecocq, A., Flick, R., Jacob, Y., Bonnefoy, E., Bouloy, M.**, 2008. A SAP30 complex inhibits IFN-beta expression in Rift Valley fever virus infected cells. *PLoS Pathogens* 4, e13. doi:10.1371/journal.ppat.0040013
- Leonard, V.H.J., Kohl, A., Hart, T.J., Elliott, R.M.**, 2006. Interaction of Bunyamwera Orthobunyavirus NSs Protein with Mediator Protein MED8: a Mechanism for Inhibiting the Interferon Response. *J Virol* 80, 9667–9675. doi:10.1128/JVI.00822-06
- Léger, P., Lara, E., Jagla, B., Sismeiro, O., Mansuroglu, Z., Coppée, J.Y., Bonnefoy, E., Bouloy, M.**, 2013. Dicer-2- and Piwi-mediated RNA interference in Rift Valley fever virus-infected mosquito cells. *J Virol* 87, 1631–1648. doi:10.1128/JVI.02795-12
- Léger, P., Lozach, P.-Y.**, 2015. Bunyaviruses: from transmission by arthropods to virus entry into the mammalian host first-target cells. *Future Virology* 10, 859–881. doi:10.2217/fvl.15.52
- Léger, P., Tetard, M., Youness, B., Cordes, N., Rouxel, R.N., Flamand, M., Lozach, P.-Y.**, 2016. Differential Use of the C-Type Lectins L-SIGN and DC-SIGN for Phlebovirus Endocytosis. *Traffic* 17, 639–656. doi:10.1111/tra.12393
- Li, X., Leung, S., Qureshi, S., Darnell, J.E., Stark, G.R.**, 1996. Formation of STAT1-STAT2 heterodimers and their role in the activation of IRF-1 gene transcription by interferon-alpha. *J. Biol. Chem.* 271, 5790–5794.
- Li, X., Stark, G.R.**, 2003. Genetic Analysis of NF-κB-Dependent Signaling Pathways in Mammalian Cells, in: Nuclear Factor κB. Springer Netherlands, Dordrecht, pp. 241–264. doi:10.1007/978-94-010-0163-2\_11
- Li, Z., Bao, C., Hu, J., Liu, W., Wang, X., Zhang, L., Ji, Z., Feng, Z., Li, L., Shen, A., Liu, X., Zhao, H., Tan, W., Zhou, J., Qi, X., Zhu, Y., Tang, F., Cardona, C.J., Xing, Z.**, 2016. Ecology of the Tick-Borne Phlebovirus Causing Severe Fever with Thrombocytopenia Syndrome in an Endemic Area of China. *PLoS Negl Trop Dis* 10, e0004574. doi:10.1371/journal.pntd.0004574
- Li, Z., Hu, J., Bao, C., Li, P., Qi, X., Qin, Y., Wang, S., Tan, Z., Zhu, Y., Tang, F., Zhou, M.**, 2014. Seroprevalence of antibodies against SFTS virus infection in farmers and animals, Jiangsu, China. *J. Clin. Virol.* 60, 185–189. doi:10.1016/j.jcv.2014.03.020
- Liang, Q., Deng, H., Li, X., Wu, X., Tang, Q., Chang, T.-H., Peng, H., Rauscher, F.J., Ozato, K., Zhu, F.**, 2011. Tripartite motif-containing protein 28 is a small ubiquitin-related modifier E3 ligase and negative regulator of IFN regulatory factor 7. *J. Immunol.* 187, 4754–4763. doi:10.4049/jimmunol.1101704

- Lihoradova, O.A., Indran, S.V., Kalveram, B., Lokugamage, N., Head, J.A., Gong, B., Tigabu, B., Juelich, T.L., Freiberg, A.N., Ikegami, T., 2013.** Characterization of Rift Valley fever virus MP-12 strain encoding NSs of Punta Toro virus or sandfly fever Sicilian virus. *PLoS Negl Trop Dis* 7, e2181. doi:10.1371/journal.pntd.0002181
- Lin, R., Heylbroeck, C., Pitha, P.M., Hiscott, J., 1998.** Virus-dependent phosphorylation of the IRF-3 transcription factor regulates nuclear translocation, transactivation potential, and proteasome-mediated degradation. *Mol. Cell. Biol.* 18, 2986–2996.
- Liniger, M., Summerfield, A., Zimmer, G., McCullough, K.C., Ruggli, N., 2012.** Chicken cells sense influenza A virus infection through MDA5 and CARDIF signaling involving LGP2. *J Virol* 86, 705–717. doi:10.1128/JVI.00742-11
- Liu, M.-M., Lei, X.-Y., Yu, H., Zhang, J.-Z., Yu, X.-J., 2017.** Correlation of cytokine level with the severity of severe fever with thrombocytopenia syndrome. *Virol. J.* 14, 6. doi:10.1186/s12985-016-0677-1
- Liu, Y., Wu, B., Paessler, S., Walker, D.H., Tesh, R.B., Yu, X.-J., 2014.** The pathogenesis of severe fever with thrombocytopenia syndrome virus infection in alpha/beta interferon knockout mice: insights into the pathologic mechanisms of a new viral hemorrhagic fever. *J Virol* 88, 1781–1786. doi:10.1128/JVI.02277-13
- Lopez, N., Müller, R., Préhaud, C., Bouloy, M., 1995.** The L protein of Rift Valley fever virus can rescue viral ribonucleoproteins and transcribe synthetic genome-like RNA molecules. *J Virol* 69, 3972–3979.
- Lowen, A.C., Boyd, A., Fazakerley, J.K., Elliott, R.M., 2005.** Attenuation of bunyavirus replication by rearrangement of viral coding and noncoding sequences. *J Virol* 79, 6940–6946. doi:10.1128/JVI.79.11.6940-6946.2005
- Lowen, A.C., Elliott, R.M., 2005.** Mutational analyses of the nonconserved sequences in the Bunyamwera Orthobunyavirus S segment untranslated regions. *J Virol* 79, 12861–12870. doi:10.1128/JVI.79.20.12861-12870.2005
- Lowen, A.C., Noonan, C., McLees, A., Elliott, R.M., 2004.** Efficient bunyavirus rescue from cloned cDNA. *Virology* 330, 493–500. doi:10.1016/j.virol.2004.10.009
- Lozach, P.-Y., Kühbacher, A., Meier, R., Mancini, R., Bitto, D., Bouloy, M., Helenius, A., 2011.** DC-SIGN as a receptor for phleboviruses. *Cell Host Microbe* 10, 75–88. doi:10.1016/j.chom.2011.06.007
- Lozach, P.-Y., Mancini, R., Bitto, D., Meier, R., Oestereich, L., Överby, A.K., Pettersson, R.F., Helenius, A., 2010.** Entry of bunyaviruses into mammalian cells. *Cell Host Microbe* 7, 488–499. doi:10.1016/j.chom.2010.05.007
- Ludwig, G.V., Israel, B.A., Christensen, B.M., Yuill, T.M., Schultz, K.T., 1991.** Role of La Crosse virus glycoproteins in attachment of virus to host cells. *Virology* 181, 564–571.
- Luster, A.D., Unkeless, J.C., Ravetch, J.V., 1985.** Gamma-interferon transcriptionally regulates an early-response gene containing homology to platelet proteins. *Nature* 315, 672–676.

- Ly, H.J., Ikegami, T.,** 2016. Rift Valley fever virus NSs protein functions and the similarity to other bunyavirus NSs proteins. *Viol. J.* 13, 118. doi:10.1186/s12985-016-0573-8
- Ma, X., Helgason, E., Phung, Q.T., Quan, C.L., Iyer, R.S., Lee, M.W., Bowman, K.K., Starovasnik, M.A., Dueber, E.C.,** 2012. Molecular basis of Tank-binding kinase 1 activation by transautophosphorylation. *Proc. Natl. Acad. Sci. U.S.A.* 109, 9378–9383. doi:10.1073/pnas.1121552109
- MACPHERSON, I., STOKER, M.,** 1962. Polyoma transformation of hamster cell clones--an investigation of genetic factors affecting cell competence. *Virology* 16, 147–151.
- Mandell, R.B., Flick, R.,** 2010. Rift Valley fever virus: an unrecognized emerging threat? *Hum Vaccin* 6, 597–601.
- Margaria, P., Bosco, L., Vallino, M., Ciuffo, M., Mautino, G.C., Tavella, L., Turina, M.,** 2014. The NSs protein of tomato spotted wilt virus is required for persistent infection and transmission by *Frankliniella occidentalis*. *J Virol* 88, 5788–5802. doi:10.1128/JVI.00079-14
- Marié, I., Durbin, J.E., Levy, D.E.,** 1998. Differential viral induction of distinct interferon-alpha genes by positive feedback through interferon regulatory factor-7. *EMBO J.* 17, 6660–6669. doi:10.1093/emboj/17.22.6660
- Marklewitz, M., Handrick, S., Grasse, W., Kurth, A., Lukashev, A., Drosten, C., Ellerbrok, H., Leendertz, F.H., Pauli, G., Junglen, S.,** 2011. Gouleako virus isolated from West African mosquitoes constitutes a proposed novel genus in the family Bunyaviridae. *J Virol* 85, 9227–9234. doi:10.1128/JVI.00230-11
- Marklewitz, M., Zirkel, F., Kurth, A., Drosten, C., Junglen, S.,** 2015. Evolutionary and phenotypic analysis of live virus isolates suggests arthropod origin of a pathogenic RNA virus family. *Proc. Natl. Acad. Sci. U.S.A.* 112, 7536–7541. doi:10.1073/pnas.1502036112
- Martin, M.L., Lindsey-Regnery, H., Sasso, D.R., McCormick, J.B., Palmer, E.,** 1985. Distinction between Bunyaviridae genera by surface structure and comparison with Hantaan virus using negative stain electron microscopy. *Arch. Virol.* 86, 17–28.
- Matsuno, K., Weisend, C., Kajihara, M., Matysiak, C., Williamson, B.N., Simuunza, M., Mweene, A.S., Takada, A., Tesh, R.B., Ebihara, H.,** 2015. Comprehensive molecular detection of tick-borne phleboviruses leads to the retrospective identification of taxonomically unassigned bunyaviruses and the discovery of a novel member of the genus phlebovirus. *J Virol* 89, 594–604. doi:10.1128/JVI.02704-14
- Mathys, V.S., Gorbunova, E.E., Gavrillovskaya, I.N., Mackow, E.R.,** 2010. Andes virus recognition of human and Syrian hamster beta3 integrins is determined by an L33P substitution in the PSI domain. *J Virol* 84, 352–360. doi:10.1128/JVI.01013-09
- Mazel-Sanchez, B., Elliott, R.M.,** 2015. Evolution of the Bunyamwera virus polymerase to accommodate deletions within genomic untranslated region sequences. *J Virol* 89, 3957–3964. doi:10.1128/JVI.03436-14

- Mazel-Sanchez, B., Elliott, R.M.**, 2012. Attenuation of bunyamwera orthobunyavirus replication by targeted mutagenesis of genomic untranslated regions and creation of viable viruses with minimal genome segments. *J Virol* 86, 13672–13678. doi:10.1128/JVI.02253-12
- Mazelier, M., Rouxel, R.N., Zumstein, M., Mancini, R., Bell-Sakyi, L., Lozach, P.-Y.**, 2016. Uukuniemi Virus as a Tick-Borne Virus Model. *J Virol* 90, 6784–6798. doi:10.1128/JVI.00095-16
- Mádr, V., Hubálek, Z., Zendulková, D.**, 1984. Experimental infection of sheep with Bhanja virus. *Folia Parasitol.* 31, 79–84.
- McMullan, L.K., Folk, S.M., Kelly, A.J., MacNeil, A., Goldsmith, C.S., Metcalfe, M.G., Batten, B.C., Albariño, C.G., Zaki, S.R., Rollin, P.E., Nicholson, W.L., Nichol, S.T.**, 2012. A New Phlebovirus Associated with Severe Febrile Illness in Missouri. *New England Journal of Medicine* 367, 834–841. doi:10.1056/NEJMoa1203378
- McWilliam, H., Li, W., Uludag, M., Squizzato, S., Park, Y.M., Buso, N., Cowley, A.P., Lopez, R.**, 2013. Analysis Tool Web Services from the EMBL-EBI. *Nucleic Acids Research* 41, W597–W600. doi:10.1093/nar/gkt376
- Mir, M.A., Duran, W.A., Hjelle, B.L., Ye, C., Panganiban, A.T.**, 2008. Storage of cellular 5' mRNA caps in P bodies for viral cap-snatching. *Proc. Natl. Acad. Sci. U.S.A.* 105, 19294–19299. doi:10.1073/pnas.0807211105
- Moss, B., Elroy-Stein, O., Mizukami, T., Alexander, W.A., Fuerst, T.R.**, 1990. New mammalian expression vectors. *Nature* 348, 91–92. doi:10.1038/348091a0
- Moss, S.R.**, 1986. Tick-borne viruses in Icelandic seabird colonies.
- Mourya, D.T., Yadav, P.D., Basu, A., Shete, A., Patil, D.Y., Zawar, D., Majumdar, T.D., Kokate, P., Sarkale, P., Raut, C.G., Jadhav, S.M.**, 2014. Malsoor virus, a novel bat phlebovirus, is closely related to severe fever with thrombocytopenia syndrome virus and heartland virus. *J Virol* 88, 3605–3609. doi:10.1128/JVI.02617-13
- Mudhasani, R., Tran, J.P., Retterer, C., Kota, K.P., Whitehouse, C.A., Bavari, S.**, 2016. Protein Kinase R Degradation Is Essential for Rift Valley Fever Virus Infection and Is Regulated by SKP1-CUL1-F-box (SCF)FBXW11-NSs E3 Ligase. *PLoS Pathogens* 12, e1005437. doi:10.1371/journal.ppat.1005437
- Muehlenbachs, A., Fata, C.R., Lambert, A.J., Paddock, C.D., Velez, J.O., Blau, D.M., Staples, J.E., Karlekar, M.B., Bhatnagar, J., Nasci, R.S., Zaki, S.R.**, 2014. Heartland virus-associated death in tennessee. *Clin Infect Dis.* 59, 845–850. doi:10.1093/cid/ciu434
- Murphy, F.A., Harrison, A.K., Whitfield, S.G.**, 1973. Bunyaviridae: morphologic and morphogenetic similarities of Bunyamwera serologic supergroup viruses and several other arthropod-borne viruses. *Intervirology* 1, 297–316.
- Müller, M., Briscoe, J., Laxton, C., Guschin, D., Ziemiecki, A., Silvennoinen, O., Harpur, A.G., Barbieri, G., Witthuhn, B.A., Schindler, C., Pellegrini, S., Wilks,**

- A.F., Ihle, J.N., Stark, G.R., Kerr, L.M.**, 1993. The protein tyrosine kinase JAK1 complements defects in interferon- $\alpha/\beta$  and - $\gamma$  signal transduction. *Nature* 366, 129–135. doi:10.1038/366129a0
- Müller, R., Poch, O., Delarue, M., Bishop, D.H., Bouloy, M.**, 1994. Rift Valley fever virus L segment: correction of the sequence and possible functional role of newly identified regions conserved in RNA-dependent polymerases. *J Gen Virol* 75 ( Pt 6), 1345–1352. doi:10.1099/0022-1317-75-6-1345
- Nakabayashi, H., Taketa, K., Miyano, K., Yamane, T., Sato, J.**, 1982. Growth of human hepatoma cells lines with differentiated functions in chemically defined medium. *Cancer Res.* 42, 3858–3863.
- Nakitare, G.W., Elliott, R.M.**, 1993. Expression of the Bunyamwera virus M genome segment and intracellular localization of NSm. *Virology* 195, 511–520. doi:10.1006/viro.1993.1402
- Nasci, R.S., Lambert, A.J., Savage, H.M.**, 2014. Novel bunyavirus in domestic and captive farmed animals, Minnesota, USA. *Emerg. Infect. Dis.* 20, 336–337. doi:10.3201/eid2002.131790
- Neumann, G., Kawaoka, Y.**, 2004. Reverse genetics systems for the generation of segmented negative-sense RNA viruses entirely from cloned cDNA. *Curr. Top. Microbiol. Immunol.* 283, 43–60.
- Neumann, G., Watanabe, T., Ito, H., Watanabe, S., Goto, H., Gao, P., Hughes, M., Perez, D.R., Donis, R., Hoffmann, E., Hobom, G., Kawaoka, Y.**, 1999. Generation of influenza A viruses entirely from cloned cDNAs. *PNAS* 96, 9345–9350.
- Ni, H., Yang, F., Li, Y., Liu, W., Jiao, S., Li, Z., Yi, B., Chen, Y., Hou, X., Hu, F., Ding, Y., Bian, G., Du, Y., Xu, G., Cao, G.**, 2015. Apodemus agrarius is a potential natural host of severe fever with thrombocytopenia syndrome (SFTS)-causing novel bunyavirus. *J. Clin. Virol.* 71, 82–88. doi:10.1016/j.jcv.2015.08.006
- Niewold, T.B.**, 2014. Type I Interferon in Human Autoimmunity. *Frontiers in Immunology* 5, 657. doi:10.3389/fimmu.2014.00306
- Ning, Y.-J., Feng, K., Min, Y.-Q., Cao, W.-C., Wang, M., Deng, F., Hu, Z., Wang, H.**, 2015. Disruption of type I interferon signaling by the nonstructural protein of severe fever with thrombocytopenia syndrome virus via the hijacking of STAT2 and STAT1 into inclusion bodies. *J Virol* 89, 4227–4236. doi:10.1128/JVI.00154-15
- Ning, Y.-J., Wang, M., Deng, M., Shen, S., Liu, W., Cao, W.-C., Deng, F., Wang, Y.-Y., Hu, Z., Wang, H.**, 2014. Viral suppression of innate immunity via spatial isolation of TBK1/IKK $\epsilon$  from mitochondrial antiviral platform. *J Mol Cell Biol* 6, 324–337. doi:10.1093/jmcb/mju015
- Nishiya, T., DeFranco, A.L.**, 2004. Ligand-regulated chimeric receptor approach reveals distinctive subcellular localization and signaling properties of the Toll-like receptors. *J. Biol. Chem.* 279, 19008–19017. doi:10.1074/jbc.M311618200
- Niu, G., Li, J., Liang, M., Jiang, X., Jiang, M., Yin, H., Wang, Z., Li, C., Zhang, Q.,**

- Jin, C., Wang, X., Ding, S., Xing, Z., Wang, S., Bi, Z., Li, D.,** 2013. Severe fever with thrombocytopenia syndrome virus among domesticated animals, China. *Emerg. Infect. Dis.* 19, 756–763. doi:10.3201/eid1905.120245
- Nuttall, P.A., Carey, D., Reid, H.W., Harrap, K.A.,** 1981. Orbiviruses and bunyaviruses from a seabird colony in Scotland. *J Gen Virol* 57, 127–137. doi:10.1099/0022-1317-57-1-127
- Nuttall, P.A., Kelly, T.C., Carey, D., Moss, S.R., Harrap, K.A.,** 1984. Mixed infections with tick-borne viruses in a seabird colony in Eire. *Arch. Virol.* 79, 35–44.
- Obijeski, J.F., Bishop, D.H., Palmer, E.L., Murphy, F.A.,** 1976. Segmented genome and nucleocapsid of La Crosse virus. *J Virol* 20, 664–675.
- Ogawa, Y., Sugiura, K., Kato, K., Tohya, Y., Akashi, H.,** 2007. Rescue of Akabane virus (family Bunyaviridae) entirely from cloned cDNAs by using RNA polymerase I. *J Gen Virol* 88, 3385–3390. doi:10.1099/vir.0.83173-0
- Ogino, M., Yoshimatsu, K., Ebihara, H., Araki, K., Lee, B.-H., Okumura, M., Arikawa, J.,** 2004. Cell fusion activities of Hantaan virus envelope glycoproteins. *J Virol* 78, 10776–10782. doi:10.1128/JVI.78.19.10776-10782.2004
- Oh, H.-M., Yu, C.-R., Lee, Y., Chan, C.-C., Maminishkis, A., Egwuagu, C.E.,** 2011. Autoreactive memory CD4+ T lymphocytes that mediate chronic uveitis reside in the bone marrow through STAT3-dependent mechanisms. *J. Immunol.* 187, 3338–3346. doi:10.4049/jimmunol.1004019
- Oker-Blom, N., Salminen, A., Brummer-Korvenkontio, M., Kaeaeriaeinen, L., Weckstroem, P.,** 1964. Isolation of some viruses other than typical tick-borne encephalitis viruses from Ixodes Ricinus ticks in Finland. *Ann Med Exp Biol Fenn* 42, 109–112.
- Olal, D., Dick, A., Woods, V.L., Liu, T., Li, S., Devignot, S., Weber, F., Saphire, E.O., Daumke, O.,** 2014. Structural insights into RNA encapsidation and helical assembly of the Toscana virus nucleoprotein. *Nucleic Acids Research* 42, 6025–6037. doi:10.1093/nar/gku229
- Oliveira, V.C., Bartasson, L., de Castro, M.E.B., Corrêa, J.R., Ribeiro, B.M., Resende, R.O.,** 2011. A silencing suppressor protein (NSs) of a tospovirus enhances baculovirus replication in permissive and semipermissive insect cell lines. *Virus Res.* 155, 259–267. doi:10.1016/j.virusres.2010.10.019
- Onoguchi, K., Onomoto, K., Takamatsu, S., Jogi, M., Takemura, A., Morimoto, S., Julkunen, I., Namiki, H., Yoneyama, M., Fujita, T.,** 2010. Virus-infection or 5'ppp-RNA activates antiviral signal through redistribution of IPS-1 mediated by MFN1. *PLoS Pathogens* 6, e1001012. doi:10.1371/journal.ppat.1001012
- Otsuki, K., Maeda, J., Yamamoto, H., Tsubokura, M.,** 1979. Studies on avian infectious bronchitis virus (IBV). III. Interferon induction by and sensitivity to interferon of IBV. *Arch. Virol.* 60, 249–255.
- Overby, A.K., Pettersson, R.F., Grünwald, K., Huiskonen, J.T.,** 2008. Insights into

- bunyavirus architecture from electron cryotomography of Uukuniemi virus. *Proc. Natl. Acad. Sci. U.S.A.* 105, 2375–2379. doi:10.1073/pnas.0708738105
- Overby, A.K., Popov, V.L., Pettersson, R.F., Neve, E.P.A.,** 2007. The Cytoplasmic Tails of Uukuniemi Virus (Bunyaviridae) GN and GC Glycoproteins Are Important for Intracellular Targeting and the Budding of Virus-Like Particles. *J Virol* 81, 11381–11391. doi:10.1128/JVI.00767-07
- Överby, A.K., Popov, V., Neve, E.P.A., Pettersson, R.F.,** 2006. Generation and analysis of infectious virus-like particles of uukuniemi virus (bunyaviridae): a useful system for studying bunyaviral packaging and budding. *J Virol* 80, 10428–10435. doi:10.1128/JVI.01362-06
- Palacios, G., da Rosa, A.T., Savji, N., Sze, W., Wick, I., Guzman, H., Hutchison, S., Tesh, R., Lipkin, W.I.,** 2011. Aguacate virus, a new antigenic complex of the genus Phlebovirus (family Bunyaviridae). *J Gen Virol* 92, 1445–1453. doi:10.1099/vir.0.029389-0
- Palacios, G., Savji, N., da Rosa, A.T., Guzman, H., Yu, X., Desai, A., Rosen, G.E., Hutchison, S., Lipkin, W.I., Tesh, R.,** 2013. Characterization of the Uukuniemi virus group (Phlebovirus: Bunyaviridae): evidence for seven distinct species. *J Virol* 87, 3187–3195. doi:10.1128/JVI.02719-12
- Panne, D., McWhirter, S.M., Maniatis, T., Harrison, S.C.,** 2007. Interferon regulatory factor 3 is regulated by a dual phosphorylation-dependent switch. *J. Biol. Chem.* 282, 22816–22822. doi:10.1074/jbc.M703019200
- Papa, A., Kontana, A., Tsioka, K., Chaligiannis, I., Sotiraki, S.,** 2016. Novel phleboviruses detected in ticks, Greece. *Ticks Tick Borne Dis* 7, 690–693. doi:10.1016/j.ttbdis.2016.02.017
- Patterson, J.L., Holloway, B., Kolakofsky, D.,** 1984. La Crosse virions contain a primer-stimulated RNA polymerase and a methylated cap-dependent endonuclease. *J Virol* 52, 215–222.
- Pattnaik, A.K., Ball, L.A., LeGrone, A.W., Wertz, G.W.,** 1992. Infectious defective interfering particles of VSV from transcripts of a cDNA clone. *Cell* 69, 1011–1020.
- Perrone, L.A., Narayanan, K., Worthy, M., Peters, C.J.,** 2007. The S segment of Punta Toro virus (Bunyaviridae, Phlebovirus) is a major determinant of lethality in the Syrian hamster and codes for a type I interferon antagonist. *J Virol* 81, 884–892. doi:10.1128/JVI.01074-06
- Persson, R., Pettersson, R.F.,** 1991. Formation and intracellular transport of a heterodimeric viral spike protein complex. *J. Cell Biol.* 112, 257–266.
- Pestka, S.,** 1987. Interferons And Their Actions. *Annual Review of Biochemistry* 56, 727–777. doi:10.1146/annurev.biochem.56.1.727
- Pestka, S., Kotenko, S.V., Muthukumar, G., Izotova, L.S., Cook, J.R., Garotta, G.,** 1997. The interferon gamma (IFN-gamma) receptor: a paradigm for the multichain cytokine receptor. *Cytokine Growth Factor Rev.* 8, 189–206.

- Pestka, S., Krause, C.D., Walter, M.R.,** 2004. Interferons, interferon-like cytokines, and their receptors. *Immunol. Rev.* 202, 8–32. doi:10.1111/j.0105-2896.2004.00204.x
- Petersen, L.R., Busch, M.P.,** 2010. Transfusion-transmitted arboviruses. *Vox Sang.* 98, 495–503. doi:10.1111/j.1423-0410.2009.01286.x
- Pettersson, R., Kääriäinen, L.,** 1973. The ribonucleic acids of Uukuniemi virus, a noncubical tick-borne arbovirus. *Virology* 56, 608–619. doi:10.1016/0042-6822(73)90062-7
- Pettersson, R.F., Bonsdorff, von, C.H.,** 1975. Ribonucleoproteins of Uukuniemi virus are circular. *J Virol* 15, 386–392.
- Pettersson, R.F., Hewlett, M.J., Baltimore, D., Coffin, J.M.,** 1977. The genome of Uukuniemi virus consists of three unique RNA segments. *Cell* 11, 51–63. doi:10.1016/0092-8674(77)90316-6
- Phoenix, I., Nishiyama, S., Lokugamage, N., Hill, T.E., Huante, M.B., Slack, O.A.L., Carpio, V.H., Freiberg, A.N., Ikegami, T.,** 2016. N-Glycans on the Rift Valley Fever Virus Envelope Glycoproteins Gn and Gc Redundantly Support Viral Infection via DC-SIGN. *Viruses* 8, 149. doi:10.3390/v8050149
- Pichlmair, A., Schulz, O., Tan, C.P., Näslund, T.I., Liljeström, P., Weber, F., Reis e Sousa, C.,** 2006. RIG-I-mediated antiviral responses to single-stranded RNA bearing 5'-phosphates. *Science* 314, 997–1001. doi:10.1126/science.1132998
- Pietrantoni, A., Fortuna, C., Remoli, M., Ciufolini, M., Superti, F.,** 2015. Bovine Lactoferrin Inhibits Toscana Virus Infection by Binding to Heparan Sulphate. *Viruses* 7, 480–495. doi:10.3390/v7020480
- Plasmeyer, M.L., Soldan, S.S., Stachelek, K.M., Martín-García, J., González-Scarano, F.,** 2005. California serogroup Gc (G1) glycoprotein is the principal determinant of pH-dependent cell fusion and entry. *Virology* 338, 121–132. doi:10.1016/j.virol.2005.04.026
- Platanias, L.C.,** 2005. Mechanisms of type-I- and type-II-interferon-mediated signalling. *Nat. Rev. Immunol.* 5, 375–386. doi:10.1038/nri1604
- Platanias, L.C., Fish, E.N.,** 1999. Signaling pathways activated by interferons. *Experimental Hematology* 27, 1583–1592. doi:10.1016/S0301-472X(99)00109-5
- Plyusnin, A., Beaty, B.J., Elliott, R.M., Goldbach, R., Kormelink, R., Lundkvist, A., Schmaljohn, C.S., Tesh, R.B.,** 2001. *Bunyaviridae*, in: King, A.M.Q., Adams, M.J., Carstens, E.B., Lefkowitz, E.J. (Eds.), *Virus Taxonomy: Ninth Report of the International Committee on Taxonomy of Viruses*. pp. 725–741.
- Plyusnin, A., Elliott, R.M.,** 2011. *Bunyaviridae*. Springer-Verlag.
- Poch, O., Sauvaget, I., Delarue, M., Tordo, N.,** 1989. Identification of four conserved motifs among the RNA-dependent polymerase encoding elements. *EMBO J.* 8, 3867–3874.
- Portolani, M., Sabbatini, A.M.T., Beretti, F., Gennari, W., Tamassia, M.G., Pecorari, M.,** 2002. Symptomatic infections by toscana virus in the Modena province in the

- triennium 1999-2001. *New Microbiol.* 25, 485–488.
- Pringle, C.R.**, 2011. The *Bunyaviridae* and their genetics - an overview, in: *Bunyaviridae*. Caister Academic Press., Berlin, pp. 1–25.
- Prins, K.C., Cárdenas, W.B., Basler, C.F.**, 2009. Ebola virus protein VP35 impairs the function of interferon regulatory factor-activating kinases IKKepsilon and TBK-1. *J Virol* 83, 3069–3077. doi:10.1128/JVI.01875-08
- Punda, V., Ropac, D., Vesenjaj-Hirjan, J.**, 1987. Incidence of hemagglutination-inhibiting antibodies for Bhanja virus in humans along the north-west border of Yugoslavia. *Zentralbl Bakteriolog Mikrobiolog Hyg A* 265, 227–234.
- Qu, B., Qi, X., Wu, X., Liang, M., Li, C., Cardona, C.J., Xu, W., Tang, F., Li, Z., Wu, B., Powell, K., Wegner, M., Li, D., Xing, Z.**, 2012. Suppression of the interferon and NF- $\kappa$ B responses by severe fever with thrombocytopenia syndrome virus. *J Virol* 86, 8388–8401. doi:10.1128/JVI.00612-12
- Qu, H., Yang, L., Meng, S., Xu, L., Bi, Y., Jia, X., Li, J., Sun, L., Liu, W.**, 2013. The differential antiviral activities of chicken interferon  $\alpha$  (ChIFN- $\alpha$ ) and ChIFN- $\beta$  are related to distinct interferon-stimulated gene expression. *PLoS ONE* 8, e59307. doi:10.1371/journal.pone.0059307
- Raftery, M.J., Lalwani, P., Krautkrämer, E., Peters, T., Scharffetter-Kochanek, K., Krüger, R., Hofmann, J., Seeger, K., Krüger, D.H., Schönrich, G.**, 2014.  $\beta$ 2 integrin mediates hantavirus-induced release of neutrophil extracellular traps. *J Exp Med* 211, 1485–1497. doi:10.1084/jem.20131092
- Ramana, C.V., Chatterjee-Kishore, M., Nguyen, H., Stark, G.R.**, 2000. Complex roles of Stat1 in regulating gene expression. *Oncogene* 19, 2619–2627. doi:10.1038/sj.onc.1203525
- Ramana, C.V., Gil, M.P., Schreiber, R.D., Stark, G.R.**, 2002. Stat1-dependent and -independent pathways in IFN-gamma-dependent signaling. *Trends Immunol.* 23, 96–101. doi:10.1016/S1471-4906(01)02118-4
- Randall, R.E., Goodbourn, S.**, 2008. Interferons and viruses: an interplay between induction, signalling, antiviral responses and virus countermeasures. *J Gen Virol* 89, 1–47. doi:10.1099/vir.0.83391-0
- Rasband, W.S.**, 1997. ImageJ, US National Institutes of Health, Bethesda, Maryland, USA, <http://imagej.nih.gov/ij>.
- Ravkov, E.V., Nichol, S.T., Compans, R.W.**, 1997. Polarized entry and release in epithelial cells of Black Creek Canal virus, a New World hantavirus. *J Virol* 71, 1147–1154.
- Raymond, D.D., Piper, M.E., Gerrard, S.R., Skiniotis, G., Smith, J.L.**, 2012. Phleboviruses encapsidate their genomes by sequestering RNA bases. *Proc. Natl. Acad. Sci. U.S.A.* 109, 19208–19213. doi:10.1073/pnas.1213553109
- Raymond, D.D., Piper, M.E., Gerrard, S.R., Smith, J.L.**, 2010. Structure of the Rift Valley fever virus nucleocapsid protein reveals another architecture for RNA

- encapsidation. *Proc. Natl. Acad. Sci. U.S.A.* 107, 11769–11774. doi:10.1073/pnas.1001760107
- Reguera, J., Weber, F., Cusack, S.**, 2010. Bunyaviridae RNA polymerases (L-protein) have an N-terminal, influenza-like endonuclease domain, essential for viral cap-dependent transcription. *PLoS Pathogens* 6, e1001101. doi:10.1371/journal.ppat.1001101
- Rehwinkel, J., Tan, C.P., Goubau, D., Schulz, O., Pichlmair, A., Bier, K., Robb, N., Vreede, F., Barclay, W., Fodor, E., Reis e Sousa, C.**, 2010. RIG-I detects viral genomic RNA during negative-strand RNA virus infection. *Cell* 140, 397–408. doi:10.1016/j.cell.2010.01.020
- Riemersma, K.K., Komar, N.**, 2015. Heartland Virus Neutralizing Antibodies in Vertebrate Wildlife, United States, 2009–2014. *Emerg. Infect. Dis.* 21, 1830–1833. doi:10.3201/eid2110.150380
- Rolin, A.I., Berrang-Ford, L., Kulkarni, M.A.**, 2013. The risk of Rift Valley fever virus introduction and establishment in the United States and European Union. *Emerg Microbes Infect* 2, e81. doi:10.1038/emi.2013.81
- Rose, J.K., Whitt, M.A.**, 2001. Rhabdoviridae, in: Knipe, D.E., Howley, P.M. (Eds.), *Fields Virology*. Lippincott Williams & Wilkins, Philadelphia, PA, pp. 1221–1244.
- Rossier, C., Patterson, J., Kolakofsky, D.**, 1986. La Crosse virus small genome mRNA is made in the cytoplasm. *J Virol* 58, 647–650.
- Saikku, P., Brummer-Korvenkontio, M.**, 1973. Arboviruses in Finland. II. Isolation and characterization of Uukuniemi virus, a virus associated with ticks and birds. *Am. J. Trop. Med. Hyg.* 22, 390–399.
- Saito, T., Hirai, R., Loo, Y.-M., Owen, D., Johnson, C.L., Sinha, S.C., Akira, S., Fujita, T., Gale, M.**, 2007. Regulation of innate antiviral defenses through a shared repressor domain in RIG-I and LGP2. *PNAS* 104, 582–587. doi:10.1073/pnas.0606699104
- Salanueva, I.J., Novoa, R.R., Cabezas, P., López-Iglesias, C., Carrascosa, J.L., Elliott, R.M., Risco, C.**, 2003. Polymorphism and structural maturation of bunyamwera virus in Golgi and post-Golgi compartments. *J Virol* 77, 1368–1381. doi:10.1128/JVI.77.2.1368-1381.2003
- Samso, A., Bouloy, M., Hannoun, C.**, 1975. [Circular ribonucleoproteins in the virus Lumbo (Bunyavirus)]. *C.R. Hebd. Seances Acad. Sci., Ser. D, Sci. Nat.* 280, 779–782.
- Sanbonmatsu-Gámez, S., Pérez-Ruiz, M., Palop-Borrás, B., Navarro-Marí, J.M.**, 2009. Unusual Manifestation of Toscana Virus Infection, Spain. *Emerg. Infect. Dis.* 15, 347–348. doi:10.3201/eid1502.081001
- Santiago, F.W., Covalada, L.M., Sanchez-Aparicio, M.T., Silvas, J.A., Diaz-Vizarreta, A.C., Patel, J.R., Popov, V., Yu, X.J., Garcia-Sastre, A., Aguilar, P.V.**, 2014. Hijacking of RIG-I Signaling Proteins into Virus-Induced Cytoplasmic Structures Correlates with the Inhibition of Type I Interferon Responses. *J Virol* 88, 4572–4585.

doi:10.1128/JVI.03021-13

- Santos, R.I.M., Rodrigues, A.H., Silva, M.L., Mortara, R.A., Rossi, M.A., Jamur, M.C., Oliver, C., Arruda, E.**, 2008. Oropouche virus entry into HeLa cells involves clathrin and requires endosomal acidification. *Virus Res.* 138, 139–143. doi:10.1016/j.virusres.2008.08.016
- Sato, M., Hata, N., Asagiri, M., Nakaya, T., Taniguchi, T., Tanaka, N.**, 1998. Positive feedback regulation of type I IFN genes by the IFN-inducible transcription factor IRF-7. *FEBS Lett.* 441, 106–110.
- Savage, H.M., Godsey, M.S., Lambert, A., Panella, N.A., Burkhalter, K.L., Harmon, J.R., Lash, R.R., Ashley, D.C., Nicholson, W.L.**, 2013. First detection of heartland virus (Bunyaviridae: Phlebovirus) from field collected arthropods. *Am. J. Trop. Med. Hyg.* 89, 445–452. doi:10.4269/ajtmh.13-0209
- Schaefer, T.M., Desouza, K., Fahey, J.V., Beagley, K.W., Wira, C.R.**, 2004. Toll-like receptor (TLR) expression and TLR-mediated cytokine/chemokine production by human uterine epithelial cells. *Immunology* 112, 428–436. doi:10.1111/j.1365-2567.2004.01898.x
- Schmaljohn, C.S., Nichol, S.T.**, 2007. *Bunyaviridae.*, in: Knipe, D.E., Howley, P.M., Griffin, D.E., Lamb, R.A., Martin, M.A., Roizman, B., Straus, S.E. (Eds.), *Fields Virology*. Lippincott Williams & Wilkins, Philadelphia, PA, pp. 1741–1789.
- Schneider, W.M., Chevillotte, M.D., Rice, C.M.**, 2014. Interferon-stimulated genes: a complex web of host defenses. *Annu. Rev. Immunol.* 32, 513–545. doi:10.1146/annurev-immunol-032713-120231
- Schnell, M.J., Mebatsion, T., Conzelmann, K.K.**, 1994. Infectious rabies viruses from cloned cDNA. *EMBO J.* 13, 4195–4203.
- Schnettler, E., Ratinier, M., Watson, M., Shaw, A.E., McFarlane, M., Varela, M., Elliott, R.M., Palmarini, M., Kohl, A.**, 2013. RNA interference targets arbovirus replication in Culicoides cells. *J Virol* 87, 2441–2454. doi:10.1128/JVI.02848-12
- Sherman, M.B., Freiberg, A.N., Holbrook, M.R., Watowich, S.J.**, 2009. Single-particle cryo-electron microscopy of Rift Valley fever virus. *Virology* 387, 11–15. doi:10.1016/j.virol.2009.02.038
- Shi, X., Botting, C.H., Li, P., Niglas, M., Brennan, B., Shirran, S.L., Szemiel, A.M., Elliott, R.M.**, 2016. Bunyamwera orthobunyavirus glycoprotein precursor is processed by cellular signal peptidase and signal peptide peptidase. *PNAS* 113, 8825–8830. doi:10.1073/pnas.1603364113
- Shi, X., Brauburger, K., Elliott, R.M.**, 2005. Role of N-linked glycans on bunyamwera virus glycoproteins in intracellular trafficking, protein folding, and virus infectivity. *J Virol* 79, 13725–13734. doi:10.1128/JVI.79.21.13725-13734.2005
- Shi, X., Elliott, R.M.**, 2009. Generation and analysis of recombinant Bunyamwera orthobunyaviruses expressing V5 epitope-tagged L proteins. *J Gen Virol* 90, 297–306. doi:10.1099/vir.0.007567-0

- Shi, X., Elliott, R.M.**, 2004. Analysis of N-linked glycosylation of hantaan virus glycoproteins and the role of oligosaccharide side chains in protein folding and intracellular trafficking. *J Virol* 78, 5414–5422. doi:10.1128/JVI.78.10.5414-5422.2004
- Shi, X., Goli, J., Clark, G., Brauburger, K., Elliott, R.M.**, 2009. Functional analysis of the Bunyamwera orthobunyavirus Gc glycoprotein. *J Gen Virol* 90, 2483–2492. doi:10.1099/vir.0.013540-0
- Shi, X., Kohl, A., Léonard, V.H.J., Li, P., McLees, A., Elliott, R.M.**, 2006. Requirement of the N-terminal region of orthobunyavirus nonstructural protein NSm for virus assembly and morphogenesis. *J Virol* 80, 8089–8099. doi:10.1128/JVI.00579-06
- Shi, X., Kohl, A., Li, P., Elliott, R.M.**, 2007. Role of the cytoplasmic tail domains of Bunyamwera orthobunyavirus glycoproteins Gn and Gc in virus assembly and morphogenesis. *J Virol* 81, 10151–10160. doi:10.1128/JVI.00573-07
- Shi, X., van Mierlo, J.T., French, A., Elliott, R.M.**, 2010. Visualizing the replication cycle of bunyamwera orthobunyavirus expressing fluorescent protein-tagged Gc glycoprotein. *J Virol* 84, 8460–8469. doi:10.1128/JVI.00902-10
- Sievers, F., Wilm, A., Dineen, D., Gibson, T.J., Karplus, K., Li, W., Lopez, R., McWilliam, H., Remmert, M., Söding, J., Thompson, J.D., Higgins, D.G.**, 2011. Fast, scalable generation of high-quality protein multiple sequence alignments using Clustal Omega. *Molecular Systems Biology* 7, 539–539. doi:10.1038/msb.2011.75
- Silvas, J.A., Popov, V.L., Paulucci-Holthausen, A., Aguilar, P.V.**, 2015. Extracellular Vesicles Mediate Receptor-Independent Transmission of Novel Tick-Borne Bunyavirus. *J Virol* 90, 873–886. doi:10.1128/JVI.02490-15
- Simon, M., Johansson, C., Mirazimi, A.**, 2009. Crimean-Congo hemorrhagic fever virus entry and replication is clathrin-, pH- and cholesterol-dependent. *J Gen Virol* 90, 210–215. doi:10.1099/vir.0.006387-0
- Simons, J.F., Hellman, U., Pettersson, R.F.**, 1990. Uukuniemi virus S RNA segment: ambisense coding strategy, packaging of complementary strands into virions, and homology to members of the genus Phlebovirus. *J Virol* 64, 247–255.
- Simons, J.F., Persson, R., Pettersson, R.F.**, 1992. Association of the nonstructural protein NSs of Uukuniemi virus with the 40S ribosomal subunit. *J Virol* 66, 4233–4241.
- Simons, J.F., Pettersson, R.F.**, 1991. Host-derived 5′ ends and overlapping complementary 3′ ends of the two mRNAs transcribed from the ambisense S segment of Uukuniemi virus. *J Virol* 65, 4741–4748.
- Smith, S., Weston, S., Kellam, P., Marsh, M.**, 2014. IFITM proteins-cellular inhibitors of viral entry. *Curr Opin Virol* 4, 71–77. doi:10.1016/j.coviro.2013.11.004
- Soldan, S.S., Hollidge, B.S., Wagner, V., Weber, F., González-Scarano, F.**, 2010. La Crosse virus (LACV) Gc fusion peptide mutants have impaired growth and fusion phenotypes, but remain neurotoxic. *Virology* 404, 139–147.

doi:10.1016/j.virol.2010.04.012

- Srivastava, S.P., Kumar, K.U., Kaufman, R.J.**, 1998. Phosphorylation of Eukaryotic Translation Initiation Factor 2 Mediates Apoptosis in Response to Activation of the Double-stranded RNA-dependent Protein Kinase. *J. Biol. Chem.* 273, 2416–2423. doi:10.1074/jbc.273.4.2416
- Stancato, L.F., David, M., Carter-Su, C., Lerner, A.C., Pratt, W.B.**, 1996. Preassociation of STAT1 with STAT2 and STAT3 in separate signalling complexes prior to cytokine stimulation. *J. Biol. Chem.* 271, 4134–4137.
- Stewart, C.E., Randall, R.E., Adamson, C.S.**, 2014. Inhibitors of the interferon response enhance virus replication in vitro. *PLoS ONE* 9, e112014. doi:10.1371/journal.pone.0112014
- Stone, R.**, 2010. Infectious diseases. Rival teams identify a virus behind deaths in central China. *Science* 330, 20–21. doi:10.1126/science.330.6000.20
- Struthers, J.K., Swanepoel, R.**, 1982. Identification of a Major Non-structural Protein in the Nuclei of Rift Valley Fever Virus-infected Cells. *J Gen Virol* 60, 381–384. doi:10.1099/0022-1317-60-2-381
- Suda, Y., Fukushi, S., Tani, H., Murakami, S., Saijo, M., Horimoto, T., Shimojima, M.**, 2016. Analysis of the entry mechanism of Crimean-Congo hemorrhagic fever virus, using a vesicular stomatitis virus pseudotyping system. *Arch. Virol.* 161, 1447–1454. doi:10.1007/s00705-016-2803-1
- Sun, Q., Jin, C., Zhu, L., Liang, M., Li, C., Cardona, C.J., Li, D., Xing, Z.**, 2015. Host Responses and Regulation by NFκB Signaling in the Liver and Liver Epithelial Cells Infected with A Novel Tick-borne Bunyavirus. *Scientific Reports* 5, 11816. doi:10.1038/srep11816
- Sun, Y., Jin, C., Zhan, F., Wang, X., Liang, M., Zhang, Q., Ding, S., Guan, X., Huo, X., Li, C., Qu, J., Wang, Q., Zhang, S., Zhang, Y., Wang, S., Xu, A., Bi, Z., Li, D.**, 2012. Host cytokine storm is associated with disease severity of severe fever with thrombocytopenia syndrome. *J Infect Dis.* 206, 1085–1094. doi:10.1093/infdis/jis452
- Suzich, J.A., Kakach, L.T., Collett, M.S.**, 1990. Expression strategy of a phlebovirus: biogenesis of proteins from the Rift Valley fever virus M segment. *J Virol* 64, 1549–1555.
- Takahashi, T., Maeda, K., Suzuki, T., Ishido, A., Shigeoka, T., Tominaga, T., Kamei, T., Honda, M., Ninomiya, D., Sakai, T., Senba, T., Kaneyuki, S., Sakaguchi, S., Satoh, A., Hosokawa, T., Kawabe, Y., Kurihara, S., Izumikawa, K., Kohno, S., Azuma, T., Suemori, K., Yasukawa, M., Mizutani, T., Omatsu, T., Katayama, Y., Miyahara, M., Ijuin, M., Doi, K., Okuda, M., Umeki, K., Saito, T., Fukushima, K., Nakajima, K., Yoshikawa, T., Tani, H., Fukushi, S., Fukuma, A., Ogata, M., Shimojima, M., Nakajima, N., Nagata, N., Katano, H., Fukumoto, H., Sato, Y., Hasegawa, H., Yamagishi, T., Oishi, K., Kurane, I., Morikawa, S., Saijo, M.**, 2014. The first identification and retrospective study of Severe Fever with Thrombocytopenia Syndrome in Japan. *J Infect Dis.* 209, 816–827.

doi:10.1093/infdis/jit603

- Takeda, K., Kaisho, T., Yoshida, N., Takeda, J., Kishimoto, T., Akira, S.,** 1998. Stat3 activation is responsible for IL-6-dependent T cell proliferation through preventing apoptosis: generation and characterization of T cell-specific Stat3-deficient mice. *J. Immunol.* 161, 4652–4660.
- Talmon, Y., Prasad, B.V., Clerx, J.P., Wang, G.J., Chiu, W., Hewlett, M.J.,** 1987. Electron microscopy of vitrified-hydrated La Crosse virus. *J Virol* 61, 2319–2321.
- Tang, X., Gao, J.-S., Guan, Y.-J., McLane, K.E., Yuan, Z.-L., Ramratnam, B., Chin, Y.E.,** 2007. Acetylation-dependent signal transduction for type I interferon receptor. *Cell* 131, 93–105. doi:10.1016/j.cell.2007.07.034
- Tani, H., Shimojima, M., Fukushi, S., Yoshikawa, T., Fukuma, A., Taniguchi, S., Morikawa, S., Saijo, M.,** 2016. Characterization of Glycoprotein-Mediated Entry of Severe Fever with Thrombocytopenia Syndrome Virus. *J Virol* 90, 5292–5301. doi:10.1128/JVI.00110-16
- Taniguchi, T., Takaoka, A.,** 2002. The interferon-alpha/beta system in antiviral responses: a multimodal machinery of gene regulation by the IRF family of transcription factors. *Curr. Opin. Immunol.* 14, 111–116.
- Terasaki, K., Murakami, S., Lokugamage, K.G., Makino, S.,** 2011. Mechanism of tripartite RNA genome packaging in Rift Valley fever virus. *Proc. Natl. Acad. Sci. U.S.A.* 108, 804–809. doi:10.1073/pnas.1013155108
- Thomas, D., Blakqori, G., Wagner, V., Banholzer, M., Kessler, N., Elliott, R.M., Haller, O., Weber, F.,** 2004. Inhibition of RNA polymerase II phosphorylation by a viral interferon antagonist. *J. Biol. Chem.* 279, 31471–31477. doi:10.1074/jbc.M400938200
- Thompson, J.D., Higgins, D.G., Gibson, T.J.,** 1994. CLUSTAL W: improving the sensitivity of progressive multiple sequence alignment through sequence weighting, position-specific gap penalties and weight matrix choice. *Nucleic Acids Research* 22, 4673–4680. doi:10.1093/nar/22.22.4673
- Tilston-Lunel, N.L., Acrani, G.O., Randall, R.E., Elliott, R.M.,** 2016. Generation of Recombinant Oropouche Viruses Lacking the Nonstructural Protein NSm or NSs. *J Virol* 90, 2616–2627. doi:10.1128/JVI.02849-15
- Tilston-Lunel, N.L., Hughes, J., Acrani, G.O., da Silva, D.E.A., Azevedo, R.S.S., Rodrigues, S.G., Vasconcelos, P.F.C., Nunes, M.R.T., Elliott, R.M.,** 2015. Genetic analysis of members of the species Oropouche virus and identification of a novel M segment sequence. *J Gen Virol* 96, 1636–1650. doi:10.1099/vir.0.000108
- Tokarz, R., Williams, S.H., Sameroff, S., Sanchez Leon, M., Jain, K., Lipkin, W.I.,** 2014. Virome analysis of Amblyomma americanum, Dermacentor variabilis, and Ixodes scapularis ticks reveals novel highly divergent vertebrate and invertebrate viruses. *J Virol* 88, 11480–11492. doi:10.1128/JVI.01858-14
- Traavik, T., Mehl, R.,** 1977. Uukuniemi group viruses isolated in Norway. *Arch. Virol.*

- 54, 317–331.
- Tu, D., Zhu, Z., Zhou, A.Y., Yun, C.-H., Lee, K.-E., Toms, A.V., Li, Y., Dunn, G.P., Chan, E., Thai, T., Yang, S., Ficarro, S.B., Marto, J.A., Jeon, H., Hahn, W.C., Barbie, D.A., Eck, M.J.**, 2013. Structure and ubiquitination-dependent activation of TANK-binding kinase 1. *Cell Rep* 3, 747–758. doi:10.1016/j.celrep.2013.01.033
- Uzé, G., Lutfalla, G., Gresser, I.**, 1990. Genetic transfer of a functional human interferon  $\alpha$  receptor into mouse cells: Cloning and expression of its c-DNA. *Cell* 60, 225–234. doi:10.1016/0092-8674(90)90738-Z
- Uzé, G., Monneron, D.**, 2007. IL-28 and IL-29: newcomers to the interferon family. *Biochimie* 89, 729–734. doi:10.1016/j.biochi.2007.01.008
- van Knippenberg, I., Carlton-Smith, C., Elliott, R.M.**, 2010. The N-terminus of Bunyamwera orthobunyavirus NSs protein is essential for interferon antagonism. *J Gen Virol* 91, 2002–2006. doi:10.1099/vir.0.021774-0
- van Knippenberg, I., Elliott, R.M.**, 2015. Flexibility of bunyavirus genomes: creation of an orthobunyavirus with an ambisense S segment. *J Virol* 89, 5525–5535. doi:10.1128/JVI.03595-14
- Varela, M., Schnettler, E., Caporale, M., Murgia, C., Barry, G., McFarlane, M., McGregor, E., Piras, I.M., Shaw, A., Lamm, C., Janowicz, A., Beer, M., Glass, M., Herder, V., Hahn, K., Baumgärtner, W., Kohl, A., Palmarini, M.**, 2013. Schmallenberg virus pathogenesis, tropism and interaction with the innate immune system of the host. *PLoS Pathogens* 9, e1003133. doi:10.1371/journal.ppat.1003133
- Varga, Z.T., Grant, A., Manicassamy, B., Palese, P.**, 2012. Influenza virus protein PB1-F2 inhibits the induction of type I interferon by binding to MAVS and decreasing mitochondrial membrane potential. *J Virol* 86, 8359–8366. doi:10.1128/JVI.01122-12
- Varga, Z.T., Ramos, I., Hai, R., Schmolke, M., García-Sastre, A., Fernandez-Sesma, A., Palese, P.**, 2011. The Influenza Virus Protein PB1-F2 Inhibits the Induction of Type I Interferon at the Level of the MAVS Adaptor Protein. *PLoS Pathogens* 7, e1002067. doi:10.1371/journal.ppat.1002067
- Vera-Otarola, J., Soto-Rifo, R., Ricci, E.P., Ohlmann, T., Darlix, J.-L., López-Lastra, M.**, 2010. The 3' untranslated region of the Andes hantavirus small mRNA functionally replaces the poly(A) tail and stimulates cap-dependent translation initiation from the viral mRNA. *J Virol* 84, 10420–10424. doi:10.1128/JVI.01270-10
- Vijaykrishna, D., Mukerji, R., Smith, G.J.D.**, 2015. RNA Virus Reassortment: An Evolutionary Mechanism for Host Jumps and Immune Evasion. *PLoS Pathogens* 11, e1004902. doi:10.1371/journal.ppat.1004902
- Waterhouse, A.M., Procter, J.B., Martin, D.M.A., Clamp, M., Barton, G.J.**, 2009. Jalview Version 2--a multiple sequence alignment editor and analysis workbench. *Bioinformatics* 25, 1189–1191. doi:10.1093/bioinformatics/btp033
- Wathelet, M.G., Lin, C.H., Parekh, B.S., Ronco, L.V., Howley, P.M., Maniatis, T.**, 1998. Virus infection induces the assembly of coordinately activated transcription

- factors on the IFN-beta enhancer in vivo. *Mol. Cell* 1, 507–518.
- Watret, G.E., Elliott, R.M.**, 1985. The proteins and RNAs of St. Abb's Head virus, a Scottish Uukuvirus. *J Gen Virol* 66 ( Pt 5), 1001–1010. doi:10.1099/0022-1317-66-5-1001
- Weber, F., Bridgen, A., Fazakerley, J.K., Streitenfeld, H., Kessler, N., Randall, R.E., Elliott, R.M.**, 2002. Bunyamwera Bunyavirus Nonstructural Protein NSs Counteracts the Induction of Alpha/Beta Interferon. *J Virol* 76, 7949–7955. doi:10.1128/JVI.76.16.7949-7955.2002
- Weber, F., Dunn, E.F., Bridgen, A., Elliott, R.M.**, 2001. The Bunyamwera virus nonstructural protein NSs inhibits viral RNA synthesis in a minireplicon system. *Virology* 281, 67–74. doi:10.1006/viro.2000.0774
- Weber, F., Elliott, R.M.**, 2002. Antigenic drift, antigenic shift and interferon antagonists: how bunyaviruses counteract the immune system. *Virus Res.* 88, 129–136.
- Weber, F., Wagner, V., Rasmussen, S.B., Hartmann, R., Paludan, S.R.**, 2006. Double-stranded RNA is produced by positive-strand RNA viruses and DNA viruses but not in detectable amounts by negative-strand RNA viruses. *J Virol* 80, 5059–5064. doi:10.1128/JVI.80.10.5059-5064.2006
- Wichgers Schreur, P.J., Kortekaas, J.**, 2016. Single-Molecule FISH Reveals Non-selective Packaging of Rift Valley Fever Virus Genome Segments. *PLoS Pathogens* 12, e1005800. doi:10.1371/journal.ppat.1005800
- Wichgers Schreur, P.J., Oreshkova, N., Moormann, R.J.M., Kortekaas, J.**, 2014. Creation of Rift Valley fever viruses with four-segmented genomes reveals flexibility in bunyavirus genome packaging. *J Virol* 88, 10883–10893. doi:10.1128/JVI.00961-14
- Williams, P.**, 2014. **Oklahoma State Health Department Confirms First Case and Death of Heartland Virus** [WWW Document]. <https://www.ok.gov/healthOrganization/OfficeofCommunications/NewsReleases/NewsReleases/OklahomaStateHealthDepartmentConfirmsFirstCaseandDeathofHeartlandVirus.html>. URL (accessed 12.3.16).
- Won, S., Ikegami, T., Peters, C.J., Makino, S.**, 2007. NSm protein of Rift Valley fever virus suppresses virus-induced apoptosis. *J Virol* 81, 13335–13345. doi:10.1128/JVI.01238-07
- Wu, X., Qi, X., Qu, B., Zhang, Z., Liang, M., Li, C., Cardona, C.J., Li, D., Xing, Z.**, 2014. Evasion of antiviral immunity through sequestering of TBK1/IKKε/IRF3 into viral inclusion bodies. *J Virol* 88, 3067–3076. doi:10.1128/JVI.03510-13
- Wu, Y., Gao, G.F.**, 2013. Severe fever with thrombocytopenia syndrome virus expands its borders. *Emerg Microbes Infect* 2, e36. doi:10.1038/emi.2013.36
- Wuerth, J.D., Weber, F.**, 2016. Phleboviruses and the Type I Interferon Response. *Viruses* 8, 174. doi:10.3390/v8060174
- Xiong, W.-Y., Feng, Z.-J., Matsui, T., Foxwell, A.R.**, 2012. Risk assessment of human infection with a novel bunyavirus in China. *Western Pac Surveill Response J* 3, 61–66.

doi:10.5365/WPSAR.2012.3.4.002

- Xu, B., Liu, L., Huang, X., Ma, H., Zhang, Y., Du, Y., Wang, P., Tang, X., Wang, H., Kang, K., Zhang, S., Zhao, G., Wu, W., Yang, Y., Chen, H., Mu, F., Chen, W.,** 2011. Metagenomic analysis of fever, thrombocytopenia and leukopenia syndrome (FTLS) in Henan Province, China: discovery of a new bunyavirus. *PLoS Pathogens* 7, e1002369. doi:10.1371/journal.ppat.1002369
- Yadani, F.Z., Kohl, A., Préhaud, C., Billecocq, A., Bouloy, M.,** 1999. The carboxy-terminal acidic domain of Rift Valley Fever virus NSs protein is essential for the formation of filamentous structures but not for the nuclear localization of the protein. *J Virol* 73, 5018–5025.
- Yanase, T., Kato, T., Aizawa, M., Shuto, Y., Shirafuji, H., Yamakawa, M., Tsuda, T.,** 2012. Genetic reassortment between Sathuperi and Shamonda viruses of the genus Orthobunyavirus in nature: implications for their genetic relationship to Schmallenberg virus. *Arch. Virol.* 157, 1611–1616. doi:10.1007/s00705-012-1341-8
- Yoneyama, M., Suhara, W., Fukuhara, Y., Fukuda, M., Nishida, E., Fujita, T.,** 1998. Direct triggering of the type I interferon system by virus infection: activation of a transcription factor complex containing IRF-3 and CBP/p300. *EMBO J.* 17, 1087–1095. doi:10.1093/emboj/17.4.1087
- Yoneyama, M., Suhara, W., Fukuhara, Y., Sato, M., Ozato, K., Fujita, T.,** 1996. Autocrine amplification of type I interferon gene expression mediated by interferon stimulated gene factor 3 (ISGF3). *J Biochem* 120, 160–169.
- Yu, C.-R., Dambuza, I.M., Lee, Y.-J., Frank, G.M., Egwuagu, C.E.,** 2013. STAT3 regulates proliferation and survival of CD8+ T cells: enhances effector responses to HSV-1 infection, and inhibits IL-10+ regulatory CD8+ T cells in autoimmune uveitis. *Mediators of Inflammation* 2013, 359674–10. doi:10.1155/2013/359674
- Yu, X.-J., Liang, M.-F., Zhang, S.-Y., Liu, Y., Li, J.-D., Sun, Y.-L., Zhang, L., Zhang, Q.-F., Popov, V.L., Li, C., Qu, J., Li, Q., Zhang, Y.-P., Hai, R., Wu, W., Wang, Q., Zhan, F.-X., Wang, X.-J., Kan, B., Wang, S.-W., Wan, K.-L., Jing, H.-Q., Lu, J.-X., Yin, W.-W., Zhou, H., Guan, X.-H., Liu, J.-F., Bi, Z.-Q., Liu, G.-H., Ren, J., Wang, H., Zhao, Z., Song, J.-D., He, J.-R., Wan, T., Zhang, J.-S., Fu, X.-P., Sun, L.-N., Dong, X.-P., Feng, Z.-J., Yang, W.-Z., Hong, T., Zhang, Y., Walker, D.H., Wang, Y., Li, D.-X.,** 2011. Fever with Thrombocytopenia Associated with a Novel Bunyavirus in China. <http://dx.doi.org/10.1056/NEJMoa1010095> 364, 1523–1532. doi:10.1056/NEJMoa1010095
- Yun, Y., Heo, S.T., Kim, G., Hewson, R., Kim, H., Park, D., Cho, N.-H., Oh, W.S., Ryu, S.Y., Kwon, K.T., Medlock, J.M., Lee, K.H.,** 2015. Phylogenetic Analysis of Severe Fever with Thrombocytopenia Syndrome Virus in South Korea and Migratory Bird Routes Between China, South Korea, and Japan. *Am. J. Trop. Med. Hyg.* 93, 468–474. doi:10.4269/ajtmh.15-0047
- Zeng, W., Xu, M., Liu, S., Sun, L., Chen, Z.J.,** 2009. Key role of Ubc5 and lysine-63 polyubiquitination in viral activation of IRF3. *Mol. Cell* 36, 315–325. doi:10.1016/j.molcel.2009.09.037

- Zhang, F.**, 2001. Binding of Double-stranded RNA to Protein Kinase PKR Is Required for Dimerization and Promotes Critical Autophosphorylation Events in the Activation Loop. *Journal of Biological Chemistry* 276, 24946–24958. doi:10.1074/jbc.M102108200
- Zhang, Y.-Z., He, Y.-W., Dai, Y.-A., Xiong, Y., Zheng, H., Zhou, D.-J., Li, J., Sun, Q., Luo, X.-L., Cheng, Y.-L., Qin, X.-C., Tian, J.-H., Chen, X.-P., Yu, B., Jin, D., Guo, W.-P., Li, W., Wang, W., Peng, J.-S., Zhang, G.-B., Zhang, S., Chen, X.-M., Wang, Y., Li, M.-H., Li, Z., Lu, S., Ye, C., de Jong, M.D., Xu, J.**, 2012a. Hemorrhagic fever caused by a novel Bunyavirus in China: pathogenesis and correlates of fatal outcome. *Clin Infect Dis*. 54, 527–533. doi:10.1093/cid/cir804
- Zhang, Y.-Z., Zhou, D.-J., Qin, X.-C., Tian, J.-H., Xiong, Y., Wang, J.-B., Chen, X.-P., Gao, D.-Y., He, Y.-W., Jin, D., Sun, Q., Guo, W.-P., Wang, W., Yu, B., Li, J., Dai, Y.-A., Li, W., Peng, J.-S., Zhang, G.-B., Zhang, S., Chen, X.-M., Wang, Y., Li, M.-H., Lu, X., Ye, C., de Jong, M.D., Xu, J.**, 2012b. The ecology, genetic diversity, and phylogeny of Huaiyangshan virus in China. *J Virol* 86, 2864–2868. doi:10.1128/JVI.06192-11
- Zhang, Y.-Z., Zhou, D.-J., Xiong, Y., Chen, X.-P., He, Y.-W., Sun, Q., Yu, B., Li, J., Dai, Y.-A., Tian, J.-H., Qin, X.-C., Jin, D., Cui, Z., Luo, X.-L., Li, W., Lu, S., Wang, W., Peng, J.-S., Guo, W.-P., Li, M.-H., Li, Z.-J., Zhang, S., Chen, C., Wang, Y., de Jong, M.D., Xu, J.**, 2011. Hemorrhagic fever caused by a novel tick-borne Bunyavirus in Huaiyangshan, China. *Zhonghua Liu Xing Bing Xue Za Zhi* 32, 209–220.

---

Chapter **12**

**PUBLICATIONS**

---

## **12 Publications**